RNA- and Chromatin-binding Proteins in Small RNA-mediated Gene Silencing

by

Danny Yang

A dissertation submitted in partial fulfillment
of the requirements for the degree of
Doctor of Philosophy
(Human Genetics)
in The University of Michigan
2015

Doctoral Committee:

Associate Professor John Kim, Chair
Associate Professor Patrick J. Hu
Assistant Professor Sundeep Kalantry
Associate Professor Donna M. Martin

ACKNOWLEDGMENTS

First, I especially need to thank John for his patience and support in training me to be a scientist. I want to thank all my colleagues in the Kim Lab, past and present. It has been a pleasure to work with them all. I specifically want to thank Mallory Freeberg for her bioinformatic expertise and all her helpful discussions over the years. I am grateful to Ting Han and Allison Billi for teaching me key techniques, Jungsook Park and Vishal Khivansara for their help with key experiments. It has been great to work with Natasha Weiser and discuss exciting science. I thank Amelia Alessi for sharing invaluable reporter strains, and Da Fang for helping us make science happen. Charlotte, Amanda, Tony and Andy: thanks for the comraderie.

I want to thank Ray Chan and Jayshree Khanikar for help with imaging. I really appreciate the help of Chase Weidmann, Jen Bohn, and Aaron Goldstrohm in cell culture experiments. For taking the time to learn about my research and providing helpful suggestions, I give thanks to my committee, Drs. Patrick Hu, Sundeep Kalantry, and Donna Martin. I thank Kärt Tomberg and Albert Chen for very helpful comments.

I thank my fiancée Mary, my parents Jie and Helena, my sister Angela, and my friends for all their love and encouragement.

PREFACE

This thesis comprises the research I conducted in Professor John Kim's lab starting from July 2010 until the present.

In Chapter 2, I present a study on *C. elegans* PUF-9, a member of the conserved Pumilio/FBF family of RNA binding proteins. We show that PUF-9 and microRNAs binding sites are physically clustered in 3'UTRs throughout the transcriptome.

In Chapter 3, I present a study on *C. elegans* MORC-1, a conserved chromatin binding protein that acts downstream of nuclear RNA interference and mediates the effects of inherited small RNAs.

In Chapter 4, I discuss the implications of our findings and present preliminary data as leads for promising avenues of research.

TABLE OF CONTENTS

LIST OF TABLES

LIST OF FIGURES

CHAPTER I - Introduction

Gene expression is finely and coordinately regulated at many levels to ensure the proper development and reproductive success of an organism. For example, canonical RNA-binding proteins (RBPs) and the conserved microRNA (miRNA) class of small, noncoding RNAs mediate post-transcriptional gene silencing through recognition of target mRNA 3' untranslated regions (UTRs). In addition, small interfering RNAs (siRNAs) contribute to mRNA degradation, as well as transcriptional gene silencing at the chromatin level. Here, I review our current understanding of the gene regulatory mechanisms mediated by the Pumilio family of RBPs, small noncoding RNAs, and chromatin binding proteins of the Microrchidia family.

1.1 *C. elegans* as a model organism

C. elegans provides many advantages as a model organism for genetic analysis [1]. First, they can be maintained as self-fertilizing hermaphrodites, which allow the study of clonal populations of uniform genetic makeup. Self-fertilization simplifies the isolation of homozygous mutations in genetic screens, facilitating the discovery of the first RNA interference (RNAi) factors in worms, including the Argonaute protein RNAi DEfective-1 (RDE-1) and the double strand RNA (dsRNA) binding protein RDE-4 [2].

Second, worms are optically clear, which facilitates the visual tracing of the precisely defined cell division and differentiation events in the *C. elegans* soma, from the one cell embryo to 558 cells at hatching and 959 cells in the adult hermaphrodite [3]. Analysis of mutants that deviate from the invariant cell lineage of wild-type *C. elegans* led to the discovery of miRNAs [4]. Third, *C. elegans* have a short generational time, facilitating the study of transgenerational epigenetic effects. Embryonic development spans about half a day, and worms progress through four larval stages (L1 to L4) to become reproductive adults in 48 to 72 hours at room temperature (20-25°C) (Figure 1.1). Thus, inherited gene silencing phenomena that span 10 or more generations can be feasibly studied in worms [5]. Finally, the *C. elegans* germline provides a rich context for RNA binding proteins and specialized small RNAs, which facilitated the characterization of Pumilio family RBP functions and the fine dissection of RNAi pathways [6, 7].

C. elegans germline development and function

During early embryogenesis, the *C. elegans* germline derives from the P cell lineage that receives maternally deposited RNA-protein complexes called P-granules and the global RNA Pol II repressor PIE-1 (reviewed in [8]). The P4 cell (P lineage germline precursor produced at the 4th embryonic division) yields two primordial germ cells that are transcriptionally and mitotically dormant until the mid-L1 stage [9]. In conjunction with cells of the somatic gonad, the primordial germ cells proliferate to generate the anterior and posterior arms of the gonad during larval development. Each arm is organized as a folded tube; germline stem cell mitosis occurs in the distal end. Meiosis proceeds as cells travel toward the spermatheca and uterus at the proximal

end. Sperm are produced in the L4 stage and stored in the spermatheca. In hermaphrodites, the germline transitions from spermatogenesis to oogenesis at the L4 to adult transition. Oocytes are produced throughout adulthood, travel through the spermatheca to the uterus, and fertilized embryos are laid through the vulva (Figure 1.2). Self-fertilizing hermaphrodites (XX) can generate both hermaphrodite and male (XO) progeny. Male progeny occur spontaneously through meiotic nondisjunction of the X-chromosome (at 0.1-0.2% frequency [10]). Males produce sperm throughout adulthood and can fertilize hermaphrodites.

A rich variety of small RNAs are generated in the germline, and several of these pathways feed into epigenetic regulation of germline chromatin. These pathways include the endogenous small interfering RNA (endo-siRNA) pathway, the PIWI-interacting RNA (piRNA) pathway, the hereditary RNAi defective (HRDE) nuclear RNAi pathway, and the chromosome segregation and RNAi defective (CSR) nuclear RNAi pathway. Altogether RBPs, small RNAs, and chromatin binding proteins control germline gene expression and protect the immortal germ cell lineage.

1.2 PUF proteins are conserved translational repressors

The Pumilio/*fem-3* binding factor (PUF) family of RBPs is conserved from yeast to humans. PUF proteins are proposed to be master regulators of stem cell function [11, 12]. For example, Pumilio and its binding partner Nanos are required to maintain totipotent primordial germ cells and germline stem cells across diverse species. In *C. elegans*, PUF proteins promote primordial germ cell viability, germline stem cell mitosis

and later promote meiotic progression [11, 13-15]. In *Drosophila*, Pumilio and Nanos promote stem cell self-renewal by preventing differentiation in primordial germ cells and adult stem cells [16]. In mice, *Pum1* mutants have smaller testes, decreased fertility, and increased *p53*-dependent apoptosis in differentiating spermatocytes [17]. From worms to humans, PUF proteins are also important regulators of neuronal function. PUF proteins regulate dendritic arborization in *Drosophila* and rat neurons [18, 19]. Mice deficient in *Pum1* display neurological defects resulting from upregulation of ATAXIN-1, the protein that aggregates in the brains of type 1 spinocerebellar ataxia patients [20]. And in worms, PUF proteins mediate olfactory adaptation in chemosensory neurons [21]. Together, multiple studies have highlighted the importance of PUF proteins in regulating key aspects of development and physiology.

Fly Pumilio provides a paradigm for understanding RBP regulation of translation

The *pumilio* gene was discovered in 1987 by Lehmann and Nüsslein-Volhard, who found that *pum* mutant embryos lack abdominal segmentation [22]. Pumilio expression is uniform in the early *Drosophila* embryo, while its cofactor Nanos is localized to the posterior pole [23-25]. Together, Pumilio and Nanos are required for repression of *hunchback*, generating an anterior-to-posterior gradient of Hunchback protein [26, 27]. Pumilio binds two specific motifs in the *hunchback* 3'UTR, originally identified as Nanos response elements (NREs) [27, 28]. The effect of Pumilio/Nanos binding on *hunchback* mRNA is translational repression accompanied by deadenylation. Hence, deadenylation was thought to be required for Pumilio mediated translational repression [29, 30]. However, Pumilio also represses non-adenylated transcripts whose

3’ ends are protected by a histone stem loop hairpin [31]. Thus, translational repression of *hunchback* by Pumilio does not require deadenylation.

The bipartite NRE was later discovered to be two separate motifs that can function independently. Box A is the Brain Tumor (Brat) response element, while the adjacent Box B is the Pumilio response element (PRE) [32]. Brat, Nanos, and Pumilio form a ternary complex on the *hunchback* mRNA, where the proteins associate through direct contacts [33, 34]. In addition, Brat and Pumilio each bind to their own adjacent RNA response elements and combine to achieve full repression [32]. In fly, Brat can recruit the eIF4E homolog 4EHP to repress translational initiation [35]. More specifically, 4EHP competes with the translation initiation factor eIF4E for 5’ mRNA cap binding. Overall, the *hunchback* 3’UTR provides a paradigm for studying combinatorial post-transcriptional gene silencing, where three RNA binding proteins and two RNA motifs collaborate to regulate the expression of a single target.

PUF protein structure facilitates target recognition

PUF proteins share a widely conserved Pumilio-Homology-Domain (PUM-HD) consisting of eight tri-α-helical repeats that specifically bind 8 nucleotides representing a PUF response element (PRE) [36, 37]. Drosophila Pumilio and Human PUM1 crystal structures show that all eight repeats pack to form a crescent shaped domain [38, 39]. On the interior of this crescent, three amino acid side chains from each repeat interact with RNA bases [40]. In each repeat, residues 12 and 16 form hydrogen bonds or van der Waals interactions with RNA bases, while residue 13 stacks in between RNA bases. Altogether, the eight tri-helical repeats provide one-to-one recognition of eight RNA

bases. Target specificity of PUF proteins can be changed by mutating the side chains that specifically interact with RNA bases, thus creating “designer” RNA binding modules [40, 41]. In *C. elegans*, FBF-1/2, PUF-3/11, and PUF-5/6/7 families possess divergent PUM-HDs [12]. As a result of extended spacing between the eight tri-helical repeats, divergent PUM-HDs accommodate RNA targets with extra nucleotides that are not coordinated by a PUF repeat [42-45].

PUF proteins repress translation with or without mRNA decay

PUF proteins are able to repress mRNAs through multiple mechanisms of translational repression and mRNA decay. In yeast, Puf4p and Puf5p bind their respective response elements in the 3’UTR of *HO*, an endonuclease required for mating type switching [46]. Puf5p directly binds Pop2p to recruit the Ccr4p/NOT deadenylase complex, which is responsible for deadenylation of the *HO* mRNA [47]. The Puf5p-bound Pop2p complex also includes decapping factors Dcp1p and Dhh1p that interact with the 5’mRNA cap. While Ccr4p is required for Puf5p to trigger deadenylation of *HO*, it is dispensable for translational repression [48, 49]. In contrast, Puf4p requires Ccr4p for both deadenylation and translational repression of *HO* [49]. It has been hypothesized that PUF homologs act through different mechanisms by recruiting incompletely overlapping sets of cofactors. Importantly, the recruitment of Pop2p/Ccr4p/NOT homologs is conserved for human PUM1, fly Pumilio, and both FBF-1 and PUF-8 in worms [14, 47, 50].

Similar to *Drosophila* Pumilio, human PUMs employ deadenylation-dependent and deadenylation-independent mechanisms of target repression [51]. Human PUM1/2

trigger 3'UTR target deadenylation, translational repression, and mRNA decay. Hence, NOT deadenylases are required for maximal repression. However, human PUMs can translationally repress histone stem loop 3'UTR reporters that lack a polyA tail [51]. Inhibition of translational initiation is a common mechanism employed by PUFs, as *Xenopus* Pum2 can bind the 5'mRNA cap to exclude cap-binding initiation factor eIF4E, providing translational repression without the need for deadenylation or decay [52].

In addition to their roles in target degradation and deadenylation, PUF proteins are important for localized translation and storage of mRNA targets. For example in yeast, Puf6p binds to *ASH1* transcription factor mRNA and represses translation until it reaches the bud tip of dividing yeast cells, where Casein Kinase 2 phosphorylates Puf6p to release *ASH1* for translation [53, 54]. In mammals, PUF proteins facilitate localized translation in neurons. Rat PUM2 represses translation of *eif4e* and sodium channel *scn1a* within dendrites, important for dendritic spine morphology and synaptic function [19].

Germline PUF binding is often associated with translational repression in the absence of mRNA decay. In the *C. elegans* germline, FBF-2 is recruited to perinuclear P-granules, the primary target site of RNA export (immediately after exit from the nuclear pore) [55]. Localization of FBF-2 at P-granules promotes target binding and translational repression instead of mRNA degradation. Loss of *fbf-2* or P-granules allows FBF-1 to degrade FBF-1/2 target *germline development-1* (*gld-1*) mRNA. Overall, FBF-1 and FBF-2 both repress *gld-1* but through distinct mechanisms. In many species, specialized RBP mechanisms have evolved to protect or degrade maternal transcripts. For example, in sea urchin primordial germ cells, Pumilio and Nanos

repress deadenylase *CNOT6*, protecting maternally inherited mRNAs from deadenylation and decay [56].

The *C. elegans* PUF proteins

The *C. elegans* genome encodes 10 PUF homologs in five groups as defined by PUM-HD structure. FBF-1/2 are the best characterized worm PUFs and are predominantly expressed in the germline [6]. PUF-3/11 and PUF-5/6/7 are expressed in maternal germline, where they nucleate oocyte RNA granules and regulate different aspects of oocyte development [57, 58]. *puf-4* and *puf-10* are pseudogenes, while PUF-12 is a divergent homolog of yeast Puf6p and human PUM-A with only 6 of 8 conserved repeats. PUF-8/9 are the closest homologs of fly Pumilio and human PUM1/2 [12]. While PUF-8 is restricted to the germline, PUF-9 is the predominant conserved canonical PUM-HD protein in the soma [59].

In *C. elegans*, *fem-3* promotes male development. In hermaphrodites, *fem-3* null mutants only produce oocytes, while *fem-3* gain-of-function mutants only produce sperm. Gain-of-function mutations cluster within the *fem-3* 3'UTR at a site called the "point mutation element" [60]. Through yeast three hybrid assays, Zhang *et al.* discovered that Pumilio homolog FBF-1 binds the "point mutation element," repressing *fem-3* to activate the switch from spermatogenesis to oogenesis [6]. Similar to Drosophila Pumilio, FBF-1 physically interacts with Nanos homolog NOS-3, a cofactor required for regulation of the sperm to oocyte switch [61].

C. elegans PUF proteins can have multiple functions in different contexts. For example, FBF-1 promotes mitosis in germline stem cells by repressing *gld-1* mRNA, a

factor that activates meiosis [11]. At the mitosis-to-meiosis transition, FBF-1 recruits the GLD-2 polyA-polymerase to polyadenylate and reactivate *gld-1* mRNA [14, 62, 63]. FBF-1 binding also mediates olfactory adaptation by activating *egg laying defective-4 (egl-4)* kinase in chemosensory neurons, through an unsolved mechanism [21]. Interestingly, FBF-1 activation of *egl-4* 3'UTR requires an adjacent *let-7* miRNA target site.

Although *C. elegans* PUFs have been shown to recruit CCR4/NOT and promote deadenylation *in vitro*, the mechanistic details of target repression have not been characterized *in vivo* [14, 47]. Germline GFP reporter assays detected robust repression of PUF-3/11 and PUF-5/6/7 targets at the protein level, but no effect on mRNA transcript levels [57].

Transcriptome-wide analyses of PUF targeting

RNA immunoprecipitation microarray (RIP-Chip) studies showed that PUF proteins bind 40-200 targets in yeast, to over a thousand targets in worms, flies, and humans [64, 65]. Indeed, photoactivatable ribonucleoside enhanced crosslinking and immunoprecipitation (PAR-CLIP) of human PUM2 revealed about 3000 potential targets in HEK293 cells [66]. PUF proteins bind to functionally related sets of mRNAs within a species, or across species. For example, 87% of yeast Puf3p targets are mitochondrial proteins [65]. However, the identity of PUF targets themselves is species-specific. About 23% of FBF-1 targets have an orthologous target bound by human PUM1, while only 40 targets are shared between worm FBF-1, human PUM1, and fly Pumilio [67]. Among the highly conserved targets of PUF proteins are cyclins B and T, MAP kinase regulator

ARAF, NFKB inhibitor A, PDK1 and FOXO [67]. Together, these studies found that targets of human PUM1/2, fly Pumilio, and yeast Puf3p are highly enriched for the UGUAHAUA motif (H=A/U/C), the canonical PUF recognition element previously used to generate RNA-protein complex crystal structures for human PUM1 and fly Pumilio. PUF proteins with divergent RNA binding domains (Puf4p, Puf5p, FBF-1) were enriched for 8-10nt motifs with a 5' UGUA, but extra bases in the 3' half. For example, FBF-1 binds the UGUAHHAUA motif because its RNA binding domain is elongated [43]. An extra spacer nucleotide provides the extra length required for the RNA motif to reach all eight PUF repeats in FBF-1 [68].

Combinatorial regulation of *cyclin B* by PUF and CPEB

PUF proteins and Cytoplasmic Polyadenylation Element Binding proteins (CPEB) exhibit cooperative binding and target regulation, a property that might also apply to binding of shared RNA targets by PUF proteins and miRNAs. In *Xenopus* oocytes, Pum1 and CPEB bind to adjacent sites in *cyclin B1* mRNA [69]. In immature oocytes, CPEB recruits Poly(A)-specific Ribonuclease and Maskin, which binds eIF4E at the 5' mRNA cap to block translation initiation. Upon oocyte activation, phosphorylated CPEB recruits Cleavage and Polyadenylation Specificity Factor and activates translation of *cyclin B1* mRNA. Pum1 contributes to both repression and activation [70]. Pum1 strongly enhances CPEB function at an adjacent weak CPEB motif, moderately enhances CPEB function at a consensus CPEB motif, but has no effect when two adjacent CPEB motifs are present in cyclin B1 3'UTR reporters [70]. Furthermore, UV crosslinking experiments suggest that Pum1 stabilizes CPEB binding at adjacent sites.

Thus, Pum1 potentiates CPEB binding, but becomes unnecessary when two CPEB monomers can cooperatively bind and regulate the 3'UTR. The interaction between CPEB and PUF is conserved in *C. elegans*, where CPB-1 directly associates with FBF-1 to promote meiosis in the male germline [71]. Furthermore, CPB-1 greatly enhances FBF-1 binding affinity for the weak target motif in *cyclin B* [72]. MicroRNAs also cooperatively regulate 3'UTRs in *C. elegans* embryo extracts [73], and the combinatorial regulation between Pum1 and CPEB could be similar to how PUFs interact with microRNAs.

1.3 MicroRNAs repress translation and trigger mRNA decay

MicroRNAs (miRNAs) are small, non-coding RNAs that bind mRNA 3'UTRs to mediate post-transcriptional regulation of gene expression. miRNA biogenesis and effector functions are conserved among metazoans (Figure 1.3), where they control diverse biological processes including cell division and death (reviewed in [74]), organogenesis (miR-1 in mouse cardiogenesis) [75], maternal-to-zygotic transition (miR-430 in zebrafish) [76], photoreceptor light adaptation (miR-183 in mouse retina) [77], and aging (*lin-4* in worms) [78]. Because miRNAs function in so many biological pathways, their misregulation is associated with a variety of diseases including cancer [79], diabetes [80], neurodegeneration [81], and autoimmune disorders [82].

Discovery of miRNAs in *C. elegans* and implications of their conservation

Genetic mutants with defects in the canonical cell division or specification pattern are classified as lineage (Lin) mutants. Analysis of genetic interactions between cell lineage mutants helped map the first miRNA pathways in *C. elegans*.

The *C. elegans lin-4* miRNA was the first endogenous small RNA, discovered in 1993 by the Ambros lab [4]. This locus produces two short transcripts, 61nt *lin-4L* and a 22nt *lin-4S*, correctly predicted to be the precursor and mature forms of *lin-4*. *lin-4* is expressed at the late L1 stage to promote hypodermal and vulval blast cell differentiation at the L1 to L2 transition. Loss of *lin-4* leads to reiteration of L1 fates in ventral blast cells, which are never able to form a functional vulva. However, the germline continues to develop, leading to the internal hatching of embryos and the "bag of worms" phenotype. *lin-4* is complementary to sequences in the *lin-14* 3'UTR, and *lin-14* null suppressed the *lin-4* vulvaless phenotype. Therefore, *lin-4* was proposed to repress *lin-14* through antisense targeting of the 3'UTR [4, 83]. Interestingly, *lin-4* repression of *lin-14* also regulates aging, as *lin-4* overexpression extends lifespan and *lin-14* gain of function shortens lifespan [78].

The second miRNA, *let-7,* was discovered in 2000 and found to be conserved among metazoans [84, 85]. As both *lin-4* and *let-7* functioned as temporal switches, the hunt for additional small temporal RNAs began. Advances in small RNA cloning and sequencing facilitated the rapid discovery of additional miRNAs in worms, flies, and humans [86-88] as well as endogenous siRNAs and piRNAs [89]. Today, there are more than 400 annotated miRNAs in *C. elegans*, although many have not been validated (miRBase [90]).

Just as *let-7* promotes neuronal and hypodermal differentiation in *C. elegans*, this conserved miRNA serves as a key regulator of stem cell function in humans [84]. Expression profiling of embryonal carcinoma cells revealed that human *let-7* is low in undifferentiated cells and upregulated during neuronal differentiation induced by retinoic acid, concomitant with a drop in *lin-28* [91]. In combination with OCT4, SOX2, and NANOG, LIN28 promotes induced pluripotent stem cell reprogramming by repressing *let-7* processing [92, 93]. Decreased *let-7* or increased *lin-28* expression were subsequently found to be associated with lung cancer [94], colon cancer [95], and hepatocellular carcinoma [96]. *let-7* represses *RAS* and *HMGA2* oncogenes to limit self-renewal and tumorigenicity in breast cancer, while chromosomal rearrangements involving the *HMGA2* 3'UTR promote tumorigenesis [79, 92, 97, 98].

General miRNA biogenesis pathway

miRNAs are transcribed by RNA Polymerase II, so primary miRNA transcripts are capped and polyadenylated [99, 100]. These primary transcripts can be over 1kb in length and include multiple miRNAs. miRNAs reside within precursor hairpins consisting of a ~35nt stem and a terminal loop. These hairpins are recognized by the Microprocessor complex consisting of Drosha (DRSH-1 in worms) and cofactor Pasha (PASH-1 in worms) [101-103]. Drosha has two RNaseIII domains that cleave within the stem to generate a ~65nt hairpin with a 2nt 3' overhang [101, 104, 105]. The hairpin precursor is bound by Exportin-5 (XPO-1 in worms), which transports it through nuclear pores to the cytoplasm [106, 107]. In the cytoplasm, Dicer (DCR-1 in worms) binds to the precursor hairpin and cuts the stem at a measured distance from the 3' overhang

[108-113]. Association with the miRNA Argonaute promotes precursor processing by Dicer [114, 115]. Mature miRNA duplexes are loaded into Argonaute proteins AGO1 in *Drosophila*, ALG-1/2 in *C. elegans*, or AGO1-4 in humans [111, 116, 117]. Heat shock proteins HSP70 and HSP90 mediate ATP-dependent loading of miRNA (and siRNA) duplexes by Argonautes; the passenger strand is cleaved or passively released, and the miRNA-loaded Argonaute complex (*i.e.* RNA-induced silencing complex, RISC) is free to regulate targets [118]. While the biogenesis of mature, functional miRNA species has been well characterized, the effector function of miRNA-loaded RISCs (miRISCs) and how this function is coordinated with regulation by other RBPs remains less well understood.

Regulation of *let-7* miRNA biogenesis

miRNA biogenesis is regulated at many levels including transcription, primary transcript processing, precursor stability, Dicer processing efficiency, Argonaute stability, and mature miRNA turnover (reviewed in [119]). In *C. elegans*, *let-7* family primary miRNAs are regulated by three transcription factors. Erythroid-Like Transcription factor-1 (ELT-1) promotes transcription, Hunchback-Like-1 (HBL-1) represses transcription, and abnormal Dauer Formation-12 (DAF-12) can either promote or repress transcription depending on steroid hormone ligand binding [120-122]. RBPs also regulate the processing of primary and precursor *let-7* miRNAs in mammals and worms. Human KH-type Splicing Regulatory Protein (KSRP) binds the terminal loop of human *let-7* to promote primary transcript processing by Drosha, as well as precursor processing by Dicer [123]. In contrast, LIN-28 binds to primary *let-7*

transcripts to mediate co-transcriptional repression of Drosha processing, or to precursor *let-7* to promote 3' uridylation by Terminal Uridyltransferase-4/7 and subsequent decay by 3'-to-5' nuclease DIS3-Like-2 [124-126]. Mature *let-7* miRNAs are stabilized by Argonaute loading and target availability. Otherwise, *let-7* is subject to degradation by 5'-to-3' exoribonuclease-1 and -2 (XRN-1/2) activity stimulated by decapping scavenger-1 (DCS-1) [127-129]. In human embryo and muscle tissue, the H19 long noncoding RNA acts as a sponge that functionally titrates *let-7* without reducing miRNA expression level, similar to circular RNA sponges [130].

miRNA induced silencing complex

The miRNA-loaded Argonaute recruits effector proteins, forming the miRNA-induced silencing complex (miRISC, reviewed in [131]). The core miRISC scaffolding protein is Glycine-tryptophan protein of 182 kD (GW182; AIN-1/2 in worms) [132]. The tryptophan motifs of GW182 proteins recruit the CCR4/NOT deadenylase complex and the PAN2/3 nucleases, key cofactors responsible for repression [133, 134]. In mammalian cells, GW182 homologs associate with the EDD E3 ubiquitin ligase, which binds TOB1/2 (Transducer of ERBB2 EGF Receptor) and DDX6 DEAD box helicase, a homolog of yeast Dhh1p (CGH-1 in worms) that participates in PUF-mediated translational repression and decapping [135]. The TOB1/2 proteins physically bridge CCR4 and PolyA Binidng Protein (PABP) to promote deadenylation [136]. In *C. elegans*, the NHL-2 RBP associates with miRISC to enhance repression of *let-7* family miRNA targets including *let-60/RAS* and *hbl-1*, as well as *lsy-6* miRNA target *cog-1* [137]. TRIM32, an NHL-2 homolog in mice, also enhances *let-7* activity during neuronal

differentiation [138]. Proteomic analyses have found additional factors associated with miRISC (i.e. VIG-1 RBP and TSN-1 nuclease), but their roles are unclear [139].

In worms, ALG-1 Interacting proteins (AIN) -1 and -2 are required for both translational repression and mRNA target degradation [140]. Polysome fractionation experiments showed that *lin-4* and *let-7* miRNAs repress translation initiation of *lin-14* and *lin-41* targets respectively, which requires AIN-1/2 [140]. AIN-1/GW182 also localizes the miRISC/target complex to cytoplasmic P-bodies, sites of mRNA decay where decapping factors DCP-1/2 and the 5'-to-3' nuclease XRN-1 reside [132].

Translational repression and/or RNA decay

miRNAs have been observed to mediate translational repression and mRNA decay, but the temporal order and relative contribution of each process is an ongoing point of debate [141]. Luciferase reporter studies indicate that robust translational repression often occurs in the absence of mRNA degradation, or before the onset of mRNA degradation [142-144]. In contrast, global analyses of actively translating ribosome footprints suggest that decreased mRNA can account for the majority of miRNA-mediated translational repression [145, 146]. Recent studies suggest that miRNA-mediated deadenylation in pregastrulation zebrafish embryos triggers translational repression without RNA decay, while RNA decay accompanies decreased translation in later developmental stages or in cultured cells [147-150]. Notably, mRNA poly-A tail length is positively correlated with translation rate in early embryos, but there is zero correlation after gastrulation [148]. Thus, miRNAs employ different repression mechanisms during different developmental stages. The mechanisms that underlie such

complexity in miRNA-mediated silencing have yet to be found. Overall, the molecular outcome of target repression is quite context dependent.

miRISC regulation by post-translational modification

miRISC components can be regulated by post-translational modification, adding to the complexity of miRNA function. For example, AGO2 phosphorylation at S387 and Y529 confer opposite effects on P-body localization and miRNA-mediated repression in HEK cells (reviewed in [131]). AGO2 ubiquitination reduces protein stability, while sumoylation increases stability. Hydroxylation of Argonaute proteins enhances stability and repression during hypoxia. TNRC6/GW182 is also phosphorylated in human cells, which reduces the efficiency of PABP binding and target repression by miRISC [151].

Combinatorial regulation by miRISC and RNA binding proteins

3'UTRs are rich environments for binding and regulation. miRNAs often collaborate or compete with other factors. In zebrafish embryos for example, miR-430 represses the expression of hundreds of targets to control the maternal to zygotic transition [76]. *Tudor domain protein 7 (TDRD7)* and *Nanos1* mRNA are potently repressed in the soma, but expressed in the primordial germ cells [152]. In order to facilitate germ cell survival and migration, Dead End 1 (DND1) binds to U-rich elements flanking the miR-430 target site of *Nanos1* and blocks miRNA target binding [153]. Similarly, Deleted in Azoospermia-Like (DAZL) binds to the *TDRD7* 3'UTR to promote polyadenylation and block the translational repression conferred by miR-430 [154].

In mammalian cells, Human antigen R (HuR) binds to AU-rich elements in 3'UTRs [155]. Conserved HuR recognition elements are ~17nt long and tend to form hairpin structures with a 6 bp stem and a 5 nt loop [156]. In general, HuR binding promotes mRNA translation and association with polysomes. In mammalian cells, HuR can promote or oppose proximal target binding by miRNAs in different contexts. HuR binding of *c-Myc* 3'UTR promotes *let-7* binding at an adjacent site, while HuR blocks *miR-122* binding of *CAT-1* mRNA [157, 158]. When HuR binding sites overlap with miRNA target sites, HuR generally blocks 3'UTR accessibility and alleviates miRNA repression [159].

Similarly, polypyrimidine-tract-binding protein (PTB) competes with miRNAs on 3'UTR targets where binding sites physically overlap. For example, PTB occludes miR-124 binding sites on *SCP1* 3'UTR to block neuronal cell fate specification in fibroblasts [160]. In addition, PTB binds adjacent to a *let-7b* target site in *GNPDA1* 3'UTR. PTB binding unfolds a hairpin to expose the *let-7b* target site, as detected *in vitro* by single strand vs double strand RNA nuclease digestion [160]. PUF proteins have been shown to promote miRNA target accessibility, possibly in a manner similar to PTB.

MOV10 helicase unwinds G-rich secondary structure; this facilitates miRNA target binding. In contrast, at sites where Fragile X Mental Retardation Protein (FMRP) binds near miRNA target sites, MOV10 and FMRP contribute to blockade of miRNA target access [161]. Strangely, FMRP inverts the effect of MOV10 helicase on miRNA target site access.

Serum starvation turns *let-7* into a translational activator of the *HMGA2* 3'UTR in HEK293 or HeLa cells, a phenomenon that can also be achieved by direct tethering of

AGO2 to 3'UTRs [162]. Fragile X mental retardation autosomal homolog 1 (FXR1) associates with AGO2 in starved cells but not proliferating cells, suggesting that FXR1 could be responsible for turning miRISC into an activation complex [163].

PUF-miRNA interactions

Mounting evidence suggests that human PUF proteins potentiate miRNA-mediated regulation of shared targets [164-167]. In BJ primary fibroblasts, PUM1/2 are required for repression of tumor suppressor *p27* by miR-221/222. The miR-221 seed target base-pairs with a PUF response element in *p27* 3'UTR, forming a stable hairpin inaccessible to miRISC. PUM1/2 binds one arm of the RNA hairpin and releases the miR-221 target site on the opposite arm. This PUM1/2-mediated structural change allows miR-221/222-loaded miRISC to access its recognition site [164]. Human PUM1/2 also bind to the 3'UTR of *E2F3* oncogene, enhancing the repression conferred by multiple miRNAs [165]. It is unknown whether PUM1/2 contributes to miRNA target binding at the *E2F3* 3'UTR, or just to repression.

Computational analyses have revealed that miRNA target sites may reside in poorly accessible regions of target 3'UTRs near predicted PUM1/2 binding sites [167]. Interestingly, PUF/miRNA co-targets were predicted to have faster mRNA decay rates for the subset of 3'UTRs where PUF binding sites are located within 50nt of an interacting miRNA seed target [166].

In Chapter 2, we present a study that examines how PUF-9 and miRNAs regulate shared targets in *C. elegans*. We apply high throughput sequencing methods to

identify the transcriptome-wide RNA binding sites of PUF-9 and ALG-1 miRISC, map the overlap, and observe functional consequences of co-regulation *in vivo*.

1.4 Epigenetic regulation of germline chromatin

A modern concept of “epigenetics” refers to “the study of changes in gene function that are mitotically and/or meiotically heritable and that do not entail a change in DNA sequence” [168]. These heritable changes in gene function can be mediated by histone modifications, noncoding RNAs, and DNA methylation [169]. In *C. elegans*, histone modifications serve to maintain gene expression patterns required for germline specification, function, and viability across generations. A growing body of evidence suggests that small noncoding RNAs collaborate with histone methyltransferases, demethylases, and chromatin binding proteins to establish or maintain epigenetic states (reviewed in [170]). For example, disruption of the nuclear RNAi pathway results in progressive depletion of heterochromatin modifications, accompanied by progressive sterility over multiple generations. The role of small RNAs and chromatin binding proteins in maintenance of the immortal germ cell lineage will be discussed in detail in this introduction and studied in Chapters 3 and 4.

As the P4 cell (P-lineage germline precursor derived at the 4th embryonic cleavage) gives rise to the two primordial germ cells in the early embryo, there is a dramatic loss of Histone 3 (H3) tail modifications proposed to be driven by histone replacement [171-173]. H3K4me2/3, H3K8Ac, and H3K18Ac marks are lost and reset in each generation, along with H3K9me2/3 [171, 174]. In contrast, the H3K36me and

H3K27me marks remain stable across primordial germ cell specification and germline development [170]. Mutations that interfere with dynamic regulation of H3K4 and H3K9 methylation or stable inheritance of H3K27 and H3K36 methylation cause dramatic defects in germline function. These two sets of methylation marks act in opposing directions, and enzymes that modify these four marks have been implicated in transcriptional gene silencing [175-177].

H3K27 versus H3K36 methylation

In the mitotic and early meiotic regions of the germline, the X chromosome is silenced via H3K27me2/3 methylation by the MES-2/3/6 Polycomb repressor complex 2 (PRC2) [177, 178]. Accordingly, germline enriched genes are depleted from the X chromosome. Loss of MES-2/3/6 leads to maternal effect sterility in progeny.

Conversely, the histone methyl transferase MET-1 deposits H3K36me2/3 methylation at expressed genes during germ cell mitosis and early meiosis [179-181]. Active transcription likely drives placement of the H3K36me2/3 mark on expressed genes [181, 182]. Hence, this mark is enriched on autosomes and depleted from the X chromosome. MES-4 acts in early embryos to maintain H3K36 methylation independent of transcription [181, 182]. Altogether, transgenerational inheritance of H3K36 methylation transmits the memory of germline gene expression from parents to offspring. Even though H3K36 methylation is associated with actively transcribed genes in the adult germline, these marks are important for maintaining transcriptional silencing in primordial germ cells. As loss of *mes-4* results in premature activation of transcription and the accumulation of H3K4me2, *mes-4* is required for primordial germ cell viability

[180, 181, 183]. Interestingly, germline mechanisms that silence high copy transgenes require both MES-4 and the MES-2/3/6 complex [175, 184, 185]. One interpretation of these results suggests that H3K36 and H3K27 methylation differentially mark euchromatin and heterochromatin; so loss of either mark removes the heterochromatin / euchromatin boundary and the ability to differentially silence heterochromatin.

H3K4 versus H3K9 methylation: antagonistic regulation

H3K4me2/3 and H3K9me2/3 methylation are globally correlated with expressed genes and silenced heterochromatin, respectively [171, 176, 177, 186, 187]. H3K4 and H3K9 methylation are also functionally and physically opposed. For example, H3K4me3 physically blocks human H3K9 methyltransferase SETDB1 from binding its substrate, via steric hindrance [188]. The correct placement of these marks is critical for regulating germline gene expression, maintaining germline identity, and ensuring the immortality of the *C. elegans* germ cell lineage. Indeed, mutation of the SETDB1 homolog *met-2* results in a germline mortal (Mrt) phenotype, characterized by progressive sterility over multiple generations due to loss of sperm, oocytes, and their precursors [179].

H3K4me2 is enriched on autosomes throughout the germline but low on the X chromosome. In contrast, H3K9me2 accumulates on the hermaphrodite X during meiosis [171, 176]. H3K9me2 is robustly deposited on the unpaired male X and on repetitive transgene arrays, contributing to their transcriptional repression [177, 189].

Histone methyltransferase SET-2, WDR-5.1, and RBBP-5 promote H3K4me2/3 in embryos and in the mitotic germline [190, 191]. On the other hand, SPR-5 and RBR-2 are histone demethylases that remove H3K4me2 and -me3 marks, respectively [173,

192, 193]. Loss of *spr-5* causes progressive sterility associated with elevated H3K4me2 and mis-expression of spermatogenesis genes [173]. While germline H3K4 methylation is usually erased in zygotic germline precursors and the primordial germ cells, *spr-5* mutants accumulate H3K4me2 over many generations [171, 173]. This progressive germline mortal (Mrt) phenotype was subsequently found in mutants of *set-2*, *wdr-5.1*, *rbbp-5*, and *rbr-2* at elevated temperatures [190-192, 194]. Thus, the ability to deposit and erase H3K4 methylation is essential for germline maintenance over many generations.

Similarly, H3K9 methylation is important for germline function. MET-2 deposits H3K9me2 in germline and embryos, while *met-2* mutants are germline mortal [179, 195]. In addition to sharing the Mrt phenotype, *spr-5* and *met-2* mutants are both deficient in repetitive transgene silencing [173, 189].

Regulating the balance of H3K4 vs H3K9 methylation is also important for cell fate specification. Somatic cells gain the ability to express spermatogenesis genes in *spr-5;met-2* mutants with too much H3K4 methylation, whereas germ cells inappropriately express somatic genes in *set-2* mutants with too little H3K4 methylation [194, 196].

1.5 Nuclear siRNA pathways in *C. elegans*

There are three general classes of small RNAs in *C. elegans*: miRNAs, small interfering RNAs (siRNAs) and Piwi-interacting RNAs (piRNAs). Each class has a unique mode of biogenesis, sequence characteristics, and effector functions (Figure

1.4). *C. elegans* have 27 Argonaute proteins, and each associates with a characteristic set of small RNAs [7]. The exogenous RNAi pathway, endogenous RNAi pathway, and piRNA pathway all feed into a common nuclear silencing pathway. I will discuss the silencing pathways, and then introduce the Chromosome Segragation and RNAi (CSR) pathway that acts in opposition to silencing.

C. elegans have 27 specialized Argonautes

The *C. elegans* Argonautes are divided into three phylogenetic clades: the PIWI clade, the AGO clade, and the Worm Argonaute (WAGO) clade [7, 197]. The PIWI clade is named for the *Drosophila* P-element induced wimpy testes (Piwi) protein, which associates with piRNAs to silence transposons in the germline [198]. There are three PIWI clade Argonautes in worms: Piwi Related Gene 1 (PRG-1), PRG-2, and Endogenous-RNAi deficient Argonaute 1 (ERGO-1). PRG-1 is the predominant piRNA Argonaute, while ERGO-1 is the female germline primary endo-siRNA Argonaute. The AGO clade includes the miRNA Argonautes ALG-1/2, the male germline primary endo-siRNA Argonautes ALG-3/4, and the primary exo-RNAi Argonaute RDE-1. The WAGO clade includes 17 worm-specific siRNA Argonautes, 12 of which mediate gene silencing and one that promotes gene expression (CSR-1) [199].

Argonautes from all three clades have a common structure: a small N-terminal domain, a PAZ domain that binds small RNA 3’ ends, a MID domain that coordinates small RNA 5’ ends together with the PIWI domain, and a C-terminal PIWI domain that harbors an endonuclease active site responsible for slicing target RNA [200].

Exogenous RNA interference in *C. elegans*

While exogenous antisense RNA or sense RNA can both repress gene expression [201, 202], dsRNA induces a much more potent silencing effect in *C. elegans* [203]. Exogenously supplied dsRNA is able to spread from cell to cell after worms are fed, injected, or soaked in dsRNA [203-205]. The ready uptake and spreading of RNAi in *C. elegans* makes it possible to perform reverse genetic screens by feeding bacterial clones that express gene-specific dsRNA [206].

Long dsRNA is bound by RDE-4 and processed into 21-23nt duplexes by Dicer homolog DCR-1, the same protein that cleaves miRNA precursor duplexes [2, 111, 207]. The resulting primary siRNA duplexes are loaded into RDE-1, the primary siRNA Argonaute required for exo-RNAi [208, 209]. RDE-1 cleavage removes the passenger strand, leaving the siRNA guide strand free to bind complementary targets (Figure 1.5) [210]. The RDE-4/DCR-1/RDE-1 complex is conserved in humans and flies; *Drosophila* R2d2 (dsRNA binding domain x 2 associated with Dicer 2) associates with Dcr-2 to load siRNA duplexes in Ago2 [211].

Amplification of RNAi contributes to robust silencing and produces nuclear siRNAs

Target RNA binding by RDE-1/siRNA RISC triggers the amplification of siRNA signal by RNA dependent RNA polymerases (RDRPs) RRF-1 and EGO-1 [212, 213]. The RNA target is used as a template, but the primary siRNA is not used as a primer [214]. siRNA amplification is required for effective gene silencing, as *rrf-1* mutants are RNAi defective (Rde) in the soma and *ego-1* mutants are Rde in the germline, meaining that these mutants fail to silence RNAi target genes. Amplified secondary siRNAs are

22nt long and begin with a G (22G RNAs) [214]. 22G secondary siRNAs are loaded into the 12 worm specific Argonautes (WAGOs) that mediate target silencing in the cytoplasm or the nucleus [197].

Three siRNA amplifaction centers have been identified in germ cells: (1) perinuclear germline granules at nuclear pores (P-granules), (2) mutator foci directly adjacent to P-granules, and (3) cytoplasmic granules nucleated by RNAi Spreading Defective-2 (RSD-2) and RSD-6 [215]. P-granules are the primary sites of RNA export from germline nuclei [216]. siRNA and piRNA Argonautes bind their targets at P-granules, triggering siRNA amplification at adjacent mutator foci. Mutator foci are named after their constituent proteins. Loss of siRNA amplification in mutator *(mut)* class mutants increases genome mutation rate associated with transoposon activity, producing the “Mutator” phenotype [217]. *rsd-2* and *rsd-6* are named for their inability to support intercellular spreading of RNAi, because germ cells that receive transported siRNAs cannot produce amplified 22G siRNAs [218].

Nuclear Argonautes mediate transcriptional gene silencing

Hereditary RNAi Defective 1 (HRDE-1) and Nuclear RNAi Defective 3 (NRDE-3) are WAGOs that bind 22G secondary siRNAs and translocate to the nucleus, where they mediate transcriptional gene silencing [5, 219]. NRDE-3 is expressed in the soma and mediates the downstream effects of exogenous siRNAs or inherited siRNAs, while HRDE-1 is expressed in the germline and mediates the multigenerational inheritance of 22G siRNAs. HRDE-1 and NRDE-3 Argonautes do not have endonuclease active site D-E-D-(D/H) catalytic tetrads that coordinate magnesium; hence they cannot cleave

siRNA targets in the manner of human or fly Argonautes [7]. Instead, they interrupt RNA Pol II elongation via Nuclear RNAi Defective 2 (NRDE-2), bind chromatin via NRDE-1 and NRDE-4, and guide the deposition of H3K9me3 by histone methyltransferases SET-25 and SET-32 [5, 219-224]. Furthermore, SET-25 has an H3K9me3 reader domain that potentially reinforces heterochromatin maintenance at nuclear RNAi target sites [189]. Downstream of nuclear RNAi, chromatin binding proteins such as Heterochromatin Protein 1 homolog HPL-2 silence target loci through unresolved mechanisms [223]. Altogether, the HRDE/NRDE nuclear RNAi pathway promotes a repressive heterochromatin state on target genes.

Nuclear Argonautes mediate RNAi inheritance and promote fertility

HRDE-1/siRNA complexes are necessary and sufficient to transmit RNAi-induced epigenetic silencing across generations [224]. Loss of germline nuclear RNAi leads to progressive sterility over multiple generations, resulting in a “germline mortality” (Mrt) phenotype characterized by loss of both sperm and oocytes, high incidence of males, and changes in oocyte chromosome number due to synapsis or segregation defects [5, 225]. Loss of HRDE-1 or NRDE-2 causes germline mortality at elevated temperature, while loss of NRDE-1 or NRDE-4 causes germline mortality at all temperatures [5].

It remains unclear why nuclear RNAi is required for germline immortality, but emerging evidence is converging on chromatin regulation. The nuclear RNAi pathway is required to silence retrotransposons and place H3K9me3 heterochromatin marks at endogenous siRNA targets [226]. Furthermore, certain mutants deficient in nuclear

RNAi also lose proper regulation of spermatogenesis genes, similar to *spr-5* histone demethylase mutants [173].

RNAi spreading defective-2 (*rsd-2*) and *rsd-6* mutants are deficient in 22G siRNA amplification, and are thus defective in HRDE-1/22G nuclear RNAi [227]. At elevated temperature (25ºC) *rsd-2/6* mutants exhibit progressive germline mortality, upregulation of spermatogenesis genes, and loss of small RNAs targeting those genes [218]. Altogether, transposon upregulation and inappropriate expression of germline genes may lead to progressive germline mortality in nuclear RNAi mutants.

In Chapter 3, we demonstrate that MORC-1 functions in the NRDE-3 somatic nuclear RNAi pathway and the HRDE-1 RNAi inheritance pathway, and we show that *morc-1* mutants are germline mortal.

26G endogenous siRNAs trigger siRNAs that function in two nuclear RNAi pathways

Deep sequencing revealed two major classes of endogenous siRNAs produced in *C. elegans* germline: the 22G RNAs described above, and a second group of RNAs 26nt long with a 5' G (26G RNAs) [89, 214]. The 26G RNAs target protein coding genes, as well as pseudogenes and long noncoding RNAs. In general, 26G RNAs silence expression from their own host transcripts [228]. ERGO-1 Argonaute associated 26G RNAs are produced in maternal germline, and their targets are depleted in germline factors; they may be more important for regulating larval development [228]. ALG-3/4 Argonaute associated 26G RNAs are produced in the male germline, and their targets are enriched for germline transcripts. Accordingly, mutants deficient in male 26G RNAs exhibit temperature sensitive sterility resulting from defective spermatogenesis

[229, 230]. While ERGO-1 26G siRNAs trigger 22G RNAs that feed into the HRDE-1/NRDE-3/WAGO silencing pathways, only a fraction of ALG-3/4 siRNA targets are repressed [5, 231]. Most ALG-3/4 26G siRNAs trigger 22G RNAs that act in the CSR-1 pathway, which supports the continued expression of germline targets [231].

26G endo-siRNAs biogenesis

The genetic requirements for 26G RNA expression are known, but the details of template selection and precursor processing remain unsolved. Spliced mRNA transcripts are bound by RRF-3, which is the RDRP that synthesizes 26G RNAs. RDE-4 binds the dsRNA precursor, which is cleaved by DCR-1 into primary siRNAs [228]. Dicer related helicase-3 (DRH-3) and ERI-1b nuclease are also required for 26G RNA biogenesis, but their mode of action is unsolved [232, 233]. These small RNAs are loaded into ERGO-1 or ALG-3/4 Argonautes, which trigger secondary siRNA amplification by RRF-1 and EGO-1 upon target binding.

Secondary siRNA amplification triggered by 26G RNAs occurs at mutator foci and in RSD-2/6 protein complexes, similar to exogenous RNAi amplification. 22G secondary siRNAs are loaded onto the WAGOs including the nuclear Argonautes, HRDE-1 in the germline and NRDE-3 in the soma.

C. elegans piRNAs trigger secondary siRNAs that function in the nuclear RNAi pathway

C. elegans piRNAs are generated from short capped RNA Pol II transcripts in the germline and processed into 21nt small RNAs that begin with a 5’ U (21U RNAs) [234]. Loaded in the Piwi-Related-Gene-1 (PRG-1) Argonaute, 21U RNAs recognize targets

with imperfect base complementarity and trigger secondary siRNA amplification by EGO-1 and RRF-1 (Figure 1.6) [235, 236]. The resulting siRNAs are loaded into the WAGO clade Argonautes to silence targets [197]. Similar to exo-RNAi, piRNA-triggered 22G RNAs are loaded into HRDE-1 to trigger heritable gene silencing [224]. A stably silenced allele can trigger the production of additional HRDE-1-dependent siRNAs and silence an active allele in trans [237]. Thus, HRDE-1/22G RNA complexes serve as epigenetic agents that mediate the inheritance of gene silencing and the paramutation of active alleles into super-silencing alleles. Paramutation is “an allele-dependent transfer of epigenetic information, which results in the heritable silencing of one allele by another” [238].

Based on their diversity, their ability to bind a wide range of targets, and their role in heritably silencing transposons and transgenes, 21U RNAs are proposed to serve as the epigenetic immune system of *C. elegans* [224]. In other words, piRNAs and the HRDE-1 nuclear RNAi pathway silence “non-self” genetic elements in the germline.

The CSR-1 nuclear Argonaute promotes germline gene expression

The CSR-1 Argonaute / 22G RNA complex promotes germline gene expression, guides centromere placement, and mediates proper segregation of mitotic chromosomes in embryos [239]. Importantly, the CSR-1 RNAi pathway serves as the counterpart to the piRNA/HRDE-1 “non-self” silencing mechanism; CSR-1 protects endogenous “self” gene expression in the germline and guides centromere placement outside of protected regions [199, 240]. Loss of either pathway leads to early embryonic lethality or progressive germline mortality [239]. Thus, balance between silencing and

activating siRNA pathways must be achieved to maintain the immortal germline. The same is true for the balance between H3K4 versus H3K9 methylation, or H3K27 versus H3K36 methylation [181, 241].

CSR-1-associated 22G RNAs are transcribed by EGO-1 in germline P-granules, located at the nuclear pore [239]. Positioning at the nuclear pore allows CSR-1 and PRG-1 to scan the transcriptome for targets as nascent RNAs are exported [239]. Upon target binding, CSR-1-associated 22G RNAs trigger the production of additional 22G RNAs by EGO-1. Hence, CSR-1-associated 22G RNAs are generally antisense to spliced exons [197, 199]. CSR-1/22G RNA complexes also bind pre-mRNAs in the nucleus, where CSR-1 tethering promotes gene expression and deposition of H3K4me2/3 [240]. Thus, CSR-1/22G RNA targeting creates a self-reinforcing loop that protects endogenous gene expression. Because CSR-1/22G RNA complexes are inherited across generations, they transmit an epigenetic memory of germline gene expression across generations [199, 240].

Mutations in *csr-1* or *ego-1* cause loss of germline H3K9me2 foci on unpaired X chromosomes and elevated H3K9me2 levels on paired autosomes [242, 243]. Thus, loss of the “self” nuclear RNAi pathway causes global dysregulation of germline histone methylation. In embryos, CSR-1 associates with mitotic chromosomes; chromatin association is guided by 22G RNAs [239]. CSR-1 is required for the correct distribution of centromeric H3 variant CENP-A in *C. elegans* holocentric chromosomes [244]. Normally, embryonic CENP-A is excluded from genes that were expressed in parental germline and enriched in adjacent genes that are not expressed in germline [245]. Consistent with its role in transmitting the epigenetic memory of parental germline gene

expression, *csr-1* mutants display global depletion of CENP-A loading in "nonexpressed" regions and inappropriate CENP-A loading in "expressed" regions [246]. Mis-specification of centromere placement may contribute to the disorganization of kinetochore proteins at metaphase, chromosome bridging at anaphase, and subsequent embryonic lethality in *csr-1* mutants [239].

1.6 Microrchidia proteins are conserved chromatin organization factors

It is clear that HRDE-1 and CSR-1 nuclear RNAi pathways regulate gene expression at the chromatin level, and that these effector functions are required for germline maintenance. Much less is known about how chromatin organization factors mediate transcriptional or transgenerational effects downstream of small RNAs.

Microrchidia (MORC) proteins are conserved from plants to humans, and their role in chromatin regulation is just beginning to emerge. The "*Microrchidia*" gene is named after a mouse mutant with small testes and sterility associated with failure of homologous chromosome pairing during prophase I [247, 248]. Germline dysfunction in *Morc-1(-/-)* male mice may result from loss of transcriptional silencing and DNA methylation on retrotransposons [249]. In *Arabidopsis*, *AtMorc1* and *AtMorc6* are required to silence transposons located in pericentromeric heterochromatin. Interestingly, *AtMorc1/6* mutants also display defects in heterochromatin compaction and localization at the nuclear periphery, without changes in DNA methylation or H3K9me2 [250]. Hence, plant MORCs were proposed to mediate ATP-dependent chromatin superstructure changes. There is a single MORC homolog in worms, MORC-

1, which has been implicated in repetitive transgene silencing [250, 251]. In Chapter 3 we show that MORC-1 is a chromatin binding protein that functions in transcriptional gene silencing downstream of HRDE-1 and NRDE-3 nuclear RNAi.

MORC protein structure

MORC proteins share a conserved N-terminal GHKL+S5 ATPase module followed by coiled coils and variable C-terminal domains (Figure 1.7) [252]. The GHKL+S5 module is named after DNA Gyrase, HSP90, Histidine Kinase, MutL and is also found in DNA Topoisomerase. The GHKL+S5 modules of MutL and Topoisomerase mediate ATP-driven changes in protein complex organization and the movement of DNA strands [252]. Humans have four MORC proteins that function in transcriptional repression or DNA damage repair [253]. In addition to the GHKL+S5 ATPase and coiled coil domains, mammalian MORCs have cysteine-tryptophan (CW) zinc fingers related to plant homeodomains that bind H3K4me2/3 [254]. Furthermore, the CW zinc finger of human Lysine-Specific Histone Demethylase 2 (LSD2) coordinates the flavin adenine dinucleotide (FAD) cofactor required for H3K4me2 demethylation [255]. In general, MORCs are predicted to bind chromatin through the CW zinc finger module, dimerize or associate with other proteins via coiled coils, and drive changes in chromatin structure through the GHKL+S5 ATPase module [253].

MORC-1 is the sole MORC homolog in *C. elegans*. It contains an N-terminal GHKL+S5 ATPase, two coiled coils, a divergent CW zinc finger, and a C-terminal nuclear localization signal. Based on its structural domains, we predict that MORC-1 may bind to methylated histones and mediate chromatin organization. Alternatively,

MORC-1 may promote histone demethylase activity by coordinating FAD cofactor through the CW domain. In Chapter 4, we present evidence that *morc-1* genetically interacts with histone methyltransferases and demethylases.

Divergent MORCs regulate chromatin organization

In mice, Structural Maintenance of Chromosomes Hinge Domain 1 (SMCHD1) has a GHKL+S5 ATPase and SMC hinge required for heterochromatin organization in X-inactivation [256]. In *Arabidopsis*, Defective in Meristem Silencing 3 (DMS3) is an SMC hinge protein that lacks an ATPase module, while AtMORC6 lacks a chromatin binding domain (no CW zinc finger). In the *Arabidopsis* small RNA-directed DNA methylation pathway, AtMORC6 can associate with the DMS3 SMC hinge, providing an ATPase module to power chromatin reorganization [257].

Human MORC3 is a molecular clamp that nucleates protein domains on chromatin

MORC proteins form dimers that act as molecular clamps, nucleating protein complexes on chromatin. For example, human MORC3 recruits p53 to promyelocytic leukemia (PML) nuclear bodies to promote cellular senescence [258]. MORC3 associates with chromatin via its CW zinc finger, while the GHKL+S5 and coiled coils mediate dimerization. Upon ATP binding, MORC3 dimers form nuclear foci [259]. Sumoylation of MORC3 coiled coil regions facilitates recruitment to PML nuclear bodies. ATP hydrolysis frees MORC3 dimers from MORC3 nuclear foci, redistributing to nucleoplasm and chromatin.

When tethered to a promoter by GAL4, MORC3 confers transcriptional repression of luciferase reporters in HEK 293T cells [260]. While it might involve p53, the mechanism of MORC3 transcriptional repression has not been determined.

MORC localization is regulated by DNA damage or pathogen stress

MORC function can be induced by cell signaling pathways. For example, human MORC2 associates with chromatin in response to phosphorylation by DNA damage respones kinases [261]. Similar to H3K4 demethylase SPR-5 in *C. elegans*, human MORC2 localizes at sites of double strand breaks to relax chromatin and promote double strand break repair in HeLa cells [261, 262]. Accordingly, *MORC2* depletion renders cells hypersensitive to DNA damage by ionizing radiation. AtMORC1 mediates resistance to viral and bacterial pathogens in plants, where it shuttles from cytoplasm to nucleus in response to immune receptor activation [263].

MORC proteins mediate gene silencing and chromatin organization in plants

In plants, 24nt siRNAs are loaded into AGO4 to direct heterochromatin formation at pericentromeric repeats and repetitive transposable elements (reviewed in [264]). AGO4-loaded-siRNAs target nascent long noncoding RNAs produced by Pol V, co-transcriptionally targeting the RNA-directed DNA methylation (RdDM) complex to place methyl modifications on cytosine nucleotides [265]. siRNA targeting of Pol V lncRNAs also directs H3K27me1 and H3K9me2 modification [266]. Altogether, the RdDM pathway maintains transcriptional gene silencing, organizing pericentromeric repeats and transposable elements into discrete heterochromatin regions at the nuclear

periphery (chromocenters) [250, 267].

Three genetic screens independently isolated mutations in Arabidopsis *morc* genes that compromise transgene and heterochromatin silencing. Moissiard *et al.* isolated mutations in the *AtMorc1* and *AtMorc6* genes that cause heterochromatin transgene desilencing without loss of cytosine methylation or H3K9me2 [250]. Transposable elements are de-repressed, while H3K9me2 chromocenters are decompacted and delocalized from the nuclear periphery. Two other groups independently identified mutations in *Atmorc6* and reported different results, perhaps due to the molecular nature of each mutation. Brabbs *et al.* reported that a mutation in *AtMorc6* results in mosaic desilencing of a GFP transgene: cells that lose silencing also lose DNA methylation [268]. Lorkovic *et al.* reported that DNA methylation and H3K27me were reduced, while histone H3 and H4 acetylation were increased at de-silenced loci in *AtMorc6* mutants [257, 269]. While it is clear that *Arabidopsis* MORCs are required for transcriptional repression and heterochromatin compaction, how MORCs function in this pathway remains unclear. Do they promote RNA Pol V recruitment and DNA methylation in the AGO4 siRNA pathway [268, 270]? Do they mediate histone modification [257]? Or do they function downstream/parallel to these modifications in the regulation of chromatin superstructure [250]?

Role of MORC-1 in *C. elegans*

morc mutants are defective in transgene silencing, transposon silencing, germline DNA and histone methylation, and chromatin organization in various species. These are all fundamental processes regulated by small RNAs. Hence, we propose that

MORC proteins form a conserved link between nuclear RNAi, chromatin regulation, and germline maintenance. The role of *C. elegans* MORC-1 in these processes will be explored in Chapter 3.

1.7 Summary

Overall, PUF proteins and miRNAs bind 3'UTRs through drastically different mechanisms, yet they activate a highly overlapping set of regulatory mechanisms in post-transcriptional gene silencing. PUF proteins are conserved in *S. cerevisiae*, while miRNAs are not; miRNAs may have co-opted ancient PUF regulatory mechanisms that already existed. Through sheer abundance and sequence diversity, miRNAs provide the ability to confer PUF-like regulation at a much wider array of targets. In multiple species, PUF proteins are able to access target sites in stable secondary structures, while miRNAs cannot do so without assistance from RBPs. Perhaps collaborative regulation between PUFs and miRNAs facilitates regulation of the most structurally- and sequence-diverse set of 3'UTR targets. In Chapter 2, I present a study that characterizes coordinated binding of PUF-9 and miRNA RISC in *C. elegans*.

Among higher eukaryotes, germ cells are the only lineage that must be completely totipotent and indefinitely replenished at every generation (with the exception of certain plants and animals that reproduce via vegetative cloning). Together, RNA binding proteins, small RNAs, histone modifying enzymes, and chromatin binding proteins control germline gene expression patterns required for germline function. While PUF proteins and miRNAs collaborate to store, transmit,

activate, and degrade gene products from maternal germline to primordial germ cells in the embryo, piRNAs and siRNAs collaborate with the chromatin regulation machinery to either transmit or reset gene expression states in each generation. In Chapter 3, I present a study that characterizes the role of *C. elegans* MORC-1 downstream of siRNA function.

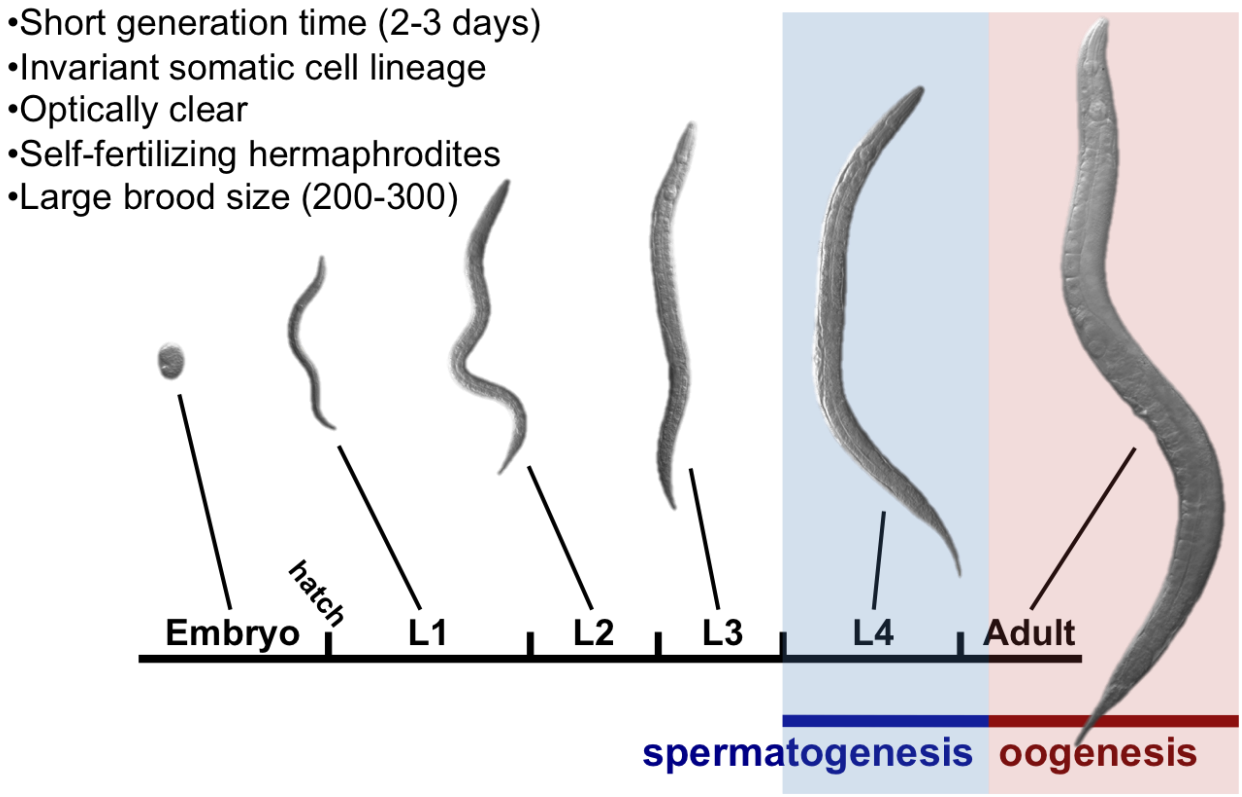

Figure 1.1 *C. elegans* life cycle.
C. elegans are self-fertilizing hermaphrodites with a short generational time, progressing through four larval stages to become reproductive adults in two to three days after hatching. Image courtesy of Aric Daul.

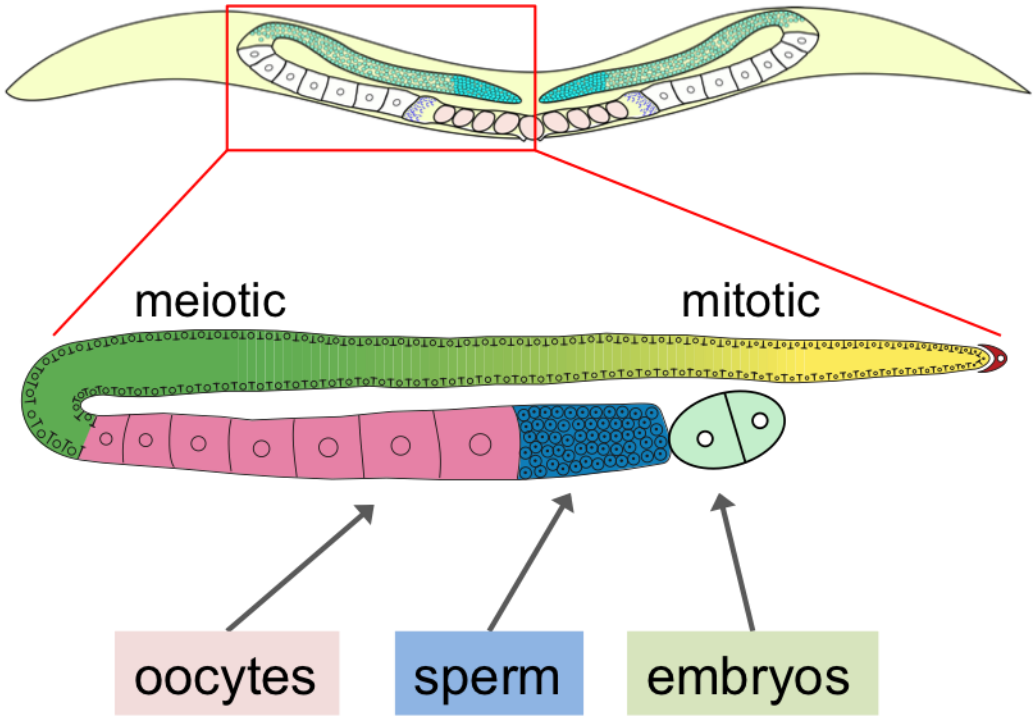

Figure 1.2 *C. elegans* adult germline.
The *C. elegans* gonad is organized as a tube. The somatic distal tip cell (red) promotes germline stem cell mitosis in the distal region. Germ cells travel through this tube and enter meiosis, producing sperm at the L4 stage and oocytes during adulthood. Illustration credit: Meng Wang.

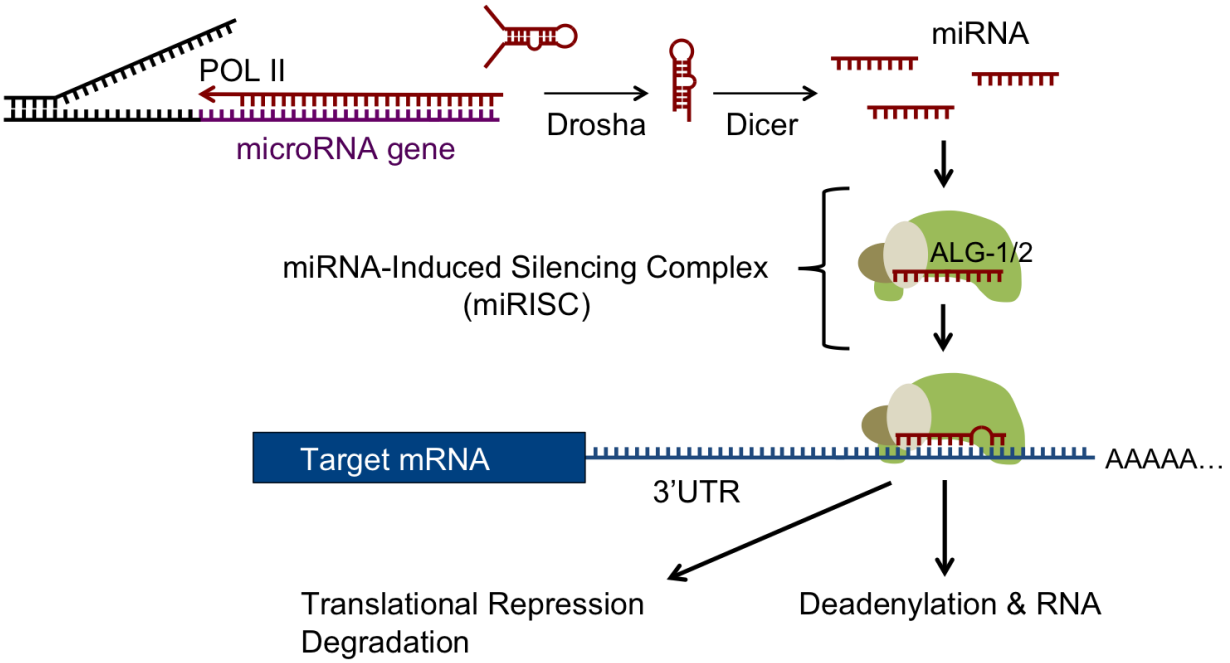

Figure 1.3 Basic schematic of the canonical microRNA pathway.
Primary miRNA transcripts are transcribed by RNA Polymerase II. These transcripts harbor hairpins that are serially cleaved by dsRNA nucleaes Drosha in the nucleus and Dicer in the cytoplasm. ~22nt mature miRNAs are loaded into the ALG-1 or ALG-2 Argonaute protein, forming the core of the miRNA-induced silencing complex. miRISC silences targets that are partially complementary to the bound miRNA.

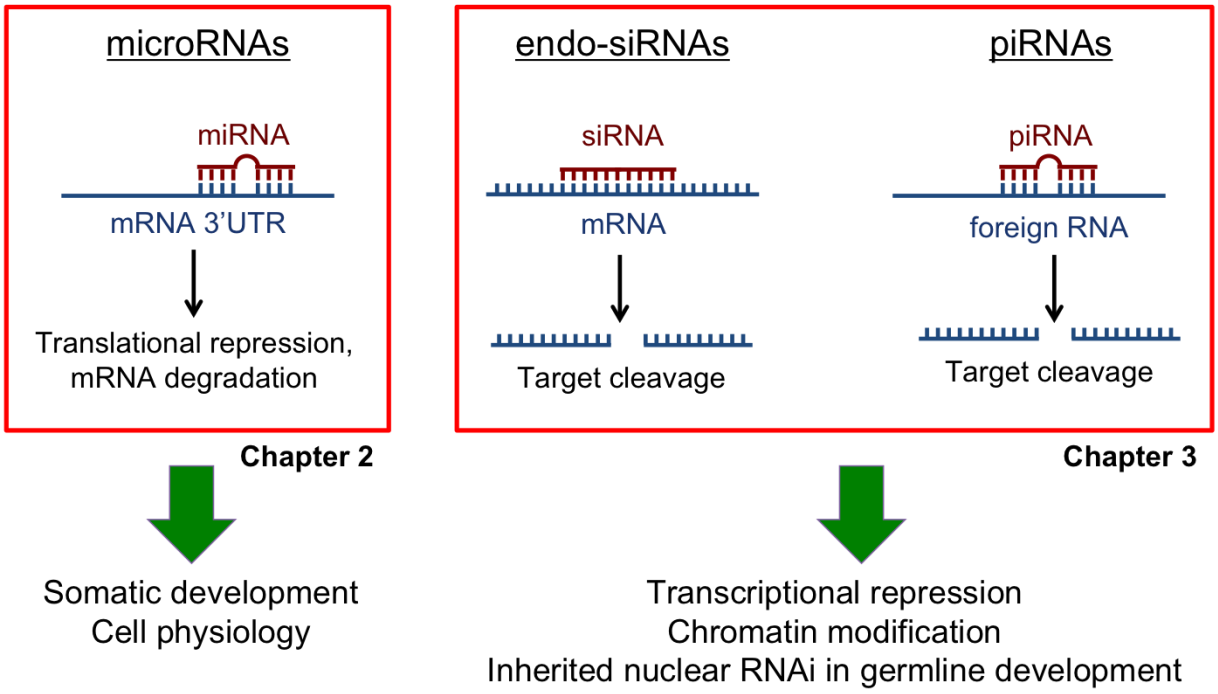

Figure 1.4 Three general classes of small RNAs in *C. elegans*.
MicroRNAs regulate many aspects of somatic development and cell physiology, while endogenous siRNAs and PIWI-interacting RNAs regulate germline gene expression. Each class of small RNAs has unique modes of biogenesis and target repression. In general, miRNAs mediate post-transcriptional repression by blocking translation or triggering mRNA deadenylation and decay in the cytoplasm. Endo-siRNAs and piRNAs trigger target RNA cleavage in the cytoplasm and guide the production of secondary siRNAs that mediate transcriptional gene silencing in the nucleus.

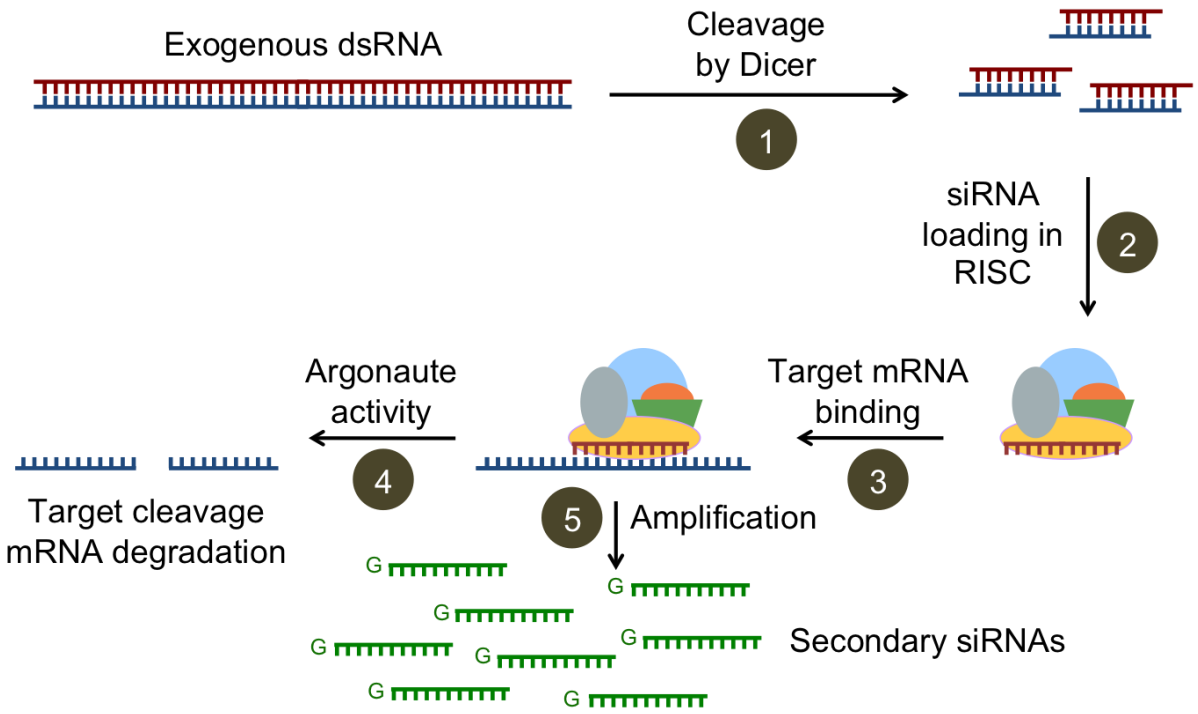

Figure 1.5 Exogenous siRNA pathway in *C. elegans*.
Double stranded RNA is cleaved by Dicer into siRNAs (1), loaded into RNA induced silencing complexes (2), recognize mRNA targets by base complementarity (3), and trigger target cleavage by Argonaute protein nuclease activity (4). Target silencing also triggers de-novo synthesis of secondary siRNAs by RNA-dependend RNA polymerases, using target mRNA as a template (5).

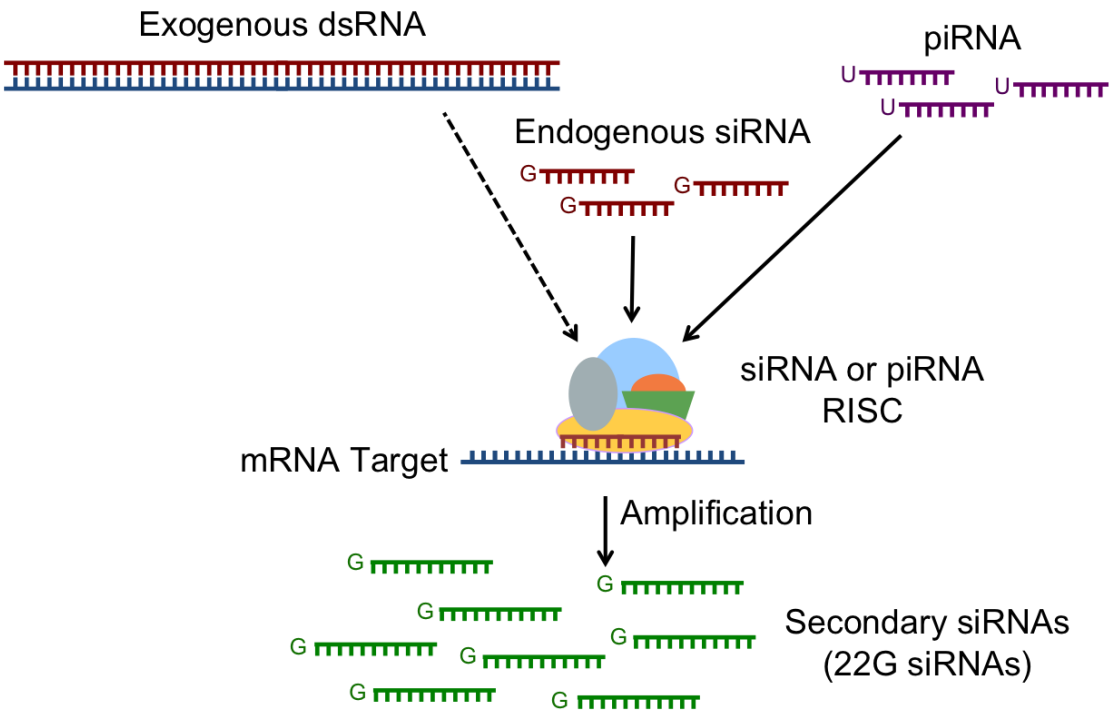

Figure 1.6 Secondary siRNAs are downstream of diverse small RNA triggers.
Exogenous dsRNAs, endogenous siRNAs, and PIWI-interacting RNAs are loaded into diverse RNA induced silencing complexes. mRNA target silencing by small RNAs also triggers *de-novo* synthesis of secondary siRNAs by RNA-dependent RNA polymerases.

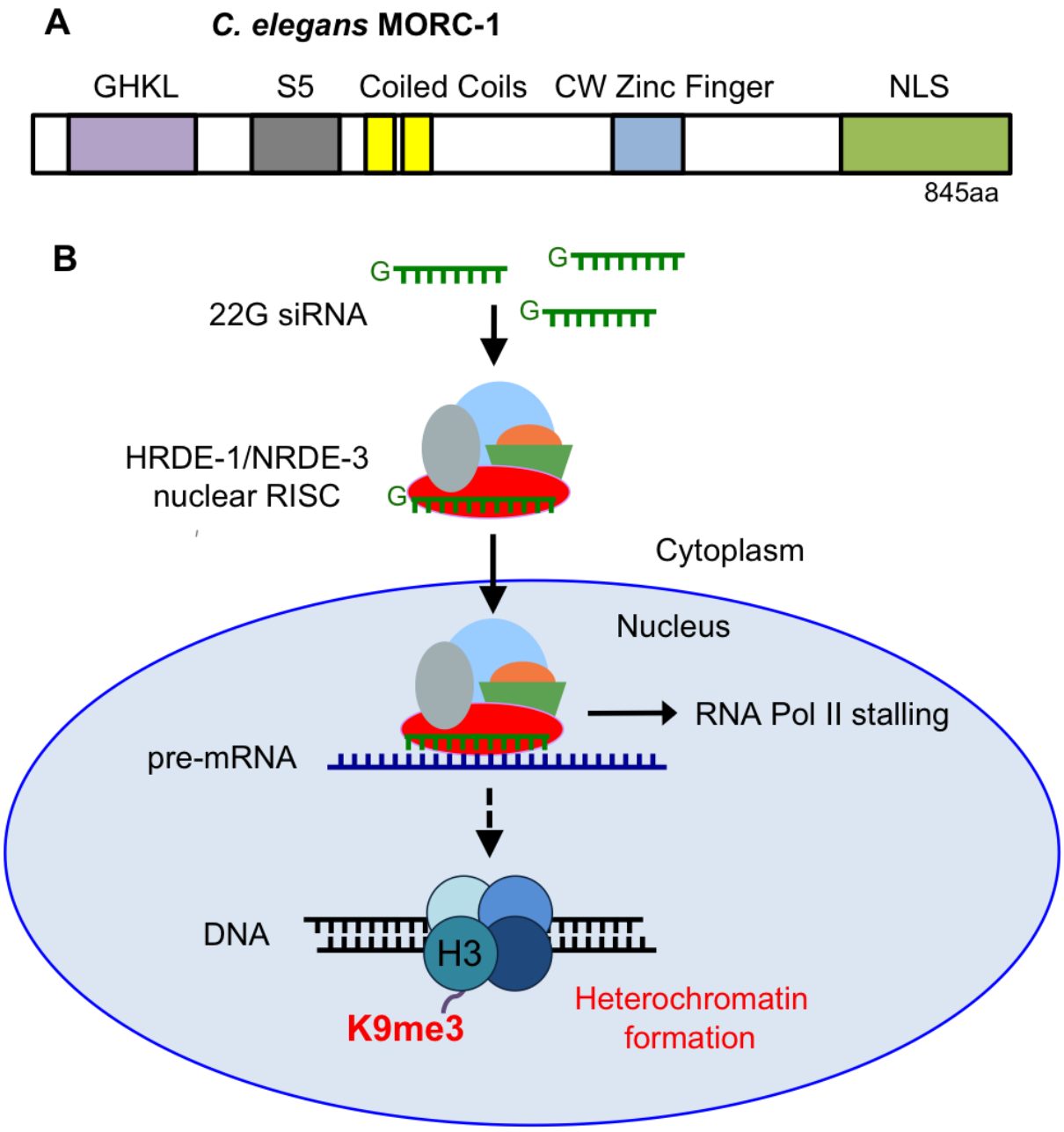

Figure 1.7 Models: MORC-1 protein and the nuclear RNAi pathway.
(A) *C. elegans* MORC-1 protein domains are indicated. GHKL+S5 comprises the ATPase domain. **(B)** *C. elegans* nuclear RNAi pathway. 22G secondary siRNAs are loaded into nuclear Argonautes, which translocate to the nucleus, inhibit Pol II transcription, and mediate heterochromatin formation.

CHAPTER II - Regulation of shared targets by PUF-9 and miRNAs

2.1 Abstract

Pumilio/*fem-3* binding factor (PUF) proteins are conserved from yeast to humans, where they bind PUF recognition elements (PREs) in mRNA 3' untranslated regions (UTRs) to direct translational repression, transcript decay, and mRNA localization. Recent studies have shown that PUF proteins mediate more complex, poorly understood mechanisms of 3'UTR regulation. In *C. elegans*, PUF proteins can activate translation in olfactory neurons and the germline. In humans, PUF binding may disrupt 3'UTR secondary structures to expose microRNA (miRNA) binding sites. *C. elegans puf-9* genetically interacts with the *let-7* miRNA to regulate epidermal stem cell differentiation and vulval integrity at the larval-to-adult transition, partially through repression of the only known PUF-9 target 3'UTR: the *let-7* target *hbl-1*. However, the full extent of *puf-9*/miRNA interaction has not been explored. In this study we use CLIP-seq to globally identify PUF-9 and miRNA binding sites *in vivo*. Global analyses reveal that PUF-9 binding sites are enriched in 3'UTR regions with secondary structure, adjacent to miRNA binding sites. We validate PUF-9 binding of miRNA targets bearing PREs by endogenous IP. We show that PUF-9 binds *lin-41* mRNA and represses a *lin-41*-3'UTR GFP reporter in the uterus. Furthermore, *lin-41* reduction of function

suppresses *puf-9* loss of function defects in the regulation of vulval integrity. Altogether, our data are consistent with a model where PUF-9 and miRNAs bind to adjacent sites in structured 3'UTRs to co-regulate shared targets.

2.2 Introduction

The highly conserved PUF (Pumilio/FBF) family of RNA-binding proteins plays diverse roles in animal development including the regulation of stem cell maintenance, proliferation, and differentiation [14, 271-273]. PUF proteins share a widely conserved Pumilio-Homology-Domain (PUM-HD) consisting of eight tri-α-helical repeats that together specifically recognize 8-12 nucleotides defining a PUF response element (PRE) [36]. PUF proteins mediate post-transcriptional regulation of their mRNA substrates by controlling target localization, translation, and stability. Canonically, PUF proteins function to repress gene expression through interactions with target 3' untranslated regions (3'UTRs) and recruitment of the CCR4/NOT deadenylase complex to trigger mRNA deadenylation and decay [47, 48]. PUFs also inhibit cap-dependent translation initiation [52]. In addition to the repressive roles for PUF proteins in gene expression, there is also support for PUF proteins acting to promote gene expression [14, 21].

C. elegans have ten PUF homologs that cluster into five distinct groups, based on conservation of the PUM-HD RNA binding domain [12]. Because PUM-HD structure dictates target specificity, each group of PUF proteins recognizes a related but distinct RNA response element, and thus different sets of mRNA targets. The FBF1/2 family is

mainly expressed in germline stem cells, where it promotes self-renewal in response to notch signaling [11]. The PUF-3/11 and PUF-5/6/7 families control different aspects of oocyte development, while PUF-12 is a member of the divergent yeast Puf6p family that binds ribosomal RNAs in the nucleus [57]. Out of all the *C. elegans* PUFs, only PUF-8/9 maintain the conserved PUM-HD structure and predicted binding specificity of yeast Puf3p, fly Pumilio, and human PUM1/2. While PUF-8 promotes proliferation of germline stem cells and their subsequent entry into meiosis [272, 273], PUF-9 functions in the soma [59]. The target repertoire, physiological function, and molecular mechanisms of PUF-9 have yet to be characterized, even though it is the canonical PUF in *C. elegans* embryogenesis, larval development, and adult soma.

Recent studies have begun to reveal the interaction between PUF proteins and the microRNA pathway for the regulation of common target mRNAs. MicroRNAs (miRNAs) are small, non-coding RNAs conserved across metazoans that regulate gene expression to control diverse biological processes including cell proliferation, organogenesis, and metabolic control [84-88]. Together with Argonaute proteins and other cofactors of the miRNA-induced silencing complex (miRISC), miRNAs bind mRNA targets through base-pairing interactions, typically at target 3'UTRs, to promote translational repression and/or mRNA degradation [147-149, 274-278]. For example, miRISC cofactor GW182 can displace PABP from polyA tails, recruit CCR4/NOT deadenylase, and localize targets to P-bodies where mRNAs are decapped and degraded [132, 277]. In addition, CCR4/NOT can directly repress translation initiation by blocking ribosome scanning of the 5'UTR via recruitment of eIF4A [278].

Among the best studied miRNAs in metazoans is the *let-7* family, which acts to regulate stem cell function [85]. In mammals, *let-7* accumulation contributes to the age-related decline of neural stem cell self-renewal, presents a barrier to induced pluripotent stem cell programming, and limits the proliferation and tumorigenicity of breast cancer cells, highlighting the importance of *let-7* family miRNAs in development and disease [92, 279, 280].

In *C. elegans*, *let-7* is a key component of the heterochronic pathway. The heterochronic gene network controls the precisely defined timing of cell division and differentiation in *C. elegans*, specifying the developmental lineage of all 959 cells in the adult hermaphrodite soma from 558 cells in newly hatched larvae (reviewed in [281]). In general, miRNA targets *lin-14*, *lin-28*, *hbl-1*, and *lin-41* regulate developmental expression programs from the first larval stage (L1) through adulthood. Cell lineage (Lin) mutants skip or re-iterate stage-specific gene expression programs, leading to a departure from the defined cell lineage of wild type *C. elegans*. For example, *lin-14* promotes L1 gene expression, whereas *lin-14* loss of function causes “precocious” expression of L2 cell fates and skips over the L1-to-L2 molt. *lin-4* downregulates *lin-14* to promote L2-specific differentiation patterns and prevent re-iteration of L1 cell fates in blast cells of the vulva and the lateral epidermal seam [4]. Thus, “retarded” *lin-4* mutants reiterate L1 expression patterns, undergo extra blast cell divisions, and fail to develop a functional vulva.

let-7 is expressed at the fourth larval (L4) stage, triggering cell cycle exit and differentiation of hypodermal blast cells of the lateral seam, ultimately leading to proper secretion of adult cuticle structures at the larval-to-adult transition through repression of

targets including *lin-41* and *hbl-1* [84, 282, 283]. *let-7* loss of function results in reiteration of L4 fates in seam cells, as well as defects in vulval morphogenesis [84, 284].

Regulation by PUFs and miRNAs is pervasive throughout metazoans, and their coordinated repression of shared targets could be vital for regulation of developmental processes. Human PUFs PUM1/2 bind to the 3'UTRs of the *p27* tumor suppressor and *E2F3* oncogene, enhancing the activity of multiple miRNAs to silence these targets [164, 165]. Computational analyses revealed that miRNA target sites reside in poorly accessible regions of target 3'UTRs near PUF binding sites [166, 167]. Furthermore, faster mRNA decay rates were correlated with closer proximity between PUF binding sites and miRNA binding sites [166]. Together, these studies suggest that PUF proteins promote miRNA target access by reducing local RNA secondary structure.

Previous studies in *C. elegans* suggest that interactions between PUF- and miRISC-mediated post-transcriptional regulatory pathways at specific targets are vital for ensuring the larval-to-adult transition. Loss of *puf-9*, but not any of the nine other *puf* genes encoded by the *C. elegans* genome, enhances *let-7(n2853)* hypomorphic defects in vulval integrity [59]. Furthermore, PUF-9 binds and represses the *hbl-1* 3'UTR, contributing to faithful terminal differentiation of seam cells and the secretion of adult alae [59]. Thus, PUF-9 collaborates with the *let-7* miRNA pathway to silence at least one common target (*hbl-1*).

While post-transcriptional gene regulation by PUF proteins and miRNAs shares a number of features, including binding to 3'UTRs and target repression by deadenylation, a comprehensive, genome-wide analysis of the interactions between these two

mechanisms has yet to be done. To further elucidate how PUF proteins interact with the miRNA pathway, we sought to determine whether coregulation of gene expression by PUF-9- and miRNAs is a general feature of miRNA target genes.

In this study, we use CLIP-seq (crosslinking immunoprecipitation and high throughput sequencing) to globally identify PUF-9 and miRISC binding sites. Our analyses reveal that PUF-9 binding sites are enriched in 3'UTR regions with secondary structure, adjacent to miRNA binding sites. In addition, miRISC binding sites reside in areas of higher predicted RNA secondary structure than upstream or downstream regions. We validate binding of miRNA targets bearing PUF-9 binding sites and motifs by endogenous PUF-9 IP. PUF-9 binds a 27nt spacer between two *let-7* target sites in the *lin-41*-3'UTR. We show that *lin-41* genetically interacts with *puf-9* in the regulation of vulval integrity, and *puf-9* represses a *lin-41*-3'UTR GFP reporter. Altogether, our data are consistent with a model where PUF-9 and miRISC bind to adjacent sites in structured 3'UTRs to co-regulate shared targets.

2.3 Results

PUF-9 physically associates with miRNA Argonaute ALG-1

Given that *puf-9* genetically interacts with *let-7* and binds *let-7* target *hbl-1* to regulate seam cell differentiation [59], we hypothesized that PUF-9 and miRISC physically associate via shared mRNA targets. To determine whether this interaction occurs *in vivo,* we tested if PUF-9 is present in immunoprecipitations (IPs) of GFP-tagged ALG-1. Using an antibody against endogenous PUF-9, we showed that PUF-9

co-immunoprecipates with GFP-ALG-1 and that this association is abrogated with RNase A treatment (Figure 2.1). In contrast, the association between GFP-ALG-1 and another miRISC component, AIN-1, is RNase-resistant (Figure 2.1; [132]). Our results suggest that PUF-9 associates with miRISC via shared RNA targets. Alternatively, but less likely, a direct PUF-9/miRISC protein association could be stabilized by RNA.

PUF-9 binds target 3'UTRs at canonical PUF recognition elements

PUF-9 associates with *hbl-1* 3'UTR, the only known PUF-9 target, in regions containing *let-7* and PUF recognition elements (PREs) [59]. We also observed predicted PREs in 3'UTRs of mRNAs targeted by *let-7* and other miRNAs (Table 2.1), suggesting that PUF-9 may interact with other miRNA targets. In order to identify directly bound target sites of PUF-9 on a global scale, we generated a transgene expressing PUF-9-GFP that rescues the bursting phenotype of *puf-9(ok1136)* mutants (Figure 2.2, Figure 2.10) and performed crosslinking and immunopurification of PUF-9-GFP in animals from several developmental stages (embryo, L1, and adult) followed by deep sequencing of PUF-9-protected RNA fragments of 20-40nt (CLIP-seq; Figure 2.2C). Altogether we identified 19,504 PUF-9 binding sites (PBSs) on 8,987 genes. Globally, PUF-9 binding was enriched in 3'UTRs (Figure 2.3A), supporting previous characterizations of PUF proteins [47, 66, 285]. Gene ontology (GO) analysis indicates that PUF-9 targets were enriched for functional categories related to growth and development, aging, cytoskeleton, and epidermal development (Figure 2.4A).

We searched 3'UTR PUF-9 binding sites for over-represented sequence motifs using MEME [286] and identified a 5'-UGUA-3' sequence followed by an A/U-rich region

with consensus 5'-HWWW-3' (H=A,C,U and W=A,U; Figure 2.3B). The full eight nucleotide motif forms a PRE similar to those identified for fly Pumilio, yeast Puf3p, and worm PUF-8 but divergent from other worm PUFs [36, 287]. Among the top 20% of PUF-9 binding sites (based on RPM coverage), 45% contain a PRE and another 26% contain just a UGUA sequence (Figure 2.3C), suggesting the presence of a PRE/UGUA promotes strong PUF-9:target interactions. Indeed, read coverage at 3'UTR PUF-9 binding sites with a full PRE or just UGUA was significantly higher than at PUF-9 binding sites with no motif (Welch's two-tailed *t*-tests: $p<10^{-17}$ (PRE) and $p<10^{-3}$ (UGUA); Figure 2.3D). Using conservation scores derived from aligning the *C. elegans* genome to six other nematode genomes, we observed that 3'UTR PUF-9 binding sites with a full PRE were significantly more conserved than sites with no motif (Figure 2.4B), suggesting a functionally conserved role for PUF-9 binding at targets sites with a full PRE motif.

PUF-9 binds 3'UTRs that are also targeted by ALG-1 miRISC

To complement our PUF-9 CLIP-seq data, we also isolated and sequenced RNAs bound by the miRNA Argonaute ALG-1 in embryo, L1, and adult worms. Collectively, we identified 2,952 ALG-1 binding sites on 2,163 genes. We observed that the majority of ALG-1 bound to 3'UTRs and exonic regions as well as mature miRNAs (Figure 2.3A). To determine whether PUF-9 and ALG-1 preferentially bind common target mRNAs, we identified genes with at least one PBS or at least one ALG-1 binding site (ABS) in the 3'UTR. At each stage, 70-84% of mRNAs bound by ALG-1 were also bound by PUF-9 (Figure 2.3E) suggesting extensive co-regulation by PUF-9 and

miRISC. To determine if the number of common targets of PUF-9 and ALG-1 is more than expected by chance, we randomly selected the same number of genes in each gene set from the list of all genes expressed at each stage [288] with the probability of selecting each gene corresponding to its expression level in the dataset. From the set of random PUF-9 and ALG-1 "targets" we calculated the number of shared genes. This process was repeated 100,000 times, and an empirical *p*-value was calculated as (number of times observed more shared genes in random control)/100,000. PUF-9 and ALG-1 co-target more genes at 3'UTRs than expected by chance (Chi-squared test $p<1e-5$). In gravid adults, 60% of PUF-9/ALG-1 co-targeted genes contained a PBS with a full PRE compared to only 40% of genes targeted only by PUF-9 (Figure 2.4C), suggesting that PUF-9/miRNA co-targeting is the most highly enriched at this stage. At embryo and L1 stages, full PRE enrichment was not observed in PUF-9/ALG-1 co-targets compared with targets bound by PUF-9 alone.

The closest PUF-9 and miRISC binding sites overlap or are adjacent to each other on shared 3'UTR targets

Based on the close proximity of predicted PUF-9 and *let-7* target sites on the *hbl-1* 3'UTR, we investigated whether PUF-9 and ALG-1 generally bind in close proximity on common target 3'UTRs. We defined the proximity of PBSs and ABSs as the distance in nucleotides between the midpoints of two binding sites. Interestingly, we observed 73%, 51%, and 78% of 3'UTR ALG-1 binding located within 25nt of a PBS in embryo, L1, and gravid adult animals, suggesting widespread proximal co-binding of PUF-9 and miRISC. Furthermore, when we centered all PBSs on their midpoints and summed

ALG-1 binding RPM surrounding each PBS, we observed strong ALG-1 binding directly overlapping PBSs only at 3'UTRs (Figure 2.3F). This trend was still observed when we limited our analysis to just the closest ABS to each PBS (Figure 2.4D). Finally, we observed an enrichment of PUF response elements in PBSs located within 25nt of an ALG-1 binding site in adult animals only (40% of PBSs ≤25nt versus 21% of PBSs >25nt, Figure 2.3G), supporting the idea that PUF-9 targeting near miRISC binding sites is particularly important in adults. Taken together, our data support a co-regulatory model in which PUF-9 and ALG-1 bind a common set of target mRNAs to orchestrate post-transcriptional regulatory mechanisms.

PUF-9 binds target 3'UTRs at structured regions near miRISC target sites

PUF proteins typically function through recognition of specific nucleotide sequences by the conserved Pumilio homology RNA-binding domain whereby each of the eight PUF repeats binds a single nucleotide base. Recent studies have provided evidence that PUF proteins can bind structured RNAs in which the PRE nucleotides are not initially accessible [289], likely due to the high affinity of PUM-HD for its target motif (Kd=0.5nM-5nM [37]). We identified PREs enriched among our PUF-9 binding sites, and we wondered whether PUF-9 in *C. elegans* could also bind structured RNA. Using the secondary structure prediction software RNAfold [290], we predicted the minimum free energy (MFE, -ΔG in kcal/mol) of all 3'UTR PBSs extended by 15nt in either direction. As a control, we also predicted the minimum free energy of RNA regions of equal length located directly upstream and downstream of each PBS. Strikingly, PBS minimum free energies were significantly lower than their length-matched upstream and

downstream control regions (Welch's two-tailed *t*-test *p*=9.1e-45; Figure 2.5A), suggesting that PUF-9 preferentially binds structured regions in 3'UTRs. Furthermore, the minimum free energy of PBSs with a PRE are lower than PBSs without a PRE, suggesting that both primary sequence and RNA secondary structure contribute to PUF-9 binding at target 3'UTRs. For example, PUF-9 may be able to bind high-affinity PREs within structured RNA regions, but not low affinity binding sites that lack a PRE.

Based on our observation that PBSs overlapping ABSs contain a higher proportion of PREs than PBSs located away from ABSs, we compared the minimum free energy of PBSs located ≤25nt from an ABS with PBSs located >25nt from an ABS. Twenty-five nucleotides were chosen as a threshold to reflect the typical footprint size of an RBP [291]. PBSs overlapping an ABS are significantly more structured compared to PBSs that are away from an ABS (Welch's two-tailed *t*-test *p*=6.6e-4; Figure 2.5B). For example, predicted structures with the lowest minimum free energy show how PREs within PBS1 and PBS2 on the *lin-41* 3'UTR might be part of hairpin structures (Figure 2.5C) and how *let-7* target site LCS1 is capable of forming a stable hairpin with the PRE in PBS1 (Figure 2.5D). It is tempting to speculate that PUF-9 binding at PBS1 prevents formation of the LCS1/PRE hairpin, thus preserving availability of the adjacent *let-7* target site. Additional RNA structure analyses *in vitro* would be required to support or refute this model.

ALG-1 binding sites also reside in more structured regions relative to flanking regions

ALG-1 binding sites reside in regions of higher predicted secondary structure than surrounding sequences (Figure 2.6). The mean free energy predicted for ALG-1

binding sites was lower than upstream or downstream sequences, summed across all target 3'UTRs. However we did not detect a correlation between ALG-1 binding site secondary structure (minimum free energy) and the presence of an adjacent PUF-9 binding site (Figure 2.6). ALG-1 binding sites within 25nt of a PBS were no more structured than ALG-1 binding sites >25nt from a PBS, while both classes of ABS had lower minimum free energy than upstream or downstream regions. Multiple studies report that miRNA seeds with low predicted secondary structure are favored over miRNA seeds that reside in structured regions [66, 292, 293]. Instead of predicting miRNA seed targets and assessing local secondary structure, we took an objective empirical approach; experimentally identified miRNA binding sites reside in regions of predicted secondary structure. Perhaps miRNA binding sites reside in regions of secondary structure so that miRISC activity can be regulated by target site availability. In other words, miRNA target sites are not constitutively available for base pairing. Secondary structure provides a layer of miRNA target site regulation controlled by helicases and RNA binding proteins [167].

Endogenous PUF-9 physically associates with miRNA targets identified by CLIP-seq

We validated PUF-9 CLIP-seq binding sites through RNA-IP of endogenous PUF-9 followed by qRT-PCR. IP of endogenous PUF-9 in wild-type L4 animals enriches for *let-7* target mRNAs that contain PREs covered by PUF-9 CLIP-seq reads, compared to *puf-9(ok1136)* mutants in which the RNA binding domain is deleted (Figure 2.7-2.9, Table 2.1). In addition to *let-7* targets, PUF-9 IP enriches for validated and predicted targets of other miRNAs including *miR-1* (*mef-2*), and *miR-35* (*sup-26*). Further, PUF-9

binds its own transcript, suggesting an autoregulatory mechanism of expression. In all cases, the PUF binding site harbors a PRE. PUF-9 IP did not enrich for mRNAs lacking both 3'UTR PREs and PBSs (*rpb-10* and *ttr-22*), an mRNA with a 3'UTR PRE but no PBS (*mdt-9*), or an mRNA with a 3'UTR PBS but no PRE (*eft-2*). In total, nine of eleven PUF-9 CLIP-seq targets were enriched ≥3-fold by RNA-IP, while zero of four PUF-9 non-targets were enriched.

As expected, endogenous ALG-1 IP in wild-type L4 animals enriches for *let-7* and other miRNA targets compared to *alg-1(tm369)* mutants lacking a PIWI domain, whereas miRNA non-targets lacking ALG-1 CLIP-seq reads are not enriched (*eft-2, rpb-10, mdt-9, ttr-22*), (Figure 2.7-2.9, Table 2.1). Eight known miRNA targets and three novel miRNA targets were assayed, the same set of eleven transcripts tested for PUF-9. Nine of eleven ALG-1 targets were enriched ≥6-fold by RNA-IP, compared to zero of four ALG-1 non-targets. Taken together, our data show that endogenous PUF-9 associates with miRNA targets that also harbor 3'UTR PREs covered by PBS clusters, validating a subset of targets identified in our CLIP-seq data.

puf-9 genetically interacts with *lin-41*, functionally validating a PUF-9 CLIP-seq target

Based on the results of our CLIP-seq studies showing that PUF-9 and miRNAs bind shared targets at close proximity, we sought to functionally validate co-regulation by PUF-9 and miRNAs by investigating the regulation of a well-characterized *let-7* target by PUF-9. *let-7* repression of *lin-41* is required for vulval integrity at the L4 to young adult transition and loss of this repression, for example in a strain expressing a *let-7* hypomorph, leads to a vulval bursting or rupture (Rup) phenotype [284]. Previous

studies have shown that *puf-9* knockdown enhances the vulval rupture defect of *let-7(n2853)* hypomorphs, where a G-to-A seed mutation severely compromises *let-7* expression and function [59, 84]. We find that *puf-9(ok1136)* loss-of-function mutants and *puf-9(ok1136);let-7(mg279)* double mutants exhibit a moderately penetrant vulval rupture phenotype (11% and 16%, respectively) (Figure 2.10A). *let-7(mg279)* is a 27 nt deletion that reduces *let-7* primary transcript processing, resulting in a less severe than *let-7(n2853)* [294]. Vulval bursting of *puf-9(ok1136)* and *puf-9(ok1136);let-7(mg279)* animals is suppressed by *lin-41* RNAi (Figure 2.10B). In addition, *puf-9(ok1136)* vulval bursting is suppressed in *puf-9(ok1136);lin-41(ma104)* double mutants (Figure 2.10A). These data suggest that *lin-41* functions downstream of or in parallel to *puf-9* in the regulation of vulval integrity.

PUF-9 represses a *lin-41* 3'UTR reporter *in vivo*

Given that PUF-9 binds *lin-41* mRNA (Figure 2.7, Table 2.1) and *lin-41* hypomorph is epistatic to *puf-9* loss of function (Figure 2.10A), we propose that PUF-9 regulates *lin-41* expression. To test this hypothesis, we generated an integrated GFP reporter regulated by the *lin-41* 3'UTR. Depletion of *alg-1* by RNAi increases GFP reporter signal throughout the soma (non-germline tissues) at the L4 stage (Figure 2.11A) as expected for loss of miRNA-mediated repression of the *lin-41* 3'UTR. In an enhanced RNAi background *(eri-1(mg366)), puf-9* RNAi causes pronounced de-repression of the *lin-41* 3'UTR reporter in early L4 uterine tissues, similar to *alg-1* RNAi (Figure 2.11B). At mid L4, *puf-9* RNAi produced a 54% increase in GFP signal in uterine cells adjacent to the vulval toroid (Figure 2.12). NHL-2 is an miRISC cofactor that

promotes *let-7* family miRNA repression of *hbl-1* at the L2-to-L3 transition [137]. Consistent with its role as a miRISC cofactor, *nhl-2* RNAi de-represses the *lin-41* GFP reporter at the mid L4 stage by 44% (Figure 2.12). There were no changes in global *lin-41* mRNA levels or *lin-41* GFP reporter protein levels in whole animals upon *puf-9* knockdown (Figure 2.13). Regulation of *lin-41* by PUF-9 may be tissue-specific or may be beyond the detection limits of our reporter system. Taken together, our results are consistent with a model in which *puf-9* is necessary for efficient repression of *lin-41* in uterine tissues.

2.4 Discussion

PUF-9 represses *lin-41*, likely through PREs bound in the 3'UTR

The *lin-41* 3'UTR contains eight UGUA sequences that are potential recognition and binding sites for PUF-9 (or the nine other worm PUFs). Two of these UGUA motifs overlap with PUF-9 CLIP-seq read clusters, suggesting that these sites (hereafter referred to as PBS1 and PBS2) most efficiently interact with PUF-9 directly. PBS1 covers a perfect PRE and is located between two *let-7* complementary sequences (LCSs), in the classic "27nt spacer" required for downregulation of *lin-41* 3'UTR reporters [293, 295, 296]. This 27nt spacer was shown to regulate secondary structure and miRNA target accessibility at adjacent *let-7* binding sites LCS1 and LCS2. Early on, the 27nt spacer was proposed to bind an RBP [296]. PUF-9 could be the predicted RBP that binds the 27nt spacer to regulate *lin-41* expression and/or local RNA secondary structure.

PUF-9 binds to a 3'UTR element that maintains miRNA target site accessibility in *lin-41*

miRNA binding site architecture is important for miRNA-mediated repression. For example, the "27nt spacer" between LCS1 and LCS2 is required for repression of the *lin-41* 3'UTR, in part because it provides a low RNA-structure context for LCS1 and LCS2 binding [293]. Our studies suggest that PUF-9 is the previously unknown RBP proposed to regulate *lin-41* expression via the 27nt spacer [296]. It remains unclear whether PUF-9 binding contributes to direct repression of *lin-41* 3'UTR and/or stabilization of an open RNA conformation spanning the LCS1 and LCS2 sites.

lin-41 is a key target that underlies the genetic interaction between *puf-9* and *let-7* in the regulation of vulval integrity

puf-9 is required for seam cells to terminally differentiate and reach adult fates in the hypodermis, in part through repression of *let-7* target *hbl-1* [59]. Based on epistasis, Nolde *et al.* proposed that *puf-9* functions downstream or parallel to *lin-41* in the differentiation of hypodermal tissues [59]. In contrast, we observe that *lin-41* functions downstream of *puf-9* in the regulation of vulval integrity, where *let-7* repression of *lin-41* is required to prevent rupture [284]. *let-7* repression of *lin-41* 3'UTR is robust in the vulval toroid, where this interaction is required for vulval morphogenesis but not cell fate specification [284]. Interestingly, *puf-9* knockdown increases *lin-41* GFP reporter expression in uterine tissues, not in cells of the L4 vulva itself. Perhaps *puf-9* repression is more important in tissues where *let-7* alone cannot adequately repress *lin-41*. Alternatively, the *lin-41* promoter may be expressed more highly in L4 uterus than L4

vulva.

PUF proteins bind thousands of 3'UTRs [64, 65], while miRNAs can potentially recognize hundreds of targets through imperfect complementarity. As a whole, our results demonstrate that genetic interactions between PUFs and miRNAs can be exceedingly complex. Different co-targets may mediate PUF/miRNA interactions in different tissues or developmental stages. Future studies are required to fully characterize the importance of proximal PUF-9- and ALG-1-mediated post transcriptional gene regulation in *C. elegans*.

miRNA binding sites reside in 3'UTR regions with predicted secondary structure

Although miRNA seed targets are more accessible when they occur in single stranded RNA than in structured regions, we observe that *C. elegans* ALG-1 miRISC binding sites tend to reside in 3'UTR regions with secondary structure, suggesting that miRNA regulation of these targets can be modulated by the activity of other factors that affect mRNA secondary structure. Notably, work in primary fibroblasts showed that human PUM1/2 binds an energetically stable stem-loop structure in the 3'UTR of *p27* to induce a structural change, allowing miR-221/222-loaded miRISC to access its recognition site [164]. The miR-221 seed target base-pairs with a PRE in *p27* 3'UTR, forming a stable hairpin inaccessible to miRISC. Hence, PUM1/2 binding on one arm of the RNA hairpin releases a miR-221 target site on the opposite arm.

PUF binding sites usage may regulate local RNA secondary structure.

Placing a PRE within secondary structure reduces PUF binding activity; yet PUF

proteins can still regulate PRE hairpins when the affinity of PUM-HD for PREs exceeds the affinity of PREs for complementary RNA [37, 289]. This might explain why PBSs with consensus PREs reside in areas of higher secondary structure than PBSs with UGUA or no motif. In other words, PUF-9 may be able to outcompete complementary RNA strands for high-affinity target PREs, but not for low-affinity target motifs. The enrichment of PBS's with PREs in structured regions adjacent to miRNA binding sites is consistent with the model proposed by several groups: PUF binding in regions of secondary structure may free miRNA target sites within those secondary structures [164, 165, 167]. In HeLa cells, Human antigen R (HuR) binds at an A/U-rich element in the *c-Myc* 3'UTR to enhance *let-7* targeting at an adjacent site [157]. Hence, RBP regulation of miRNA target access may be a common theme [159].

2.5 Methods

Strains & worm maintenance

C. elegans were maintained using standard procedures at 20°C unless otherwise noted. Bristol strain N2 was used for wild type control. Alleles used in this study are listed by chromosome. LGX: *let-7(n2853), let-7(mg279), alg-1(tm369), ain-1(tm3681), puf-9(ok1136), xkIs53(puf-9p::puf-9::gfp::puf-9utr; myo-2p::rfp), zaIs5[alg-1p::GFP::alg-1 + pRF4(rol-6(su1006))],* LGI: *lin-41(ma104),* LGIV: *eri-1(mg366),* unmapped: *xkIs52[sur-5p::gfp::3xmiR-35-target::unc-54-3'utr; myo-2p::rfp], xkIs[lin-41p::gfp::lin-41-3'utr; myo-2p::mcherry; myo-3p::mcherry; rab-3p::mcherry].* The CT20 strain (*zaIs5*) was generously provided by Frank Slack.

Transgenic constructs

The *puf-9-gfp* construct in *xkIs53*(*puf-9p::puf-9::gfp::puf-9utr; myo-2p::rfp*) was generated by introducing the following fragments into pJK210 plasmid: 5.1kb genomic fragment of *puf-9* (*W06B11.2*: 1.9kb promoter and 3.2kb coding region with mutated termination codon), gfp coding region (0.9kb with synthetic introns and termination codon), *puf-9* endogenous 3'UTR (1.3kb immediately after termination codon). The *puf-9-gfp* construct was injected at 5ng/µl in a high copy array with *myo-2p::rfp* marker (2ng/µl) and pBluescript carrier DNA (93ng/µl) in N2 worms. Extrachromosomal arrays were integrated by UV irradiation and the resulting strains were backcrossed 5 times.

The *lin-41* 3'UTR reporter construct pJK290*(lin-41p::gfp::lin-41-3'utr)* (Alessi, manuscript in preparation) was generated by introducing the following fragments into the pCFJ151 plasmid: 4.1kb *lin-41* promoter, 0.9kb gfp coding sequence with synthetic introns and termination codon, 1.2kb *lin-41* 3'utr downstream of termination codon.

The *sur-5p::gfp::3xmir-35-target::unc-54utr* transgene was generated by inserting the following fragments into pJK227 plasmid: *sur-5* promoter fragment, 0.9kb *gfp* coding sequence with synthetic introns and termination codon, artificial 3X miR-35 target fragment, and *unc-54* 3'UTR.

lin-41 3'UTR GFP reporter imaging

Reporter plasmids were generated as described in supplemental experimental procedures, injected as high copy extrachromosomal arrays, and integrated by 254nm UV irradiation. Integrants were backcrossed at least 3X before analysis. Synchronized

L1 worms were grown on feeding RNAi clones at 20°C. L4 worms were immobilized on 3% agarose pads in 1mg/ml levamisole. Representative images in Figures 2.11-12 were captured on an Olympus BX61 microscope at 60X magnification, with 250nm *z*-stacks. Deconvolution of GFP *z*-stacks was performed in Huygens Essential software. Maximum-projection of *z*-stacks was performed in ImageJ. Final images represent one DIC plane with the vulva and UV cells in focus, along with the corresponding GFP maximum projection of seven *z*-planes across 1.5µm. Raw, unprocessed images were used for GFP quantification in Fig 2B. Images for GFP quantification were captured on an Olympus BX63 microscope at 20X magnification, with 1.34µm *z*-stacks. The *z*-plane with maximum signal over UV cells was used for GFP quantification in Image J. Average GFP signal was measured in circles of 10 pixel diameter (3.24µm) over the anterior and posterior UV cells. Each worm is represented by a single data point: quantification = anterior circle GFP + posterior circle GFP. *p*-values were calculated in PRISM using a two-tailed student's *t*-test with unequal standard deviations.

RNA Isolation and Quantitative Real-Time PCR

Synchronized L1 worms were grown at 20°C for the indicated number of hours on *E. coli* from the Ahringer RNAi library. Samples were processed by three rounds of freeze/thaw lysis in Tri Reagent (Ambion) and RNA was extracted according to manufacturer's protocol with the following modifications: RNA was precipitated in isopropanol at -80°C for 1 hour, pelleted by centrifugation at 4°C for 30 minutes, and washed three times in 75% ethanol; RNA was resuspended in water. cDNA was generated from 100ng total RNA using MultiScribe Reverse Transcriptase (Applied

Biosystems) following the vendor's protocol with the following modifications: 25 units of RT and 7.6 units of RNase Out (Invitrogen) were used per reaction. Quantitative real-time PCR was performed in a Realplex thermocycler (Eppendorf) using Absolute Blue SYBR Green Master Mix (Thermo) in a 20µl reaction. Relative mRNA levels were calculated based on the ddCT method using *eft-2* for normalization [297]. *U18* and *let-7* cDNA were generated from 50ng total RNA using *Ce-U18* or *Hs-let-7a* Taqman RT primers (Applied Biosystems) according to manufacturer's instructions. Quantitative real-time PCR was performed in a Realplex thermocycler using Taqman Universal PCR Master Mix, No AmpErase UNG (Applied Biosystems) in a 20µl reaction. Relative *let-7* levels were calculated based on the ddCT method using U18 for normalization. *eft-2* and *U18* were not used to normalize immunoprecipitated RNA, but served as negative controls.

Immunopurification of PUF-9 or ALG-1 associated RNA

Wild type N2, *puf-9(ok1136),* or *alg-1(tm369)* synchronized L1 worms were grown at 20°C and collected at mid L4. Worm pellets were flash frozen in liquid nitrogen and pulverized in a ball mill homogenizer (Retsch MM400). Worm homogenates were resuspended in lysis buffer (50 mM HEPES (pH 7.4), 1 mM EGTA, 1 mM $MgCl_2$, 100 mM KCl, 10% glycerol, 0.05% NP-40) with 200U/ml RNase Out (Invitrogen) and 1X Complete, Mini, EDTA-free Protease Inhibitor Cocktail (Roche; 1 tablet per 10ml buffer). Lysates were clarified by centrifugation (12000x g for 12 minutes, 12000x g for 2 minutes at 4°C) and lysate protein concentration was adjusted to be equal across samples. Lysate aliquots (50µl) were collected to show equal protein concentration of

input material, and to provide RNA for input normalization. Lysate was brought up 300 mM KCl concentration in 1ml volume (by addition of 100µl 2M KCl) and pre-cleared with 15µl of Protein G Dynabeads for 15 minutes at 4°C. Lysates were incubated with 6µg rabbit polyclonal anti-PUF-9 (Proteintech) for 2 hours or anti-ALG-1 (Thermo) for 1 hour, and PUF-9 or ALG-1 were immunoprecipitated with 50µl Protein G Dynabeads for 1 hour. Beads were washed 4 times (50 mM Tris-HCl (pH 7.5), 200 mM KCl, 0.05% NP-40) and split in two aliquots: half were resuspended in 1ml Tri Reagent for RNA extraction as described above; half were resuspended in 60µl 1X Tris-Glycine SDS Sample Buffer (Invitrogen) and heated at 55°C for 12 minutes to elute protein for Western blot analysis.

Co-immunopurification of GFP-ALG-1 and PUF-9

CT20(*Is[alg-1::gfp-alg-1::alg-1*]) or CT20;*puf-9(ok1136)* synchronized L1 worms were grown at 25°C and collected at mid L4. Worm homogenates were processed as above with the following modifications: Purelink RNaseA (Invitrogen) was added to lysis buffer at 10µg/ml instead of RNaseOut for RNase-treated samples. Immunoprecipitation was performed as above with the following modifications: lysates were pre-cleared with 20µl Protein A Dynabeads; GFP-ALG-1 was immunoprecipitated by 1 hour incubation with 2.5µg anti-GFP (Invitrogen clone 3E6) cross-linked to 50µl Protein A Dynabeads (Invitrogen).

Western Blot Analysis

Proteins were immobilized on Immobilon FL transfer membrane (Millipore) and

blotted with rabbit anti-GFP (Proteintech custom, antigen = GFP protein), rabbit anti-AIN-1(1:1000 Proteintech custom, antigen = WGDPPLSDVQYPLQPHASFC peptide), rabbit anti-ALG-1 (1:2000; Thermo PA1-031), rabbit anti-PUF-9 (1:2000; Proteintech custom, antigen = WAYAPPTNYYADHSIAKPIC peptide), and rabbit anti-γ-Tubulin (1:2000; Sigma LL-17).

Vulval rupture assays

Synchronized L1 worms were plated on OP50 or feeding RNAi clones in HT115 *E. coli* [206], maintained at 22.5°C, and monitored for vulval rupture at L4 and young adult stages. Mean and standard deviation were calculated from three biological replicate experiments. *p*-values were calculated in PRISM using Fisher's exact test.

CLIP-seq procedures

PUF-9-GFP and GFP-ALG-1 CLIP-seq were performed similarly to Puf3p PAR-CLIP [291] with modifications for application in *C. elegans*, and each step is described below.

Worm culture for PUF-9-GFP and GFP-ALG-1 strains

Worms expressing PUF-9-GFP (*xkIs53[puf-9-promoter::puf-9-gfp::puf-9-3'UTR]*) or GFP-ALG-1 (CT20, *zaIs5[alg-1-promoter::gfp-alg-1::alg-1-3'UTR]*) were grown at 25°C. Synchronized L1 worms were prepared by hypochlorite preparation of embryos and nutation for 22-26 hours in M9. Gravid adults were grown for 50 hours, washed 3 times in M9 solution, and rocked in M9 for 15 minutes. Embryo samples were prepared

by hypochlorite preparation of Day 1 gravid adults (50-60 hours). Embryos were nutated for 22-26 hours in M9 and L1 worm samples were filtered through 20 µm filters.

UV crosslinking of protein & RNA

Live samples (worms or embryos) were washed once with water, resuspended in 10ml water on 15cm glass cell culture dishes and placed on ice. Samples were irradiated with 254nm UV at 150 mJ/cm^2 four times in a Stratalinker 2400 (Stratagene). Samples were centrifuged for 1 minute at 3000xg and water was removed. Samples were flash frozen in liquid nitrogen and ground to a fine powder in a ball-mill homogenizer (Retsch MM400).

Extract preparation

100mg of frozen, homogenized worm sample was resuspended in 1ml Lysis Buffer (1xPBS, 0.5%NP-40, 1xComplete Mini Protease Inhibitor, EDTA-free). Lysates were cleared by sequential spins at 1,300Xg for 5 minutes and 20,000Xg for 10 minutes at 4°C. 500µl of clarified lysate was passed through a Costar Spin-X filter (Corning), mixed with RNase T1 (Fermentas) to 1 U/µl, and incubated at 24°C for 15 minutes in an Eppendorf Thermomixer (with 15 seconds shaking at 1,000 rpm followed by a 2 minute rest interval) followed by a 5 minute incubation on ice.

RNP immunoprecipitation and RNase T1 treatment

Lysates were mixed with 25µl anti-GFP magnetic bead slurry (prepared by DMP-mediated crosslinking of 5µg monoclonal anti-GFP antibody (Invitrogen clone 3E6) to

100µl Protein A Dynabeads (Invitrogen) and resuspended in 200µl Lysis Buffer) to pull down PUF-9-GFP or GFP-ALG-1 at 4°C for 1 hr. Beads were washed twice with 1x PBS + 0.1% NP-40, then incubated with 20 µl of 50 U/µl RNase T1 (Fermentas, 1:20 dilution in 1× PBS) at 24°C for 15 minutes on a Thermomixer (15 seconds shaking at 1,000 rpm followed by a 2 minute rest interval), followed by a 5 minute incubation on ice. Beads were washed twice with wash buffer (1× PBS, 0.1% SDS, 0.5% deoxycholate, 0.5% NP-40), twice with high-salt wash buffer (5× PBS, 0.1% SDS, 0.5% deoxycholate, 0.5% NP-40) and twice with 1× PNK buffer (50 mM Tris pH 7.4, 10 mM $MgCl_2$, 0.5% NP-40).

On-bead CIP treatment

Beads were incubated with 20 µl of CIP mix (50 mM Tris pH 7.9, 100 mM NaCl, 10 mM $MgCl_2$, 0.5 U/µl calf intestinal alkaline phosphatase (CIP); NEB) at 37°C for 15 minutes, with 15 seconds shaking at 1,000 rpm followed by a 2 minute rest interval on a Thermomixer. After CIP treatment, beads were washed twice with 1× PNK+EGTA buffer (50 mM Tris pH 7.4, 20 mM EGTA, 0.5% NP-40) and twice with 1× PNK buffer.

On-bead 3’ DNA linker ligation

Beads were incubated with 20 µl of ligation mix (50 mM Tris pH 7.4, 10 mM $MgCl_2$, 0.5 mM DTT, 2 µM pre-adenylated 3' DNA linker, 25% PEG-8000, 10 U/µl T4 RNA ligase 2, truncated K227Q; NEB M0351S) at 16°C overnight (≥16 hr), with 15 seconds shaking at 1,000 rpm followed by a 2 minute interval on a Thermomixer. After linker ligation, beads were washed three times with 1× PNK+EGTA buffer.

SDS-PAGE and nitrocellulose transfer

Beads were mixed with 15 µl of 1× PNK+EGTA buffer and 15 µl of 4× NuPAGE LDS sample buffer (Invitrogen NP0007), and incubated at 70°C for 10 minutes. Beads were removed, and the supernatant was loaded onto NuPAGE 4-12% Bis-Tris gel (Invitrogen) and run at 150 V for 1 hr. The gel was transferred to Protran BA 85 nitrocellulose membrane (pore size 0.45 µm, Whatman) using Novex wet transfer at 30 V for 1 hr. A membrane band corresponding to each RNP was excised and transferred to a microfuge tube.

On-bead ^{32}P labeling of RNA 5' ends identifies membrane regions for excision

A diagnostic CLIP experiment was performed in parallel, for the sole purpose of identifying RNP bands on nitrocellulose membranes. Extract preparation, RNP immunoprecipitation, and RNase T1 digestion were performed as described above. 5' end phosphorylation was performed on-bead in 15 µl of PNK mix (70 mM Tris pH 7.6, 10 mM $MgCl_2$, 5 mM DTT, 0.75 µl ^{32}P rATP (6000 Ci/mmol 10 mCi/ml Perkin Elmer BLU502Z500UC), 1 U/µl T4 polynucleotide kinase (NEB)) and incubated at 37°C for 15 minutes. After SDS-PAGE and transfer, crosslinked RNAs were visualized by autoradiography.

RNA isolation and purification

Non-radioactive membrane bands were excised for RNA isolation and library construction. Excised membranes were incubated with 200 µl of 4 mg/ml Proteinase K prepared in 1× PK buffer (100 mM Tris pH 7.5, 50 mM NaCl, 10 mM EDTA) for 20

minutes at 37°C on a Thermomixer. We added 200 µl of 7 M urea prepared in 1× PK buffer to the tube followed by another 20 minute incubation at 37°C. The Proteinase K digestion reaction was mixed with 1 ml of phenol:chloroform:isoamyl alcohol 25:24:1 (Sigma-Aldrich P2069) by vortexing and spun for 5 minutes at 20,000Xg. The liquid phase was transferred into a new tube, mixed with 50 µl of 3 M NaOAc, 1 ml of 100% ethanol and 1 µl of 15 mg/ml Glycoblue (Invitrogen), and precipitated for 2 hr at -80°C. RNAs were collected by centrifugation for 20 minutes at 20,000Xg at room temperature followed by two washes with cold 75% ethanol.

RNA 5' end phosphorylation

RNA pellets were air-dried briefly, resuspended in 10 µl of PNK mix (70 mM Tris pH 7.6, 10 mM $MgCl_2$, 5 mM DTT, 1 mM ATP, 1 U/µl T4 polynucleotide kinase (NEB)) and incubated at 37°C for 30 minutes. The reaction was combined with 90 µl of H_2O and 100 µl of phenol:chloroform:isoamyl alcohol 25:24:1, mixed well and spun for 5 minutes at 20,000Xg. The liquid phase was mixed with 12.5 µl of 3 M NaOAc, 250 µl of 100% ethanol, 1 µl of 15 mg/ml glycoblue and precipitated for 2 hr at -80°C. RNAs were collected by centrifugation for 20 minutes at 20,000Xg at room temperature, followed by two washes with cold 75% ethanol.

5' RNA linker ligation

RNA pellets were resuspended in 10 µl of ligation mix (50 mM Tris pH 7.5, 10 mM $MgCl_2$, 10 mM DTT, 1 mM ATP, 0.1 mg/ml bovine serum albumin, 2 µM 5' RNA linker, 1 U/µl T4 RNA ligase (Fermentas EL0021), 10% DMSO) and incubated at 15°C

for 2 hr.

RNA size selection

Ligation reaction was terminated by adding 10 µl of 2X formamide gel loading buffer (Invitrogen AM8546G), heated for 2 minutes at 70°C and then quickly chilled on ice. Samples were loaded onto a 6% TBE UREA gel (Invitrogen EC6865) and run at 150 V for 45 minutes. After staining with 1× Sybr Gold Stain (Invitrogen S-11494), a gel piece corresponding to a 70 to 90 nucleotide RNA (80 to 100 nucleotide single-stranded DNA) was excised, crushed, and soaked in 400 µl of 0.3 M NaOAc overnight at room temperature. After removing gel pieces, the solution was combined with 1 ml of 100% ethanol and 1 µl of 15 mg/ml glycoblue and precipitated for 2 h at -80°C. RNAs were collected by centrifugation for 20 minutes at 20,000Xg at room temperature, followed by two washes with cold 75% ethanol. After brief drying, RNAs were resuspended in 15 µl of H_2O.

Reverse Transcriptase PCR

The ligated RNA (10 µl) was combined with 2 µl of 5 µM RT primer, heated at 65°C for 5 minutes, and then quickly chilled on ice, and followed by the addition of 1 µl of water, 1 µl of 10 mM dNTP, 1 µl of 0.1 M DTT, 4 µl of 5X First strand buffer, and 0.5 µl of SuperScript III Reverse transcriptase (Invitrogen, 200 U/µl). The RT reaction was kept at 50°C for 45 minutes, 55°C for 15 minutes and 90°C for 5 minutes. A test PCR was performed with 2.5 µl of RT product in 20 µl PCR mix: 1× AccuPrime PCR buffer I, 0.5 µM P5 long primer, 0.5 µM P7 primer, 0.2 µl AccuPrime Taq High Fidelity

(Invitrogen, 5 U/µl). PCR was carried out with an initial 3 minute denaturation at 98°C, followed by 14 to 22 cycles of 80 s denaturation at 98°C, 90 s annealing and extension at 65°C, and termination with a final 5 minute extension at 65°C. PCR product (15 µl) was collected after 14, 18, and 22 cycles and analyzed on a 10% TBE gel (Invitrogen) at 150 V for 1 hr to determine the optimal amplification cycles (the lowest cycle number required to generate 96 to 116 bp amplicons detected by Sybr Gold staining).

Preparation of sequencing libraries

A 50 µl PCR reaction was carried out with the determined cycle number. Amplicons were purified using DNA clean and concentrator-5 (Zymo D4013; Irvine, CA, USA), run on 10% TBE gels at 150 V for 1 hr and stained with Sybr Gold. A gel piece corresponding to 96 to 116 bp DNA was excised, crushed, and soaked overnight in 400 µl 0.3 M NaOAc at room temperature. After removing gel pieces, the solution was combined with 1 ml of 100% ethanol and 1 µl of 15 mg/ml glycoblue and precipitated for 2 h at -80°C. DNAs were collected by centrifugation for 20 minutes at 20,000Xg at room temperature, followed by two washes with cold 75% ethanol. After brief drying, amplicons were resuspended in 20 µl of H_2O. Purified amplicons (5 µl) were used to seed a second round of PCR in 50 µl: 1× AccuPrime PCR buffer I, 0.5 µM Illumina Primer A, 0.5 µM Illumina Primer B, 0.2 µl AccuPirme Taq High Fidelity for 6 to 12 cycles. Second PCR amplicons were purified with DNA clean and concentrator-5 (Zymo) and sequenced on an Illumina HiSeq 2000 sequencer.

Sequence read processing

Sequencing reads were processed to remove linkers and low-quality reads. Reads from ALG-1 HITS-CLIP libraries were mapped to miRBase v19 using BWA 0.6.2 [298], and reads mapping to miRNA sequences were identified. Remaining ALG-1 sequencing reads and all PUF-9 sequencing reads >15nt were aligned to the masked *C. elegans* genome version WS220 using BWA 0.6.2. The single most optimal alignment for each read was kept based on mismatches per read length, and reads aligning to multiple genomic loci with the same number of mismatches were discarded. Read clusters were generated from single nucleotide overlapping reads, and Gaussian smoothing was applied to resolve multi-peak clusters as described in [291]. Read clusters were annotated to genic regions from WS220 including predicted 3'UTRs, which we defined as 1.5kb downstream from any ORF with no annotated 3'UTR. Clusters aligned anti-sense to annotated genes were removed from downstream analyses. Cluster read counts were normalized to the total number of million mapped reads in each library (RPM) and additionally to gene RPKM values [288] for the gene to which each cluster was aligned.

Functional category enrichment analysis and identification of sequence motifs

DAVID was used to derive enriched functional categories for genes targeted by PUF-9 in each stage [299, 300]. Background gene lists were restricted to genes expressed in each specific stage as determined by the modENCODE group [288]. MEME was used to search 3'UTR PUF-9 binding sites in each stage for over-represented sequence motifs [286]. The following parameters were used: -zoops -minw

6 -maxw 9.

RNA structure prediction

RNAfold from the ViennaRNA Package 2.0 [290] was used to determine optimal minimum free energy (MFE) scores for all PUF-9 and ALG-1 binding sites. Each binding site was extended 15 nucleotides in either direction for prediction. As matched controls for each binding site, RNA regions immediately upstream and downstream of each site were chosen, with the same length, and used as input to RNAfold to derive minimum free energy scores. The RNAfold web server [290] (http://rna.tbi.univie.ac.at/cgi-bin/RNAfold.cgi) was used to generate example RNA structures for select PUF-9 binding sites.

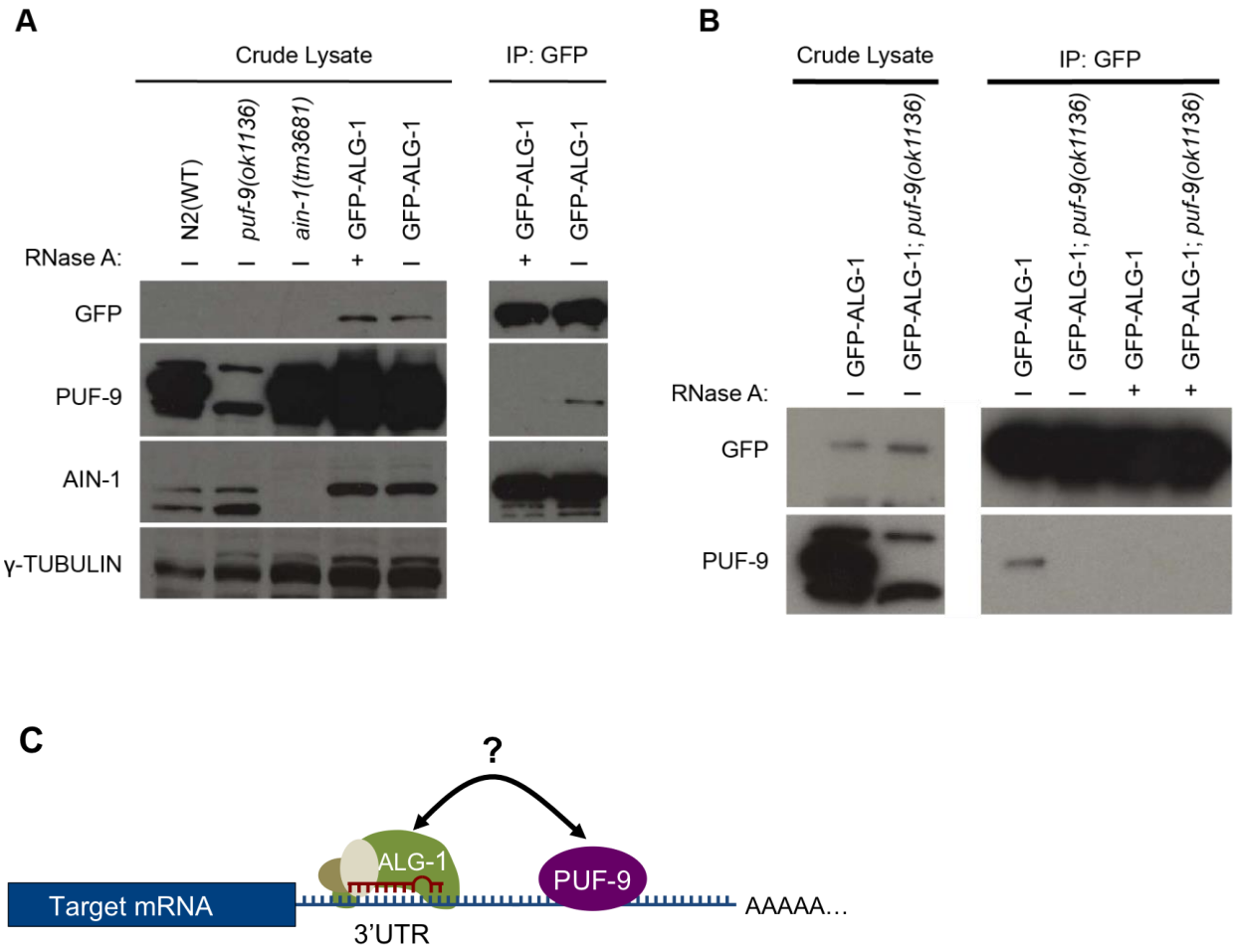

Figure 2.1 PUF-9 physically associates with ALG-1 in an RNA-dependent manner.
(A) Immunoprecipitation of GFP-ALG-1 pulls down endogenous PUF-9 in L4 animals. CoIP of GFP-ALG-1 and PUF-9 is disrupted by RNase A, while coIP of GFP-ALG-1 and AIN-1 is unaffected. N2 wild type, *puf-9(ok1136)* and *ain-1(tm3681)* deletion mutants serve as Western blot controls. **(B)** The PUF-9 band does not co-precipitate with GFP-ALG-1 in *puf-9(ok1136)* mutant worms. **(C)** Model: ALG-1 and PUF-9 may associate via shared mRNA targets.

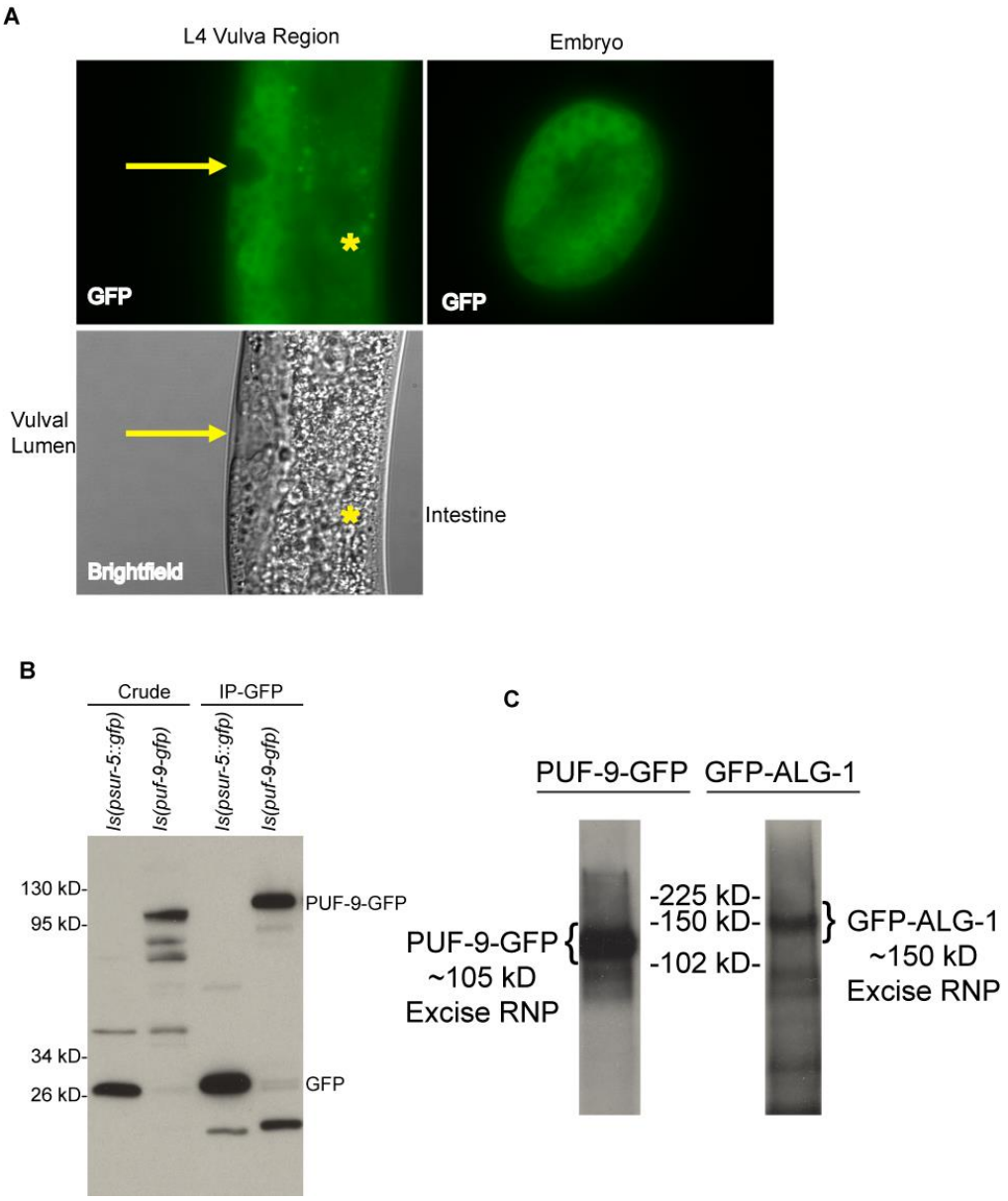

Figure 2.2 PUF-9-GFP expression, immunoprecipitation, and bound RNA fragments.
(A) Cytoplasmic PUF-9-GFP is visible in early L4 vulva and uterus, as well as in embryos undergoing morphogenesis. Images were taken at 60X magnification in GFP or Brightfield channels. Arrow indicates vulval lumen, surrounded by vulval and uterine tissue. Asterisk (*) = intestine. **(B)** Western blot confirms PUF-9-GFP is expressed at ~105 kD. Ubiquitous somatic GFP driven by a *sur-5* promoter runs at ~27 kD. Embryo crude lysate and GFP-IP samples are shown. **(C)** Autoradiography detects PUF-9-GFP and GFP-ALG-1 ribonucleoprotein complexes. RBPs were crosslinked to RNA targets *in vivo* by 254nm UV. RNPs were immunopurified and digested with RNaseT1. Protected RNA fragments were 5'-end-labeled with P32. RNPs were resolved on LDS PAGE and transferred to nitrocellulose membranes. Autoradiography detects protected RNA fragments crosslinked to RNPs. The corresponding membrane regions were excised for RNA isolation and high throughput sequencing.

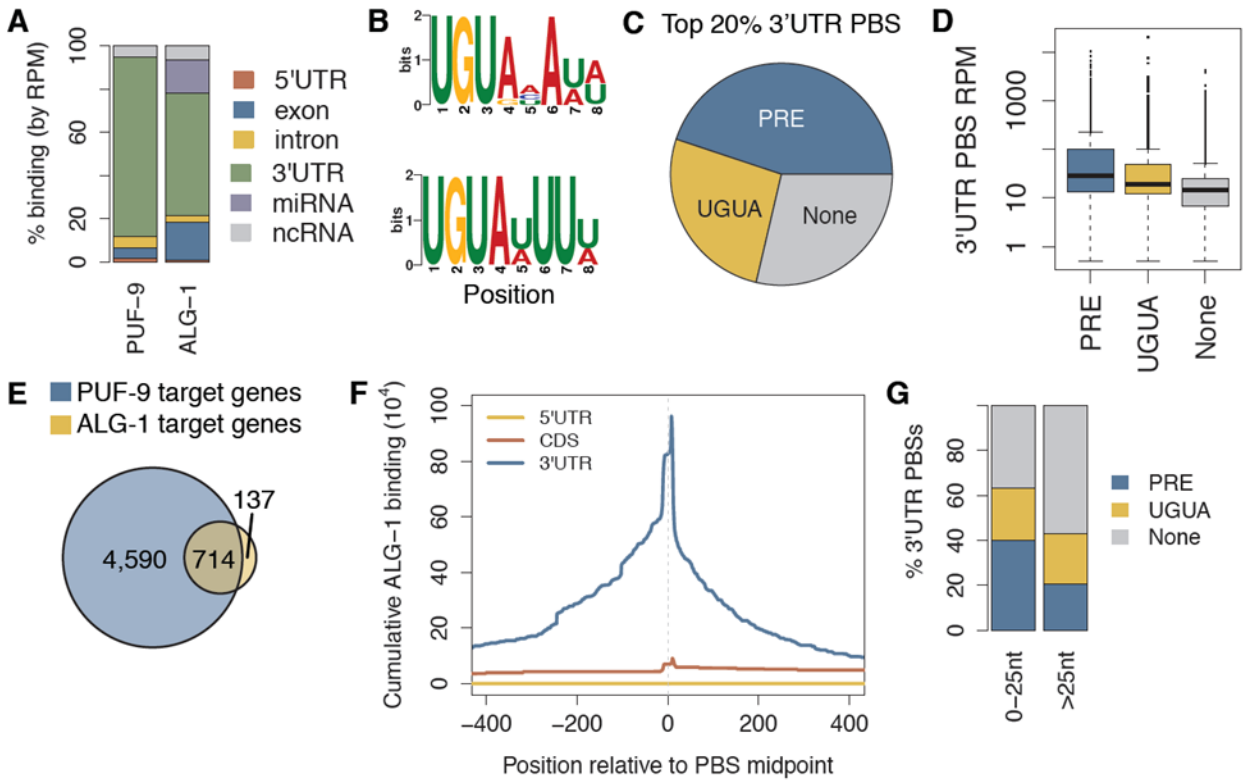

Figure 2.3 PUF-9 and ALG-1 globally bind common targets.
(A) CLIP-seq data reveals that PUF-9 and ALG-1 preferentially bind target 3'UTRs. ALG-1 also binds exons and miRNAs. The binding site distribution graph is based on gravid adult CLIP-seq datasets. Similar distributions are present in embryo and L1 datasets. **(B)** The top two enriched motifs in adult PUF-9 CLIP-seq binding sites resemble the conserved UGUANAUA motif. **(C)** A majority of the highest bound PUF-9 binding sites (top 20% ranked by RPM) contain either a full PRE (motif in B) or a truncated UGUA motif. **(D)** PUF-9 binding sites containing a PRE are more highly bound than sites with a UGUA motif or no motif. **(E)** Most ALG-1 target genes are also bound by PUF-9. **(F)** Globally, PUF-9 binding sites overlap or are directly adjacent to ALG-1 binding sites only on shared target 3'UTRs. The distribution of ALG-1 reads is plotted cumulatively, relative to the PUF-9 binding site midpoint, across all 714 shared targets. **(G)** PUF-9 binding sites that reside within 25nt of ALG-1 binding sites are more likely to contain a PRE than PUF-9 binding sites located more distal from ALG-1 binding sites.

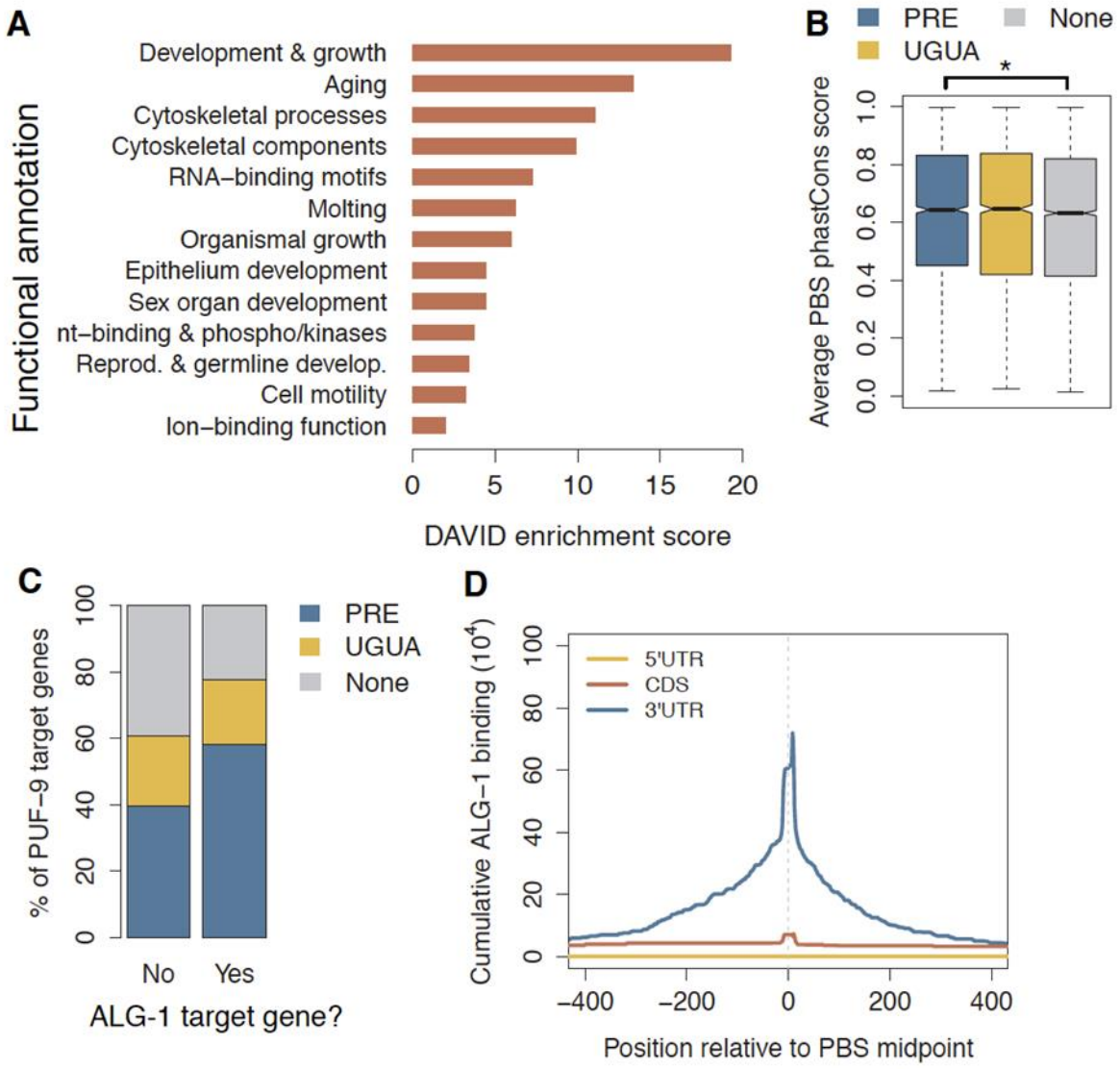

Figure 2.4 PUF-9 binding site characteristics.
(A) PUF-9 CLIP-seq targets are enriched for functional annotations related to development, growth, aging, cytoskeleton, RNA-binding proteins, and molting. **(B)** PUF-9 binding sites with a PRE are significantly more conserved than sites with no motif. Asterisk: two-tailed *t*-test $p<0.05$. **(C)** PUF-9 binding sites on ALG-1 target genes are more likely to have PREs than binding sites on ALG-1 non-target genes. **(D)** PUF-9 binding sites overlap or are directly adjacent to ALG-1 binding sites on shared target 3'UTRs. Adult CLIP-seq datasets were used to construct a representative graph. Embryo and L1 datasets show a similar pattern.

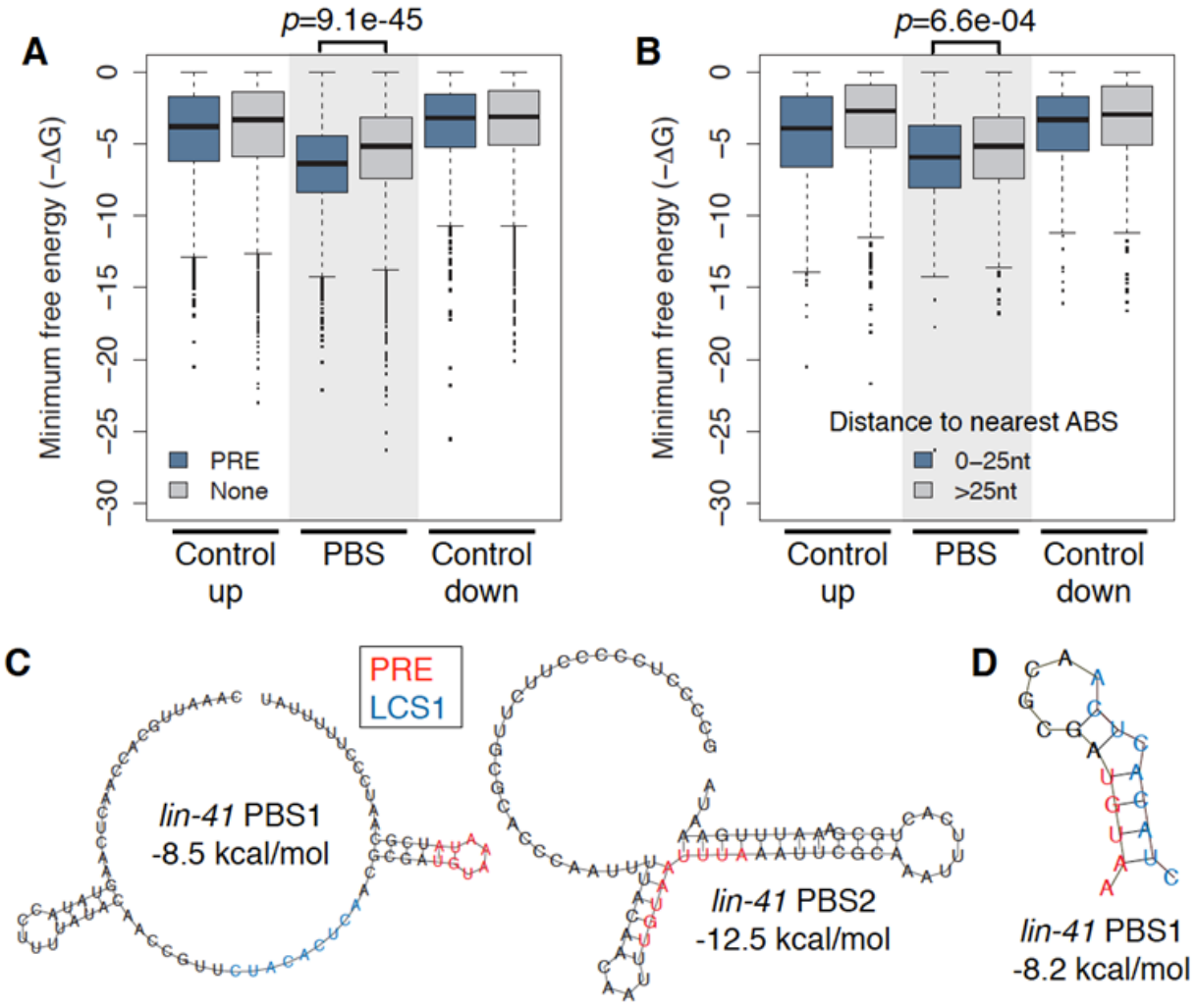

Figure 2.5 PUF-9 binds 3'UTRs at structured regions near miRISC target sites.
(A) PUF-9 binding sites are predicted to reside in 3'UTR regions with higher secondary structure (lower ΔG) than regions 50nt upstream or downstream. PUF-9 binding sites with PREs have lower minimum free energy of folding than sites without a PRE. Adult CLIP-seq datasets were used to make representative graphs. **(B)** PUF-9 binding sites within 25nt of ALG-1 binding sites are predicted to be more structured than PUF-9 binding sites >25nt from ALG-1 binding sites. **(C)** The two PUF-9 binding sites in *lin-41* 3'UTR can form stable secondary structures predicted in Vienna Package RNA Fold. **(D)** The second most stable structure predicted for the *lin-41* 3'UTR PBS1 region is a hairpin containing the LCS1 *let-7* seed target and the PBS1 PUF-9 response element.

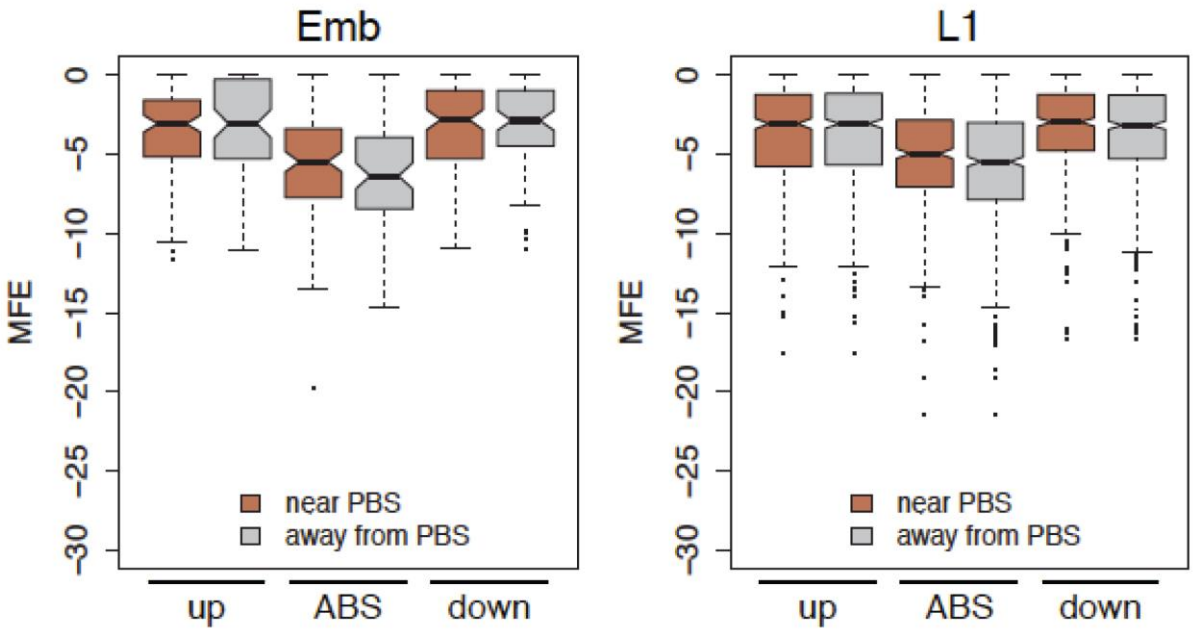

Figure 2.6 ALG-1 binding sites have high predicted secondary structure.
ALG-1 binding sites within 25nt of PUF-9 binding sites are predicted to be more structured than ALG-1 binding sites >25nt from PUF-9 binding sites. Minimum free energy calculated as in Figure 2.5.

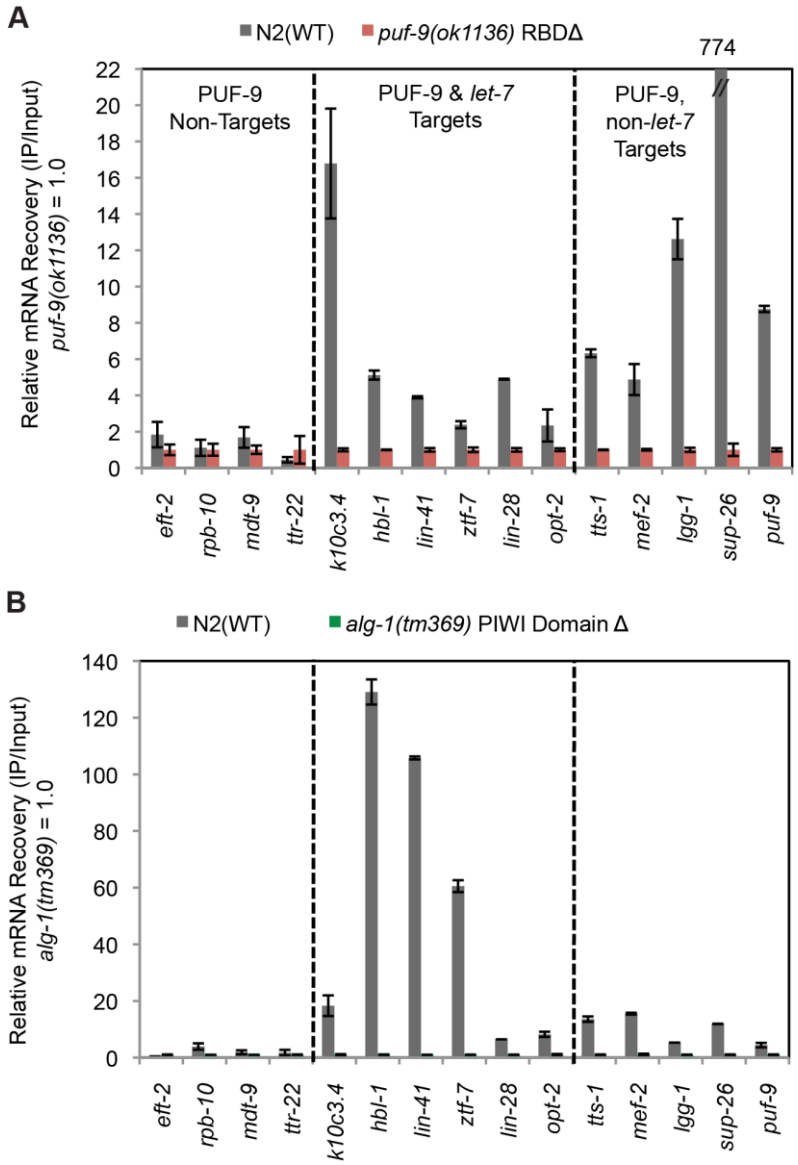

Figure 2.7 Endogenous PUF-9 binds *let-7* target mRNAs.
(A) Immunoprecipitation of endogenous PUF-9 from L4 worms enriches for *let-7* targets and other mRNAs that contain 3'UTR PBSs with PREs. **(B)** Immunoprecipitation of endogenous ALG-1 from L4 worms enriches *let-7* targets and the *miR-1* target *mef-2* mRNA. Non-target control mRNAs lack 3'UTR ABSs and 3'UTR PBSs with PREs. Technical duplicate average and standard deviation are shown.

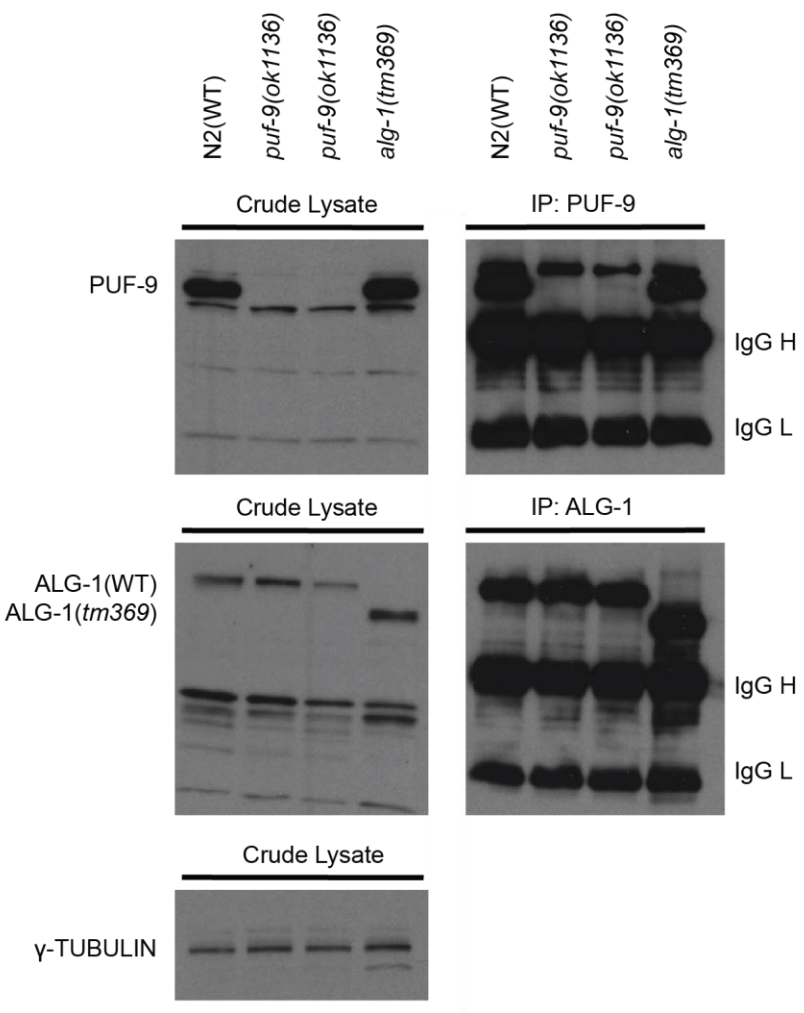

Figure 2.8 Western blot controls for Figure 2.7 RNA-IP.
Western blot confirms endogenous PUF-9 immunoprecipitation from L4 worms. PUF-9 protein is detected in N2 WT crude lysate and recovered by immunoprecipitation with a rabbit polyclonal antibody generated against an N-terminal peptide in PUF-9. PUF-9 protein is not detected in crude lysate or IP samples from *puf-9(ok1136)* mutants that harbor a C-terminal deletion of PUM-HD. Western blot confirms endogenous ALG-1 immunoprecipitation from L4 worms. Full length ALG-1 is detected in crude lysate and recovered by immunoprecipitation in N2 WT worms. Truncated ALG-1 protein is detected in crude lysate and recovered by immunoprecipitation in *alg-1(tm369)* mutants. (Lane 3: an extra replicate IP was performed in *puf-9(ok1136)* to test whether *puf-9* is required for efficient ALG-1 target binding. However, this analysis was not performed because less ALG-1 is present in crude lysate of the extra sample.)

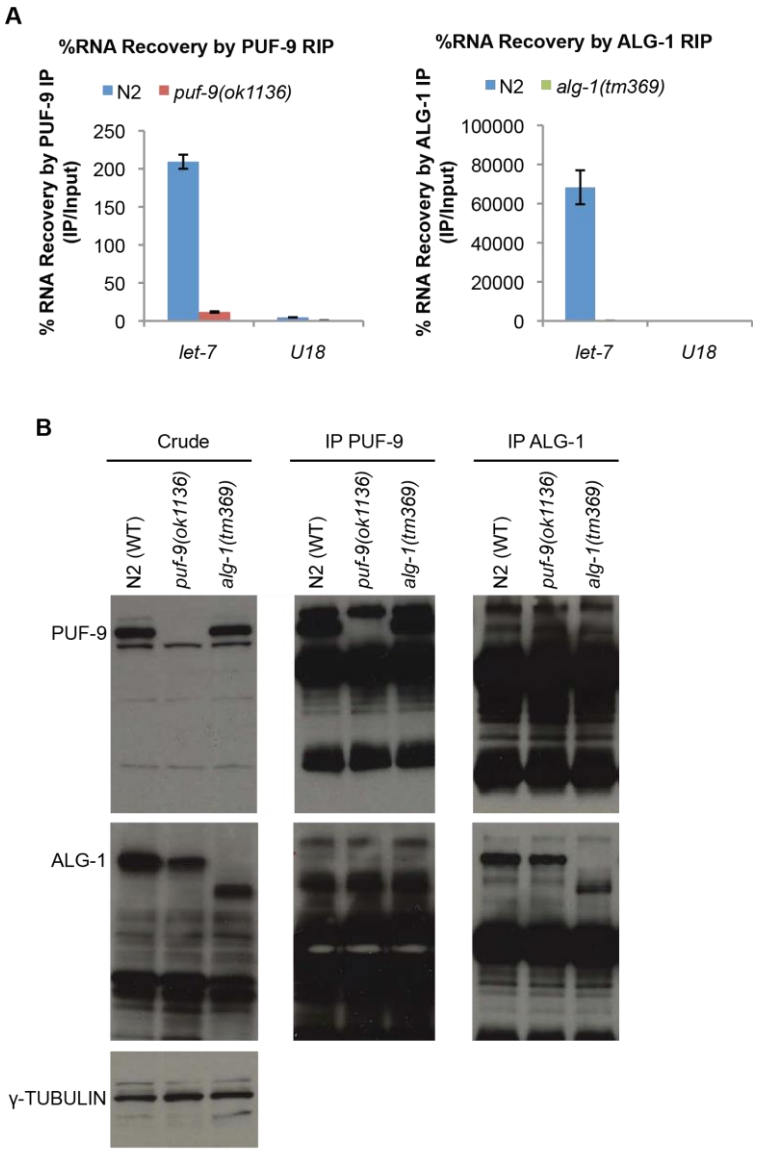

Figure 2.9 PUF-9 physically associates with *let-7* miRNA weakly or indirectly.
(A) Immunoprecipitation of PUF-9 moderately enriches *let-7* miRNA but not U18 small RNA negative control, as measured by Taqman qRT-PCR. Immunoprecipitation of ALG-1 enriches *let-7* miRNA to a much greater degree. Technical duplicate average and standard deviation are shown. **(B)** Endogenous coIP for PUF-9 and ALG-1 does not detect an association in L4 animals. This Western blot is also the confirmation for RNA-IP in part A.

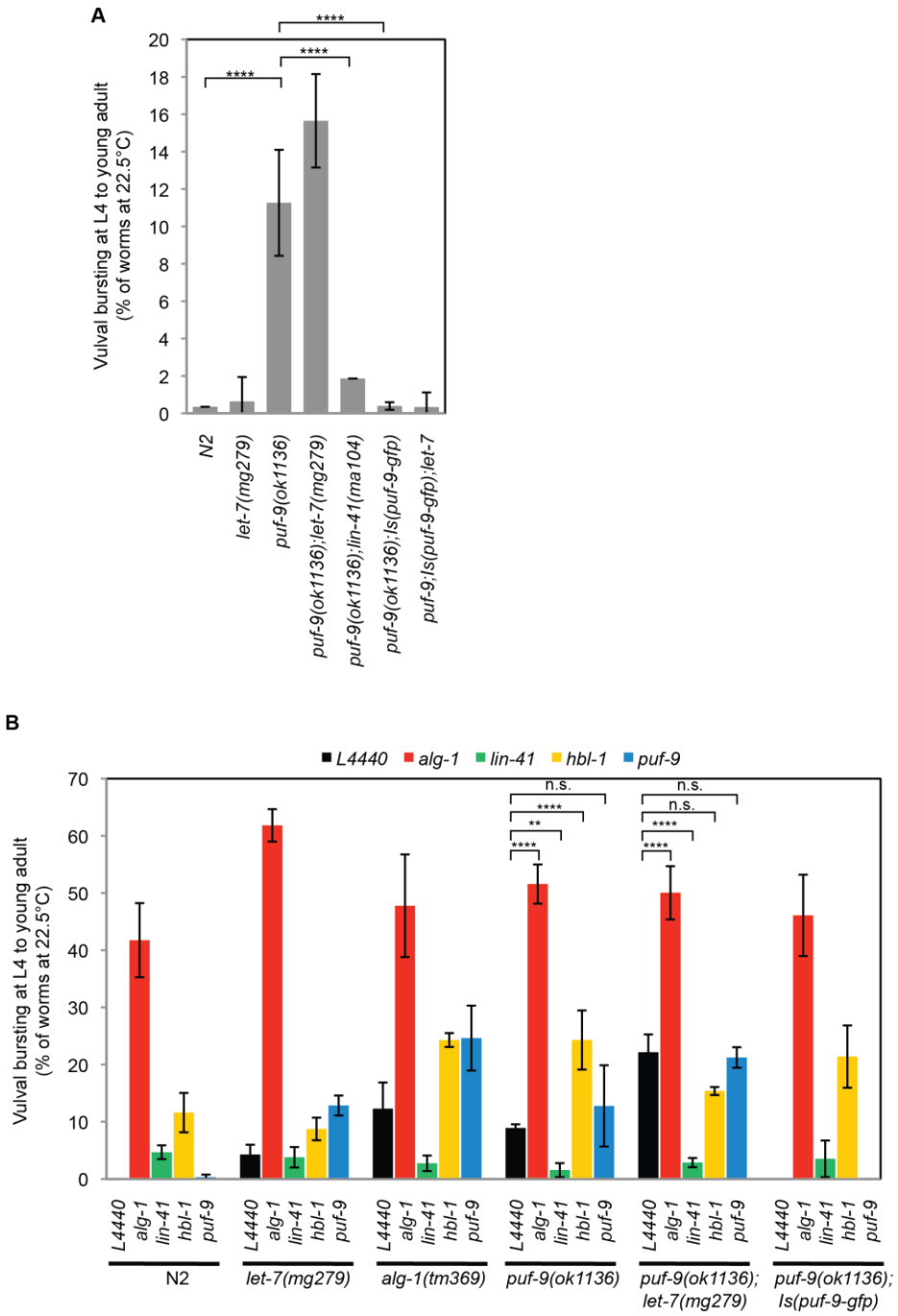

Figure 2.10. *puf-9* genetically interacts with *let-7* and *lin-41* to regulate vulval integrity at the L4 to young adult transition.

(A) *puf-9(ok1136)* loss of function mutants exhibit a low rate of vulval rupture (11.25%) that is suppressed in the *puf-9(ok1136);lin-41(ma104)* double mutant (1.86%) or by an integrated *puf-9-gfp* transgene (0.39%). **(B)** Vulval rupture of *puf-9(ok1136)* mutants and *puf-9(ok1136) let-7(mg279*) *X* double mutants is suppressed by RNAi knockdown of *lin-41* but not *hbl-1*. Experiments were performed at 22.5°C. Biological triplicate average and standard deviation are shown. *p*-values were calculated by Fisher's exact test: *<.05 **<.01 ***<.001 ****<.0001.

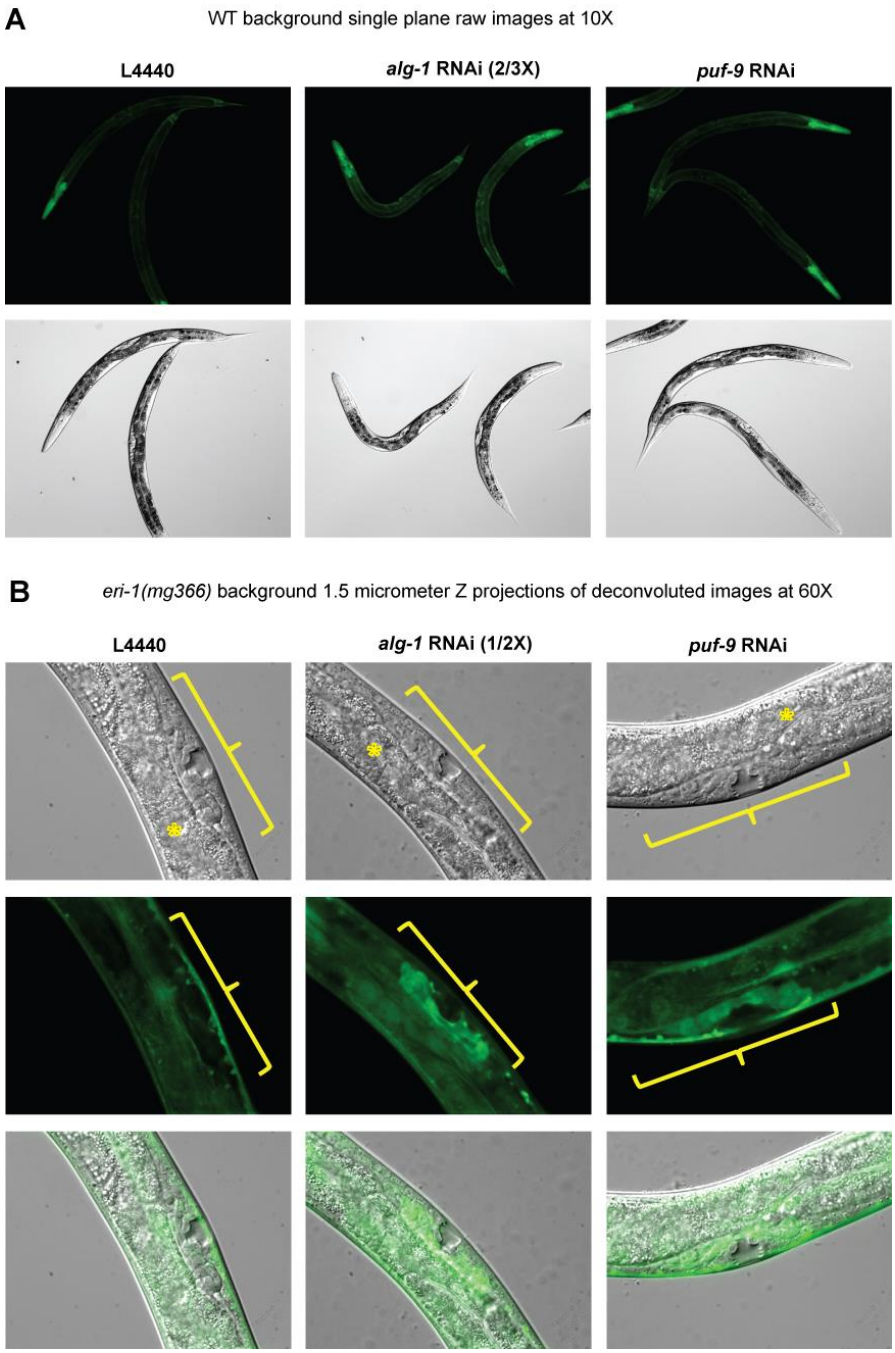

Figure 2.11 A *lin-41* 3'UTR GFP reporter is regulated by *alg-1* and *puf-9*.
(A) Single plane images at 10X magnification show that *alg-1* RNAi increases *lin-41* GFP reporter signal in a wild type genetic background. DIC and GFP channels are shown at mid L4 stage. Reporter = *Is[lin-41-promoter::gfp::lin-41-3'utr]*. **(B)** Deconvolved images at 60X magnification show that *alg-1* RNAi and *puf-9* RNAi increase uterine *lin-41* GFP reporter signal in an *eri-1(mg366)* enhanced RNAi background at early L4 stage. Single plane raw images are shown for DIC. GFP images are 1.5 µm maximum projections (seven *z*-stacks at 250 nm). Reporter = *eri-1(mg366);Is[lin-41-promoter::gfp::lin-41-3'utr]*). Bracket = vulva and uterus region. Asterisk * = intestine.

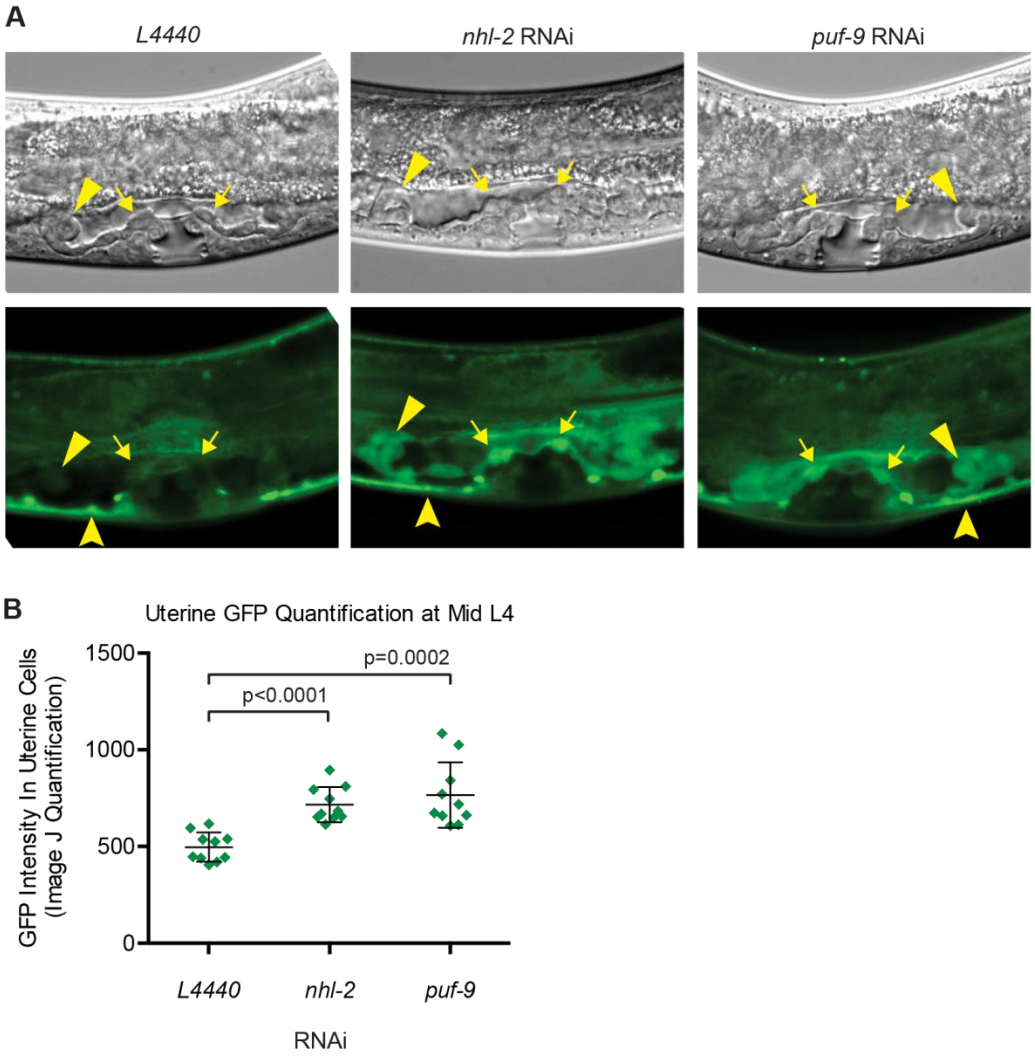

Figure 2.12 Quantification of *lin-41* 3'UTR GFP reporter expression.
(A) GFP is weakly expressed in vulval and uterine tissues at mid L4, but strongly expressed in the ventral neural cord (notched arrowheads). *nhl-2* RNAi or *puf-9* RNAi increases GFP expression in cells of the uterine toroid (solid arrowheads) and in uterine cells at the vulval interface (arrows). **(B)** GFP was quantified with Image J in uterine cells adjacent to the vulva (arrows). Each data point represents the sum of two cells from one animal, N=10. *nhl-2* RNAi and *puf-9* RNAi increased GFP signal over L4440 vector by 44% and 54% respectively. *p*-values were calculated by two-tailed unpaired student's T-test. Reporter = *eri-1(mg366);Is[lin-41-promoter::gfp::lin-41-3'utr]*).

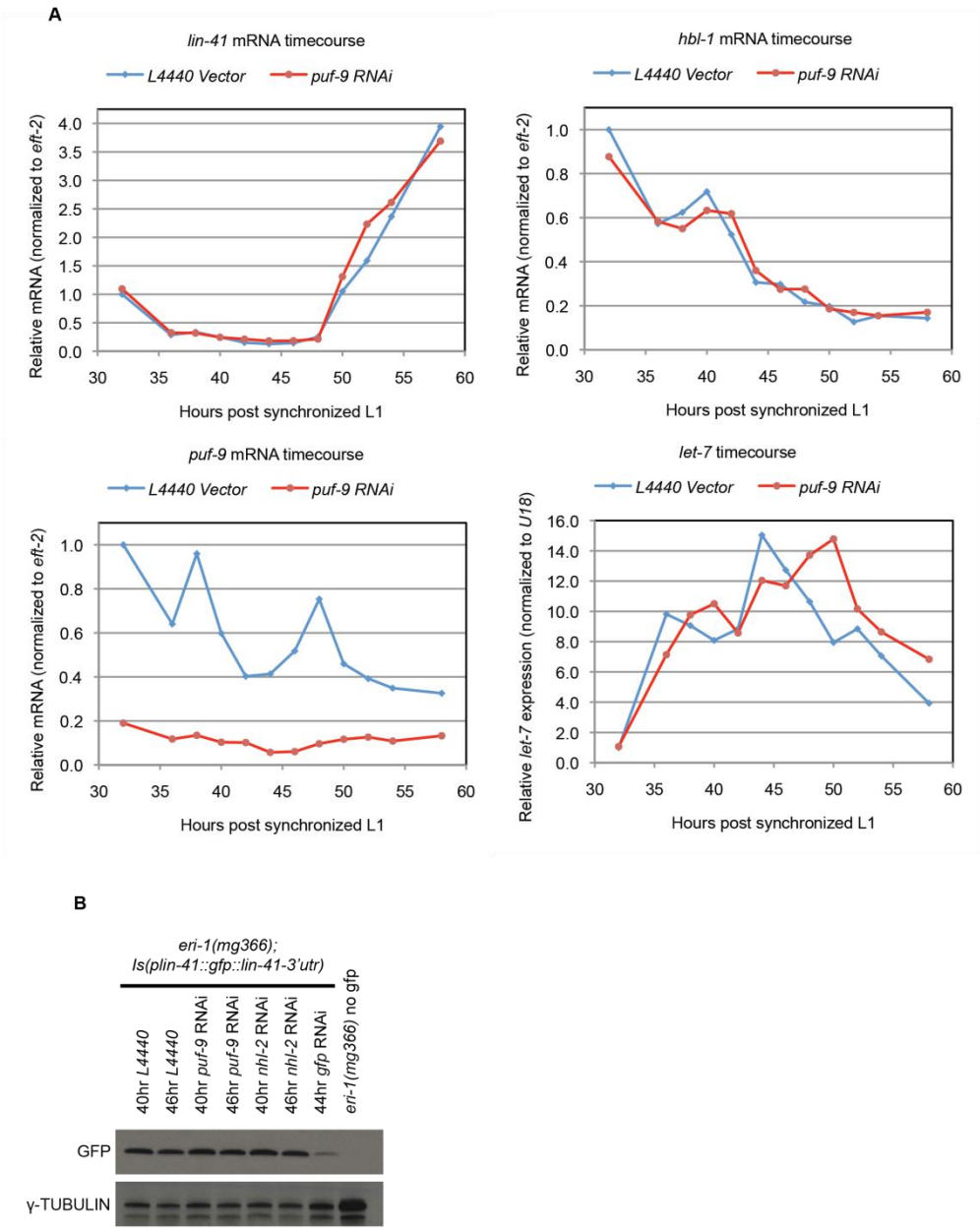

Figure 2.13 Quantification of endogenous *lin-41* mRNA and *lin-41* 3'UTR GFP reporter protein levels in *puf-9* RNAi.
(A) Global *lin-41* mRNA levels are unchanged upon *puf-9* knockdown in *eri-1(mg366)* worms grown at 20°C for the indicated number of hours after feeding of synchronized L1s. qRT-PCR confirms *puf-9* knockdown, while *hbl-1* and *let-7* levels are also displayed. Each point represents the average of technical duplicates. **(B)** Global *lin-41* GFP reporter protein levels are unchanged upon *puf-9* knockdown in *eri-1(mg366)* worms grown at 20°C for the indicated number of hours after feeding of synchronized L1 worms. Western blot membranes were probed for GFP and γ-Tubulin.

Table 2.1 List of PREs in miRNA target 3'UTRs bound by PUF-9

3'UTR	PBS Motif 1	PBS Motif 2	PBS Motif 3	Max PBS RPM	Description
hbl-1	TGTACAAT			3946.85	*let-7* target
lin-28	TGTATTTT			1.06	*let-7* target
lin-41	TGTAAATA	TGTAATTT		132.46	*let-7* target
K10C3.4	TGTATATA	TGTACATT		2076.74	*let-7* target
opt-2	TGTATAAA			12.94	*let-7* target
ztf-7	TGTAATTT	TGTAATTT		250.75	*let-7* target
T27D12.1	TGTACAAA			27.94	*let-7* target
let-526	TGTATAAC			142.37	*let-7* target
die-1	TGTAATCT			13.41	*let-7* target
mef-2	TGTATAAA	TGTATTTT		788.40	miR-1 target
sup-26	TGTACATA			3275.37	miR-35 target
lin-14	TGTATCAC			197.73	*lin-4* target
lgg-1	TGTAATAA	TGTACAAT		1724.29	new PUF-9 target
tts-1	TGTATATA			75542.09	new PUF-9 target ncRNA
puf-9	TGTAAATT	TGTAATCT	TGTAAACC	501.98	new PUF-9 target
eft-2	None			100.61	high expression control
rpb-10	None			0	high expression control
mdt-9	TGTAAAAT			0	medium expression control
ttr-22	None			0	low expression control

* Nucleotides matching the consensus PUF response element 5' end UGUA are in red.
Note: CLIP-seq reads are sequenced as cDNA, and T in cDNA = U in RNA.

Table 2.2 Oligonucleotide sequences

PUF-9-GFP cloning primers with restriction sites underlined	
Name	**Sequence (5' to 3')**
puf-9 promoter & CDS F	CTAAGGCGCGCCCAGACCTCGTTATAGCCAT
puf-9 promoter & CDS R	ACTAGCGGCCGCAAACGGGTGATTACTAAAAT
puf-9 3'UTR F	ATGGACGCGTCGGAAACTGGACGACGATG
puf-9 3'UTR R	GTCTCCGCGGGGAAAACAAATTCAACAGAAAGAAC
lin-41 reporter sequences	
lin-41 promoter F	TATCTTGTTGGCTTTTTGTT
lin-41 promoter R	TTCACTTTTTCCAAGTCTGAA
lin-41 3'UTR F	ACACTTTCTTCTTGCTCTTTAC
lin-41 3'UTR R	TCGAGTTCTTCAATTGATGTGT

Table 2.3 Quantitative RT-PCR primers

Gene	**Forward (5' to 3')**	**Reverse (5' to 3')**
eft-2	ACGCTCGTGATGAGTTCAAG	ATTTGGTCCAGTTCCGTCTG
rpb-10	GCTTCACATGCGGCAAAGTC	TCGAGAGCATCTCCTTCACTG
mdt-9	TCCATCTTGTGAACTCCGTGG	CGGCGATTTTCCGTCTTTCC
ttr-22	TGATTCATTGCTCCGATGCTT	CGAGTCATATATCGTTCCATCGTC
lin-41	GGTTCCAAATGCCACAAGAG	AGGTCCAACTGCCAAATCAG
hbl-1	ATGGAGAAAGATGGCGAGAG	AAACTCATTCGGCTGTGGAG
k10c3.4	TGACGAGGCACATGATCCAG	ACGGGGACTCTGGTCAACTC
opt-2	GCGTTAGCTCGAAAGGCAAAA	GTTCGCAGAATTCGTTGGACAC
ztf-7	AGCCATTGAGTCACCTTCCG	GCTGCTGCAAGTGATTTCGT
lin-28	GATAGGCTGCCAGATGTAGTTG	TGAGCCAAAGTATCGAGGTG
tts-1	AACTTGACCGGCTCAACCATGT	CATTTGAAGAAGTGCTTCCATTTACG
mef-2	GGCTGCACTACAAGCATCAA	TGAGGATGAGGAAGGAGCAA
lgg-1	TCCTCGTGATGGTCCTGGTA	GTTAGACGACGCCTCCAACT
puf-9	GAATCATTCGGACAATCAGTTACTA	GAACGGTGTTGTGGTGAAATAG
sup-26	CCATGGACGTGTCCAAAACC	AAGGAGTCGAGTCGTGATGC

Table 2.4 Sequencing library barcodes

Core ID	Name	Barcode	Sample
13053	THM1	ATCACG	PUF-9-GFP Adult
13054	THM2	CGATGT	PUF-9-GFP Embryo
13055	THM3	TTAGGC	PUF-9-GFP L1
13056	THM4	TGACCA	GFP-ALG-1 Adult
13057	THM5	ACAGTG	GFP-ALG-1 Embryo
13058	THM6	GCCAAT	GFP-ALG-1 L1

Table 2.5 HITS-CLIP barcodes and primers

3' DNA linker oligos* (5' phosphorylated, and 3' block with inverted deoxythymidine)	
Index 1	5' p ATCACGTCGTATGCCGTCTTCTGCTTGidT 3'
Index 2	5' p CGATGTTCGTATGCCGTCTTCTGCTTGidT 3'
Index 3	5' p TTAGGCTCGTATGCCGTCTTCTGCTTGidT 3'
Index 4	5' p TGACCATCGTATGCCGTCTTCTGCTTGidT 3'
Index 5	5' p ACAGTGTCGTATGCCGTCTTCTGCTTGidT 3'
Index 6	5' p GCCAATTCGTATGCCGTCTTCTGCTTGidT 3'
5' RNA linker	
5' RNA linker	5' GUUCAGAGUUCUACAGUCCGACGAUC 3'
Barcoded RT primers	
Index 1	5' CAAGCAGAAGACGGCATACGACGTGAT 3'
Index 2	5' CAAGCAGAAGACGGCATACGAACATCG 3'
Index 3	5' CAAGCAGAAGACGGCATACGAGCCTAA 3'
Index 4	5' CAAGCAGAAGACGGCATACGATGGTCA 3'
Index 5	5' CAAGCAGAAGACGGCATACGACACTGT 3'
Index 6	5' CAAGCAGAAGACGGCATACGAATTGGC 3'
Other primers	
P7 primer	5' CAAGCAGAAGACGGCATACGA 3'
P5 long primer	5' AATGATACGGCGACCACCGACAGGTTCAGAGTTCTACAGTCCGA 3'
Illumina primer A	5' AATGATACGGCGACCACCGA 3'
Illumina primer B	5' CAAGCAGAAGACGGCATACGA 3'

CHAPTER III – MORC-1 in nuclear RNAi

3.1 Abstract

Small noncoding RNAs are essential for germline function throughout the animal kingdom. Their functions include silencing foreign genetic elements, organizing euchromatin and heterochromatin regions, and transmitting an epigenetic memory of germline gene expression across generations. In *C. elegans*, different classes of small RNAs are well defined, and their basic biogenesis and effector pathways have been characterized. The endogenous small interfering RNA (endo-siRNA) pathway and the Piwi-interacting RNA (piRNA) pathway converge on two downstream nuclear pathways important for germline function. The hereditary RNAi (HRDE) pathway directs the establishment and maintenance of silenced heterochromatin, while the chromosome segregation RNAi (CSR) pathway promotes target gene expression in addition to the proper organization and function of centromeres on holocentric chromosomes. The coordinated function of these antagonistic pathways is essential for fertility, and their small RNA effector complexes are passed down across generations to program and protect the immortal germ cell lineage.

In this chapter, I present a study that identifies *microrchidia-1* (*morc-1*) as an effector protein in the somatic Nuclear RNAi (NRDE) and HRDE germline nuclear RNAi

pathways. I show that *morc-1* is required for repetitive transgene silencing by the exogenous RNAi pathway and that *morc-1* functions in the silencing of operon pre-mRNAs in the nucleus. In addition, I show that *morc-1* is required for RNAi inheritance across generations, but not for the biogenesis or inheritance of siRNAs themselves. Therefore, *morc-1* is likely an effector protein downstream of nuclear siRNA targeting. Most importantly, *morc-1* is required to maintain germline immortality at elevated temperatures, and loss of *morc-1* results in mislocalization of transgene heterochromatin.

3.2 Introduction

The nuclear RNAi pathway mediates transcriptional gene silencing.

In *C. elegans*, primary siRNAs and piRNAs are loaded into cytoplasmic Argonaute proteins including RDE-1, ALG-3/4, ERGO-1, and PRG-1 [7, 208, 228, 235]. Primary siRNAs guide Argonaute complexes to complementary target sequences on mRNA targets, recruiting RNA-dependent RNA polymerases (RDRPs) EGO-1 and RRF-1 to transcribe secondary siRNAs from Argonaute-RISC bound mRNAs [212, 301]. Secondary siRNAs are loaded into worm-specific Argonautes (WAGOs) to amplify the effects of RNA degradation in the cytoplasm, or into the NRDE-3 and HRDE-1 WAGOs that shuttle into the nucleus to mediate transcriptional and co-transcriptional gene silencing [5, 7, 197, 219].

NRDE-3 is expressed in the soma and mediates the downstream effects of inherited siRNAs and exogenous siRNAs, while HRDE-1 is expressed in the germline

and mediates the multigenerational inheritance of small RNAs [5, 219]. HRDE-1 and NRDE-3 do not have functional D-E-D-(D/H) catalytic tetrads in the Argonaute PIWI domain [200]. Hence, these secondary Argonautes do not possess endonucleolytic "slicer" activity present in the primary siRNA Argonautes that cleaves target mRNAs. Instead, they interrupt RNA Pol II elongation through NRDE-2, bind chromatin via NRDE-1 and NRDE-4, and guide the deposition of H3K9me3 by SET-25 and SET-32 methyltransferases [5, 219-224]. In concert, SET-25 has an H3K9me3 reader domain that potentially reinforces heterochromatin maintenance at nuclear RNAi target sites [189]. Downstream of nuclear RNAi, chromatin-binding proteins such as H3K9 methylation reader HPL-2 (Heterchromatin Protein 1 Like 2) silence target loci through unresolved mechanisms [224]. Altogether, the HRDE/NRDE nuclear RNAi pathway promotes a repressive heterochromatin state on target genes.

Nuclear RNAi mediates epigenetic inheritance of gene silencing through the germline and promotes fertility.

Recent studies have demonstrated that HRDE-1/siRNA complexes are necessary and sufficient to transmit RNAi-induced epigenetic silencing across generations [5, 223, 302]. Loss of germline nuclear RNAi leads to progressive sterility over multiple generations, resulting in a "germline mortality" (Mrt) phenotype characterized by loss of both sperm and oocytes, high incidence of males, and changes in oocyte chromosome number due to synapsis or segregation defects [5, 225, 227]. Loss of HRDE-1 or NRDE-2 causes germline mortality at elevated temperature, while loss of NRDE-1 or NRDE-4 causes germline mortality at all temperatures [5]. Because

NRDE-1 directly binds chromatin, and NRDE-4 is required for NRDE-1 recruitment on genes targeted by nuclear RNAi, NRDE-1 and NRDE-4 may be important for chromatin regulation in general. Recent studies suggest the nuclear RNAi pathway is required to silence retrotransposons and repetitive elements [226], and to prevent ectopic expression of spermatogenesis genes [227]. Still, it remains unclear why nuclear RNAi is required for germline immortality.

Microrchidia (MORC) proteins are conserved from plants to humans.

The “Microrchidia” *Morc-1* gene is named for a mouse mutant that exhibited small testes and sterility associated with failure of homologous chromosome pairing during prophase I [247, 248]. Germline dysfunction in *Morc-1(-/-)* males may result from loss of transcriptional silencing and DNA methylation on retrotransposons, combined with elevated H3K4 methylation [249]. In Arabidopsis, *AtMorc1* and *AtMorc6* are required to silence transposons located in pericentromeric heterochromatin. Interestingly, *AtMorc1/6* mutants also display defects in heterochromatin compaction and localization at the nuclear periphery, without changes in DNA or H3K9me2 methylations [250]. Hence, plant MORCs were proposed to mediate ATP-dependent changes in chromatin superstructure. All MORC proteins share a conserved N-terminal GHKL ATPase – coiled coil module. The GHKL ATPase is named after DNA Gyrase, HSP90, Histidine Kinase, MutL and is also found in DNA Topoisomerase [252].

Here, we present evidence that *C. elegans morc-1* functions in nuclear RNAi effector mechanisms, including pre-mRNA silencing of operons, multigenerational

inheritance of RNAi, and maintenance of germline immortality. We also find that *morc-1* is required for transgene silencing and transgene heterochromatin localization at the nuclear periphery. These data suggest that MORC-1 functions as a conserved link between nuclear RNAi, heterochromatin organization, and the epigenetic inheritance of gene silencing required to maintain the immortal germ cell lineage.

3.3 Results

morc-1 is required for transgene silencing in *C. elegans*

The JR672 worm strain has an integrated high copy transgene array, expressing GFP in blast cells of the lateral seam [303]. The exogenous RNAi pathway efficiently silences high copy transgene arrays in the *eri-1(mg366)* enhanced RNAi background, where *eri-1*-dependent endo-siRNAs are depleted; they no longer compete with transgene-derived siRNAs for limiting factors in target repression [251, 304]. Knockdown of genes required for exogenous RNAi, or factors required for both exogenous and endogenous RNAi, desilences the seam cell GFP reporter, forming the basis of an early screen for RNAi factors. This genome-wide RNAi screen found the *syn-16/morc-1* operon to be required for silencing of JR672 seam cell GFP in the *eri-1* background [251].

The microrchidia family of ATPases was found to be required for heterochromatin compaction and transgene silencing in *Arabidopsis* [250]. Further, our lab showed that RNAi targeting *morc-1* desilences JR672 seam cell GFP in the *eri-1* background [250]. Therefore, we hypothesized that worm *morc-1* could be a conserved link between the

RNAi pathway and chromatin organization. However, nuclear RNAi silences entire operons in the *eri-1* enhanced RNAi background. *eri-1* mutation also increases off-target RNAi effects [219, 305]. Thus, we needed to confirm a genetic requirement for *morc-1* in transgene silencing using a mutant allele that does not affect other genes in the operon. The *gk174232* nonsense allele truncates the predicted CW zinc finger in MORC-1, reduces *morc-1* mRNA expression by 8-fold in embryos, and leads to germline mortality at elevated temperatures (Figure 3.1). The *eri-1;JR672;morc-1(gk174232)* strain robustly expressed seam cell GFP from L2 to L4 stages, whereas seam cell GFP was silenced in *eri-1;JR672* worms (Figure 3.2). Thus, the genetic mutant phenotype is consistent with the *morc-1* RNAi phenotype.

morc-1 mediates efficient nuclear RNAi

Unlike the miRNA pathway that mediates post-transcriptional repression of mature mRNAs, the nuclear RNAi pathway mediates transcriptional repression and co-transcriptional repression [222]. More specifically, small RNAs guide the somatic NRDE-3 and germline HRDE-1 Argonautes to repress pre-mRNAs in the nucleus. *C. elegans* operons are expressed as long transcripts that are trans-spliced to 5' splice leader RNA sequences in the nucleus, and then exported to the cytoplasm. As a result, multi-gene operons can be silenced by nuclear targeting of a single pre-mRNA, but not by cytoplasmic targeting of a single mature mRNA in the absence of nuclear RNAi. The *lir-1/lin-26* operon is required for larval development. Loss of *lir-1* is has no obvious phenotype, while loss of *lin-26* is lethal due to defects in epithelial differentiation [219]. RNAi against *lir-1* also silences *lin-26* in the nucleus in wild-type worms but not in

nuclear RNAi defective mutants. Thus, wild type worms larvally arrest or die in the presence of *lir-1* RNAi, while nuclear RNAi defective mutants develop normally (Figure 3.3) [219].

The *lir-1* RNAi assay was used characterize nuclear RNAi sensitivity in *morc-1* null mutants. *morc-1(tm6048)* deletion mutants are resistant to *lir-1* RNAi, but *eri-1;morc-1* double mutants are sensitive to *lir-1* RNAi. In contrast, *nrde-2(gg91)* mutants and *eri-1;nrde-2* double mutants are completely resistant to the *lir-1* nuclear RNAi phenotype (Figure 3.4).

While canonical NRDE complex components such as *nrde-2* and *nrde-3* are essential for somatic nuclear RNAi [222], our data indicate that *morc-1* loss of function can be overcome by increased RNAi dosage. This observation could be explained by the hypothesis that *morc-1* mediates only a subset of nuclear RNAi mechanisms: heterochromatin repression but not co-transcriptional RNA Pol II stalling.

To further explore the requirement of *morc-1* in operon silencing by nuclear RNAi, we examined repression at a second locus that serves as readout for nuclear RNAi function [219]. *Abnormal cell lineage-15b* (*lin-15b)* and *lin-15a* form an operon that encodes two chromatin binding proteins important for cell fate specification in the six vulval precursor cells. Normally, only one vulval precursor adopts a primary vulval cell fate. Loss of both *lin-15b* and *lin-15a* results in mis-specification of the vulval precursor cells, so multiple pseudo-vulvae can develop, causing a multivulva (Muv) phenotype. Loss of either *lin-15b* or *lin-15a* alone does not produce the Muv phenotype [306].

In an enhanced RNAi background, knockdown of *lin-15b* also silences *lin-15a*, resulting in the development of multiple pseudo-vulvae (Figure 3.5). *eri-1;morc-1*

mutants are completely non-Muv on *lin-15b* RNAi, even though >90% of *eri-1* worms develop Muv (Figure 3.6). Hence, *morc-1* is required for nuclear silencing of the *lin-15b/lin-15a* operon.

Nuclear RNAi also mediates the spreading of repression from one member of a gene family to close homologs. For example, genetic mutation of the *dumpy-13* (*dpy-13)* collagen results in short, fat worms. However, nuclear RNAi against *dpy-13* can produce much more severe phenotypes by depleting closely related collagens [305].

morc-1 is moderately resistant to *dpy-13* RNAi in both wild-type and enhanced RNAi backgrounds (Figure 3.7-3.8). While about half of *eri-1;morc-1* worms become “dumpy balls” like *eri-1* worms, *eri-1;nrde-2* worms are completely resistant to the “dumpy ball” phenotype. Altogether, we observed a reduced penetrance of somatic nuclear RNAi phenotypes in *morc-1* mutants.

morc-1 is not required for Exogenous RNAi

Although *morc-1* mutants are partially defective in nuclear operon silencing and nuclear RNAi spreading, the exogenous RNAi pathway remains intact. *Posterior segregation-1* (*pos-1*) is a maternally deposited mRNA required for embryonic patterning. Knockdown of *pos-1* in the maternal germline produces highly penetrant embryonic lethality [2]. This phenotype was used to identify the some of the first factors required for RNAi, including the RNAi-Defective-1 (RDE-1) Argonaute that binds primary siRNAs [208]. *pos-1* is expressed as an independent mRNA transcript, not an operon, so nuclear RNAi is not required to produce the *pos-1* RNAi phenotype.

RNAi against *pos-1* causes embryonic lethality in wild-type worms, *nrde-2* and

morc-1 mutants, but not RNAi-defective *rde-4* mutants (Figure 3.9A). When *pos-1* RNAi dosage is reduced to 20% by dilution in L4440 vector control, *nrde-2* and *morc-1* worms are moderately resistant to the embryonic lethality phenotype. This result suggests that *morc-1* is not essential for exogenous RNAi but enhances the potency of RNAi, consistent with previous reports of nuclear RNAi function [307].

The *uncoordinated-22 (unc-22)* twitch/paralysis phenotype was originally used to characterize the RNAi response to dsRNA versus sense or antisense RNA [203]. At low doses, dsRNA against the *unc-22* muscle myosin kinase causes twitching. At high doses of dsRNA, *unc-22* knockdown causes complete paralysis.

nrde-2 and *morc-1* mutants are susceptible to twitching and paralysis induced by dsRNA targeting *unc-22* (Figure 3.9B). Paralysis occurs in 31% of *eri-1* worms and 29% or *eri-1;morc-1* worms, while twitching occurs in 69% of *eri-1* worms and 71% of *eri-1;morc-1* worms. Together, the classical *pos-1* and *unc-22* RNAi phenotypes demonstrate that *morc-1* is not required for exogenous RNAi in maternal germline or muscle tissue.

morc-1 mediates transgenerational RNAi inheritance in the soma

dpy-11 encodes a thioredoxin enzyme expressed in the hypodermis. *dpy-11* knockdown causes a moderate dumpy (Dpy) phenotype in the P0 generation grown on RNAi [221]. As somatic RNAi can be inherited for one generation, F1 progeny grown in the absence of RNAi are also Dpy. Importantly, inheritance of somatic RNAi requires Argonaute NRDE-3 and the nuclear RNAi pathway [221].

morc-1 mutants are susceptible to the *dpy-11* RNAi phenotype in the P0

generation, but are resistant to the Dpy phenotype at F1 (Figure 3.10). In contrast, wild type and *eri-1* mutants are Dpy at both P0 and F1. Therefore, somatic RNAi is functional in *morc-1* mutants, but somatic RNAi inheritance is attenuated.

morc-1 mediates transgenerational RNAi inheritance in the germline

The YY513 strain expresses a GFP-Histone-2B transgene driven by a *pie-1* promoter in the germline [5]. In YY513 worms, *gfp* RNAi silences GFP signal. In the absence of additional RNAi treatment, GFP silencing persists for six generations in a wild-type background. However, *hrde-1* mutants do not inherit GFP silencing because they lack the germline nuclear Argonaute that transmits inherited small RNAs across generations and mediates their downstream silencing effects [5] (Figure 3.11).

gfp RNAi silences the YY513 GFP reporter in wild type worms, *hrde-1* mutants, and *morc-1* mutants (Figure 3.12-13). GFP silencing persists for multiple generations in wild-type worms but is lost in *hrde-1* mutants at the F1 generation. *morc-1* mutants display an intermediate phenotype, where GFP silencing persists for only one generation after RNAi treatment (Figure 3.12-13). Like *hrde-1* mutants, *morc-1* mutants are defective in inherited RNAi but not exogenous RNAi in the germline.

morc-1 is not required for biogenesis or inheritance of 22G siRNAs across generations

Next, we sought to determine whether *morc-1* mutants are deficient in small RNA inheritance and/or their downstream effector functions. Wild-type, *hrde-1* mutant, and *morc-1* mutant YY513 GFP reporter worms were treated with L4440 vector or *gfp* RNAi for one generation, and their progeny were grown in the absence of RNAi for three

generations. RNA was collected from adult worms at each generation, and *gfp* small RNA levels were measured by Taqman qRT-PCR. Wild-type levels of 22nt antisense *gfp* siRNAs were detected in *hrde-1* and *morc-1* mutants treated with *gfp* RNAi (by feeding *E. coli* that express long dsRNA from the *gfp* coding sequence) (Figure 3.14). Therefore, production of 22G secondary siRNAs from long dsRNA precursors was not impaired in the P0 generation treated with RNAi. In the F1 progeny, GFP siRNAs are inherited in wild-type worms, *hrde-1* mutants, and *morc-1* mutants. By the F2 and F3 generations, *morc-1* mutants inherited wild type levels of GFP small RNA, in contrast to *hrde-1* mutants which exhibit a moderate reduction in siRNA levels (Figure 3.14). HRDE-1 is a germline Argonaute protein that binds nuclear small RNAs to transmit and maintain RNAi across generations. As expected, inherited siRNAs are depleted in *hrde-1* mutants.

Overall, *morc-1* mutants are not defective in small RNA biogenesis, exogenous RNAi in the cytoplasm, or inheritance of small RNAs across generations. However, *morc-1* mutants are defective in nuclear RNAi and the functional inheritance of RNAi. Together, these results indicate that *morc-1* functions in the effector mechanism downstream of nuclear small RNAs and inherited small RNAs. RNAi against transcriptional gene silencing factors de-represses transgene reporters in the P0 generation [251], while loss of an overlapping set of factors in the germline causes de-repression after two to three generations [184]. The timing of transgene de-silencing in *morc-1* soma (P0) and germline (F2) is consistent with the timing observed for other transcriptional silencing factors such as *hpl-2*, which binds and represses heterochromatin at H3K9me3 [308]. Differences in the timing of transgene desilencing

in soma versus germline might reflect the fact that chromatin modifications are reset during embryogenesis at each generation [173, 181]. While germline Argonautes (HRDE-1 and CSR-1) and the associated chromatin modification machinery are able to re-establish germline expression patterns based on which genes were expressed in the previous generation, the memory of somatic gene expression is not transmitted beyond one generation.

morc-1 is required for germline immortality at elevated temperatures

Small RNA pathways regulate important processes in the germline, including chromosome segregation, foreign DNA element silencing, and the control of spermatogenic and oogenic gene expression patterns. Mutations in core RNAi factors such as *eri-1* or *rde-4* are sterile at elevated temperatures of 25°C due, in part, to loss of ALG-3/4-associated male 26G RNAs. 22G RNAs triggered by male 26G RNAs can mediate silencing through the WAGO secondary Argonautes [228]. However, most 22G RNAs triggered by male 26G RNAs associate with the CSR-1 Argonaute required for chromosome segregation during mitosis and meiosis. The CSR-1/22G RNA complex promotes germline gene expression in progeny, transmitting the paternal load of germline “memory” downstream of ALG-3/4 [231]. Similarly, mutations in *C. elegans* piRNA Argonaute *prg-1* results in reduced brood size and progressive sterility over 50 generations, resulting from desilencing of repetitive DNA elements [225]. Intermediate in severity, nuclear RNAi pathway mutations cause progressive sterility at normal or elevated temperature over five to seven generations [5]. Nuclear RNAi mutants display a high incidence of males (Him) phenotype, suggesting defects in chromosome

synapsis or segregation. Progressive sterility occurs in both male and female germline, unlike the temperature sensitive sterility caused by loss of 26G RNAs. The mechanism behind germline mortality in nuclear RNAi mutants remains unsolved.

Consistent with its role in nuclear RNAi, *morc-1* worms also display a germline mortal phenotype. *morc-1* worms are fertile at 20°C but become sterile within five to seven generations after a shift to 25°C (Figure 3.15A). In addition, germline nuclei appear grossly abnormal with disorganized chromatin after four generations at elevated temperature (Figure 3.15B). The *tm6048* deletion truncates most of the conserved N-terminal ATPase domain, resulting in a frameshift and early stop codon in the coiled coil domain, upstream of the CW Zinc finger domain and C-terminal nuclear localization signal. Therefore, *tm6048* is a predicted null allele. Both the *tm6048* deletion and *gk174232* nonsense alleles are germline mortal.

morc-1 is required for transgene heterochromatin localization at the nuclear periphery

Because MORC proteins mediate chromatin compaction in Arabidopsis and chromatin unwinding in mammalian cells, we hypothesized that *morc-1* functions in chromatin organization downstream of nuclear RNAi. Repetitive transgenes are silenced by RNAi pathways in *C. elegans*, leading to transcriptional repression, H3K9me2/3 deposition, heterochromatin compaction, and anchoring at the nuclear periphery [189, 195, 251]. Because *morc-1* is required for both nuclear RNAi and efficient transgene silencing, we hypothesized that *morc-1* might be required for peripheral localization of heterochromatinized transgenes. Indeed, H3K9me2 and H3K9me3 are required for heterochromatin anchoring at the nuclear periphery, marks

that may be placed by nuclear RNAi [189].

The *gwIS4* transgene contains ~300 copies of a *gfp-lacI/lacO* array, which is integrated in the genome, maintained in compacted heterochromatin, and anchored to the nuclear periphery [189]. GFP-LacI binds to the *lacO* sequences, labeling the *gwIS4* array within the nucleus. Thus, two GFP foci appear in each diploid cell, anchored at the nuclear membrane. H3K9me2/3 is required for heterochromatin anchoring at the nuclear periphery. Knockdown or mutation of H3K9me3 methyltransferase *set-25* causes the transgene array to detach from the periphery [189].

We crossed the *gwIS4* reporter into *morc-1(tm6048)* and *nrde-2(gg91)*. Similar to *set-25* mutants, *morc-1* mutants and *nrde-2* mutants display a shift in localization of the *gwIS4* array away from the nuclear periphery (Figure 3.16-17). These results suggest that *morc-1* and the nuclear RNAi pathway are important for maintaining the heterochromatin state of the *gwIS4* array, or for anchoring the array at the nuclear lamina.

MORC-1 is likely dispensible for biogenesis of endogenous siRNAs

Preliminary experiments show that *morc-1(tm6048)* worms express wild-type levels of a representative 26G RNA (26G-O3) in embryos, wild-type levels of mRNA targets silenced by 26G RNAs, and wild-type levels of a pre-mRNA target silenced by the nuclear RNAi pathway downstream of 26G RNAs. In contrast, 26G-O3 was depleted in *eri-1(mg366)* and *rde-4(ne301)* mutants, while pre-mRNA and mature mRNA levels of 26G RNA targets were elevated (Figure 3.18). This result is consistent with the finding that *morc-1* is not required for the biogenesis of 22G siRNAs downstream of exogenous

gfp dsRNA (Figure 3.14). Therefore, we hypothesize that *morc-1* functions downstream of small RNA biogenesis, in the effector phase of nuclear RNAi function.

A recent study showed that *hrde-1* and *nrde-2* mutants are not depleted of small RNAs that map to nuclear RNAi target genes; 22G secondary siRNAs are produced despite the loss of transcriptional silencing or H3K9me3 on targets [226]. Similarly, we did not detect a requirement for *morc-1* in the biogenesis or inheritance of secondary siRNAs. Perhaps *morc-1* must be grown at elevated temperature to elicit defects in small RNA biogenesis or inheritance, which is true for *rsd-2/6* siRNA amplification mutants [227]. Indeed, *morc-1* and *rsd-2/6* mutants display temperature-sensitive germline mortality at 25°C.

A *morc-1::gfp* transgene rescues the nuclear RNAi and fertility defects of *morc-1(-)*

morc-1 is required for germline maintenance, nuclear RNAi in the soma, and inherited RNAi in the germline. *morc-1* is the second gene in an operon, making it difficult to define the endogenous promoter region. Therefore, we made a transgene driven by the ubiquitously expressed *dpy-30* promoter and a permissive *tbb-2* 3'UTR: *xkEx50[dpy-30p::morc-1::gfp::tbb-2utr; myo-2p::rfp]*. When crossed into the *morc-1(tm6048)* background, this transgene restores somatic nuclear RNAi function in the *lir-1* assay (Figure 3.19).

This complex array was UV-integrated in the genome and outcrossed. The resulting transgenic worm strain expressed nuclear GFP throughout the soma and germline. When crossed into the *morc-1(tm6048)* background, *xkIs50[dpy-30p::morc-1::gfp::tbb-2utr; myo-2p::rfp]* restores germline immortality at elevated temperature

(25°C). *morc-1* worms become sterile after five generations at 25°C, while *morc-1* worms with transgene are fertile for at least nine generations (Figure 3.20). Hence, the *morc-1* transgene is functionally active in both soma and germline. In worm lysates, MORC-1-GFP is in the chromatin-associated pellet upon low speed centrifugation (12,000xg for 12 minutes), but released into the supernatant fraction after sonication. Imaging of this transgene shows that GFP colocalizes with DAPI within the nucleus. Surprisingly, antibody staining shows that MORC-1-GFP is excluded from H3K9me3 foci in adult intestinal nuclei (Figure 3.21). This result is unexpected because H3K9 methyltransferase homologs recruit AtMORC1/6 dimers to AGO4-siRNA target sites in *Arabidopsis* [270].

3.4 Discussion

MORC proteins have been implicated in heterochromatin organization, and transposon silencing in plants and mammals. However, the molecular mechanisms of MORC proteins remain elusive. We show that *morc-1* forms a link between nuclear RNAi, heritable gene silencing, chromatin organization, and the maintenance of germline immortality. Importantly, we demonstrate that *morc-1* mediates multigenerational siRNA inheritance, beyond functions restricted to a single generation as previously reported for MORC homologs [250, 258]. So far, heritable gene silencing through the HRDE-1 nuclear RNAi pathway has been studied in two phases: establishment and maintenance [5, 302]. Primary small RNAs and their Argonaute cofactors, such as piRNAs and PRG-1, are necessary for triggering secondary siRNAs

in the establishment of germline silencing. In turn, HRDE-1 is required for establishment of silencing in the germline, mediating inheritance of secondary siRNAs to the next generation, and re-establishing silencing at the level of histone modification and chromatin organization. Inherited gene silencing is lost when downstream chromatin binding proteins such as MORC-1 are mutated. It is not known whether factors such as *morc-1* are required for amplification of silencing signals in the nucleus during establishment, or in the inheriting generations during maintenance. Our data suggests that *morc-1* is dispensable for inheritance of secondary siRNAs but required for their downstream effects.

Importantly, the HRDE-1 nuclear RNAi pathway functions downstream of piRNAs, protecting the genome from transposons and other repetitive elements. Our collaborators recently reported that MORC1 is required for silencing retrotransposons in the mouse germline, including LINE1 elements [249]. The transposon expression profile of *Morc1(-)* mutant mouse testes is similar to pre-pachytene piRNA mutants such as *Miwi2(-)*. Since piRNA expression levels are not perturbed in *Morc1(-)* mutant mice, MORC1 might be a downstream effector of mammalian piRNAs at the chromatin level. An exciting implication is that MORC proteins may promote fertility downstream of small RNAs throughout the animal kingdom.

When tethered to a promoter by GAL4, human MORC3 confers transcriptional repression of luciferase reporters in HEK 293T cells [260]. However, the mechanism of transcriptional repression is unknown. In *C. elegans*, tethering of CSR-1 Argonaute to pre-mRNA induces the production of heritable 22G RNAs that activate gene expression in *cis* and in *trans* [240]. We hypothesize that the NRDE-3 and HRDE-1 nuclear RNAi

complexes endogenously tether MORC-1 to small RNA target sites, silencing transcription. In the future, it will be informative to see whether artificial MORC-1 tethering can (1) induce transcriptional silencing in *cis*, (2) induce transcriptional silencing in *trans*, (3) induce heritable silencing, and (4) counteract CSR-1 on shared targets. If MORC-1 tethering induces transcriptional silencing in *cis* but not *trans*, it may only be important in the effector phase of nuclear RNAi, not the amplification phase. If MORC-1 tethering induces silencing in “tethered” P0 worms, but not in “untethered” F1 progeny, we can infer that MORC-1 mediates epigenetic changes that are reset each generation.

Our results suggest that *morc-1* is required for the localization of transgene heterochromatin arrays to the nuclear periphery. It is currently unclear how *morc-1* functions to silence heterochromatin–whether it regulates H3K9 methylation, directs chromatin compaction, or plays a direct role in anchoring. Emerging studies suggest that H3K9me1/2 marks mediate anchoring through chromo-domain proteins (International Worm Meeting 2013). We hypothesize that nuclear RNAi and *morc-1* promote H3K9 methylation to drive transcriptional repression, heterochromatin compaction, and peripheral anchoring. This model is consistent with new data from Natasha Weiser suggesting that *morc-1* regulates the balance of germline H3K9 vs H3K4 methylation (see Chapter 4.2).

AGO1 directs transcriptional gene silencing in humans [309]. Nuclear DICER resides at sites of overlapping sense and antisense transcription, processing dsRNA into endogenous siRNAs in HEK293 cells [310]. These small RNAs are loaded into AGO1, which represses transcription and triggers H3K9me2 deposition. NRDE-2 and

MORC-1 homologs are conserved in humans, so it would be interesting to see if human NRDE2 is involved in Pol II co-transcriptional inhibition, and whether any of the four human MORCs are required for heterochromatin formation or organization on endogenous siRNA targets.

C. elegans tertiary siRNAs were recently described as heritable agents of paramutation, “an allele-dependent transfer of epigenetic information, which results in the heritable silencing of one allele by another” [237, 238]. piRNA target binding triggers RDRP-mediated synthesis of 22G secondary siRNAs. These secondary siRNAs are bound by HRDE-1, which enters the nucleus and transcriptionally silences active alleles. Through uncharacterized mechanisms, HRDE-1-bound secondary siRNAs trigger another round of siRNA synthesis, producing “tertiary” siRNAs [237]. Once an allele is stably silenced by HRDE-1, it becomes “paramutated” if it produces secondary and tertiary siRNAs that propagate silencing in *trans*. “Paramutated” alleles can transmit tertiary siRNAs throught the germline to mediate paramutation in subsequent generations [237].

It will be interesting to see whether chromatin-modifying effectors of nuclear RNAi are required for the propagation of tertiary siRNAs. For example, *set-25* H3K9me3 methyltransferase mutants are unable to heterochromatinize and efficiently silence nuclear RNAi targets. Hence, they are defective in the effector phase of inherited germline RNAi [224]. Even though chromatin-level effector mutants *set-25* and *hpl-2* fail to silence targets, it is unclear whether inherited small RNA/HRDE-1 complexes can still trigger the generation of new tertiary siRNAs that propagate to the next generation. In other words, can heterochromatin modification be dissociated from inherited small RNA

propagation? It is already known that small RNA/HRDE-1 complexes can propagate silencing across generations without also inheriting the silenced alleles themselves [311, 312]. Does a tertiary small RNA need to heterochromatinize a target allele in order to trigger new tertiary small RNAs? Is *morc-1* required for this process? Encompassing all of these questions is the central question of whether there is a partial state of paramutation, where the allele is not silenced but still produces heritable siRNAs.

MORC-1 is intricately tied to nuclear RNAi, epigenetic inheritance, and maintenance of the immortal germline. In the future, studying mechanisms of MORC-1 function could uncover fundamental principles of chromatin biology.

3.5 Methods

Strains & worm maintenance

C. elegans were maintained using standard procedures at 20°C unless otherwise noted. Bristol N2 strain was used for wild-type control. Alleles used in this study include *eri-1(mg366), rde-4(ne301), nrde-2(gg091), hrde-1(tm1200), morc-1(tm6048), morc-1(gk174232), set-25(n5021), met-2(n4256), pkIs32[pie-1p::gfp::h2b]* (YY513), *wIs54[scm::gfp]* (JR672), *xkIs51(ges-1p::morc-1::gfp::unc-54-3'utr; myo-2p::rfp], xkEx50(dpy-30p::morc-1::gfp::tbb-2-3'utr; myo-2p::rfp], xkIs50(dpy-30p::morc-1::gfp::tbb-2-3'utr; myo-2p::rfp], gwIs4[baf-1::gfp-lacI::let-858-3'utr; myo3::rfp]* (GW76).

Transgene silencing assay in *eri-1*;JR672

eri-1(mg366);JR672 reporter worms were crossed into *morc-1(gk174232).* Wild

type and *morc-1(-/-)* F2 sibling strains were derived from the same heterozygous F1 parent. Synchronized L1 worms were grown on OP50 food at 20ºC and GFP-positive seam cells were counted at L2, L3, and L4 stages. Worms were immobilized with 1mg/ml tetramisole on 2% to 3% agarose pads and imaged in GFP and brightfield channels on an Olympus BX61 microscope with a 4X objective.

RNAi sensitivity assays

Synchronized L1 worms were grown on 6cm RNAi plates seeded with feeding RNAi clones in HT115 *E. coli*. *lir-1* larval arrest / lethality, *dpy-13* dumpy, and *unc-22* twitching / paralysis phenotypes were scored in P0 adults at 72 hours. *pos-1* embryonic lethality was scored in F1 embryos. *lin-15b* multivulva was scored in F1 adults. *dpy-11* dumpiness was scored in P0 adults treated with RNAi and their F1 progeny grown without RNAi.

Germline mortality assays

Worms were maintained at 20ºC, embryos were isolated through hypochlorite preparation, and synchronized L1 worms were plated on OP50 food at 25ºC, designated as the P0 generation at elevated temperature. 30 L4 hermaphrodites were transferred to new plates at 25ºC, which produced the next generation. This protocol was applied at F1, F2, F3, and so on. For each generation tested, single hermaphrodites were transferred to 6 cm plates with OP50 food at 25ºC, and fertility was measured by counting live progeny.

RNAi inheritance assays

YY513 reporter worms stably express GFP in germline nuclei. YY513 reporter worms in wild-type, *hrde-1(tm1200),* and *morc-1(tm6048)* background were maintained at 20°C on OP50 food. Embryos were isolated by hypochlorite preparation, and synchronized L1 worms were plated on *L4440* vector or *gfp* feeding RNAi in HT115 *E. coli*. P0 gravid adults were subjected to hypochlorite egg prep. F1, F2, and F3 synchronized L1 worms were plated on OP50 *E. coli* without RNAi. At each generation, gravid adults were imaged with an Olympus BX61 microscope or collected in Tri Reagent for RNA extraction. Germline nuclear GFP brightness was categorically scored as on, dim, or off (N≥100 worms). GFP 22G small RNA levels were quantified by Taqman qRT-PCR, normalized by U18 small RNA Taqman qRT-PCR.

gwIS4 transgene array localization assays

gwIS4 transgene expresses GFP-LacI driven by a baf-1 promoter, which is highly expressed in embryos. GFP-LacI binds to *lacO* sequences in the *gwIS4* transgene integrated within the genome. gwIS4 reporter worms in the wild type, *set-25*, and *morc-1(tm6048)* backgrounds were maintained at 20ºC. L4 hermaphrodites were picked to plates at 25C to lay “P0” generation eggs at elevated temperature. P0 L4s were picked to new plates to produce the F1 generation. F2 embryos were dissected from day 1 adults, freeze-cracked, and DAPI stained by Seydoux protocol. Embryos were imaged in GFP and DAPI channels with an Olympus BX61 microscope at 60X magnification, across 10um of Z-stacks at 250nm intervals. Deconvolution was performed in Huygens Essential software. DAPI-labeled nuclear diameters were measured in ImageJ, and

nuclei were divided into three zones of equal volume. The distance from nuclear boundary to GFP arrays was measured in ImageJ, and array localization was assigned to Zone 1 (peripheral third), Zone 2 (intermediate third), or Zone 3 (interior third).

Quantification of small RNA, mRNA, and pre-mRNA in embryos

Wild type and mutant worms were grown at 20ºC for 72 hours, embryos were isolated by bleach prep and collected in Tri Reagent. RNA was isolated as described in Chapter 2. 26G and 22G small RNA quantification were performed by Taqman qRT-PCR as described in Chapter 2, using custom Taqman probes (Applied Biosystems) based on the sequences listed below. cDNA was generated from mRNA using oligo dT primer as described in Chapter 2. mRNA was quantified by qRT-PCR, using *eft-2* for normalization as described in Chapter 2. cDNA was generated from pre-mRNA using random hexamer primers. Pre-mRNA was quantified by qRT-PCR with primers that span exon-intron junctions, using *eft-2* for normalization.

morc-1::gfp expression plasmids

A 2.3kb *ges-1* promoter fragment, 2.9kb *morc-1* genomic coding fragment with no termination codon, 0.9kb *gfp* coding fragment with introns, and 0.8kb *unc-54* 3'UTR fragment were inserted into cloning vector pJK211 to generate plasmid pJK532*[ges-1p::morc-1::gfp::unc-54-3'utr].* A 4.1kb *dpy-30* promoter fragment and 0.6kb *tbb-2* 3'UTR fragment were swapped in to generate plasmid pJK499[*dpy-30p::morc-1::gfp::tbb-2-3'utr*]. The *ges-1* promoter and *unc-54* 3'UTR fragments were subcloned from plasmid pJK332. Other fragments were generated by PCR (primers in Table 3.2).

morc-1::gfp transgenic animals

Complex array injection mixes consisted of 120ng/µl E. coli genomic DNA, 2ng/µl *myo-2p::rfp*, 0.2ng/µl *dpy-30p::morc-1::gfp::tbb-2-3'utr*. Transgene arrays were injected into N2 wild type *C. elegans* gonads. Extrachromosomal array strain *xkEx50[dpy-30p::morc-1::gfp::tbb-2-3'utr; myo-2p::rfp]* was crossed into the *morc-1(tm6048)* mutant to test for rescue of somatic nuclear RNAi deficiency. Transgene arrays were integrated in N2 wild type worms by 254nm UV. The integrated strain *xkIs50[dpy-30p::morc-1::gfp::tbb-2-3'utr; myo-2p::rfp]* was backcrossed five times and crossed into the *morc-1(tm6048)* background to test for rescue of germline mortality. A second transgenic strain *xkIs51[ges-1p::morc-1::gfp::unc-54-3'utr; myo-2p::rfp]* was generated similarly, except that simple array injection mixes consisted of 95ng/µl *pBlueScript*, 2ng/µl *myo-2p::rfp*, and 3ng/µl *ges-1p::morc-1::gfp::unc-54-3'utr*.

Immunofluorescence microscopy for H3K9me3 in intestinal nuclei

Adult worms expressing the *xkIs51[ges-1p::morc-1::gfp::unc-54-3'utr; myo-2p::rfp]* array were dissected and freeze-cracked on poly-lysine slides. Slides were fixed in methanol at -20°C and washed at room temperature with PBS+0.2% Tween-20. Slides were incubated with primary antibody (Millipore 07-523) in a humid chamber overnight at 4°C. Slides were washed at room temperature and then incubated with secondary antibody (anti-rabbit Alexa 674) in a humid chamber for one hour at room temperature. Slides were washed and then incubated in DAPI for 15 minutes at room temperature. Slides were imaged in GFP, Cy5, and DAPI channels with an Olympus

BX61 microscope at 60X magnification.

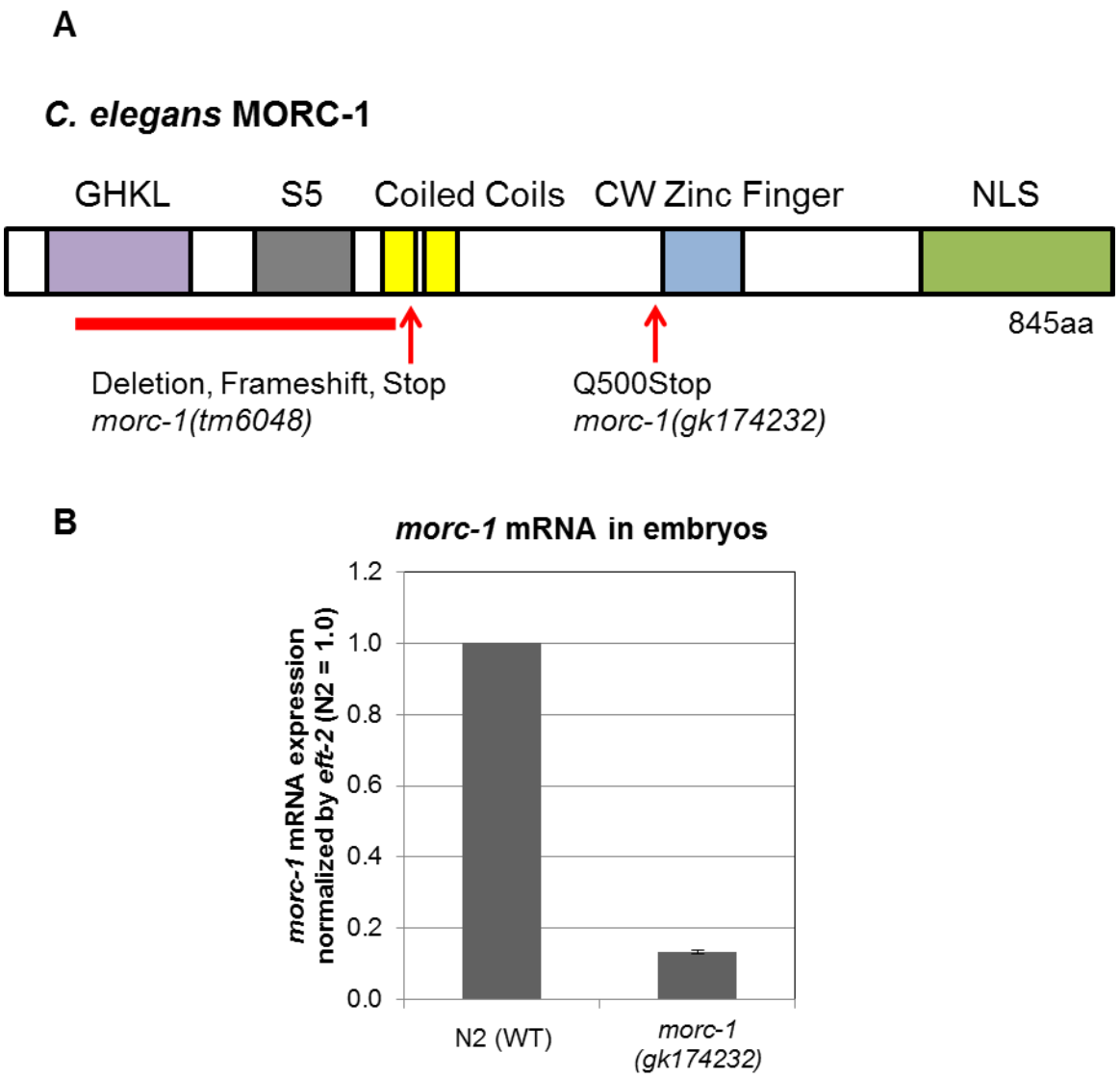

Figure 3.1 MORC-1 protein domains and genetic mutants.
(A) *morc-1(tm6048)* is a predicted null allele that deletes the GHKL+S5 ATPase, resulting in a frameshift and early termination codon in the coiled coil domain. *morc-1(gk174232)* is a point mutation that introduces a stop codon upstream of the CW zinc finger. (**B)** Compared to wild type, *morc-1(gk174232)* mRNA expression is reduced, likely by nonsense mediated RNA decay.

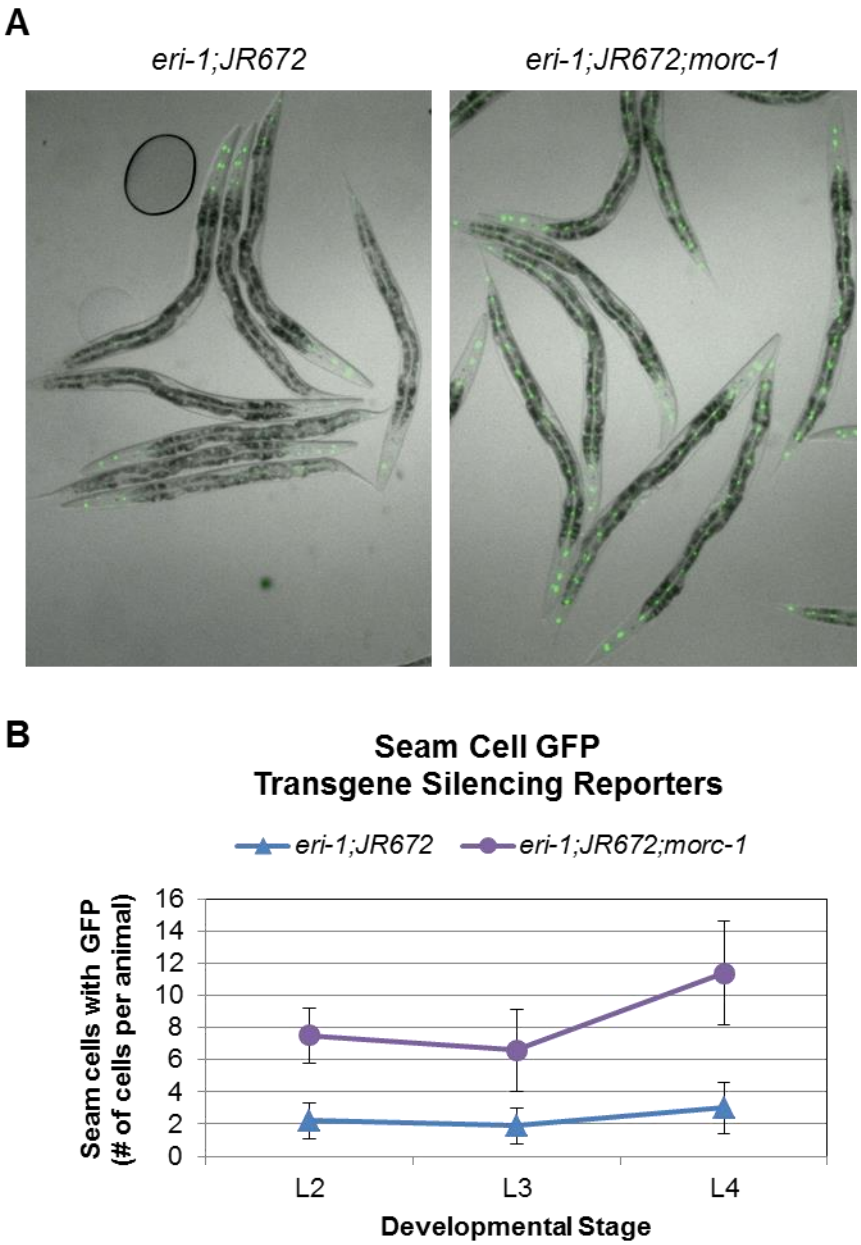

Figure 3.2. *morc-1* is required for efficient transgene silencing.
(A) Seam cell GFP reporter is visible in a few head and tail cells in *eri-1;JR672* worms at L4 stage. Seam cell GFP is desilenced in *eri-1;JR672;morc-1(gk174232)* mutants. (**B)** Quantification of seam cell GFP expression at L2, L3, and L4 stages. Mean +/- standard deviation are shown for three biological replicates. N=10 worms in each biological replicate, (N=30 worms total for each data point).

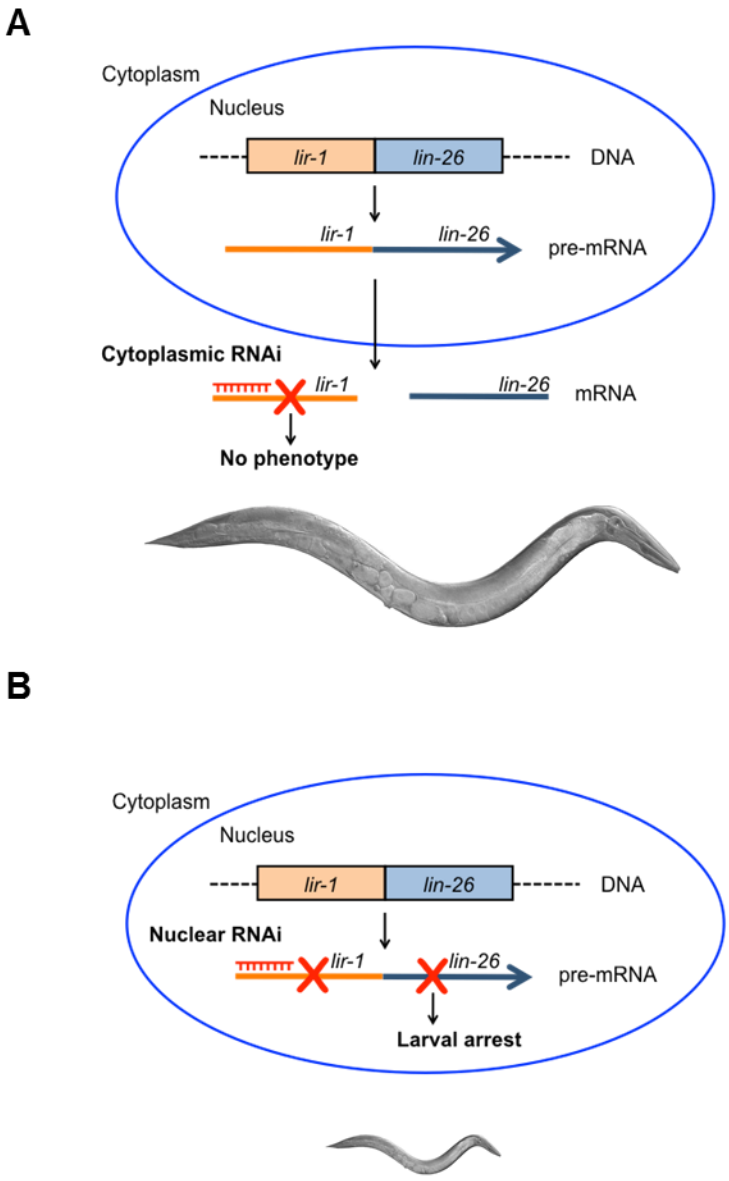

Figure 3.3 Model: the *lir-1* nuclear RNAi phenotype.
(A) Cytoplasmic RNAi knockdown of *lir-1* has no phenotype. (**B)** Nuclear RNAi knockdown of *lir-1* also silences *lin-26*, a part of the *lir-1* operon. Loss of *lin-26* causes larval arrest or lethality. Thus, sensitivity to *lir-1* RNAi serves as a readout for nuclear RNAi function. Worm images are not drawn to scale; the small worm signifies early larval arrest. Image credit: WormAtlas.

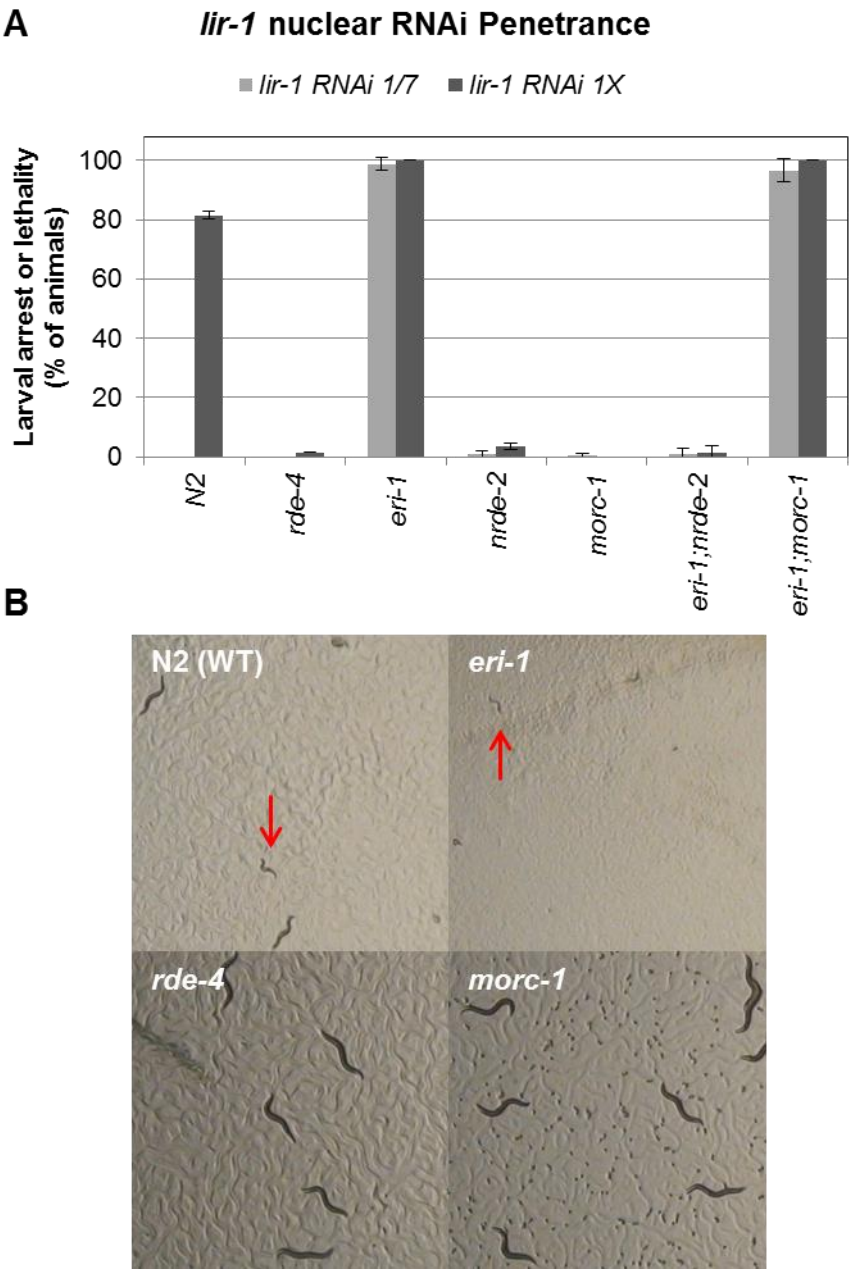

Figure 3.4 *morc-1* is required for efficient *lir-1* nuclear RNAi.
(A) *lir-1* RNAi sensitivity assay. *morc-1(tm6048)* worms are resistant to full strength *lir-1* RNAi (1X), similar to *nrde-2* nuclear RNAi deficient worms. *eri-1;morc-1* worms are sensitive to dilute *lir-1* RNAi (1/7), similar to *eri-1* enhanced RNAi worms. (**B)** Representative images showing full strength *lir-1* RNAi phenotypes at 72 hours, 20°C. Red arrows indicate worms with larval arrest.

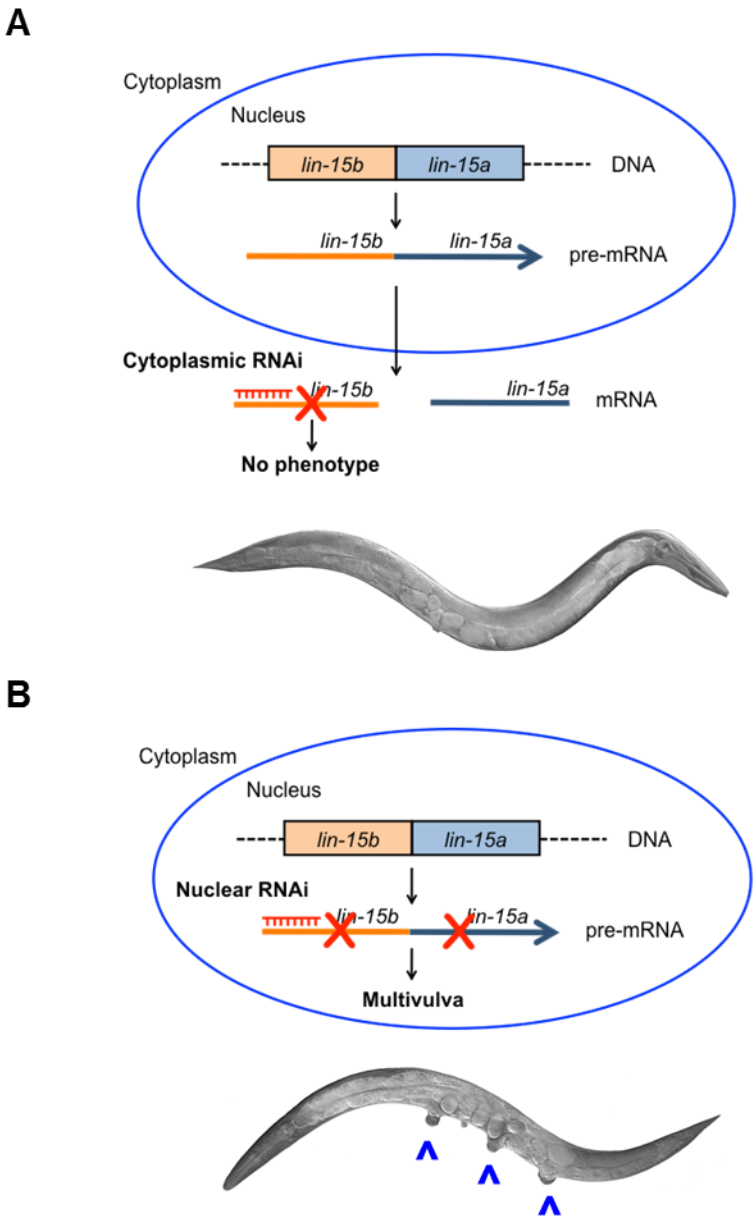

Figure 3.5 Model: the *lin-15b* RNAi phenotype.
(A) Cytoplasmic RNAi knockdown of *lin-15b* has no phenotype. (**B)** Nuclear RNAi knockdown of *lin-15b* also silences *lin-15a*, a part of the *lin-15* operon. Loss of *both lin-15b and lin-15a* produces a synthetic mulitivulva phenotype. Thus, sensitivity to *lin-15b* RNAi serves as a readout for nuclear RNAi function. Worm images from WormAtlas. Three blue arrowheads point to two pseudovulvae flanking the true vulva.

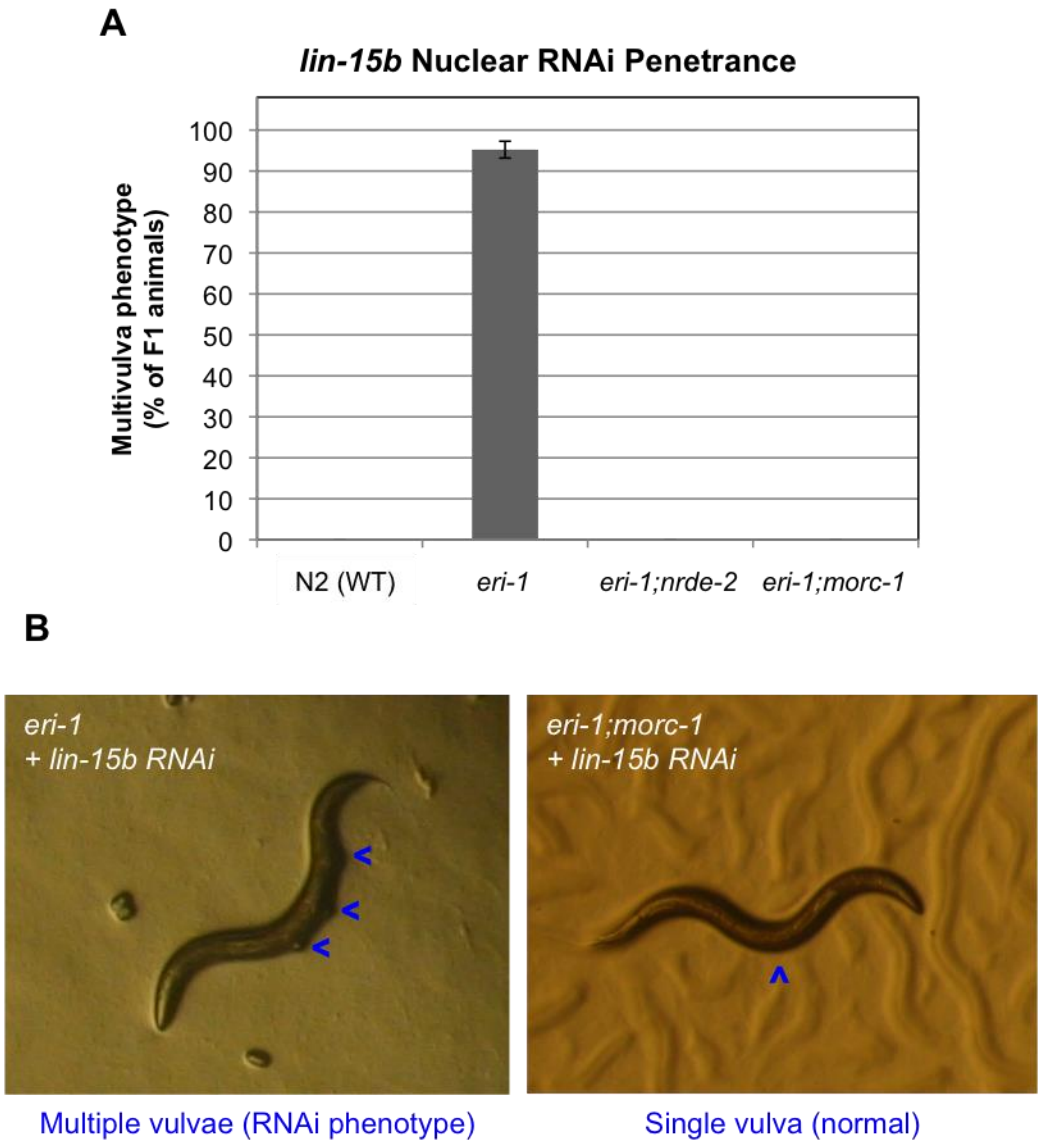

Figure 3.6 *morc-1* is required for *lin-15b* operon silencing by nuclear RNAi.
(A) *lin-15b* RNAi sensitivity assay. *eri-1;morc-1(tm6048)* worms are resistant to *lin15b* RNAi, similar to *eri-1;nrde-2* nuclear RNAi deficient worms. *eri-1* worms develop multiple ectopic vulvae on *lin-15b* RNAi (**B)** Representative images showing *lin-15b* F1 RNAi phenotypes at 20°C. Blue arrows indicate vulvae.

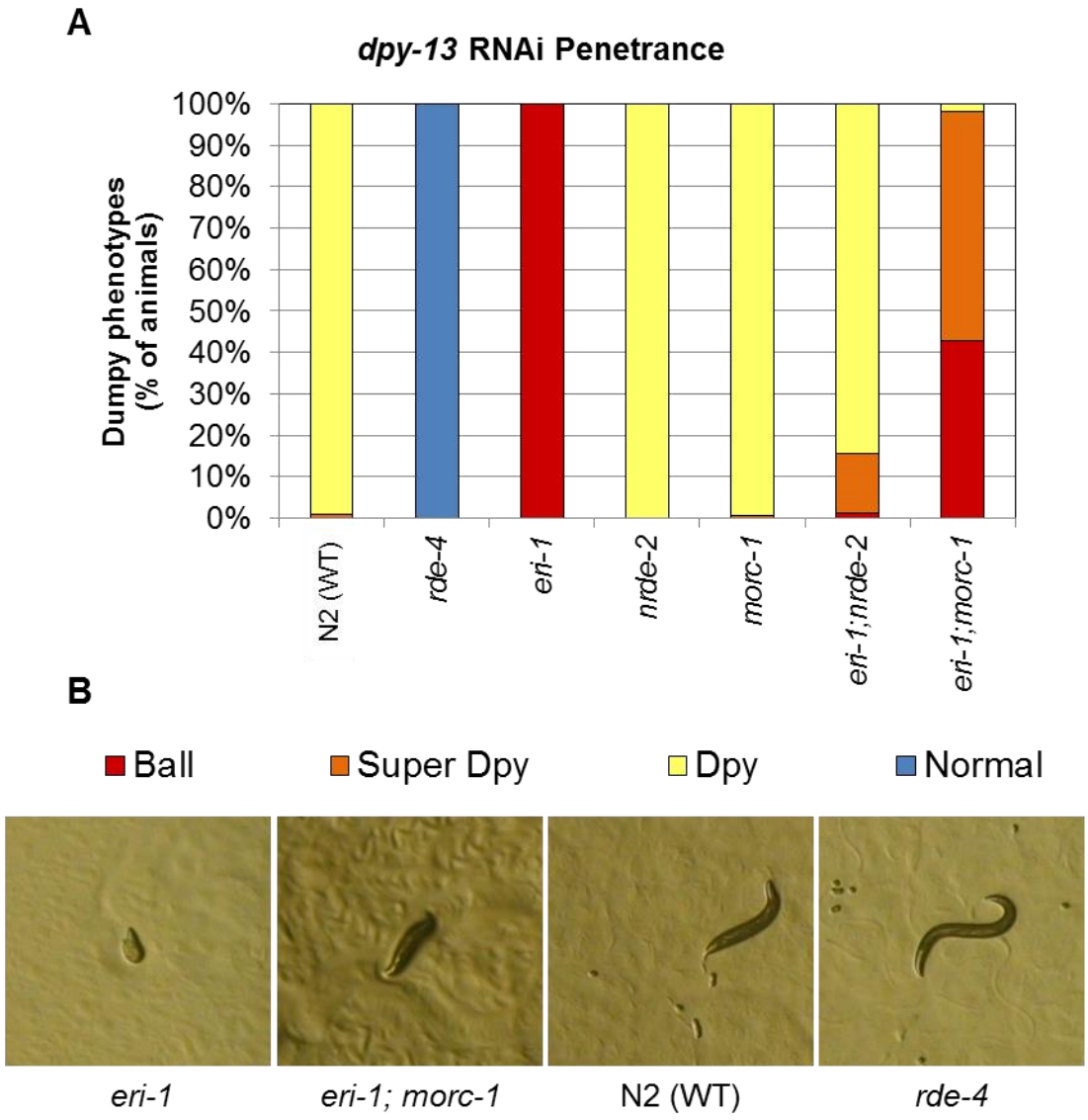

Figure 3.7 *dpy-13* nuclear RNAi assay.
(A) *eri-1;morc-1(tm6048)* worms are moderately resistant to *dpy-13* RNAi compared to *eri-1* worms, but not as resistant as *eri-1;nrde-2* nuclear RNAi deficient worms. (**B)** Representative images showing *dpy-13* RNAi phenotypes at 72 hours at 20°C.

Figure 3.8 Representative images of *dpy-13* nuclear RNAi assay.
These are images of the assay quantified in Figure 3.7.

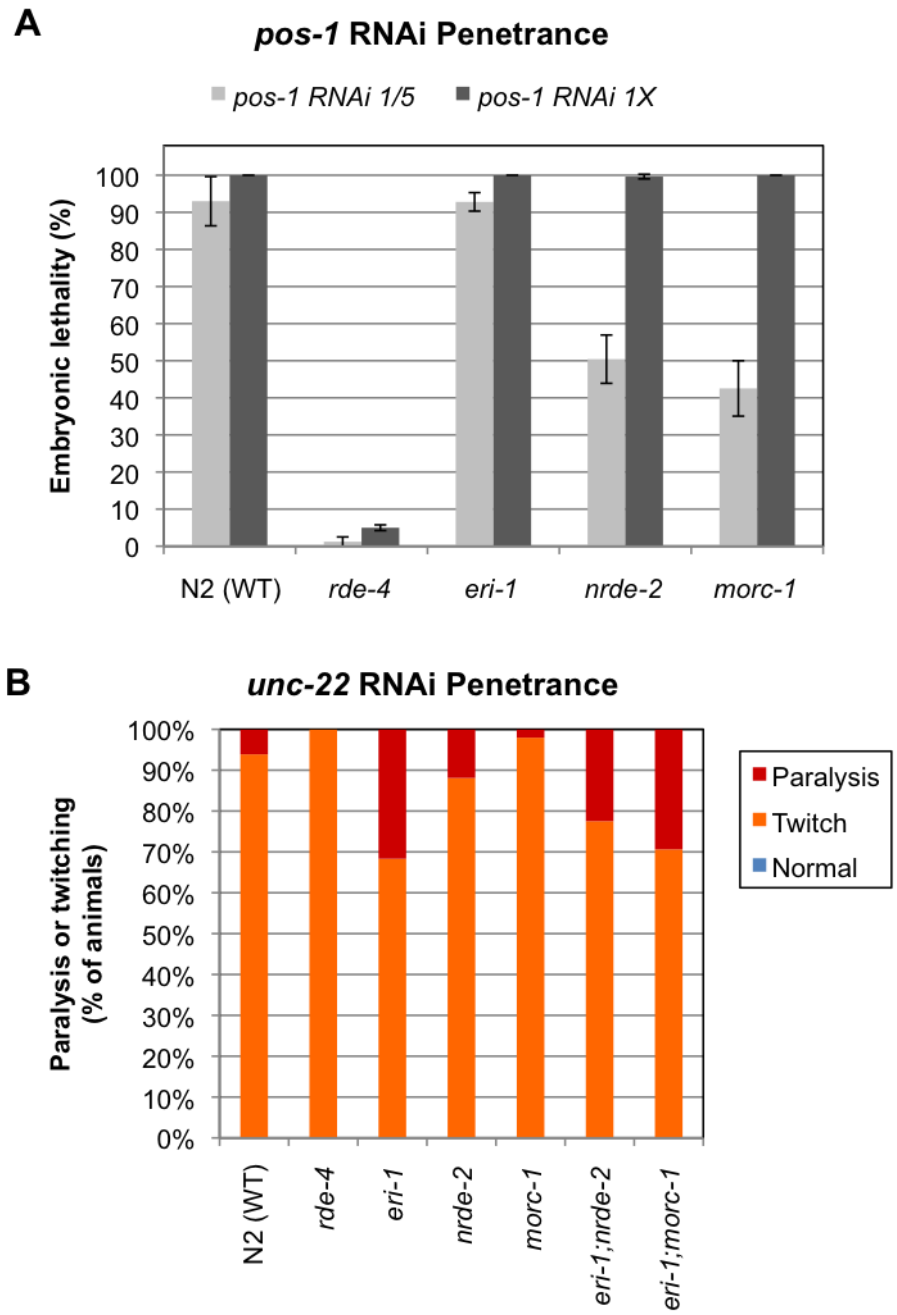

Figure 3.9 *morc-1* is not required for Exogenous RNAi.
(A) *pos-1* RNAi sensitivity assay. *morc-1(tm6048)* worms are slightly resistant to embryonic lethality in dilute *pos-1* RNAi (1/5 dilution in vector), similar to *nrde-2* nuclear RNAi deficient worms. (**B)** *unc-22* RNAi sensitivity assay. *morc-1(tm6048)* worms and *nrde-2* mutants are susceptible to twitch and paralysis phenotypes.

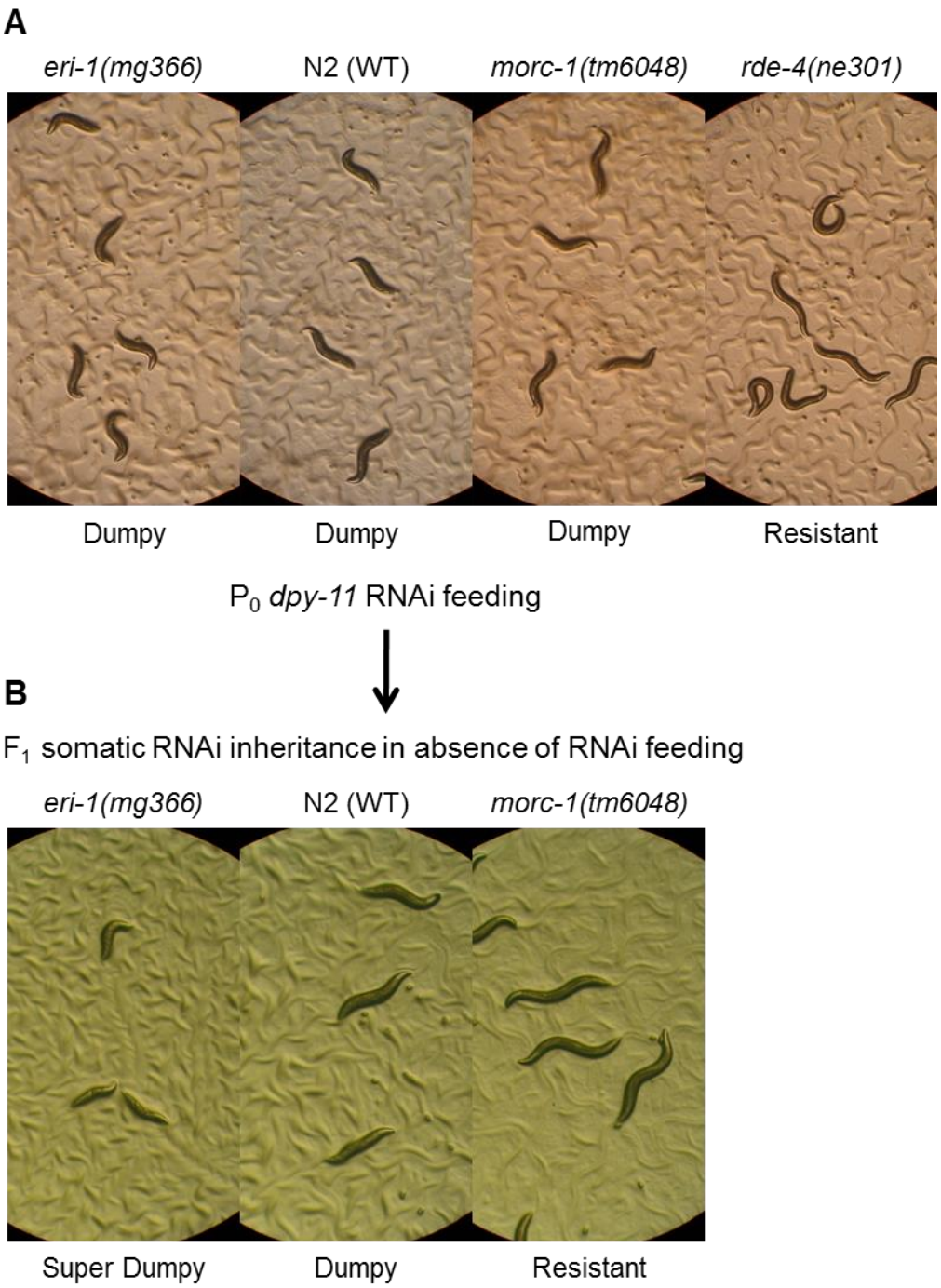

Figure 3.10 *morc-1* is required for efficient somatic RNAi inheritance
(A) RNAi against *dpy-11* produces a dumpy phenotype. *morc-1(tm6048)* worms are susceptible to RNAi against *dpy-11*. **(B)** F_1 progeny inherit the dumpy phenotype in wild type worms and *eri-1* mutants, but not in *morc-1* mutants.

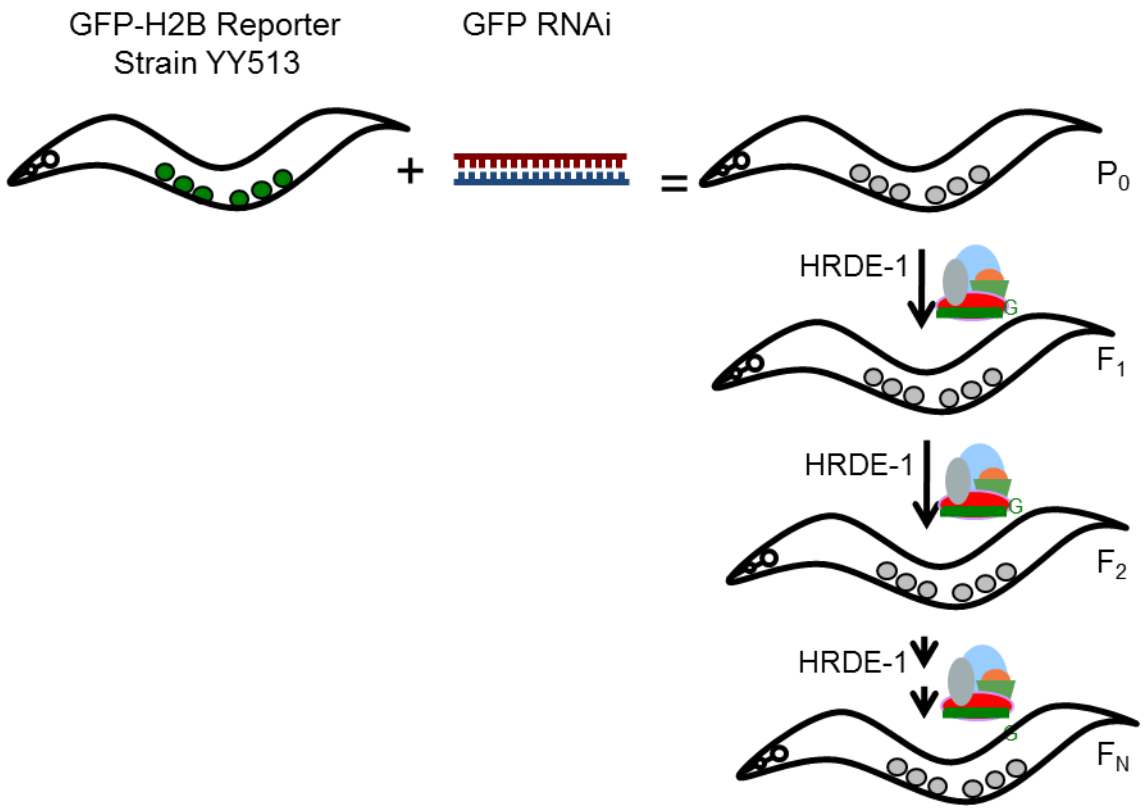

Figure 3.11 Model: germline RNAi inheritance assay.
gfp RNAi silences a germline GFP-Histone-2B reporter transgene. RNAi silencing can be inherited for many generations in the absence of additional RNAi treatment. Germline nuclear Argonaute HRDE-1 and 22G siRNAs mediate RNAi inheritance across generations.

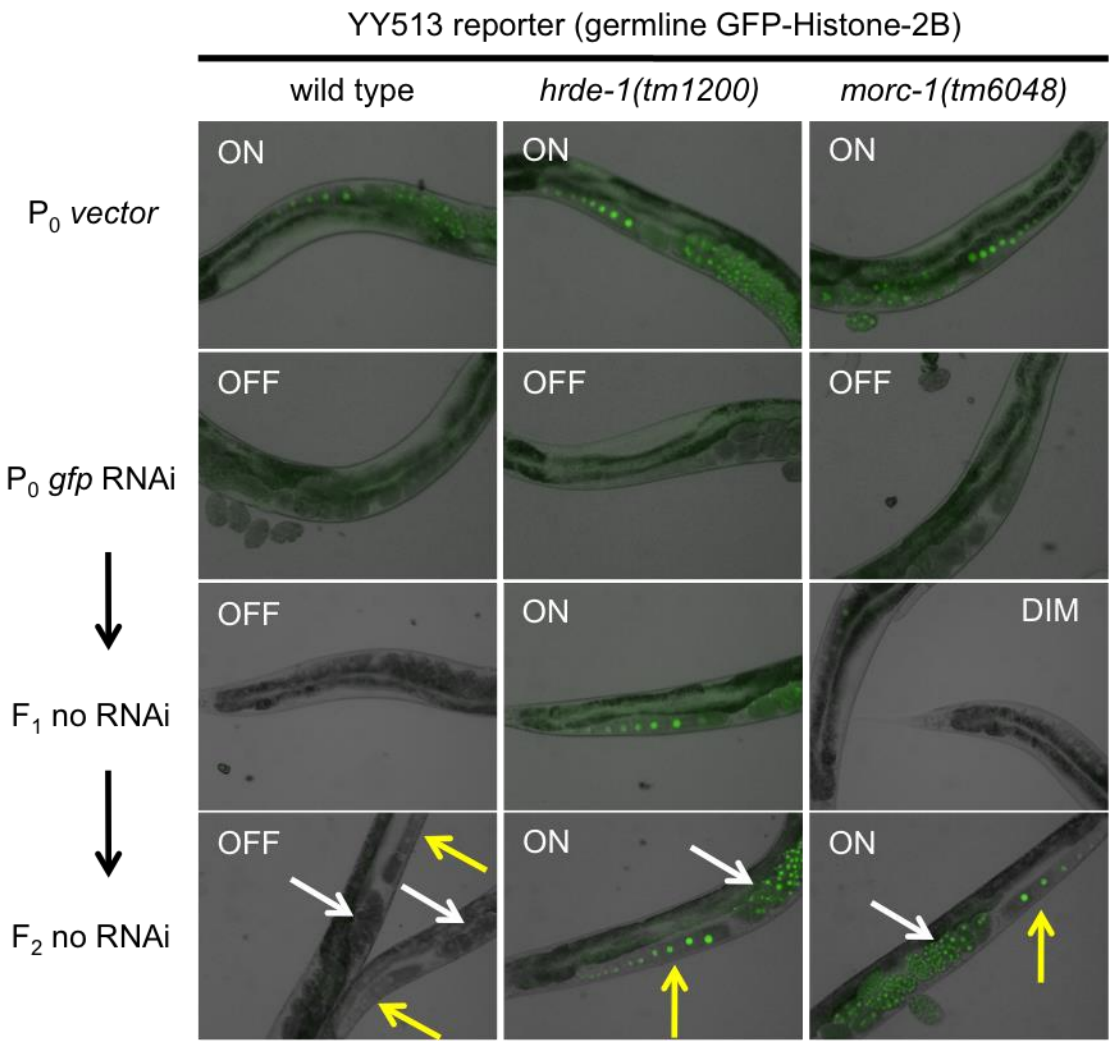

Figure 3.12 *morc*-1 is required for germline RNAi inheritance.
gfp RNAi silences a germline GFP reporter. GFP silencing is inherited in the absence of additional RNAi treatment in WT worms. Germline nuclear Argonaute *hrde-1* mutants do not inherit RNAi silencing in F_1 or F_2 generations. Inherited GFP silencing is weak in *morc-1* mutants in the F_1 generation and absent by the F_2 generation. Yellow arrows indicate oocytes, which may express nuclear GFP. White arrows indicate embryos within the uterus.

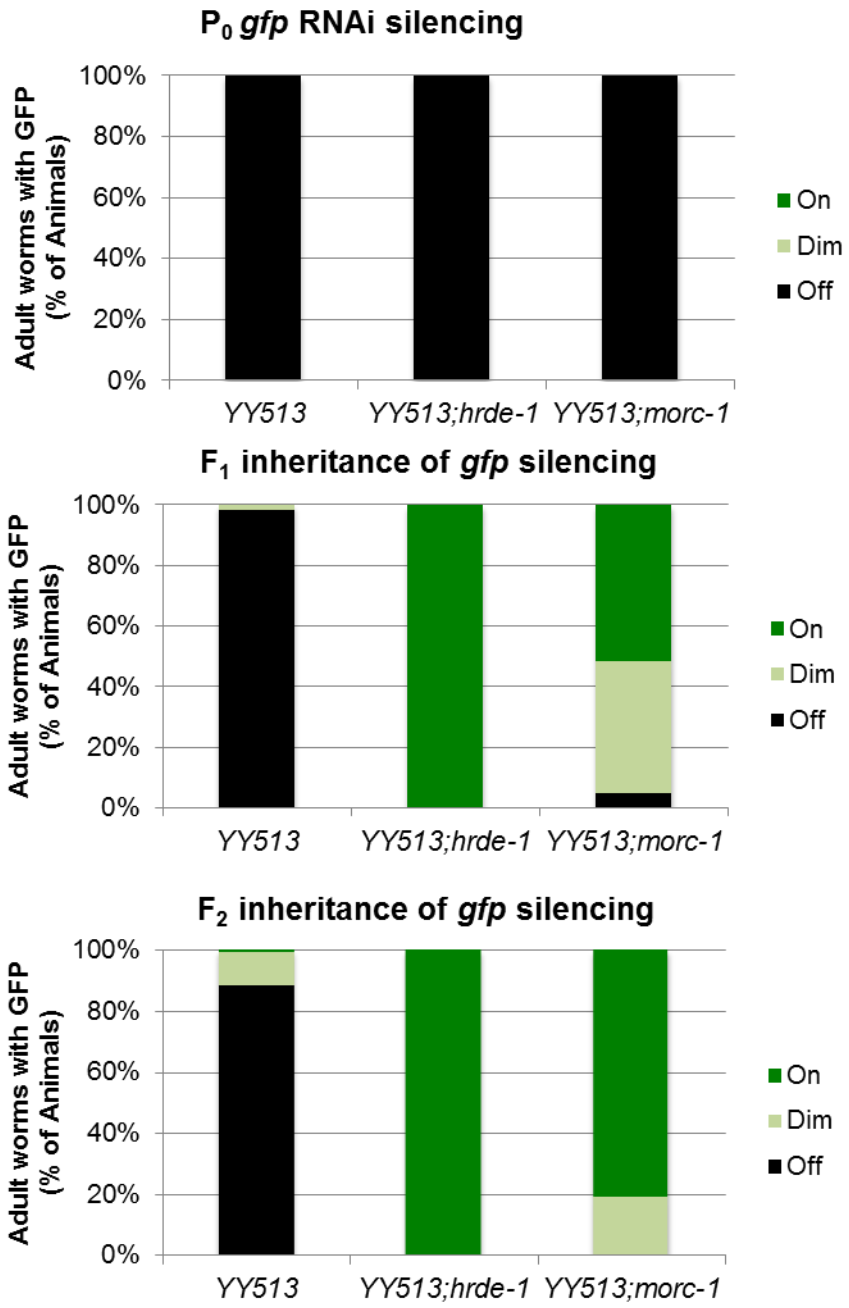

Figure 3.13 Quantification of germline GFP silencing for Figure 3.12.
gfp RNAi silences a germline GFP reporter. GFP silencing is inherited in the absence of additional RNAi treatment in WT worms. Germline nuclear Argonaute *hrde-1* mutants do not inherit RNAi silencing in F_1 or F_2 generations. Inherited GFP silencing is weak in *morc-1* mutants in the F_1 generation and absent by the F_2 generation. GFP signal was scored as on, dim, or off. N≥100 for each strain at each generation.

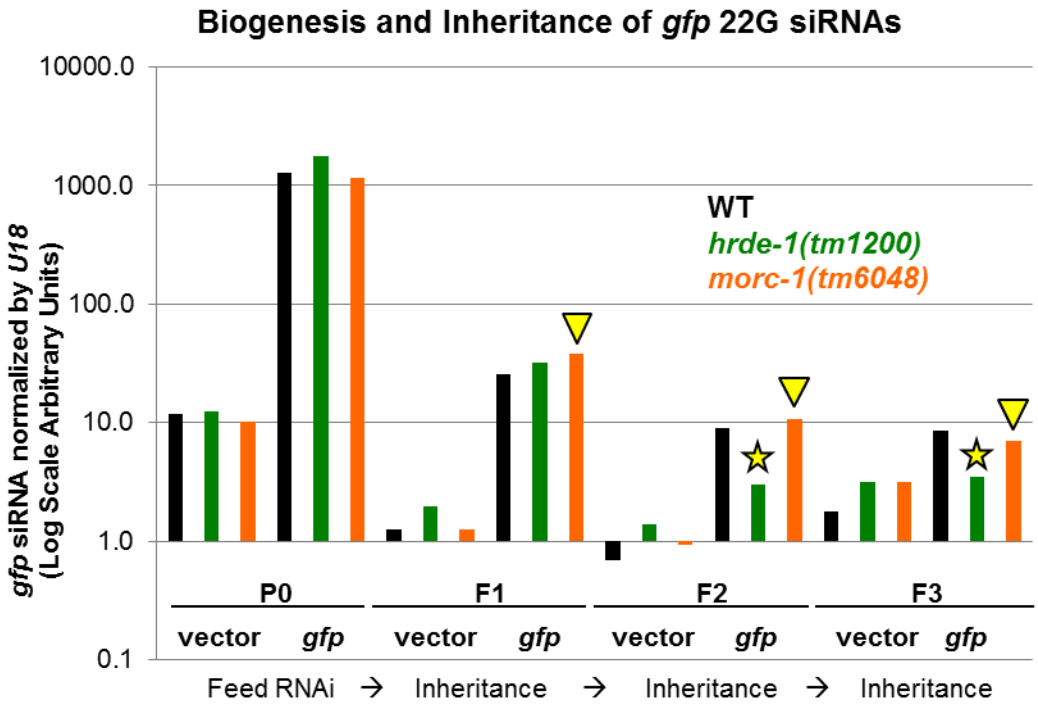

Figure 3.14 Quantification of *gfp* 22G secondary siRNA levels in YY513 GFP reporter worms from Figure 3.12 and 3.13.

gfp RNAi feeding induces the production of 22G secondary siRNAs in P_0 animals, which are inherited in F_1, F_2, and F_3 generations. Stars: *hrde-1* mutants are deficient in 22G siRNA inheritance at F_2 and F_3 generations. Triangles: *morc-1* mutants are not deficient in 22G siRNA inheritance at F_1, F_2, or F_3. 22G siRNAs were quantified by Taqman qRT-PCR and normalized to U18 snoRNA.

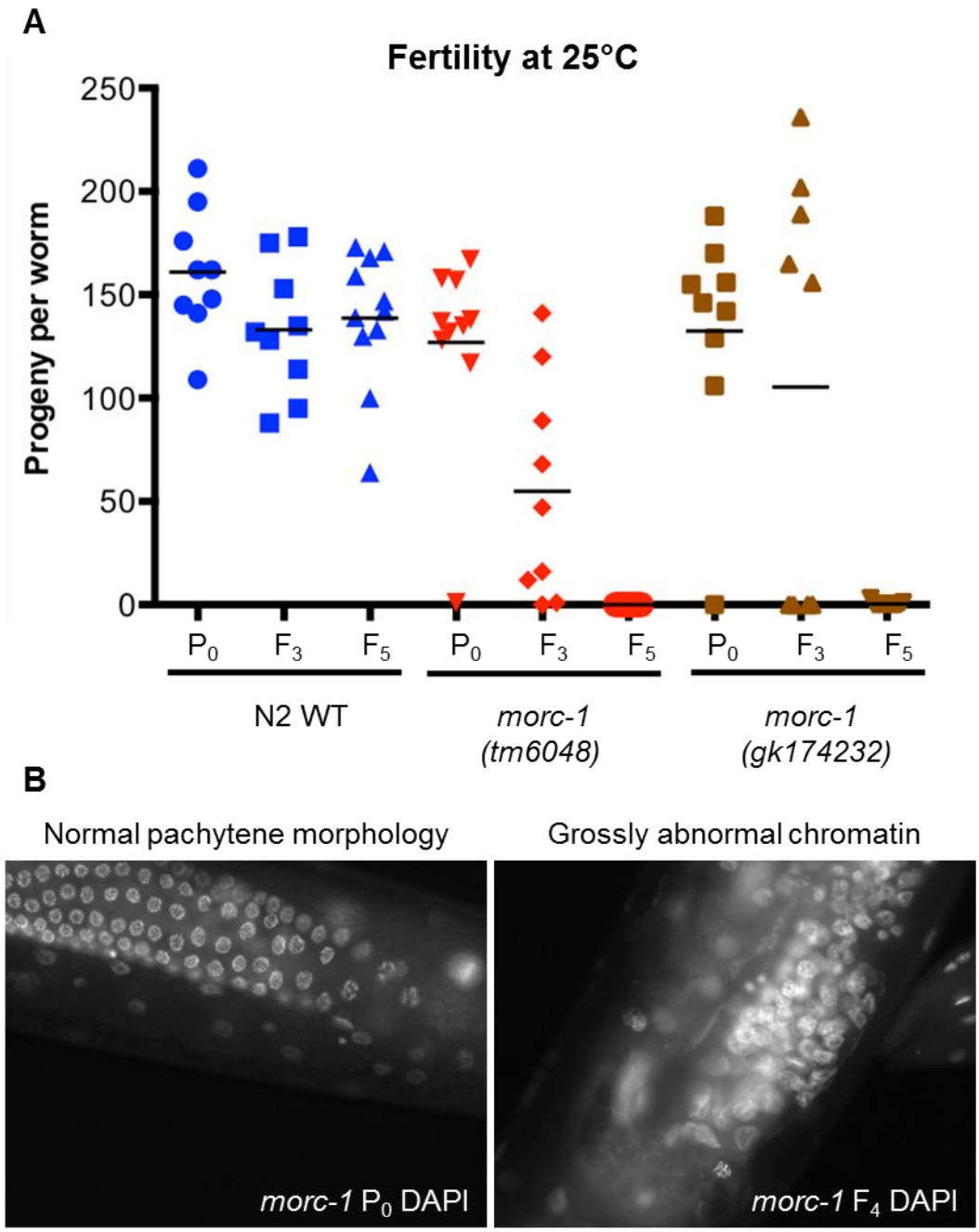

Figure 3.15 *morc-1* mutants are germline mortal.
(A) Wild type worms are fertile at 25°C. In contrast, *morc-1* deletion (*tm6048*) and nonsense (*gk174232*) mutants are initially fertile but become progressively sterility over multiple generations, a stereotypical demonstration of the germline mortal phenotype. Both *morc-1* mutants become sterile by the F_5 generation at elevated temperature. **(B)** Representative images showing adult *morc-1* mutants DAPI stained at P_0 (mostly fertile) and F_4 (mostly sterile) generations at 25°C. F_4 pachytene chromatin appears grossly abnormal.

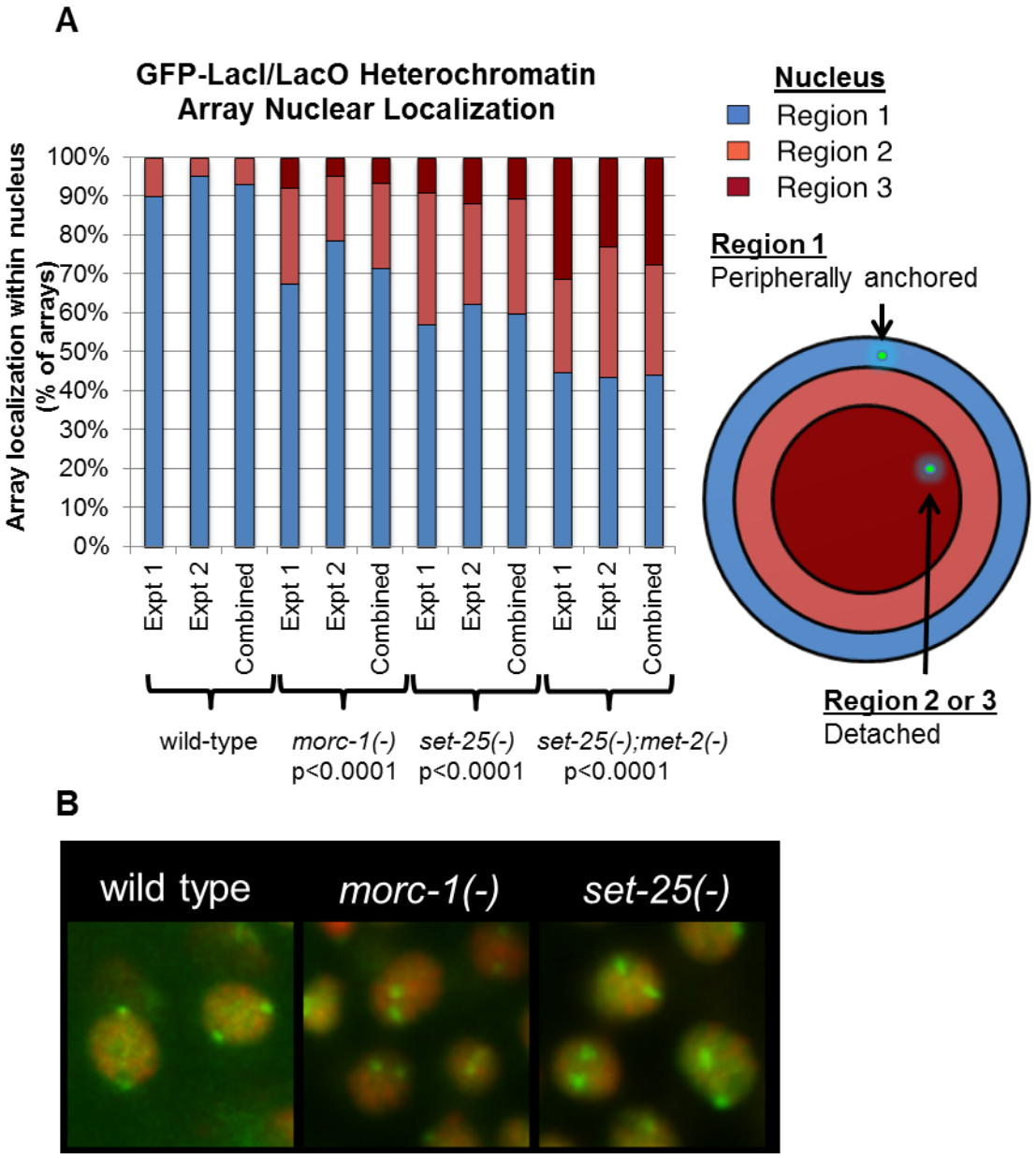

Figure 3.16 *morc-1* functions in heterochromatin localization.
(A) *gwIs4[baf-1p::gfp-lacI; lacO]* heterochromatin array nuclear localization in wild type versus mutant embryos. Worms were maintained at 20°C and shifted to 25°C for two generations before imaging. Nuclei were divided into three regions of equal volume. GFP-LacI/LacO arrays are peripheral in wild type embryos, but detached in *morc-1* mutants, *set-25* and *set-25;met-2* mutant controls. (*set-25;met-2* mutant embryos lack H3K9me1/2/3 which further disrupts heterochromatin anchoring [189].) *p*-values were calculated by chi-square test for wild type vs mutants. N>100. **(B)** Representative images of GFP-LacI/LacO localization in DAPI stained nuclei. GFP arrays are peripheral in wild type nuclei, but detached in *morc-1* and *set-25* mutants. Credit: Jayshree Khanikar.

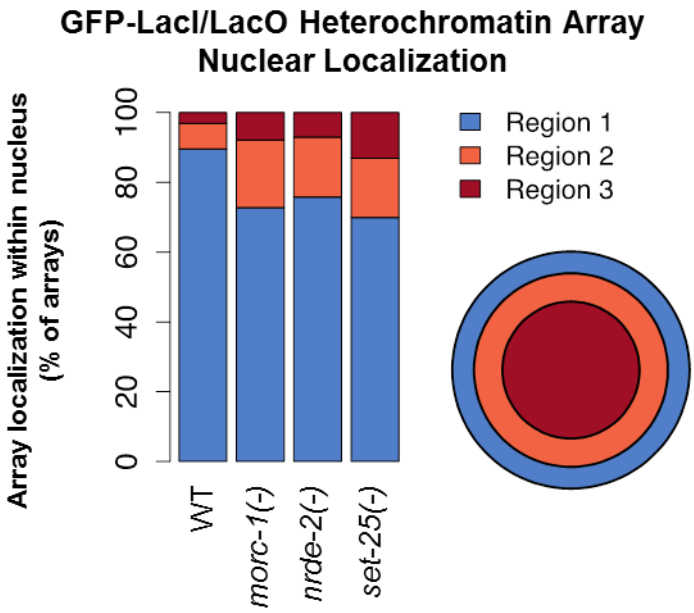

Figure 3.17 Nuclear RNAi functions in heterochromatin localization.
gwIs4[baf-1p::gfp-lacI; lacO] heterochromatin array nuclear localization in wild type versus mutant embryos. Worms were maintained at 20°C and shifted to 25°C for two generations before imaging. Nuclei were divided into three regions of equal volume. GFP-LacI/LacO arrays are peripherally localized in wild type embryos, but moderately delocalized in *morc-1* mutants, *nrde-2* mutants, and *set-25* mutant controls. Credit: Jayshree Khanikar.

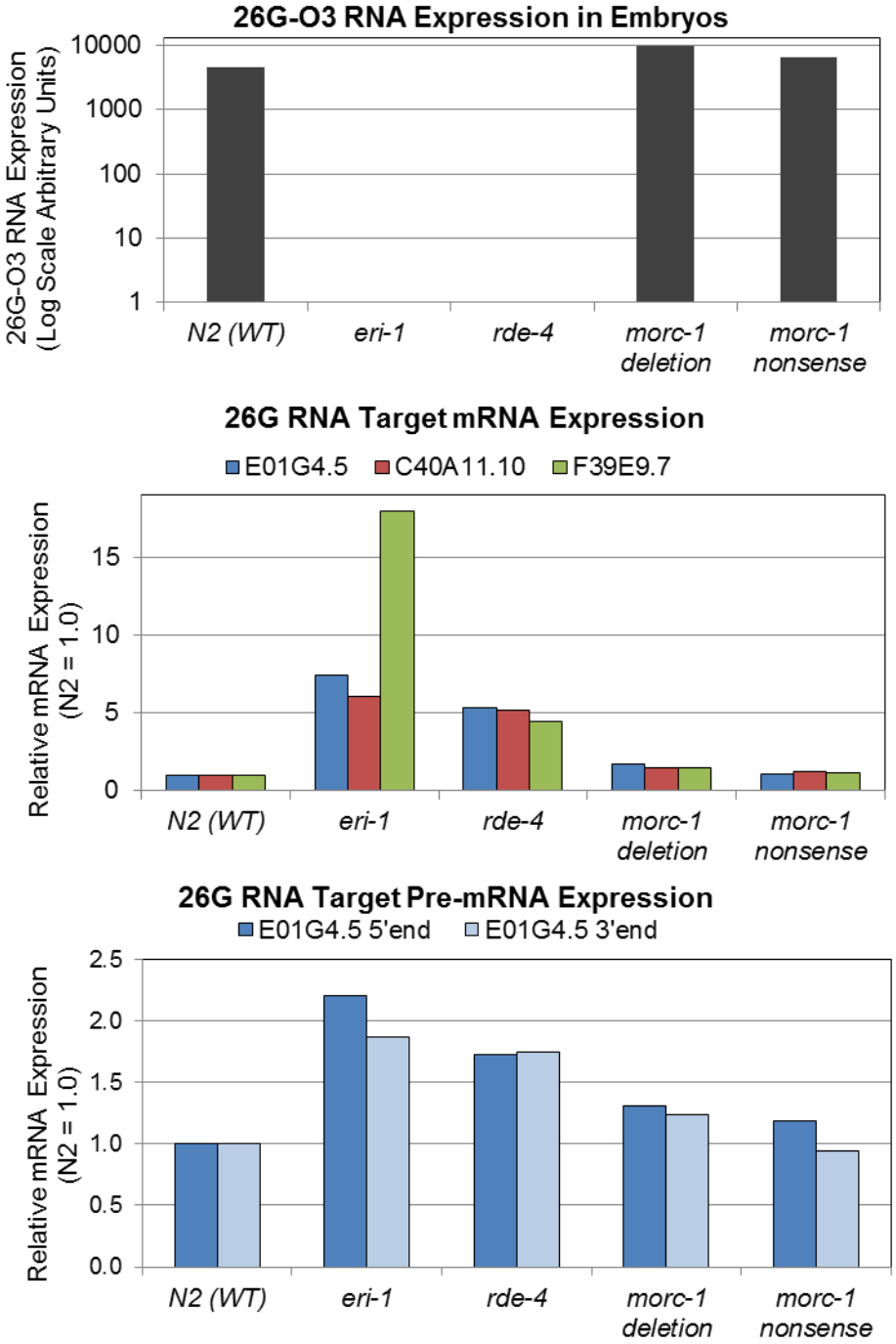

Figure 3.18 *morc-1* is not required for 26G endo-siRNA target repression.
(A) 26G-O3 siRNA is expressed at wild type levels in *morc-1* mutant embryos but depleted in *eri-1* and *rde-4* mutants. **(B)** 26G target mRNAs are elevated in *eri-1* and *rde-4* mutants but not in *morc-1* mutants. **(C)** Nuclear RNAi target *E01G4.5* pre-mRNA is upregulated in *eri-1* and *rde-4* mutants that lack 26G RNAs, but not in *morc-1* mutants.

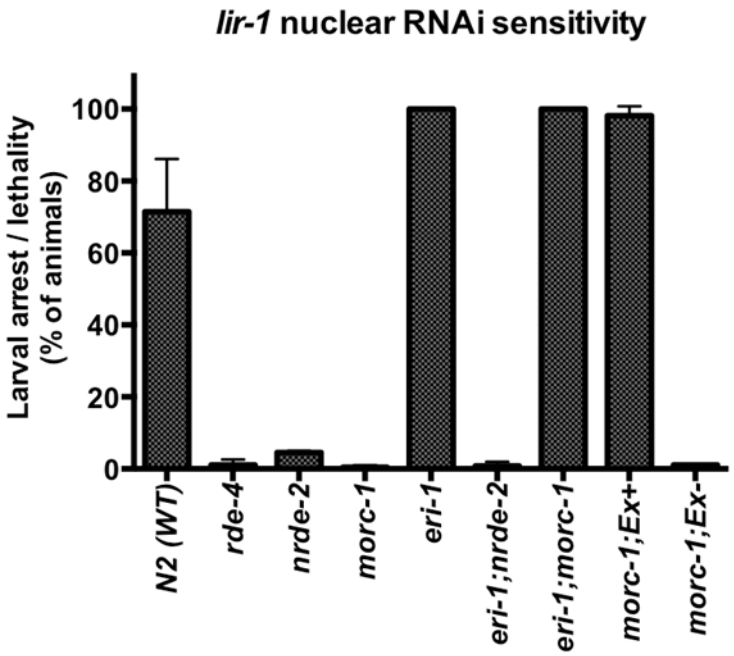

Figure 3.19 *morc-1::gfp* transgene restores nuclear RNAi function.
An extrachromosomal *morc-1-gfp* transgene *xkEx50*(*dpy-30p::morc-1::gfp::tbb2-3'utr*) restores *lir-1* nuclear RNAi sensitivity in *morc-1(tm6048)* mutants. *morc-1* mutants that inherit the transgene array *(Ex+)* arrest on *lir-1* RNAi, but worms that lose the array *(Ex-)* are resistant to *lir-1* nuclear RNAi.

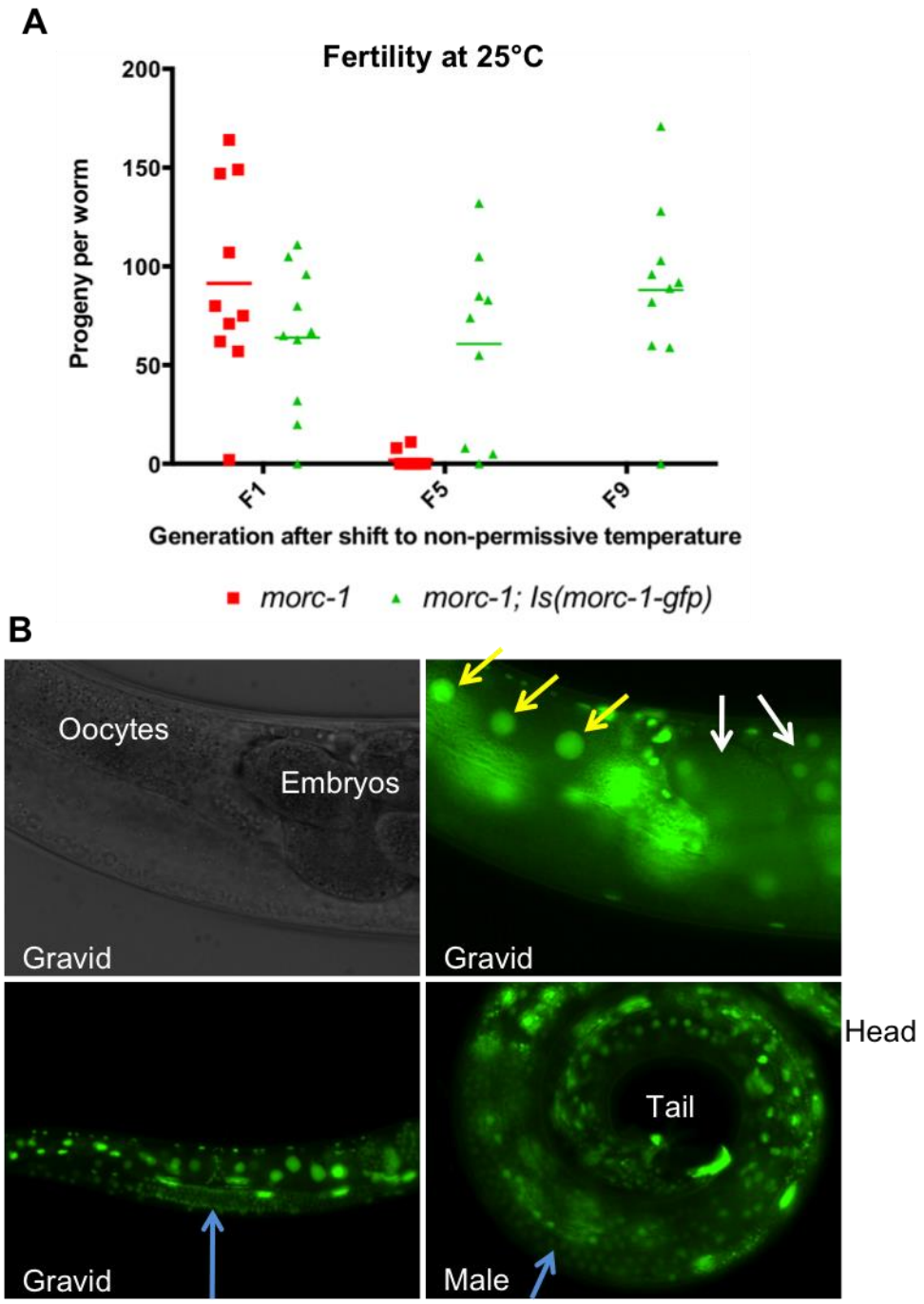

Figure 3.20 *morc-1-gfp* transgene rescues germline mortality.
(A) An integrated *morc-1-gfp* transgene *xkIs50*(*dpy-30p::morc-1::gfp::tbb2-3'utr*) rescues germline mortality in *morc-1(tm6048)* mutants grown at the non-permissive temperature of 25°C. **(B)** The *morc-1-gfp* transgene is ubiquitously expressed in germline and somatic nuclei of adults and embryos. Yellow arrows: oocyte nuclei with GFP. White arrows: embryos with nuclear GFP signal. Blue arrows: distal germline with GFP in developing germ cell nuclei.

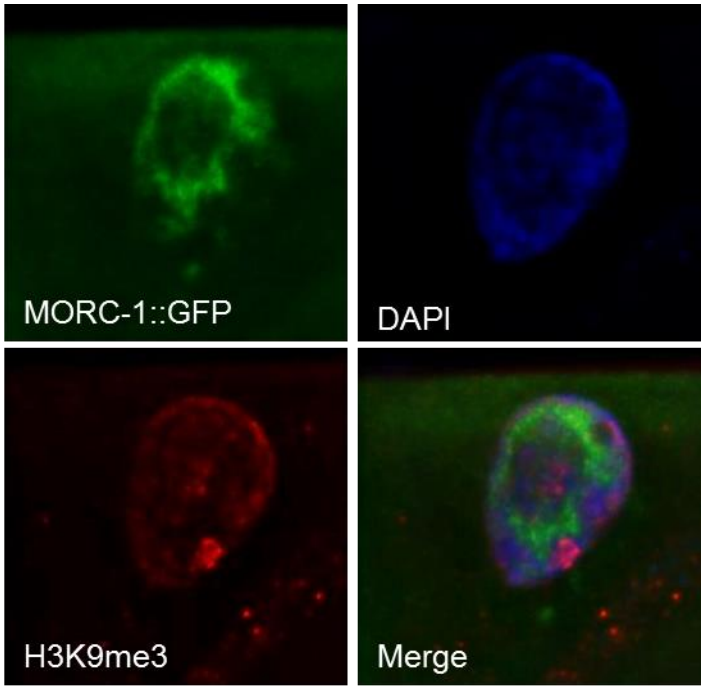

Figure 3.21 MORC-1-GFP colocalizes with chromatin but is depleted from H3K9me3 foci. Adult worms expressing integrated transgene *xkIs51*(*ges-1p::morc-1::gfp::unc-54-3'utr*) were stained with DAPI and anti-H3K9me3 for immunofluorescence microscopy. Native intestinal MORC-1-GFP signal was captured in the GFP channel. Images were taken at 60X on an Olympus BX61 microscope and z-stacks were deconvolved using Huygens Essential software. An adult intestinal nucleus is shown. Credit: Natasha Weiser.

Table 3.1 Quantitative RT-PCR primer sequences

Gene	Forward (5' to 3')	Reverse (5' to 3')
morc-1	GTGCTATGGGGCGTTTATGGATAC	AGGTTCGGCACATTTGACACAG
eft-2	TGTGTTTCCGGAGTGTGTGT	CCATCGTCGTCTCCGTAAGT
C40A11.10	AATGGCTCCTTGAAAAGATCG	TACATTTCCGCCACGTTGAAA
F39E9.7	CCCAGTGGCCCAATTAAACG	GCACAAGGTTTCGTTCTTGGTG
E01G4.5	TATGATGGTCACTACGAGGTTGT	AACTGGTAGCACTTGTCACAGAA
E01G4.5 pre-mRNA 5'	CAGAGCTTCACTACCACCCAA	CTCCAAATGTGTGCTCCTGTAA
E01G4.5 pre-mRNA 3'	TATGATGGTCACTACGAGGTTGT	TCACAGAAACTGGAAAGAACAAT
eft-2 pre-mRNA	CAAGCAGTTCGCTGAGATGT	TTCATGAGCTTGTCAACCTGTA
Taqman probes		
26G-O3 sequence for Taqman probe design		GACAAACTCGAAAGTCGGATACTTTT
22G-gfp sequence for Taqman probe design		GUGUCCAAGAAUGUUUCCAUCU

Table 3.2 *morc-1* transgene cloning primers

Gene	Forward (5' to 3')	Reverse (5' to 3')
morc-1 coding region	GATGAGGCGCGCCCATTTACGAAAATAATGATGC	AGATCTGGTACCACGCGTCTATTTGTATAGTTCA
dpy-30 promoter	GTTACCTGCAGGATTCAGAGGGGTGGGATTATTG	CTAAGGCGCGCCACTTGGTTTTTGCTCGATTTCTG
tbb-2 3'UTR	CTAAGGTACCATGCAAGATCCTTTCAAGCATTCC	TCTAGGGCCCCTAGGCGATCGCGA

CHAPTER IV – Conclusions and future directions

This chapter provides a succinct summary of our results, discusses their significance, and provides an overview of promising future directions for PUF-9 in part 1 and MORC-1 in part 2.

4.1 Conclusions and future directions on PUF-9

We have shown that PUF-9 associates with miRISC in an RNA dependent manner, that PUF-9 and miRISC bind overlapping sets of targets, and that PUF-9 binds two target sites in the *lin-41* 3'UTR. We validated endogenous PUF-9 and ALG-1 binding of mRNAs that were classified as shared PUF-9/miRISC targets by CLIP-seq. We also showed that *lin-41* reduction of function suppresses vulval rupture in *puf-9* mutants, and that *puf-9* represses a *lin-41* 3'UTR GFP reporter. These results indicate that *puf-9* interacts with *let-7* via the shared target *lin-41*.

The transcriptome-wide binding sites of PUF-9 and ALG-1 miRISC were enriched in RNA regions with high predicted secondary structure. PUF-9 and ALG-1 binding sites also occurred in close proximity across hundreds of shared targets. Perhaps physical clustering of PUF and miRNA target sites produces cooperative binding or cooperative repression. In HEK cells, miRNAs target sites separated by 8 to 40 nucleotides trigger

cooperative repression greater than the sum of individual target sites [313]. In *C. elegans* embryo lysates, multiple miRNA binding sites must be present on 3'UTRs to trigger target deadenylation; thus miRNA binding sites exhibit cooperativity in target repression [73].

Remaining questions and future directions

While our current study identifies shared targets of PUF-9 and miRISC, the core mechanism of PUF-9-mediated repression remains unsolved, along with the purpose of PUF-9/miRNA target clustering. In the future, we could use an embryo lysate system to measure deadenylation of artificial reporters bearing different combinations of PUF-9 and miRNA binding sites. In *C. elegans* embryo lysates, miRNAs trigger deadenylation and translational repression, without any detectable mRNA decay [73]. This system should also be able to determine if PUF-9 represses translation, triggers deadenylation, and promotes mRNA decay in worms. In addition, we should be able to determine if PUF-9 is additive, competitive, potentiating, or synergistic with miRNA repression.

In the next three subsections, I will describe (1) the identification of a novel *puf-9* isoform of unknown significance, (2) the identification of novel PUF-9 cofactors, and (3) the characterization of PUF-9 as a translational repressor in a heterologous *Drosophila* S2 cell culture system. These experiments present promising leads for future studies.

Novel isoform of PUF-9 in *C. elegans* embryos and maternal germline

The modENCODE mRNA-seq datasets across development contain reads in the final *puf-9* intron that could indicate a novel spliced isoform (Figure 4.1A). Sanger

sequencing of cDNA from embryos confirmed the presence of two splice donor sites for exon 8 and a single splice acceptor site in exon 9 (Figure 4.1B). RT-qPCR confirmed that the novel *puf-9* isoform (long) was enriched in early embryos and rapidly declined over embryonic development, similar to maternal transcript *glp-1* (Figure 4.2-3). In contrast, the annotated *puf-9* isoform (short) accumulated over embryonic development, similar to zygotic transcripts *elt-2* and *myo-3* (Figure 4.2-3). We hypothesize that the new isoform of *puf-9* is a maternal transcript that functions in oocytes, early embryos, or primordial germ cells. The only predicted difference in novel versus annotated PUF-9 protein sequence is replacement of the 40 amino acid C-terminal tail. This tail region is not conserved among PUF proteins and does not align to other known protein sequences.

PUF-9-GFP translational fusions were made from genomic *puf-9* DNA, *puf-9-long* cDNA (novel early embryo isoform), and *puf-9-short* cDNA (annotated mid embryo to adult isoform). These transgenes were integrated into the N2 wild-type genome as high-copy arrays and crossed into the *puf-9(ok1136)* deletion mutant to test for functional rescue. The *puf-9-long-gfp* (early embryo isoform) transgene did not rescue developmental delay observed in *puf-9(ok1136)* (Figure 4.4). In contrast, the *puf-9-short-gfp* (annotated isoform) transgene rescued developmental delay. The genomic *puf-9-gfp* transgene can express both isoforms, and it also rescues the developmental delay of *puf-9* mutants. Thus, our results suggest that the early embryo isoform of *puf-9* may not confer the same function as the larval isoform of *puf-9*. The main caveat of our analysis is that early embryo isoform *puf-9* transgene is expressed at 2 to 3 times the level of our larval isoform and genomic transgenes (Figure 4.5). Future work to dissect

the specific functions of each *puf-9* isoform could benefit from CRISPR-mediated mutation of splice donor sites to enforce constitutive expression of early embryo or larval isoforms.

It would be interesting to determine which isoform mediates clearance of embryonic miRNAs in newly hatched larvae, rescues the vulval rupture phenotype, and binds *let-7* targets *hbl-1* and *lin-41*. PUF protein families 3/11 and 5/6/7 are known to mediate oocyte RNA granule formation [58], nucleating RNA storage bodies that disperse upon oocyte activation and fertilization. PUF-9 was previously reported to be a somatic factor. However, the presence of the new *puf-9-long* isoform in early embryos and its rapid clearance during zygotic development suggest it could be maternally expressed and deposited in oocytes/embryos. *In situ* hybridization could show the extent of *puf-9* mRNA expression, and highlight differences in isoform distribution. In particular, *in situ* hybridization could show whether maternal *puf-9* is deposited in oocytes. Our rabbit polyclonal antibody binds endogenous PUF-9 by IP and recognizes PUF-9 by Western blot. The antibody epitope resides in the N-terminus shared by both puf-9 isoforms. Therefore, antibody staining in wild type versus *puf-9* null worms may show whether endogenous PUF-9 protein is expressed in maternal germline, germline precursors in embryos, or primordial germ cells. We noticed that phosphomutant PUF-9-GFP transgenes are lethal in *puf-9* maternal(-)zygotic(+) embryos, but are not lethal in *puf-9* maternal(+)zygotic(+) embryos. This observation suggests that endogenous maternal *puf-9* prevents transgene toxicity in embryos, providing circumstantial evidence that the novel *puf-9* isoform functions *in vivo*.

Identification of PUF-9 cofactors that interact with the miRNA pathway

PUF-9-GFP protein complexes were immunopurified from gravid adults, embryos, and L1 animals. Associated cofactors were identified by mass spectrometry by James Moresco at Scripps Research Institute. Across three stages, we identified only 9 proteins that associated with PUF-9-GFP but not GFP alone (Figure 4.6). Several protein interactors were known components of worm miRISC: AIN-2, NHL-2, PABP, TSN-1, and RACK-1. Two novel PUF-9 interactors of unknown function include ATAXIN-2 (homolog of the human spinocerebellar ataxia type 2 gene) and SQUID-1 (homolog of *Drosophila* Squid). Ataxin-2 is required for miRNA reporter repression in *Drosophila*, so it could be a RISC cofactor [314]. SQUID-1 is an RNA binding protein that is ubiquitously identified in many RBP mass spectrometry datasets [73, 132]. Although our PUF-9 cofactor list is likely far from comprehensive, I set out to determine whether loss of each cofactor could phenocopy *puf-9* defects in the miRNA pathway.

PUF-9 protein cofactors were knocked down in the *let-7(n2853)* and *alg-1(tm369)* mutants to assay for enhanced bursting. RNAi of *atx-2* and *sqd-1* enhanced vulval bursting, suggesting that they may be cofactors for *let-7* family miRNAs. Interestingly, *atx-2* and *sqd-1* RNAi enhanced bursting in both *let-7* and *alg-1* mutants, but not *puf-9(ok1136)* mutants, suggesting that these genes might act in the same pathway as *puf-9* but in parallel to *let-7* and *alg-1* (Figure 4.7). *puf-9;cofactor* double mutants should be generated for epistasis analysis. Unfortunately, *atx-2* or *sqd-1* loss of function results in sterility. Because *let-7*-mediated repression of *lin-41* 3'UTR is required for vulval morphogenesis and integrity, I tested whether *atx-2* or *sqd-1* knockdown affects *lin-41*-3'UTR GFP reporter expression. *sqd-1* RNAi increases GFP reporter signal in the

uterus (Figure 4.8), similar to knockdown of *puf-9*, *nhl-2*, or *alg-1* (Figure 2.11-12). However, *atx-2* knockdown did not desilence the *lin-41*-3'UTR GFP reporter. Thus, we predict that *sqd-1* interacts with *let-7* through silencing of the *lin-41* 3'UTR, whereas *atx-2* interacts with *let-7* through vulval development pathways parallel to or downstream of *lin-41*.

Additional studies are required to determine how *sqd-1* interacts with *let-7* targets and whether *sqd-1* is important for regulation by additional miRNAs. *sqd-1* is a conserved hnRNP that shuttles mRNA targets from the nucleus to the cytoplasm. Notably, Drosophila Squid controls the apical localization of *fushi tarazu* (pair rule gene) mRNA in oocytes [315], delivers *gurken* (epidermal growth factor ligand) mRNA to translational repressor Bruno, and regulates both anterior-posterior and dorsal-ventral axis patterning in oocytes [316]. Squid interacts with specific 3'UTR targets through its two RNA recognition motifs and c-terminal arginine-glycine box (2xRBD-gly) [315-317]. CLIP-seq analysis of SQD-1 should reveal a diverse array of RNA targets, some of which may function in miRNA pathways. We expect to find the preferred motif of SQD-1, as well as potential binding sites in the *lin-41* 3'UTR. Perhaps SQD-1 is important for delivering nuclear mRNA targets to cytoplasmic translational repressors like PUF-9 or miRISC.

PUF-9 represses 3xPRE reporters in *Drosophila* S2 cells

Cell culture systems have provided detailed insights into the mechanism of action for miRNAs and PUF proteins in humans and flies [51, 143]. Thus, I set out to determine the effects of PUF-9 binding in cell culture. Does PUF-9 mediate translational

repression and RNA decay like fly Pumilio? Dmel-2 cells derived from the Drosophila S2 cell line do not have detectable levels of Pumilio protein or activity [318, 319]. Dmel-2 cells were co-transfected with PUF protein expression plasmids and Renilla luciferase reporters regulated by 3'UTRs bearing PREs or mutant PREs, along with non-target Firefly luciferase control plasmid. PUF-9 represses luciferase expression of poly-adenylated mRNA reporters, but not mRNA reporters bearing a 3' histone stem loop (Figure 4.9A). PUF-9-mediated repression of luciferase protein signal was accompanied by roughly equivalent reductions in mRNA (Figure 4.9B). Our preliminary results suggest that PUF-9 repression in Drosophila S2 cells requires a 3'UTR PRE motif and a polyA tail that can be de-adenylated. The polyA-tail-independent translational inhibition activity of fly Pumilio does not appear to be conserved in worm PUF-9, at least in this heterologous system. Additional reporter studies will need to be performed in worms to definitively address the repressive mechanisms of worm PUF-9.

Given that PUF-9 represses PRE target reporters, I set out to establish a system in which to study PUF-9/*let-7* combinatorial regulation of the *lin-41* 3'UTR. Drosophila *let-7* expression vector [320] was co-transfected with Renilla luciferase reporters bearing wild type or mutant *lin-41* 3'UTR. Drosophila *let-7* is identical to *C. elegans let-7* and human *let-7a*, except that Drosophila *let-7* is one U nucleotide shorter at the 3' end [90]. Fly *let-7* repressed wild type *lin-41* 3'UTR, but not *lin-41* 3'UTR with point mutations in the LCS1 and LCS2 *let-7* binding sites.

I planned to test whether *let-7*-mediated repression of *lin-41* 3'UTR depends on PUF-9, or whether *let-7* repression is synergistic, additive, or competitive with PUF-9-mediated repression. Unfortunately, I was unable to answer these questions due to

artifacts in non-specific PUF-9 repression of the *lin-41* 3'UTR reporter. In brief, PUF-9 repressed wild-type *lin-41* 3'UTR reporters in addition to *lin-41* 3'UTR mutant reporters that lack PUF-9 binding sites.

4.2 Conclusions and future directions on MORC-1

Our results indicate that *morc-1* is required for efficient nuclear RNAi in the soma, inheritance of RNAi in soma and germline, and the maintenance of germline immortality. In addition, *morc-1* and the nuclear RNAi pathway are required for repetitive transgene silencing through heterochromatin organization and/or anchoring at the nuclear periphery. Altogether, we have uncovered a role for *morc-1* in the NRDE-3/HRDE-1 nuclear RNAi pathway downstream of siRNAs.

We propose that *morc-1* mutation disrupts the balance between germline small RNA silencing and activation, with important implications for chromatin regulation. More recently, our work has uncovered genetic interactions between *morc-1* and two major regulatory axes important for germline gene expression and the immortal germ cell lineage: H3K4 versus H3K9 methylation, and H3K27 versus H3K36 methylation. In the future, dissecting the mechanism of MORC-1 function could provide insight into how nuclear RNAi pathways collaborate with histone methylation networks in the germline.

In the next three subsections, I describe the Kim Lab's continuing efforts to explore the role of MORC-1 in germline maintenance through the following studies: (1) a mutagenesis screen that isolated suppressors of *morc-1* germline mortality, (2) identification of MORC-1 protein cofactors by IP-mass spectrometry, and (3) analysis of

genetic interactions between *morc-1* and histone methyltransferases in germline maintenance.

ENU mutagenesis screen to identify suppressors of *morc-1* germline mortality

Based on the finding that *morc-1* mutants are germline mortal at elevated temperature, we performed a genetic screen to identify mutations that extend fertility in *morc-1* mutants (Figure 4.10A). We mutagenized L4 worms in 0.5mM ENU and plated ~100 L4 worms in 32 pools at 20°C on 10cm OP50 bacterial food. F1 animals were grown at 20C to allow potential heterozygous suppressor mutants to reproduce under non-selective conditions. F2 embryos were isolated by bleach prep and plated at 25°C to select for suppressor mutations. Twitching is a stereotypical phenotype for mutants of *unc-22*, a large gene that spans 38kb. 12 pools were examined and twitching worms were found in 5 pools, suggesting that ENU treatment successfully generated mutations. All 32 pools were maintained until the F14 generation at 25°C, isolating embryos by hypochlorite prep and transferring to new plates at each generation. 16 single worms were picked to 6cm plates from each fertile pool, to identify the most fertile worms that are likely to have homozygous suppressor mutations (Figure 4.10B). *lir-1* nuclear RNAi sensitivity and GFP RNAi inheritance were scored for promising candidates (Figure 4.11). Whole genome sequencing was performed for clonal mutants from 18 separate pools, alongside the unmutagenized parental strain, to identify genes with multiple deleterious mutations in different pools. Five independent homozygous alleles of suppressor of *morc-1* (*smorc-1*) were isolated in our screen. RNAi of *smorc-1* extended *morc-1* fertility by seven generations at elevated temperature, suggesting that

smorc-1 is a real *morc-1* suppressor (data not shown). Candidate suppressors are now being characterized by Natasha Weiser. These genes could have important roles in the nuclear RNAi pathway, chromatin organization, and germline maintenance. Interestingly, *smorc-1* is a methylatransferase that functions in germline chromatin organization.

How does MORC-1 interact with histone modification factors in germline maintenance?

The first candidate suppressor of *morc-1* germline mortality (*smorc-1*) is a histone methyltransferase. Histone modifying enzymes mediate the inheritance of transcriptional states from one generation to the next. In embryos, MES-4 maintains H3K36 methylation of genes that were previously expressed in the maternal germline. Maternal loss of *mes-4* disrupts H3K36 methylation patterns (originally deposited by MET-1) in primordial germ cells and results in sterility [182]. In primordial germ cells, *spr-5* erases H3K4me2 to reset transcriptional states for the new generation in concert with *met-2* H3K9me2 methyltransferase [173, 196]. Hence, *spr-5* and *met-2* single mutants develop progressive sterility, while double mutants fail to suppress spermatogenic gene expression in the soma and become sterile in the first generation [196]. These examples illustrate that different kinds of epigenetic information must be selectively retained or reset across generations to maintain the immortal germline and to specify germline cell fate. Interestingly, disrupting H3K36 methyltransferases, H3K4 demethyalases, and H3K9 methyltransferases can all have the same end result: disruptions of euchromatin-heterochromatin boundaries that cause ectopic gene expression in tissues and stages where those genes should be silenced [173, 181, 196].

Recent results suggest that *morc-1* regulates the balance of H3K4 vs H3K9 methylation in the germline. *morc-1* germline mortality (Mrt) can be rescued by loss of H3K4 methyltransferases or H3K9 demethylases (Figure 4.12). Hence, *morc-1* loss of function may tip the balance in favor of H3K4 methylation (Figure 4.13). The next step is to establish whether *morc-1* mutants exhibit defects in histone methylation patterns by ChIP-seq and immunofluorescence microscopy. We hypothesize that H3K4 methylation will be globally elevated in *morc-1* mutants, consistent with *morc-1* Mrt rescue through loss of H3K4 methyltransferases. Furthermore, we hypothesize that H3K9me2 or H3K27me3 heterochromatin domains may be reduced in size or misplaced across the genome in *morc-1* animals.

Similar to *morc-1*, *spr-5* germline mortality can be suppressed by mutation of H3K4 histone methyltransferases or H3K9 methyltransferases [241]. Hence, balance of H3K4 and H3K9 methylation is important for maintaining germline immorality across generations. Interestingly, the HRDE/NRDE nuclear RNAi pathway promotes transcriptional gene silencing and H3K9 methylation [5, 220, 321], while the CSR-1 22G RNA pathway promotes H3K4 methylation and promotes germline transcription.

A recent study [227] showed that the RSD-2/RSD-6 complex is required for generation of 22G secondary siRNAs that promote germline immortality at high temperatures. Presumably, these 22G RNAs act through the HRDE-1/NRDE pathway, as *rsd* and *nrde* mutations produce similar germline mortality phenotypes that are not additive or synergistic in *rsd-6;nrde-2* double mutants. RSD-2 and RSD-6 function to repress repeat elements and spermatogenesis genes. Loss of *rsd-2* and *rsd-6* results in massive germline apoptosis, chromosome mis-segregation, and high incidence of

males: phenotypes that may be present in *morc-1* mutants. Importantly, it seems that RSD-2/6 does not enhance the expression of spermatogenesis genes targeted by ALG-3/4 and CSR-1, nor does it repress a mostly overlapping set of genes regulated by the *spr-5* H3K4 demethylase. Overall, it appears that the HRDE/NRDE/RSD pathway acts in parallel to *spr-5* to regulate germline gene expression.

In the absence of PRG-1 and piRNA function, 22G RNAs that rescue germline immortality require the function of downstream H3K4 demethylases such as *rbr-2* [225]. Together, these studies suggest that the nuclear RNAi pathway may regulate germline immortality through histone modification. We propose that *morc-1* functions in the regulation of histone methylation, or as a reader of histone modifications, to promote germline immortality. Because *morc-1* participates in the HRDE-1 nuclear RNAi pathway, we hypothesize that HRDE-1 guides MORC-1 to its genomic target sites. We plan to test whether RNAi treatment enriches MORC-1-GFP on target genes using ChIP-qPCR.

Identification of MORC-1 protein cofactors

In *Arabidopsis*, AtMORC6 forms heterodimers with AtMORC1 or AtMORC2, and these dimers are recruited to chromatin via interactions with SUVH9, a homolog of MET-2 in worms and Cryptic Loci Regulator 4 H3K9 methyltransferase active in *S. pombe* nuclear RNAi [250, 270]. In addition, AtMORC6 associates with structural maintenance of chromosomes hinge domain protein DMS3 [257]. We hypothesize that *C. elegans* MORC-1 may also associate with histone methyltransferases (like MET-2), demethylases, and other chromatin organization factors that function in nuclear RNAi,

akin to its homologs in *Arabidopsis*. To identify binding partners, MORC-1-GFP protein complexes will be immunopurified and subjected to mass spectrometry analysis (Figure 4.14). MORC-1 cofactors will be functionally validated by rapid secondary screens, including an RNAi screen for suppression or enhancement of the *morc-1* germline mortal phenotype. Viable mutants will be assessed for germline mortality, nuclear RNAi sensitivity, and RNAi inheritance phenotypes.

Our *dpy-30*-promoter driven MORC-1-GFP transgene rescues nuclear RNAi function in the soma as well as germline maintenance at elevated temperature (Figure 3.20). IP of MORC-1-GFP from benzonase treated lysate should enrich direct protein interactions in the absence of chromatin. For example, we might infer that MORC-1 makes direct contact with NRDE-1, suggesting a possible route for MORC-1 recruitment at nuclear RNAi target sites. Overall, identification of MORC-1 interacting partners will provide clues for its mechanism of action.

4.3 Concluding remarks

The field of small RNA-mediated gene regulation has grown tremendously since the discovery of the first miRNAs in *C. elegans*. Small RNAs have been shown to be important regulators of almost every biological process in higher eukaryotes. Now is a truly exciting time for the field, as small RNA pathways are being integrated with the functions of RNA binding proteins, histone methylation pathways, and chromatin organization mechanisms.

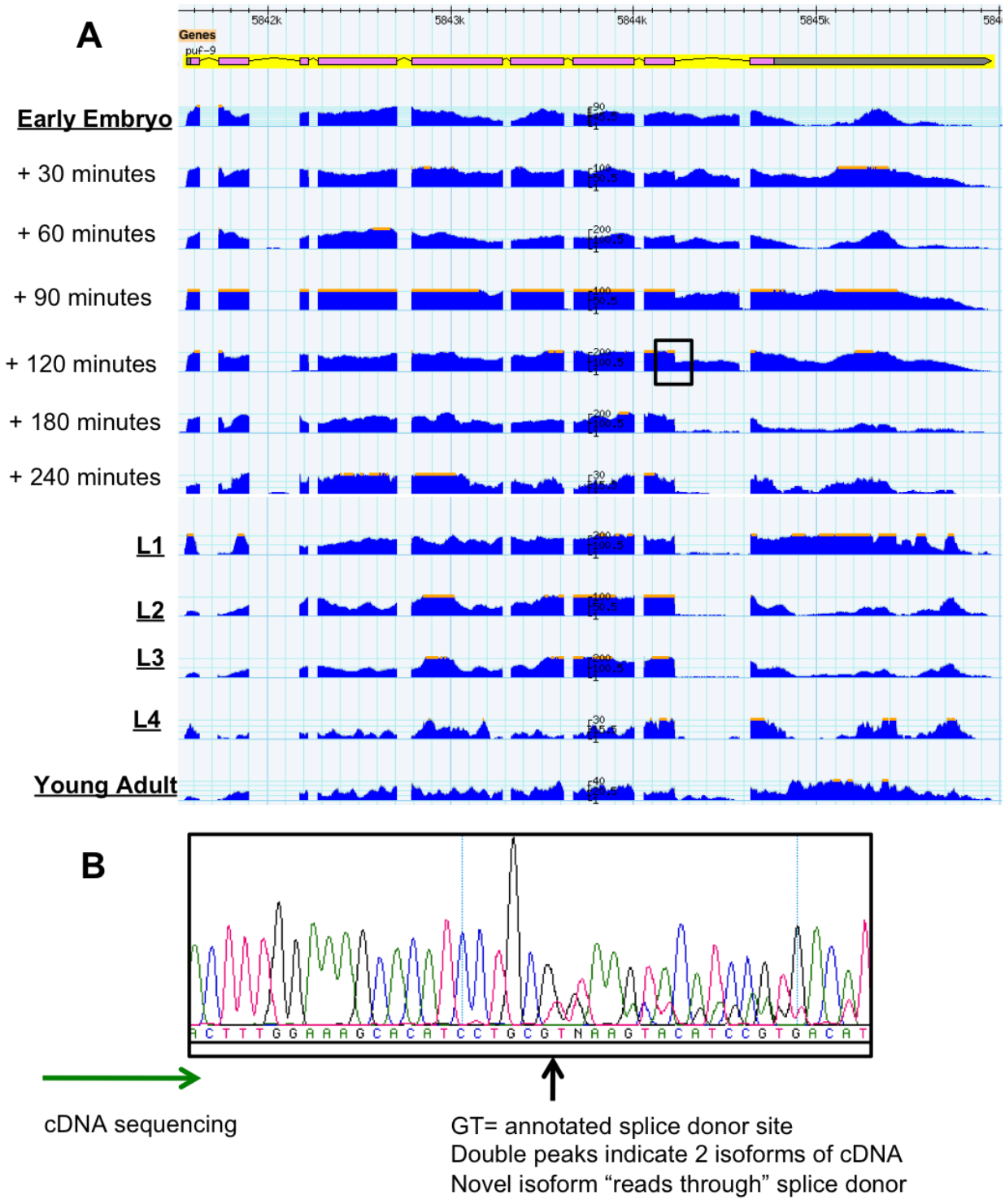

Figure 4.1 ModENCODE mRNA-seq reveals a novel isoform of *puf-9* mRNA.
(A) ModENCODE mRNA-seq browser tracks reveal an extension of *puf-9* exon 8 specific to early embryos. **(B)** Sanger sequencing of cDNA from wild type embryos confirms that new isoform reads through the annotated splice donor site. The box in part A highlights the *puf-9* region sequenced in part B.

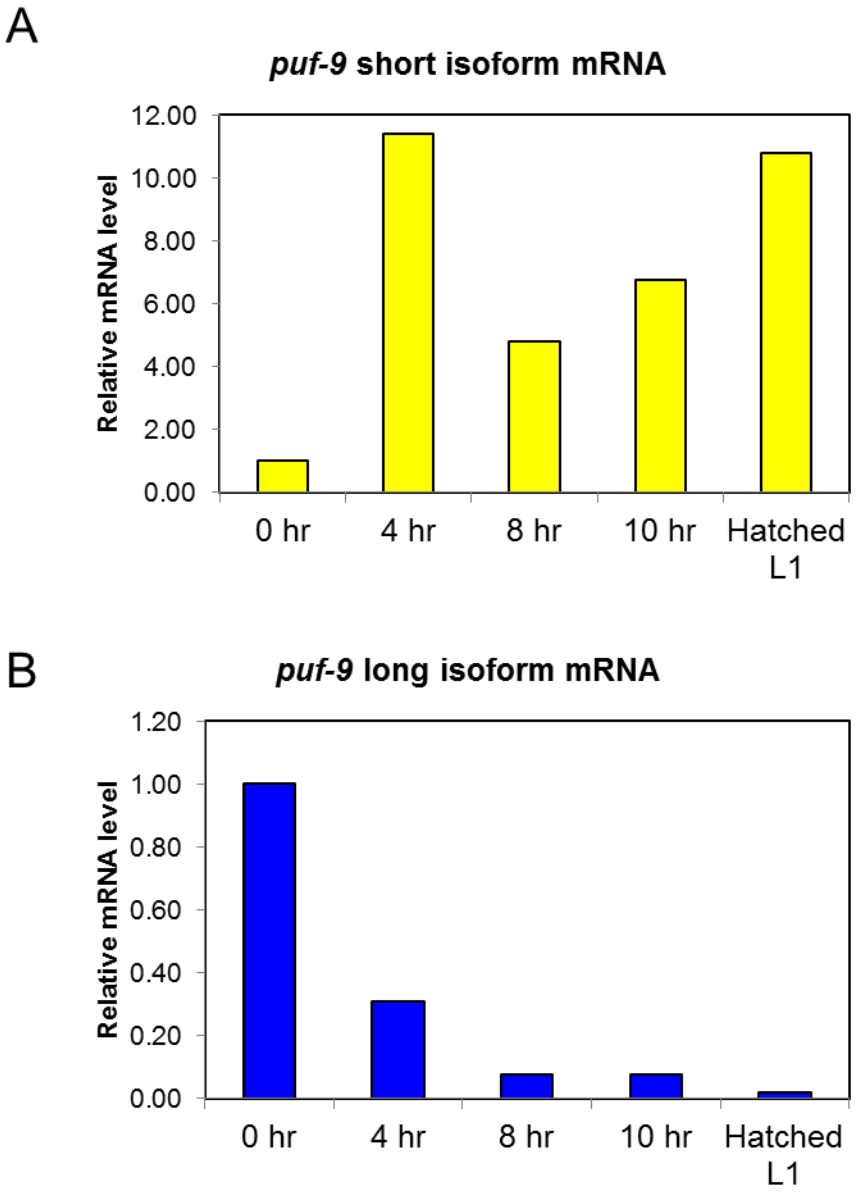

Figure 4.2 *puf-9* isoform expression across embryonic development.
(A) Expression of the annotated *puf-9* isoform (short mRNA) increases over embryonic development and persists in hatched larvae. **(B)** The novel puf-9 isoform is highly expressed in early embryos and is depleted over the course of embryonic development, becoming nearly undetectable at hatching. qRT PCR was performed with primers that span splice junctions.

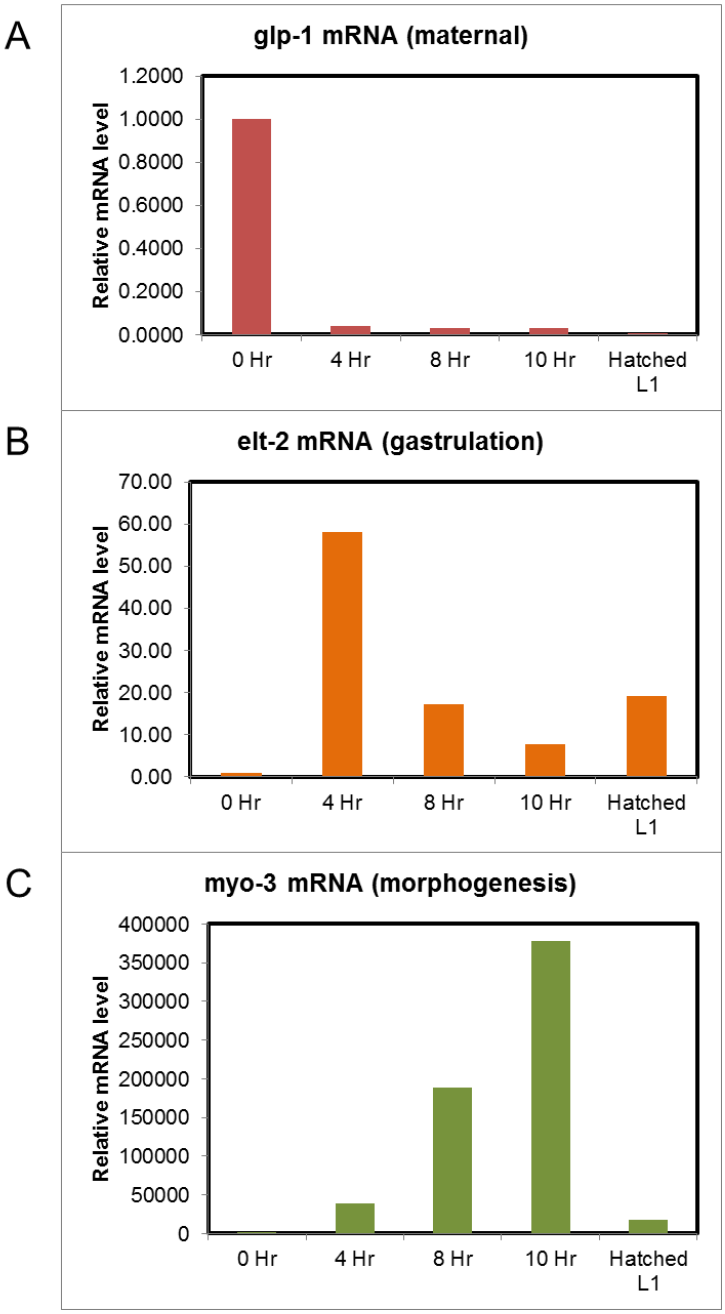

Figure 4.3 Developmental staging controls for embryo mRNA qRT-PCR.
(A) *glp-1* is a maternal mRNA in early embryos that is rapidly degraded. **(B)** *elt-2* mRNA is enriched during gastrulation. (C) *myo-3* mRNA is enriched during morphogenesis.

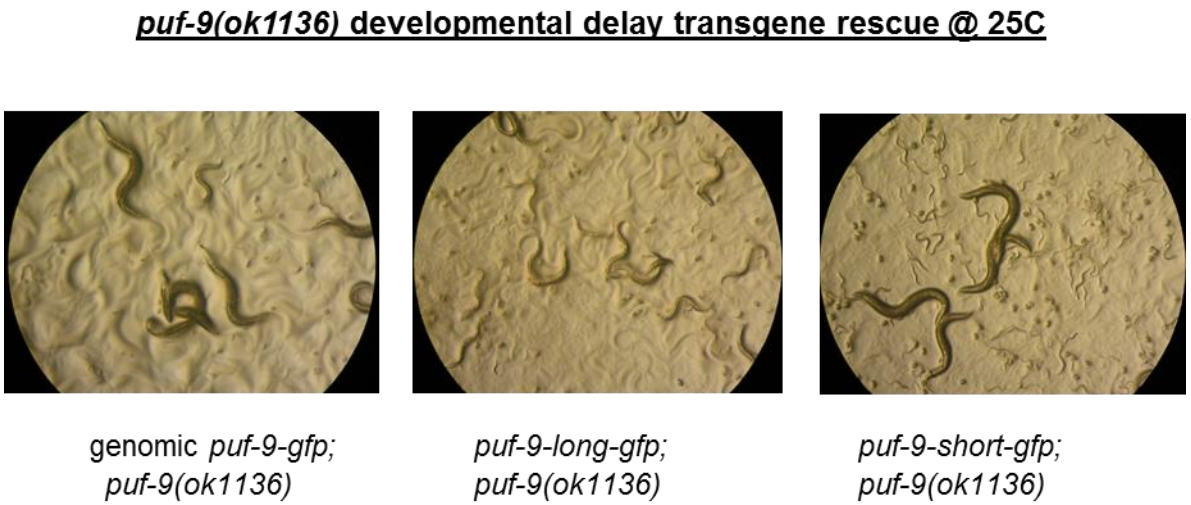

Figure 4.4 *puf-9::gfp* transgene rescue.
Genomic *puf-9-gfp* and annotated isoform *puf-9-gfp* transgenes can rescue the developmental delay of *puf-9(ok1136)* mutants. The novel, early embryo isoform *puf-9-gfp* transgene does not rescue delay in larval development. (Two integrated lines of long isoform *puf-9-gfp* were tested). Data not shown in this preliminary image set: non-transgenic *puf-9(ok1136)* mutants are also developmentally delayed.

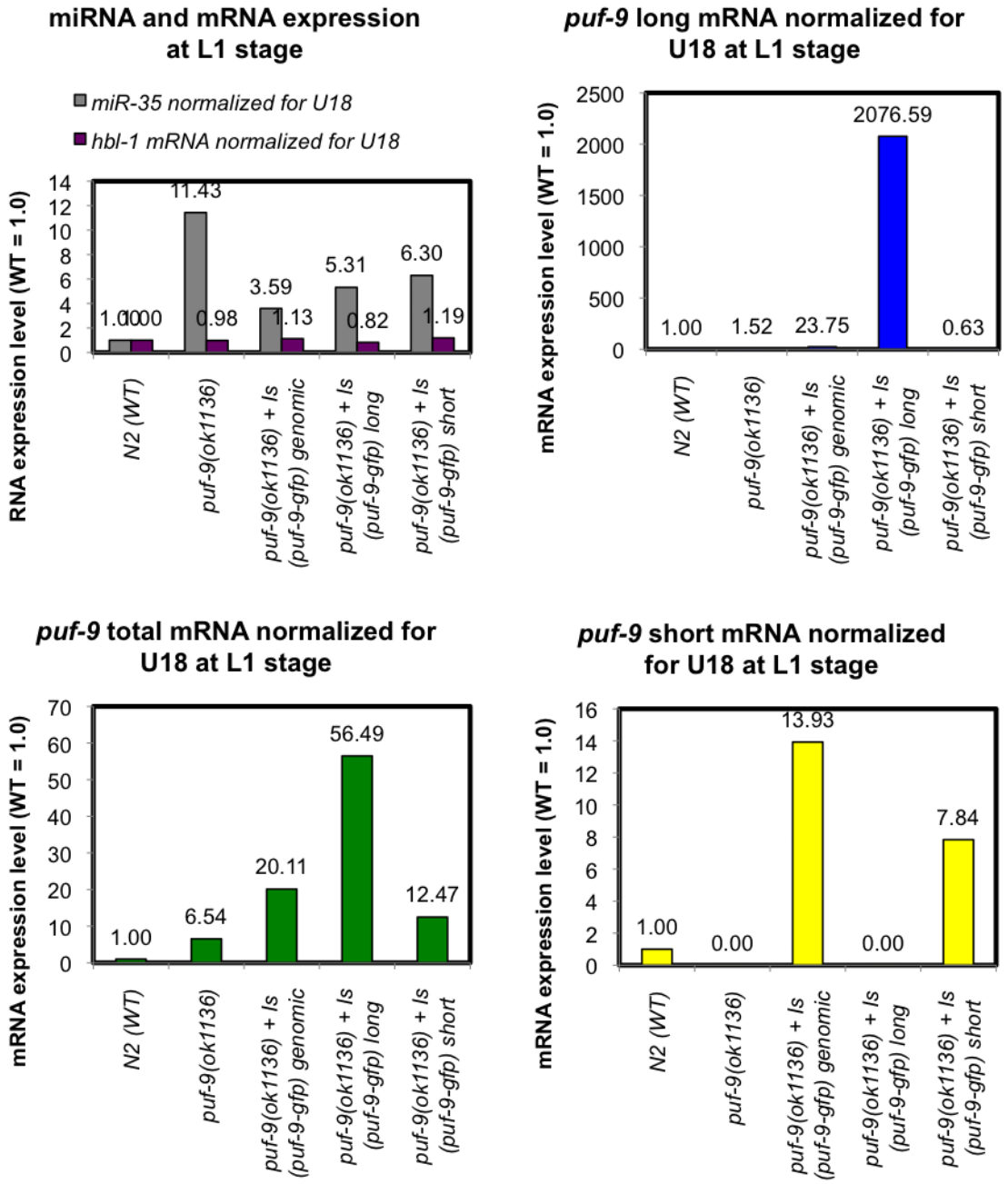

Figure 4.5 *puf-9*, target mRNA, and miRNA expression levels.
Embryonic miR-35 levels are elevated in *puf-9* mutant L1 worms for unknown reasons. This phenotype is partially rescued by genomic *puf-9-gfp*. *hbl-1* is a known target of *puf-9* translational repression, and is highly bound in PUF-9 HITS-CLIP in embryos and L1. *hbl-1* mRNA levels are not affected in *puf-9* mutants or *puf-9-gfp* transgenics. The expression level of total *puf-9* transcript, short isoform, and long isoform are displayed in the remaining graphs.

Mass Spectrometry

Protein	PUF-9-GFP Spec Count	GFP Control Spec Count
PUF-9	290	0
TSN-1	2	0
NHL-2	2	0
RACK-1	3	0
AIN-2	2	0
PAB-1	19	0
PAB-2	6	0
PAR-5	4	0
MEX-6	2	0
SQD-1	4	0
ATX-2	2	0
BRP-1	37	0

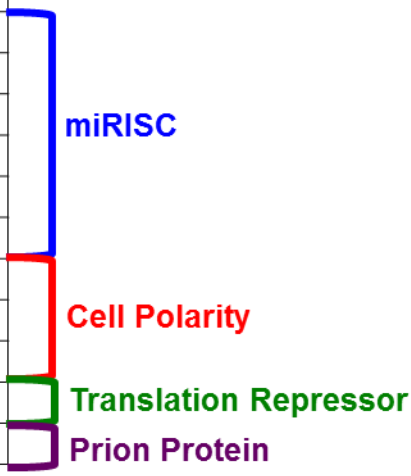

Figure 4.6 LCMS-mass spectrometry reveals PUF-9 candidate cofactors.
PUF-9-GFP complexes were immunopurified, and protein components were identified by LCMS-mass spectrometry. miRNA-RISC components and RBPs were pulled out.

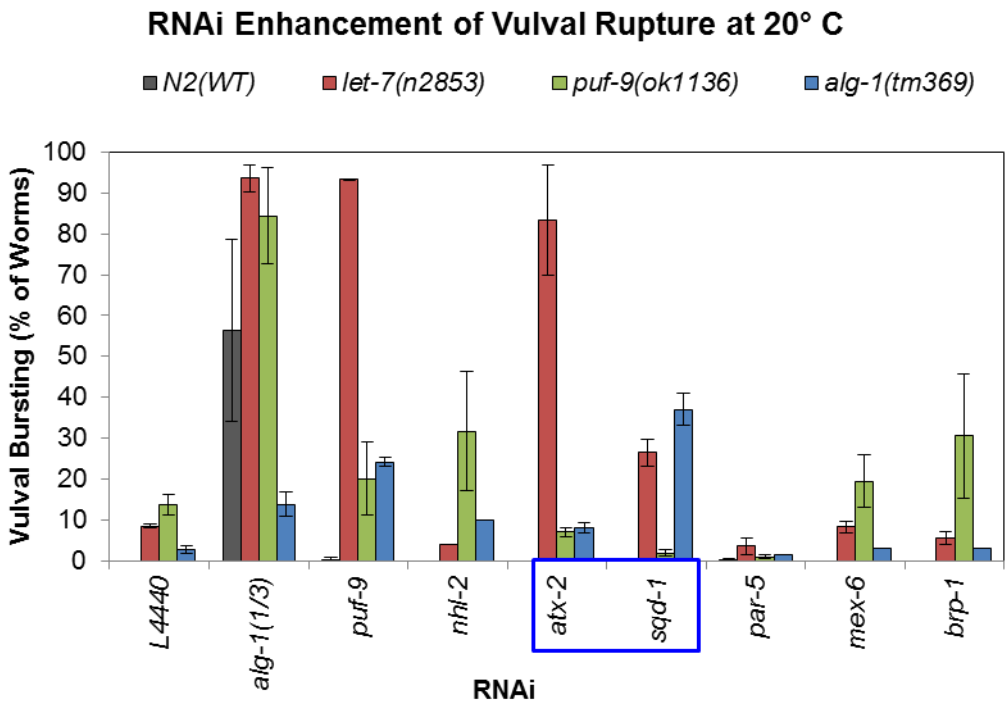

Figure 4.7 RNAi knockdown of PUF-9 candidate cofactors.
atx-2 RNAi enhances vulval rupture in *let-7(n2853)* mutants, while *sqd-1* RNAi enhances vulval rupture in *let-7(n2853)* and *alg-1(tm369)* mutants.

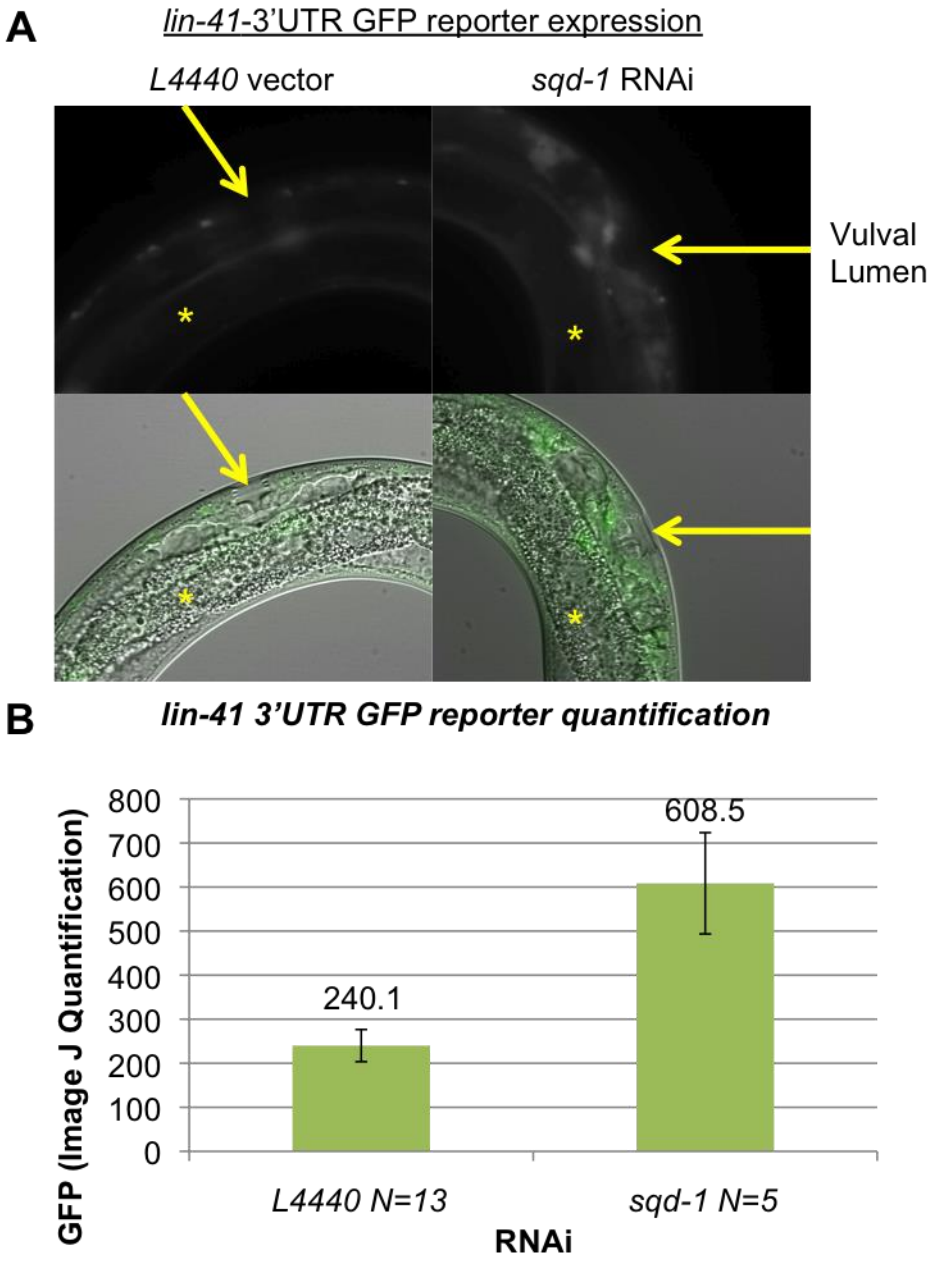

Figure 4.8 *sqd-1* RNAi increases expression of a *lin-41*-3'UTR GFP reporter.
(A) *eri-1;Is(lin-41p::gfp::lin-41-3'utr)* worms were grown on vector vs RNAi food at 20°C. Images of mid-L4 worms were taken at 60X on an Olympus BX63 microscope. Top: GFP channel. Bottom: GFP & DIC overlay. GFP signal is seen in uterine tissues adjacent to the vulval lumen (arrow). The asterisk * indicates the intestine. **(B)** GFP signal was quantified in cells surrounding the vulva at mid-L4 stage. Mean and standard deviation are plotted.

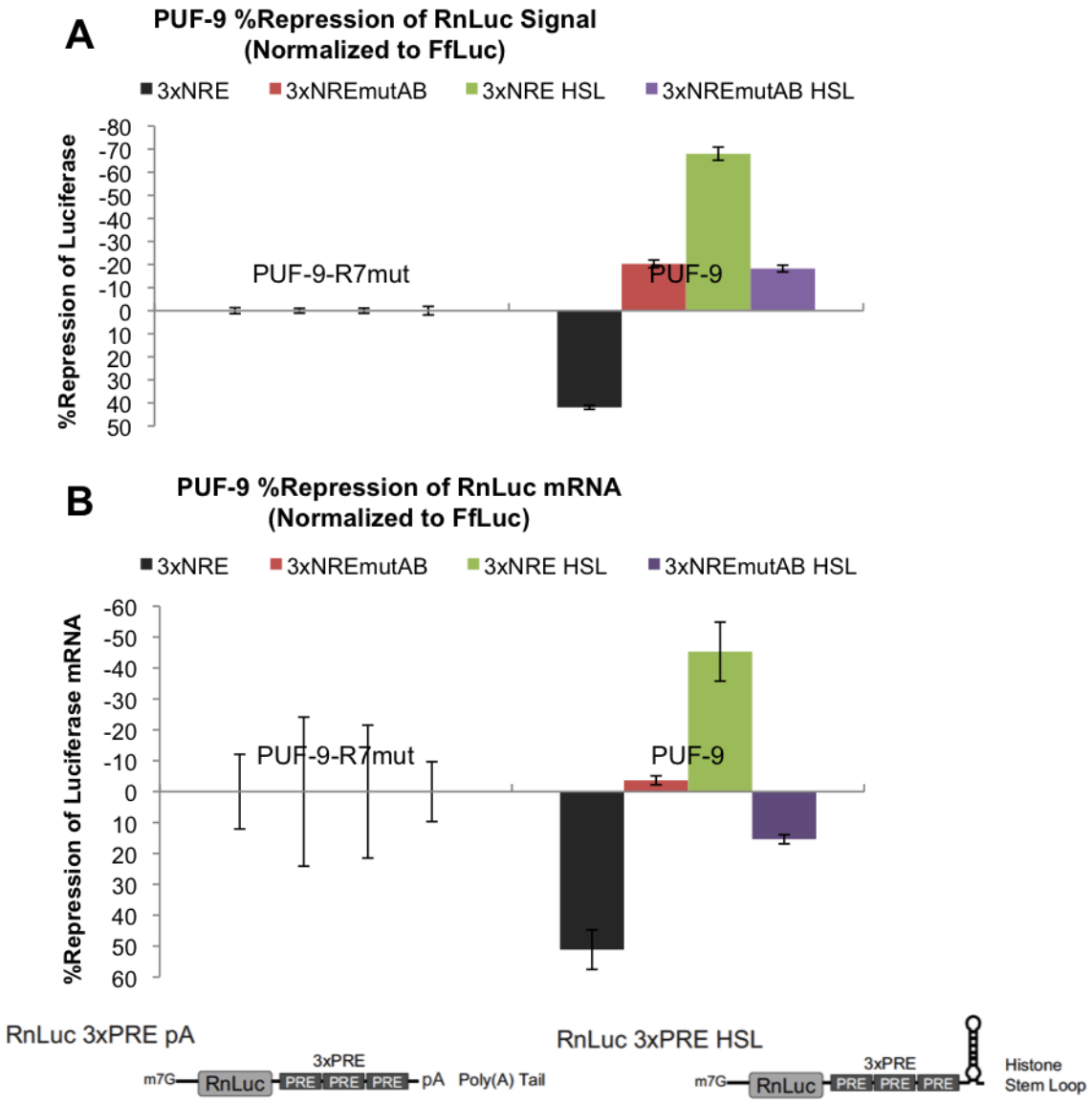

Figure 4.9 PUF-9 represses PUF target reporters in S2 cells.
(A) Luciferase reporter assays in *Drosophila* S2(D-mel2) cells. PUF-9 transfection represses a *Renilla* luciferase reporter with three nanos response elements in the 3'UTR (3xNRE), but not when the PUF binding sites are mutated (3xNREmutAB). PUF-9 increases expression of a 3xNRE 3'UTR reporter protected at the 3' end by a histone stem loop that is not polyadenylated (3xNRE HSL). These effects are lost when the PUF binding sites are mutated (3xNREmutAB HSL). Mutations in PUF-9 repeat 7 abrogate RNA binding, so PUF-9-R7mut serves as negative control. (**B)** PUF-9 transfection represses mRNA and protein levels by roughly the same amount for these reporters. PUF-9 can trigger mRNA repression and degradation when PUF binding sites are intact and a polyA tail is present. Bottom schematics: 3XNRE reporters with polyA tail or HSL. Illustration credit: Chase Weidmann [319]. 3xPRE = 3xNRE.

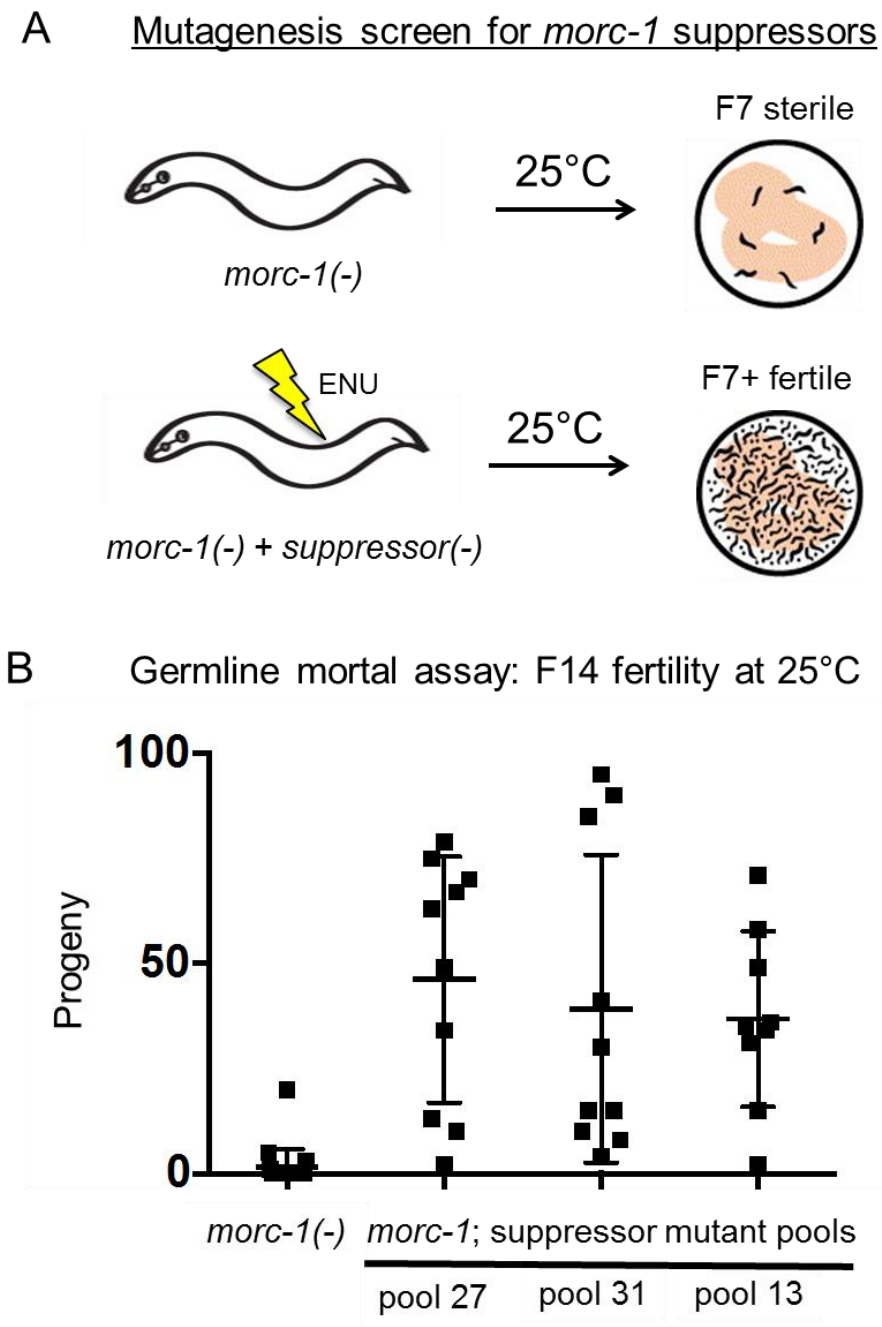

Figure 4.10 ENU mutagenesis screen for suppressors of morc-1 germline mortality.
(A) *morc-1* worms become sterile after 7 generations at 25°C. ENU mutagenesis produced suppressor mutations that preserve morc-1 fertility for 14 generations at 25°C. **(B)** Suppressor mutants were obtained in multiple pools of F14 progeny. Each pool displays variable fertility. Credit: Natasha Weiser. Worm illustration credit: [322, 323].

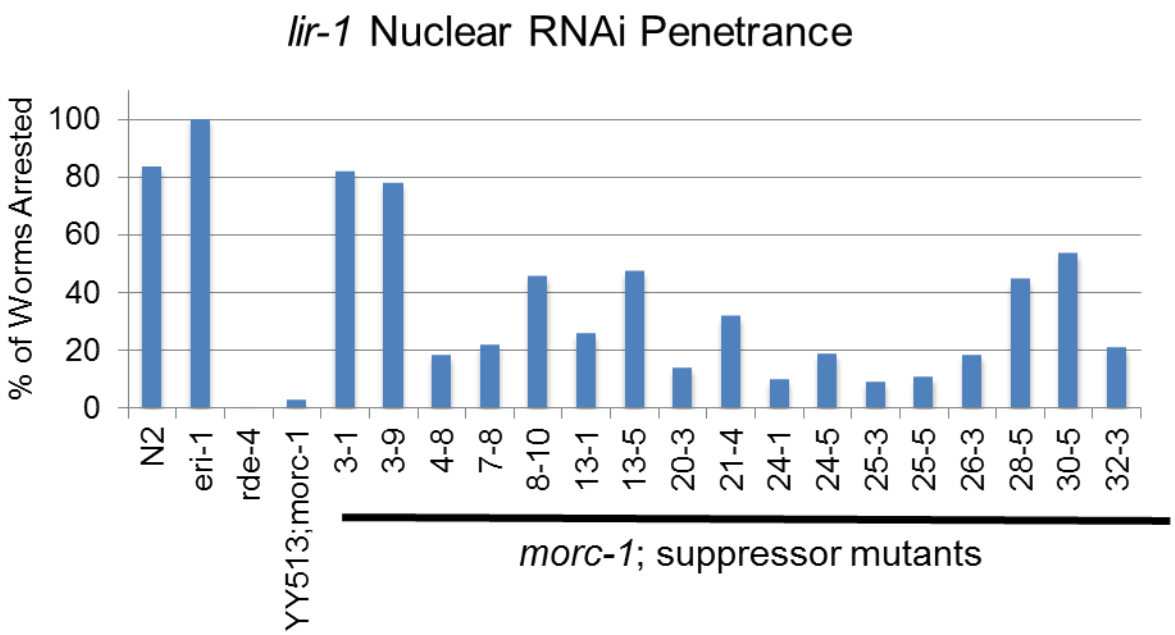

Figure 4.11 *morc-1* suppressor mutations variably restore sensitivity to nuclear RNAi. *morc-1* suppressor mutants were clonally expanded and tested for nuclear RNAi sensitivity. Credit: Natasha Weiser.

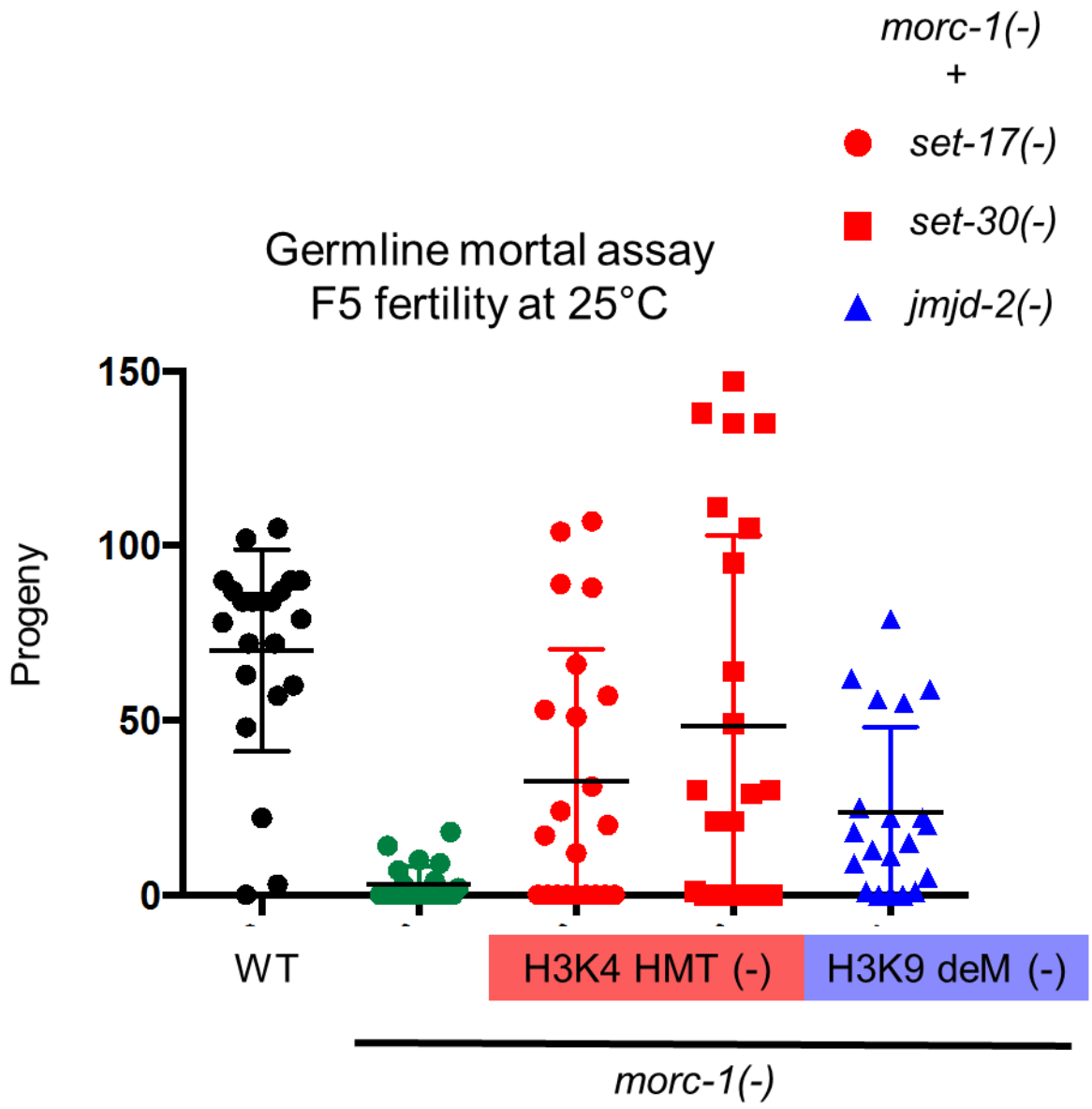

Figure 4.12 Mutations in histone methyltransferases and demethylases extend *morc-1* fertility.
morc-1 worms are germline mortal after 5 generations at 25°C. H3K9 demethylase or H3K4 methyltransferase mutations extend *morc-1* fertility. Credit: Natasha Weiser.

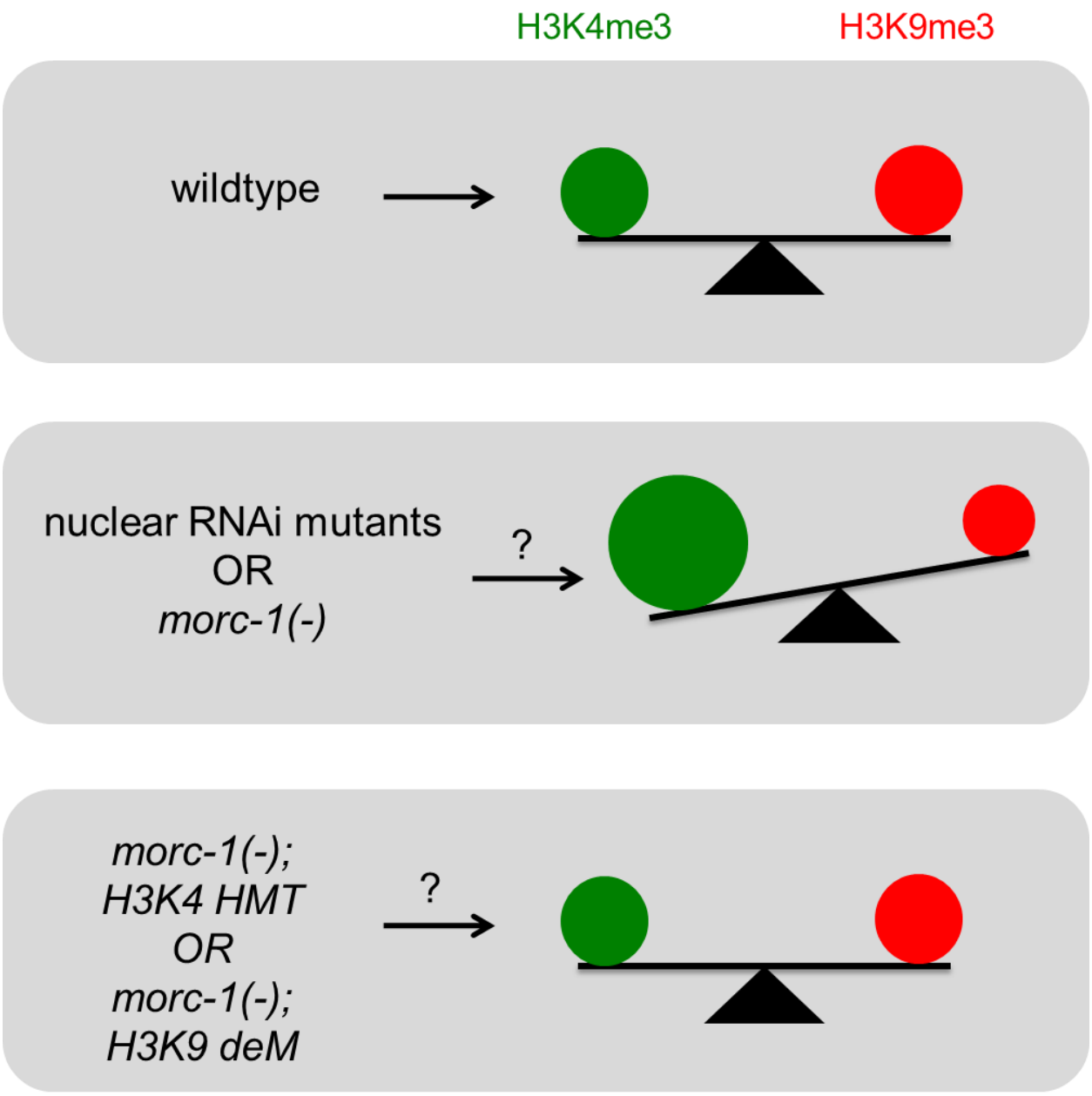

Figure 4.13 Model of H3K4 vs H3K9 methylation balance in germline maintenance.
morc-1 and nuclear RNAi mutants may be defective in H3K9 methylation or H3K4 demethylation, resulting in germline mortality. This balance can be restored by compensatory mutations in HMTs.

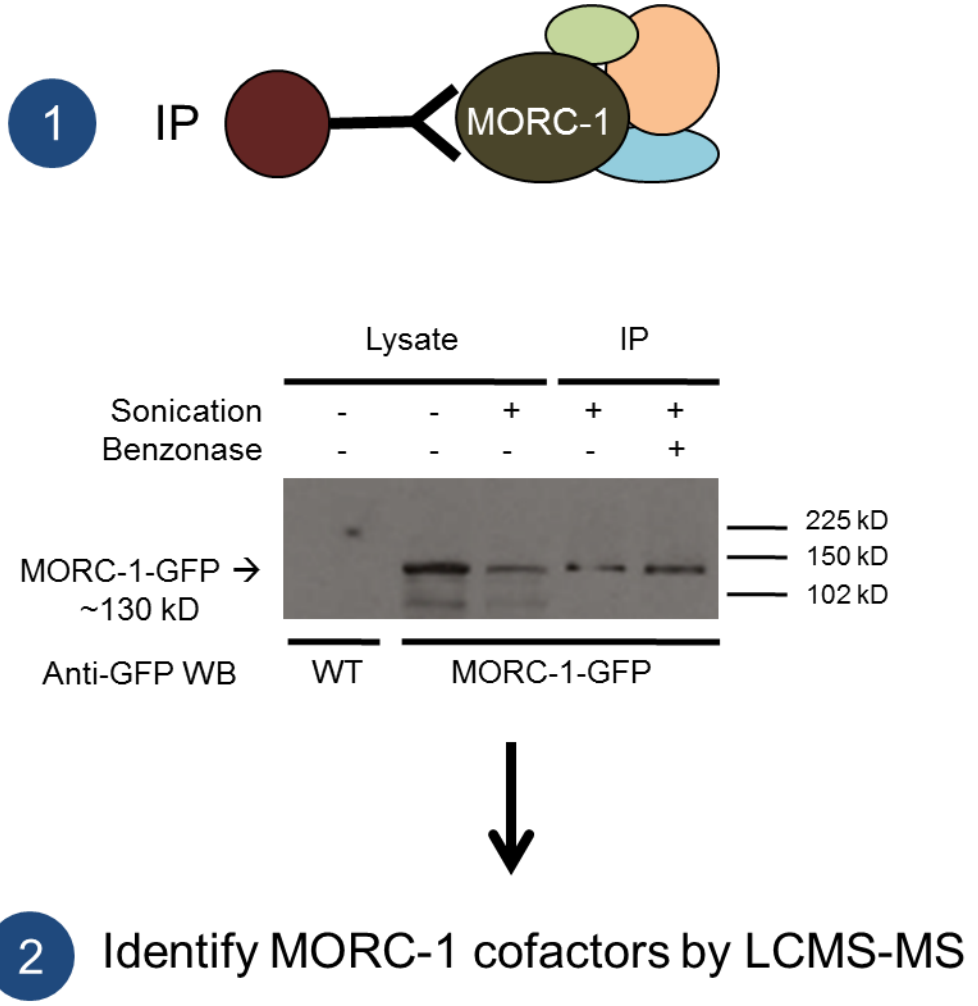

Figure 4.14 Strategy to identify MORC-1 cofactors.
MORC-1-GFP immunopurification has been worked out. Next, we will identify cofactors by LCMS-mass spectrometry. Benzonase is a nuclease that degrades both RNA and DNA, which mediates isolation of chromatin-independent protein complexes.

BIBLIOGRAPHY

1. Brenner, S., *The genetics of Caenorhabditis elegans*, in *Genetics*. 1974. p. 71-94.
2. Tabara, H., et al., *The rde-1 gene, RNA interference, and transposon silencing in C. elegans*, in *Cell*. 1999. p. 123-132.
3. Sulston, J.E. and H.R. Horvitz, *Post-embryonic cell lineages of the nematode, Caenorhabditis elegans.* Dev Biol, 1977. **56**(1): p. 110-56.
4. Lee, R.C., R.L. Feinbaum, and V. Ambros, *The C. elegans heterochronic gene lin-4 encodes small RNAs with antisense complementarity to lin-14.* Cell, 1993. **75**(5): p. 843-54.
5. Buckley, B.A., et al., *A nuclear Argonaute promotes multigenerational epigenetic inheritance and germline immortality*, in *Nature*. 2012.
6. Zhang, B., et al., *A conserved RNA-binding protein that regulates sexual fates in the C. elegans hermaphrodite germ line.* Nature, 1997. **390**(6659): p. 477-84.
7. Yigit, E., et al., *Analysis of the C. elegans Argonaute family reveals that distinct Argonautes act sequentially during RNAi*, in *Cell*. 2006. p. 747-757.
8. Schaner, C.E. and W.G. Kelly, *Germline chromatin.* WormBook, 2006: p. 1-14.
9. Seydoux, G., et al., *Repression of gene expression in the embryonic germ lineage of C. elegans.* Nature, 1996. **382**(6593): p. 713-6.
10. Ward, S. and J.S. Carrel, *Fertilization and sperm competition in the nematode Caenorhabditis elegans.* Dev Biol, 1979. **73**(2): p. 304-21.
11. Crittenden, S.L., et al., *A conserved RNA-binding protein controls germline stem cells in Caenorhabditis elegans.* Nature, 2002. **417**(6889): p. 660-3.
12. Wickens, M., et al., *A PUF family portrait: 3'UTR regulation as a way of life.* Trends Genet, 2002. **18**(3): p. 150-7.
13. Subramaniam, K. and G. Seydoux, *nos-1 and nos-2, two genes related to Drosophila nanos, regulate primordial germ cell development and survival in Caenorhabditis elegans.* Development, 1999. **126**(21): p. 4861-71.
14. Suh, N., et al., *FBF and its dual control of gld-1 expression in the Caenorhabditis elegans germline.* Genetics, 2009. **181**(4): p. 1249-60.
15. Bachorik, J.L. and J. Kimble, *Redundant control of the Caenorhabditis elegans sperm/oocyte switch by PUF-8 and FBF-1, two distinct PUF RNA-binding proteins.* Proc Natl Acad Sci U S A, 2005. **102**(31): p. 10893-7.
16. Wang, Z. and H. Lin, *Nanos maintains germline stem cell self-renewal by preventing differentiation.* Science, 2004. **303**(5666): p. 2016-9.
17. Chen, D., et al., *Pumilio 1 suppresses multiple activators of p53 to safeguard spermatogenesis.* Curr Biol, 2012. **22**(5): p. 420-5.

18. Ye, B., et al., *Nanos and Pumilio are essential for dendrite morphogenesis in Drosophila peripheral neurons.* Curr Biol, 2004. **14**(4): p. 314-21.
19. Vessey, J.P., et al., *Mammalian Pumilio 2 regulates dendrite morphogenesis and synaptic function.* Proc Natl Acad Sci U S A, 2010. **107**(7): p. 3222-7.
20. Gennarino, V.A., et al., *Pumilio1 haploinsufficiency leads to SCA1-like neurodegeneration by increasing wild-type Ataxin1 levels.* Cell, 2015. **160**(6): p. 1087-98.
21. Kaye, J.A., et al., *A 3'UTR pumilio-binding element directs translational activation in olfactory sensory neurons.* Neuron, 2009. **61**(1): p. 57-70.
22. Lehmann, R. and C. Nusslein-Volhard, *Involvement of the pumilio gene in the transport of an abdominal signal in the Drosophila embryo*, in *Nature*. 1987. p. 167-170.
23. Barker, D.D., et al., *Pumilio is essential for function but not for distribution of the Drosophila abdominal determinant Nanos.* Genes Dev, 1992. **6**(12A): p. 2312-26.
24. Smith, J.L., J.E. Wilson, and P.M. Macdonald, *Overexpression of oskar directs ectopic activation of nanos and presumptive pole cell formation in Drosophila embryos.* Cell, 1992. **70**(5): p. 849-59.
25. Macdonald, P.M., *The Drosophila pumilio gene: an unusually long transcription unit and an unusual protein.* Development, 1992. **114**(1): p. 221-32.
26. Lehmann, R. and C. Nusslein-Volhard, *The maternal gene nanos has a central role in posterior pattern formation of the Drosophila embryo.* Development, 1991. **112**(3): p. 679-91.
27. Wharton, R.P. and G. Struhl, *RNA regulatory elements mediate control of Drosophila body pattern by the posterior morphogen nanos.* Cell, 1991. **67**(5): p. 955-67.
28. Murata, Y. and R.P. Wharton, *Binding of pumilio to maternal hunchback mRNA is required for posterior patterning in Drosophila embryos.* Cell, 1995. **80**(5): p. 747-56.
29. Wreden, C., et al., *Nanos and pumilio establish embryonic polarity in Drosophila by promoting posterior deadenylation of hunchback mRNA.* Development, 1997. **124**(15): p. 3015-23.
30. Wharton, R.P., et al., *The Pumilio RNA-binding domain is also a translational regulator.* Mol Cell, 1998. **1**(6): p. 863-72.
31. Chagnovich, D. and R. Lehmann, *Poly(A)-independent regulation of maternal hunchback translation in the Drosophila embryo.* Proc Natl Acad Sci U S A, 2001. **98**(20): p. 11359-64.
32. Loedige, I., et al., *The NHL domain of BRAT is an RNA-binding domain that directly contacts the hunchback mRNA for regulation.* Genes Dev, 2014. **28**(7): p. 749-64.
33. Sonoda, J. and R.P. Wharton, *Recruitment of Nanos to hunchback mRNA by Pumilio.* Genes Dev, 1999. **13**(20): p. 2704-12.
34. Sonoda, J. and R.P. Wharton, *Drosophila Brain Tumor is a translational repressor.* Genes Dev, 2001. **15**(6): p. 762-73.
35. Cho, P.F., et al., *Cap-dependent translational inhibition establishes two opposing morphogen gradients in Drosophila embryos.* Curr Biol, 2006. **16**(20): p. 2035-41.

36. Zamore, P.D., J.R. Williamson, and R. Lehmann, *The Pumilio protein binds RNA through a conserved domain that defines a new class of RNA-binding proteins.* RNA, 1997. **3**(12): p. 1421-33.
37. Zamore, P.D., et al., *The PUMILIO-RNA interaction: a single RNA-binding domain monomer recognizes a bipartite target sequence.* Biochemistry, 1999. **38**(2): p. 596-604.
38. Edwards, T.A., et al., *Structure of Pumilio reveals similarity between RNA and peptide binding motifs.* Cell, 2001. **105**(2): p. 281-9.
39. Wang, X., P.D. Zamore, and T.M. Hall, *Crystal structure of a Pumilio homology domain.* Mol Cell, 2001. **7**(4): p. 855-65.
40. Wang, X., et al., *Modular recognition of RNA by a human pumilio-homology domain.* Cell, 2002. **110**(4): p. 501-12.
41. Campbell, Z.T., C.T. Valley, and M. Wickens, *A protein-RNA specificity code enables targeted activation of an endogenous human transcript.* Nat Struct Mol Biol, 2014. **21**(8): p. 732-8.
42. Bernstein, D., et al., *Binding specificity and mRNA targets of a C. elegans PUF protein, FBF-1.* RNA, 2005. **11**(4): p. 447-58.
43. Opperman, L., et al., *A single spacer nucleotide determines the specificities of two mRNA regulatory proteins.*, in *Nat Struct Mol Biol*. 2005. p. 945-951.
44. Stumpf, C.R., J. Kimble, and M. Wickens, *A Caenorhabditis elegans PUF protein family with distinct RNA binding specificity.* RNA, 2008. **14**(8): p. 1550-7.
45. Koh, Y.Y., et al., *A single C. elegans PUF protein binds RNA in multiple modes.* RNA, 2009. **15**(6): p. 1090-9.
46. Tadauchi, T., et al., *Post-transcriptional regulation through the HO 3'-UTR by Mpt5, a yeast homolog of Pumilio and FBF.* EMBO J, 2001. **20**(3): p. 552-61.
47. Goldstrohm, A.C., et al., *PUF proteins bind Pop2p to regulate messenger RNAs.* Nat Struct Mol Biol, 2006. **13**(6): p. 533-9.
48. Goldstrohm, A.C., et al., *PUF protein-mediated deadenylation is catalyzed by Ccr4p.* J Biol Chem, 2007. **282**(1): p. 109-14.
49. Hook, B.A., et al., *Two yeast PUF proteins negatively regulate a single mRNA.* J Biol Chem, 2007. **282**(21): p. 15430-8.
50. Kadyrova, L.Y., et al., *Translational control of maternal Cyclin B mRNA by Nanos in the Drosophila germline.* Development, 2007. **134**(8): p. 1519-27.
51. Van Etten, J., et al., *Human Pumilio proteins recruit multiple deadenylases to efficiently repress messenger RNAs.*, in *J Biol Chem*. 2012. p. 36370-36383.
52. Cao, Q., K. Padmanabhan, and J.D. Richter, *Pumilio 2 controls translation by competing with eIF4E for 7-methyl guanosine cap recognition.* RNA, 2010. **16**(1): p. 221-7.
53. Deng, Y., R.H. Singer, and W. Gu, *Translation of ASH1 mRNA is repressed by Puf6p-Fun12p/eIF5B interaction and released by CK2 phosphorylation.*, in *Genes Dev*. 2008. p. 1037-1050.
54. Gu, W., et al., *A new yeast PUF family protein, Puf6p, represses ASH1 mRNA translation and is required for its localization.*, in *Genes Dev*. 2004. p. 1452-1465.

55. Voronina, E., A. Paix, and G. Seydoux, *The P granule component PGL-1 promotes the localization and silencing activity of the PUF protein FBF-2 in germline stem cells*, in *Development*. 2012. p. 3732-3740.
56. Swartz, S.Z., et al., *Deadenylase depletion protects inherited mRNAs in primordial germ cells.* Development, 2014. **141**(16): p. 3134-42.
57. Hubstenberger, A., et al., *A network of PUF proteins and Ras signaling promote mRNA repression and oogenesis in C. elegans.*, in *Developmental Biology*. 2012. p. 218-231.
58. Hubstenberger, A., et al., *Translation Repressors, an RNA Helicase, and Developmental Cues Control RNP Phase Transitions during Early Development.*, in *Dev Cell*. 2013. p. 161-173.
59. Nolde, M.J., et al., *The Caenorhabditis elegans pumilio homolog, puf-9, is required for the 3'UTR-mediated repression of the let-7 microRNA target gene, hbl-1.* Dev Biol, 2007. **305**(2): p. 551-63.
60. Ahringer, J. and J. Kimble, *Control of the sperm-oocyte switch in Caenorhabditis elegans hermaphrodites by the fem-3 3' untranslated region.* Nature, 1991. **349**(6307): p. 346-8.
61. Kraemer, B., et al., *NANOS-3 and FBF proteins physically interact to control the sperm-oocyte switch in Caenorhabditis elegans.* Curr Biol, 1999. **9**(18): p. 1009-18.
62. Suh, N., et al., *The GLD-2 poly(A) polymerase activates gld-1 mRNA in the Caenorhabditis elegans germ line.* Proc Natl Acad Sci U S A, 2006. **103**(41): p. 15108-12.
63. Wang, L., et al., *A regulatory cytoplasmic poly(A) polymerase in Caenorhabditis elegans.* Nature, 2002. **419**(6904): p. 312-6.
64. Galgano, A., et al., *Comparative analysis of mRNA targets for human PUF-family proteins suggests extensive interaction with the miRNA regulatory system.* PLoS One, 2008. **3**(9): p. e3164.
65. Gerber, A.P., D. Herschlag, and P.O. Brown, *Extensive association of functionally and cytotopically related mRNAs with Puf family RNA-binding proteins in yeast.*, in *PLoS Biol*. 2004. p. E79.
66. Hafner, M., et al., *Transcriptome-wide identification of RNA-binding protein and microRNA target sites by PAR-CLIP.* Cell, 2010. **141**(1): p. 129-41.
67. Kershner, A.M. and J. Kimble, *Genome-wide analysis of mRNA targets for Caenorhabditis elegans FBF, a conserved stem cell regulator.* Proc Natl Acad Sci U S A, 2010. **107**(8): p. 3936-41.
68. Wang, Y., et al., *Structural basis for specific recognition of multiple mRNA targets by a PUF regulatory protein.* Proc Natl Acad Sci U S A, 2009. **106**(48): p. 20186-91.
69. Nakahata, S., et al., *Involvement of Xenopus Pumilio in the translational regulation that is specific to cyclin B1 mRNA during oocyte maturation.* Mech Dev, 2003. **120**(8): p. 865-80.
70. Pique, M., et al., *A combinatorial code for CPE-mediated translational control.* Cell, 2008. **132**(3): p. 434-48.

71. Luitjens, C., et al., *CPEB proteins control two key steps in spermatogenesis in C. elegans.* Genes Dev, 2000. **14**(20): p. 2596-609.
72. Menichelli, E., et al., *Biochemical characterization of the Caenorhabditis elegans FBF.CPB-1 translational regulation complex identifies conserved protein interaction hotspots.* J Mol Biol, 2013. **425**(4): p. 725-37.
73. Wu, E., et al., *Pervasive and cooperative deadenylation of 3'UTRs by embryonic microRNA families.* Mol Cell, 2010. **40**(4): p. 558-70.
74. Esquela-Kerscher, A. and F.J. Slack, *Oncomirs - microRNAs with a role in cancer.* Nat Rev Cancer, 2006. **6**(4): p. 259-69.
75. Zhao, Y., E. Samal, and D. Srivastava, *Serum response factor regulates a muscle-specific microRNA that targets Hand2 during cardiogenesis.* Nature, 2005. **436**(7048): p. 214-20.
76. Giraldez, A.J., et al., *Zebrafish MiR-430 promotes deadenylation and clearance of maternal mRNAs.* Science, 2006. **312**(5770): p. 75-9.
77. Krol, J., et al., *Characterizing light-regulated retinal microRNAs reveals rapid turnover as a common property of neuronal microRNAs.* Cell, 2010. **141**(4): p. 618-31.
78. Boehm, M. and F. Slack, *A developmental timing microRNA and its target regulate life span in C. elegans.* Science, 2005. **310**(5756): p. 1954-7.
79. Mayr, C., M.T. Hemann, and D.P. Bartel, *Disrupting the pairing between let-7 and Hmga2 enhances oncogenic transformation.* Science, 2007. **315**(5818): p. 1576-9.
80. Trajkovski, M., et al., *MicroRNAs 103 and 107 regulate insulin sensitivity.* Nature, 2011. **474**(7353): p. 649-53.
81. Kim, J., et al., *A MicroRNA feedback circuit in midbrain dopamine neurons.* Science, 2007. **317**(5842): p. 1220-4.
82. Du, C., et al., *MicroRNA miR-326 regulates TH-17 differentiation and is associated with the pathogenesis of multiple sclerosis.* Nat Immunol, 2009. **10**(12): p. 1252-9.
83. Wightman, B., I. Ha, and G. Ruvkun, *Posttranscriptional regulation of the heterochronic gene lin-14 by lin-4 mediates temporal pattern formation in C. elegans*, in *Cell*. 1993. p. 855-862.
84. Reinhart, B.J., et al., *The 21-nucleotide let-7 RNA regulates developmental timing in Caenorhabditis elegans.* Nature, 2000. **403**(6772): p. 901-6.
85. Pasquinelli, A.E., et al., *Conservation of the sequence and temporal expression of let-7 heterochronic regulatory RNA.* Nature, 2000. **408**(6808): p. 86-9.
86. Lagos-Quintana, M., et al., *Identification of novel genes coding for small expressed RNAs.* Science, 2001. **294**(5543): p. 853-8.
87. Lau, N.C., et al., *An abundant class of tiny RNAs with probable regulatory roles in Caenorhabditis elegans.* Science, 2001. **294**(5543): p. 858-62.
88. Lim, L.P., et al., *The microRNAs of Caenorhabditis elegans.* Genes Dev, 2003. **17**(8): p. 991-1008.
89. Ruby, J.G., et al., *Large-scale sequencing reveals 21U-RNAs and additional microRNAs and endogenous siRNAs in C. elegans*, in *Cell*. 2006. p. 1193-1207.

90. Kozomara, A. and S. Griffiths-Jones, *miRBase: annotating high confidence microRNAs using deep sequencing data.* Nucleic Acids Res, 2014. **42**(Database issue): p. D68-73.
91. Sempere, L.F., et al., *Expression profiling of mammalian microRNAs uncovers a subset of brain-expressed microRNAs with possible roles in murine and human neuronal differentiation.* Genome Biol, 2004. **5**(3): p. R13.
92. Yu, F., et al., *let-7 regulates self renewal and tumorigenicity of breast cancer cells.* Cell, 2007. **131**(6): p. 1109-23.
93. Viswanathan, S.R., et al., *Lin28 promotes transformation and is associated with advanced human malignancies.*, in *Nature Genetics*. 2009. p. 843-848.
94. Takamizawa, J., et al., *Reduced expression of the let-7 microRNAs in human lung cancers in association with shortened postoperative survival.* Cancer Res, 2004. **64**(11): p. 3753-6.
95. Akao, Y., Y. Nakagawa, and T. Naoe, *let-7 microRNA functions as a potential growth suppressor in human colon cancer cells.* Biol Pharm Bull, 2006. **29**(5): p. 903-6.
96. Guo, Y., et al., *Identification and characterization of lin-28 homolog B (LIN28B) in human hepatocellular carcinoma.* Gene, 2006. **384**: p. 51-61.
97. Johnson, S.M., et al., *RAS is regulated by the let-7 microRNA family.* Cell, 2005. **120**(5): p. 635-47.
98. Lee, Y.S. and A. Dutta, *The tumor suppressor microRNA let-7 represses the HMGA2 oncogene.* Genes Dev, 2007. **21**(9): p. 1025-30.
99. Cai, X., C.H. Hagedorn, and B.R. Cullen, *Human microRNAs are processed from capped, polyadenylated transcripts that can also function as mRNAs.* RNA, 2004. **10**(12): p. 1957-66.
100. Lee, Y., et al., *MicroRNA genes are transcribed by RNA polymerase II.* EMBO J, 2004. **23**(20): p. 4051-60.
101. Gregory, R.I., et al., *The Microprocessor complex mediates the genesis of microRNAs.* Nature, 2004. **432**(7014): p. 235-40.
102. Lee, Y., et al., *The nuclear RNase III Drosha initiates microRNA processing.* Nature, 2003. **425**(6956): p. 415-9.
103. Denli, A.M., et al., *Processing of primary microRNAs by the Microprocessor complex.* Nature, 2004. **432**(7014): p. 231-5.
104. Han, J., et al., *The Drosha-DGCR8 complex in primary microRNA processing.* Genes Dev, 2004. **18**(24): p. 3016-27.
105. Landthaler, M., A. Yalcin, and T. Tuschl, *The human DiGeorge syndrome critical region gene 8 and Its D. melanogaster homolog are required for miRNA biogenesis.* Curr Biol, 2004. **14**(23): p. 2162-7.
106. Yi, R., et al., *Exportin-5 mediates the nuclear export of pre-microRNAs and short hairpin RNAs.* Genes Dev, 2003. **17**(24): p. 3011-6.
107. Lund, E., et al., *Nuclear export of microRNA precursors.* Science, 2004. **303**(5654): p. 95-8.
108. Ketting, R.F., et al., *Dicer functions in RNA interference and in synthesis of small RNA involved in developmental timing in C. elegans.* Genes Dev, 2001. **15**(20): p. 2654-9.

109. Hutvagner, G., et al., *A cellular function for the RNA-interference enzyme Dicer in the maturation of the let-7 small temporal RNA.* Science, 2001. **293**(5531): p. 834-8.
110. Bernstein, E., et al., *Role for a bidentate ribonuclease in the initiation step of RNA interference.* Nature, 2001. **409**(6818): p. 363-6.
111. Grishok, A., et al., *Genes and mechanisms related to RNA interference regulate expression of the small temporal RNAs that control C. elegans developmental timing.* Cell, 2001. **106**(1): p. 23-34.
112. Knight, S.W. and B.L. Bass, *A role for the RNase III enzyme DCR-1 in RNA interference and germ line development in Caenorhabditis elegans.* Science, 2001. **293**(5538): p. 2269-71.
113. Zhang, H., et al., *Single processing center models for human Dicer and bacterial RNase III.* Cell, 2004. **118**(1): p. 57-68.
114. Tahbaz, N., et al., *Characterization of the interactions between mammalian PAZ PIWI domain proteins and Dicer.* EMBO Rep, 2004. **5**(2): p. 189-94.
115. Zinovyeva, A.Y., et al., *Mutations in conserved residues of the C. elegans microRNA Argonaute ALG-1 identify separable functions in ALG-1 miRISC loading and target repression.* PLoS Genet, 2014. **10**(4): p. e1004286.
116. Hutvagner, G. and P.D. Zamore, *A microRNA in a multiple-turnover RNAi enzyme complex.* Science, 2002. **297**(5589): p. 2056-60.
117. Mourelatos, Z., et al., *miRNPs: a novel class of ribonucleoproteins containing numerous microRNAs.* Genes Dev, 2002. **16**(6): p. 720-8.
118. Iwasaki, S., et al., *Hsc70/Hsp90 chaperone machinery mediates ATP-dependent RISC loading of small RNA duplexes.* Mol Cell, 2010. **39**(2): p. 292-9.
119. Ha, M. and V.N. Kim, *Regulation of microRNA biogenesis.* Nat Rev Mol Cell Biol, 2014. **15**(8): p. 509-24.
120. Cohen, M.L., et al., *The GATA factor elt-1 regulates C. elegans developmental timing by promoting expression of the let-7 family microRNAs.* PLoS Genet, 2015. **11**(3): p. e1005099.
121. Roush, S.F. and F.J. Slack, *Transcription of the C. elegans let-7 microRNA is temporally regulated by one of its targets, hbl-1.* Dev Biol, 2009. **334**(2): p. 523-34.
122. Bethke, A., et al., *Nuclear hormone receptor regulation of microRNAs controls developmental progression.* Science, 2009. **324**(5923): p. 95-8.
123. Trabucchi, M., et al., *The RNA-binding protein KSRP promotes the biogenesis of a subset of microRNAs.* Nature, 2009. **459**(7249): p. 1010-4.
124. Heo, I., et al., *Lin28 mediates the terminal uridylation of let-7 precursor MicroRNA.*, in *Mol Cell*. 2008. p. 276-284.
125. Heo, I., et al., *TUT4 in concert with Lin28 suppresses microRNA biogenesis through pre-microRNA uridylation.*, in *Cell*. 2009. p. 696-708.
126. Van Wynsberghe, P.M., et al., *LIN-28 co-transcriptionally binds primary let-7 to regulate miRNA maturation in Caenorhabditis elegans.* Nat Struct Mol Biol, 2011. **18**(3): p. 302-8.
127. Chatterjee, S., et al., *Target-mediated protection of endogenous microRNAs in C. elegans.* Dev Cell, 2011. **20**(3): p. 388-96.

128. Chatterjee, S. and H. Grosshans, *Active turnover modulates mature microRNA activity in Caenorhabditis elegans.* Nature, 2009. **461**(7263): p. 546-9.
129. Bossé, G.D., et al., *The decapping scavenger enzyme DCS-1 controls microRNA levels in Caenorhabditis elegans.*, in *Mol Cell*. 2013. p. 281-287.
130. Hansen, T.B., et al., *Natural RNA circles function as efficient microRNA sponges.*, in *Nature*. 2013.
131. Wilczynska, A. and M. Bushell, *The complexity of miRNA-mediated repression.* Cell Death Differ, 2015. **22**(1): p. 22-33.
132. Ding, L., et al., *The developmental timing regulator AIN-1 interacts with miRISCs and may target the argonaute protein ALG-1 to cytoplasmic P bodies in C. elegans.* Mol Cell, 2005. **19**(4): p. 437-47.
133. Fabian, M.R., et al., *Mammalian miRNA RISC recruits CAF1 and PABP to affect PABP-dependent deadenylation*, in *Mol Cell*. 2009. p. 868-880.
134. Braun, J.E., et al., *GW182 proteins directly recruit cytoplasmic deadenylase complexes to miRNA targets.* Mol Cell, 2011. **44**(1): p. 120-33.
135. Su, H., et al., *Mammalian hyperplastic discs homolog EDD regulates miRNA-mediated gene silencing.* Mol Cell, 2011. **43**(1): p. 97-109.
136. Funakoshi, Y., et al., *Mechanism of mRNA deadenylation: evidence for a molecular interplay between translation termination factor eRF3 and mRNA deadenylases.* Genes Dev, 2007. **21**(23): p. 3135-48.
137. Hammell, C.M., et al., *nhl-2 Modulates microRNA activity in Caenorhabditis elegans.* Cell, 2009. **136**(5): p. 926-38.
138. Schwamborn, J.C., E. Berezikov, and J.A. Knoblich, *The TRIM-NHL protein TRIM32 activates microRNAs and prevents self-renewal in mouse neural progenitors.* Cell, 2009. **136**(5): p. 913-25.
139. Caudy, A.A., et al., *A micrococcal nuclease homologue in RNAi effector complexes.*, in *Nature*. 2003. p. 411-414.
140. Ding, X.C. and H. Grosshans, *Repression of C. elegans microRNA targets at the initiation level of translation requires GW182 proteins.*, in *EMBO J*. 2009. p. 213-222.
141. Selbach, M., et al., *Widespread changes in protein synthesis induced by microRNAs.* Nature, 2008. **455**(7209): p. 58-63.
142. Eulalio, A., et al., *Deadenylation is a widespread effect of miRNA regulation.* RNA, 2009. **15**(1): p. 21-32.
143. Chekulaeva, M., et al., *miRNA repression involves GW182-mediated recruitment of CCR4-NOT through conserved W-containing motifs.*, in *Nat Struct Mol Biol*. 2011. p. 1218-1226.
144. Djuranovic, S., A. Nahvi, and R. Green, *miRNA-mediated gene silencing by translational repression followed by mRNA deadenylation and decay.* Science, 2012. **336**(6078): p. 237-40.
145. Ingolia, N.T., et al., *Genome-Wide Analysis in Vivo of Translation with Nucleotide Resolution Using Ribosome Profiling*, in *Science*. 2009. p. 218-223.
146. Guo, H., et al., *Mammalian microRNAs predominantly act to decrease target mRNA levels*, in *Nature*. 2010. p. 835-840.

147. Bazzini, A.A., M.T. Lee, and A.J. Giraldez, *Ribosome profiling shows that miR-430 reduces translation before causing mRNA decay in zebrafish.* Science, 2012. **336**(6078): p. 233-7.
148. Subtelny, A.O., et al., *Poly(A)-tail profiling reveals an embryonic switch in translational control.* Nature, 2014. **508**(7494): p. 66-71.
149. Eichhorn, S.W., et al., *mRNA destabilization is the dominant effect of mammalian microRNAs by the time substantial repression ensues.* Mol Cell, 2014. **56**(1): p. 104-15.
150. Kronja, I., et al., *Widespread changes in the posttranscriptional landscape at the Drosophila oocyte-to-embryo transition.* Cell Rep, 2014. **7**(5): p. 1495-508.
151. Huang, K.L., et al., *Phosphorylation at intrinsically disordered regions of PAM2 motif-containing proteins modulates their interactions with PABPC1 and influences mRNA fate.* RNA, 2013. **19**(3): p. 295-305.
152. Mishima, Y., et al., *Differential regulation of germline mRNAs in soma and germ cells by zebrafish miR-430.* Curr Biol, 2006. **16**(21): p. 2135-42.
153. Kedde, M., et al., *RNA-binding protein Dnd1 inhibits microRNA access to target mRNA.* Cell, 2007. **131**(7): p. 1273-86.
154. Takeda, Y., et al., *DAZL relieves miRNA-mediated repression of germline mRNAs by controlling poly(A) tail length in zebrafish.* PLoS One, 2009. **4**(10): p. e7513.
155. Lopez de Silanes, I., et al., *Identification of a target RNA motif for RNA-binding protein HuR.* Proc Natl Acad Sci U S A, 2004. **101**(9): p. 2987-92.
156. Dassi, E., et al., *Hyper conserved elements in vertebrate mRNA 3'-UTRs reveal a translational network of RNA-binding proteins controlled by HuR.* Nucleic Acids Res, 2013. **41**(5): p. 3201-16.
157. Kim, H.H., et al., *HuR recruits let-7/RISC to repress c-Myc expression.* Genes Dev, 2009. **23**(15): p. 1743-8.
158. Bhattacharyya, S.N., et al., *Relief of microRNA-mediated translational repression in human cells subjected to stress.* Cell, 2006. **125**(6): p. 1111-24.
159. Lu, Y.C., et al., *ELAVL1 modulates transcriptome-wide miRNA binding in murine macrophages.* Cell Rep, 2014. **9**(6): p. 2330-43.
160. Xue, Y., et al., *Direct conversion of fibroblasts to neurons by reprogramming PTB-regulated microRNA circuits.* Cell, 2013. **152**(1-2): p. 82-96.
161. Kenny, P.J., et al., *MOV10 and FMRP regulate AGO2 association with microRNA recognition elements.* Cell Rep, 2014. **9**(5): p. 1729-41.
162. Vasudevan, S., Y. Tong, and J.A. Steitz, *Switching from repression to activation: microRNAs can up-regulate translation.* Science, 2007. **318**(5858): p. 1931-4.
163. Vasudevan, S. and J.A. Steitz, *AU-rich-element-mediated upregulation of translation by FXR1 and Argonaute 2.* Cell, 2007. **128**(6): p. 1105-18.
164. Kedde, M., et al., *A Pumilio-induced RNA structure switch in p27-3' UTR controls miR-221 and miR-222 accessibility.* Nat Cell Biol, 2010. **12**(10): p. 1014-20.
165. Miles, W.O., et al., *Pumilio facilitates miRNA regulation of the E2F3 oncogene.* Genes Dev, 2012. **26**(4): p. 356-68.

166. Jiang, P., M. Singh, and H.A. Coller, *Computational Assessment of the Cooperativity between RNA Binding Proteins and MicroRNAs in Transcript Decay.*, in *PLoS Comput Biol*. 2013. p. e1003075.
167. Incarnato, D., et al., *MREdictor: a two-step dynamic interaction model that accounts for mRNA accessibility and Pumilio binding accurately predicts microRNA targets.*, in *Nucleic Acids Res*. 2013.
168. Wu, C. and J.R. Morris, *Genes, genetics, and epigenetics: a correspondence.* Science, 2001. **293**(5532): p. 1103-5.
169. Deans, C. and K.A. Maggert, *What do you mean, "epigenetic"?* Genetics, 2015. **199**(4): p. 887-96.
170. Kelly, W.G., *Transgenerational epigenetics in the germline cycle of Caenorhabditis elegans.* Epigenetics Chromatin, 2014. **7**(1): p. 6.
171. Schaner, C.E., et al., *A conserved chromatin architecture marks and maintains the restricted germ cell lineage in worms and flies.* Dev Cell, 2003. **5**(5): p. 747-57.
172. Checchi, P.M. and W.G. Kelly, *emb-4 is a conserved gene required for efficient germline-specific chromatin remodeling during Caenorhabditis elegans embryogenesis.* Genetics, 2006. **174**(4): p. 1895-906.
173. Katz, D.J., et al., *A C. elegans LSD1 demethylase contributes to germline immortality by reprogramming epigenetic memory.* Cell, 2009. **137**(2): p. 308-20.
174. Shi, Y., et al., *Histone demethylation mediated by the nuclear amine oxidase homolog LSD1.* Cell, 2004. **119**(7): p. 941-53.
175. Kelly, W.G., et al., *Distinct requirements for somatic and germline expression of a generally expressed Caernorhabditis elegans gene.* Genetics, 1997. **146**(1): p. 227-38.
176. Reuben, M. and R. Lin, *Germline X chromosomes exhibit contrasting patterns of histone H3 methylation in Caenorhabditis elegans.* Dev Biol, 2002. **245**(1): p. 71-82.
177. Kelly, W.G., et al., *X-chromosome silencing in the germline of C. elegans.* Development, 2002. **129**(2): p. 479-92.
178. Bender, L.B., et al., *The MES-2/MES-3/MES-6 complex and regulation of histone H3 methylation in C. elegans.* Curr Biol, 2004. **14**(18): p. 1639-43.
179. Andersen, E.C. and H.R. Horvitz, *Two C. elegans histone methyltransferases repress lin-3 EGF transcription to inhibit vulval development.* Development, 2007. **134**(16): p. 2991-9.
180. Bender, L.B., et al., *MES-4: an autosome-associated histone methyltransferase that participates in silencing the X chromosomes in the C. elegans germ line.* Development, 2006. **133**(19): p. 3907-17.
181. Furuhashi, H., et al., *Trans-generational epigenetic regulation of C. elegans primordial germ cells.* Epigenetics Chromatin, 2010. **3**(1): p. 15.
182. Rechtsteiner, A., et al., *The histone H3K36 methyltransferase MES-4 acts epigenetically to transmit the memory of germline gene expression to progeny.* PLoS Genet, 2010. **6**(9): p. e1001091.

183. Capowski, E.E., et al., *Identification of grandchildless loci whose products are required for normal germ-line development in the nematode Caenorhabditis elegans.* Genetics, 1991. **129**(4): p. 1061-72.
184. Robert, V.J., et al., *Chromatin and RNAi factors protect the C. elegans germline against repetitive sequences.* Genes Dev, 2005. **19**(7): p. 782-7.
185. Kelly, W.G. and A. Fire, *Chromatin silencing and the maintenance of a functional germline in Caenorhabditis elegans*, in *Development*. 1998. p. 2451-2456.
186. Bannister, A.J., et al., *Selective recognition of methylated lysine 9 on histone H3 by the HP1 chromo domain.* Nature, 2001. **410**(6824): p. 120-4.
187. Bernstein, B.E., et al., *Methylation of histone H3 Lys 4 in coding regions of active genes.* Proc Natl Acad Sci U S A, 2002. **99**(13): p. 8695-700.
188. Binda, O., et al., *Trimethylation of histone H3 lysine 4 impairs methylation of histone H3 lysine 9: regulation of lysine methyltransferases by physical interaction with their substrates.* Epigenetics, 2010. **5**(8): p. 767-75.
189. Towbin, B.D., et al., *Step-wise methylation of histone H3K9 positions heterochromatin at the nuclear periphery.* Cell, 2012. **150**(5): p. 934-47.
190. Li, T. and W.G. Kelly, *A role for Set1/MLL-related components in epigenetic regulation of the Caenorhabditis elegans germ line.* PLoS Genet, 2011. **7**(3): p. e1001349.
191. Xiao, Y., et al., *Caenorhabditis elegans chromatin-associated proteins SET-2 and ASH-2 are differentially required for histone H3 Lys 4 methylation in embryos and adult germ cells.* Proc Natl Acad Sci U S A, 2011. **108**(20): p. 8305-10.
192. Alvares, S.M., et al., *H3K4 demethylase activities repress proliferative and postmitotic aging.*, in *Aging Cell*. 2014. p. 245-253.
193. Christensen, J., et al., *RBP2 belongs to a family of demethylases, specific for tri- and dimethylated lysine 4 on histone 3*, in *Cell*. 2007. p. 1063-1076.
194. Robert, V.J., et al., *The SET-2/SET1 histone H3K4 methyltransferase maintains pluripotency in the Caenorhabditis elegans germline.* Cell Rep, 2014. **9**(2): p. 443-50.
195. Bessler, J.B., E.C. Andersen, and A.M. Villeneuve, *Differential localization and independent acquisition of the H3K9me2 and H3K9me3 chromatin modifications in the Caenorhabditis elegans adult germ line.* PLoS Genet, 2010. **6**(1): p. e1000830.
196. Kerr, S.C., et al., *SPR-5 and MET-2 function cooperatively to reestablish an epigenetic ground state during passage through the germ line.* Proc Natl Acad Sci U S A, 2014. **111**(26): p. 9509-14.
197. Gu, W., et al., *Distinct argonaute-mediated 22G-RNA pathways direct genome surveillance in the C. elegans germline*, in *Mol Cell*. 2009. p. 231-244.
198. Vagin, V.V., et al., *A distinct small RNA pathway silences selfish genetic elements in the germline*, in *Science*. 2006. p. 320-324.
199. Seth, M., et al., *The C. elegans CSR-1 Argonaute Pathway Counteracts Epigenetic Silencing to Promote Germline Gene Expression.*, in *Dev Cell*. 2013.
200. Song, J.J., et al., *Crystal structure of Argonaute and its implications for RISC slicer activity.* Science, 2004. **305**(5689): p. 1434-7.

201. Fire, A., et al., *Production of antisense RNA leads to effective and specific inhibition of gene expression in C. elegans muscle.* Development, 1991. **113**(2): p. 503-14.
202. Guo, S. and K.J. Kemphues, *par-1, a gene required for establishing polarity in C. elegans embryos, encodes a putative Ser/Thr kinase that is asymmetrically distributed.* Cell, 1995. **81**(4): p. 611-20.
203. Fire, A., et al., *Potent and specific genetic interference by double-stranded RNA in Caenorhabditis elegans*, in *Nature*. 1998. p. 806-811.
204. Timmons, L. and A. Fire, *Specific interference by ingested dsRNA*, in *Nature*. 1998. p. 854.
205. Winston, W.M., C. Molodowitch, and C.P. Hunter, *Systemic RNAi in C. elegans requires the putative transmembrane protein SID-1.* Science, 2002. **295**(5564): p. 2456-9.
206. Kamath, R.S. and J. Ahringer, *Genome-wide RNAi screening in Caenorhabditis elegans.* Methods, 2003. **30**(4): p. 313-21.
207. Zamore, P.D., et al., *RNAi: double-stranded RNA directs the ATP-dependent cleavage of mRNA at 21 to 23 nucleotide intervals*, in *Cell*. 2000. p. 25-33.
208. Parrish, S. and A. Fire, *Distinct roles for RDE-1 and RDE-4 during RNA interference in Caenorhabditis elegans.* RNA, 2001. **7**(10): p. 1397-402.
209. Tabara, H., et al., *The dsRNA binding protein RDE-4 interacts with RDE-1, DCR-1, and a DExH-box helicase to direct RNAi in C. elegans*, in *Cell*. 2002. p. 861-871.
210. Steiner, F.A., et al., *RDE-1 slicer activity is required only for passenger-strand cleavage during RNAi in Caenorhabditis elegans.* Nat Struct Mol Biol, 2009. **16**(2): p. 207-11.
211. Okamura, K., et al., *R2D2 organizes small regulatory RNA pathways in Drosophila.* Mol Cell Biol, 2011. **31**(4): p. 884-96.
212. Sijen, T., et al., *On the role of RNA amplification in dsRNA-triggered gene silencing.* Cell, 2001. **107**(4): p. 465-76.
213. Smardon, A., et al., *EGO-1 is related to RNA-directed RNA polymerase and functions in germ-line development and RNA interference in C. elegans.* Curr Biol, 2000. **10**(4): p. 169-78.
214. Sijen, T., et al., *Secondary siRNAs result from unprimed RNA synthesis and form a distinct class.* Science, 2007. **315**(5809): p. 244-7.
215. Yang, H., et al., *The RDE-10/RDE-11 complex triggers RNAi-induced mRNA degradation by association with target mRNA in C. elegans*, in *Genes Dev*. 2012. p. 846-856.
216. Sheth, U., et al., *Perinuclear P granules are the principal sites of mRNA export in adult C. elegans germ cells*, in *Development*. 2010. p. 1305-1314.
217. Phillips, C.M., et al., *MUT-16 promotes formation of perinuclear mutator foci required for RNA silencing in the C. elegans germline.* Genes Dev, 2012. **26**(13): p. 1433-44.
218. Han, W., et al., *The Caenorhabditis elegans rsd-2 and rsd-6 genes are required for chromosome functions during exposure to unfavorable environments.* Genetics, 2008. **178**(4): p. 1875-93.

219. Guang, S., et al., *An Argonaute transports siRNAs from the cytoplasm to the nucleus.* Science, 2008. **321**(5888): p. 537-41.
220. Burkhart, K.B., et al., *A Pre-mRNA-Associating Factor Links Endogenous siRNAs to Chromatin Regulation*, in *PLoS Genet*. 2011. p. e1002249.
221. Burton, N.O., K.B. Burkhart, and S. Kennedy, *Nuclear RNAi maintains heritable gene silencing in Caenorhabditis elegans*, in *Proc Natl Acad Sci USA*. 2011. p. 19683-19688.
222. Guang, S., et al., *Small regulatory RNAs inhibit RNA polymerase II during the elongation phase of transcription*, in *Nature*. 2010. p. 1097-1101.
223. Shirayama, M., et al., *piRNAs Initiate an Epigenetic Memory of Nonself RNA in the C. elegans Germline*, in *Cell*. 2012. p. 65-77.
224. Ashe, A., et al., *piRNAs Can Trigger a Multigenerational Epigenetic Memory in the Germline of C. elegans*, in *Cell*. 2012. p. 88-99.
225. Simon, M., et al., *Reduced Insulin/IGF-1 Signaling Restores Germ Cell Immortality to Caenorhabditis elegans Piwi Mutants.*, in *Cell Rep*. 2014.
226. Ni, J.Z., E. Chen, and S.G. Gu, *Complex coding of endogenous siRNA, transcriptional silencing and H3K9 methylation on native targets of germline nuclear RNAi in C. elegans.* BMC Genomics, 2014. **15**: p. 1157.
227. Sakaguchi, A., et al., *Caenorhabditis elegans RSD-2 and RSD-6 promote germ cell immortality by maintaining small interfering RNA populations.* Proc Natl Acad Sci U S A, 2014. **111**(41): p. E4323-31.
228. Han, T., et al., *26G endo-siRNAs regulate spermatogenic and zygotic gene expression in Caenorhabditis elegans.* Proc Natl Acad Sci U S A, 2009. **106**(44): p. 18674-9.
229. Conine, C.C., et al., *Argonautes ALG-3 and ALG-4 are required for spermatogenesis-specific 26G-RNAs and thermotolerant sperm in Caenorhabditis elegans*, in *Proc Natl Acad Sci USA*. 2010. p. 3588-3593.
230. Vasale, J.J., et al., *Sequential rounds of RNA-dependent RNA transcription drive endogenous small-RNA biogenesis in the ERGO-1/Argonaute pathway*, in *Proc Natl Acad Sci USA*. 2010. p. 3582-3587.
231. Conine, C.C., et al., *Argonautes Promote Male Fertility and Provide a Paternal Memory of Germline Gene Expression in C. elegans.*, in *Cell*. 2013. p. 1532-1544.
232. Pavelec, D.M., et al., *Requirement for the ERI/DICER complex in endogenous RNA interference and sperm development in Caenorhabditis elegans*, in *Genetics*. 2009. p. 1283-1295.
233. Duchaine, T.F., et al., *Functional proteomics reveals the biochemical niche of C. elegans DCR-1 in multiple small-RNA-mediated pathways*, in *Cell*. 2006. p. 343-354.
234. Gu, W., et al., *CapSeq and CIP-TAP Identify Pol II Start Sites and Reveal Capped Small RNAs as C. elegans piRNA Precursors.*, in *Cell*. 2012. p. 1488-1500.
235. Batista, P.J., et al., *PRG-1 and 21U-RNAs interact to form the piRNA complex required for fertility in C. elegans*, in *Mol Cell*. 2008. p. 67-78.

236. Das, P.P., et al., *Piwi and piRNAs act upstream of an endogenous siRNA pathway to suppress Tc3 transposon mobility in the Caenorhabditis elegans germline (Supp)*, in *Mol Cell*. 2008. p. 79-90.
237. Sapetschnig, A., et al., *Tertiary siRNAs mediate paramutation in C. elegans.* PLoS Genet, 2015. **11**(3): p. e1005078.
238. Alleman, M., et al., *An RNA-dependent RNA polymerase is required for paramutation in maize.* Nature, 2006. **442**(7100): p. 295-8.
239. Claycomb, J.M., et al., *The Argonaute CSR-1 and its 22G-RNA cofactors are required for holocentric chromosome segregation*, in *Cell*. 2009. p. 123-134.
240. Wedeles, C.J., M.Z. Wu, and J.M. Claycomb, *Protection of Germline Gene Expression by the C. elegans Argonaute CSR-1.*, in *Dev Cell*. 2013.
241. Greer, E.L., et al., *A histone methylation network regulates transgenerational epigenetic memory in C. elegans.* Cell Rep, 2014. **7**(1): p. 113-26.
242. She, X., et al., *Regulation of heterochromatin assembly on unpaired chromosomes during Caenorhabditis elegans meiosis by components of a small RNA-mediated pathway.* PLoS Genet, 2009. **5**(8): p. e1000624.
243. Maine, E.M., et al., *EGO-1, a putative RNA-dependent RNA polymerase, is required for heterochromatin assembly on unpaired dna during C. elegans meiosis.* Curr Biol, 2005. **15**(21): p. 1972-8.
244. Cecere, G., et al., *Global effects of the CSR-1 RNA interference pathway on the transcriptional landscape.* Nat Struct Mol Biol, 2014. **21**(4): p. 358-65.
245. Gassmann, R., et al., *An inverse relationship to germline transcription defines centromeric chromatin in C. elegans.* Nature, 2012. **484**(7395): p. 534-7.
246. Cecere, G., et al., *Global effects of the CSR-1 RNA interference pathway on the transcriptional landscape.*, in *Nat Struct Mol Biol*. 2014. p. 358-365.
247. Watson, M.L., et al., *Identification of morc (microrchidia), a mutation that results in arrest of spermatogenesis at an early meiotic stage in the mouse.* Proc Natl Acad Sci U S A, 1998. **95**(24): p. 14361-6.
248. Inoue, N., et al., *New gene family defined by MORC, a nuclear protein required for mouse spermatogenesis.* Hum Mol Genet, 1999. **8**(7): p. 1201-7.
249. Pastor, W.A., et al., *MORC1 represses transposable elements in the mouse male germline.* Nat Commun, 2014. **5**: p. 5795.
250. Moissiard, G., et al., *MORC family ATPases required for heterochromatin condensation and gene silencing.* Science, 2012. **336**(6087): p. 1448-51.
251. Kim, J.K., et al., *Functional genomic analysis of RNA interference in C. elegans.* Science, 2005. **308**(5725): p. 1164-7.
252. Iyer, L.M., S. Abhiman, and L. Aravind, *MutL homologs in restriction-modification systems and the origin of eukaryotic MORC ATPases.* Biol Direct, 2008. **3**: p. 8.
253. Li, D.Q., S.S. Nair, and R. Kumar, *The MORC family: new epigenetic regulators of transcription and DNA damage response.* Epigenetics, 2013. **8**(7): p. 685-93.
254. He, F., et al., *Structural insight into the zinc finger CW domain as a histone modification reader.* Structure, 2010. **18**(9): p. 1127-39.
255. Zhang, Q., et al., *Structure-function analysis reveals a novel mechanism for regulation of histone demethylase LSD2/AOF1/KDM1b.* Cell Res, 2013. **23**(2): p. 225-41.

256. Blewitt, M.E., et al., *SmcHD1, containing a structural-maintenance-of-chromosomes hinge domain, has a critical role in X inactivation.* Nat Genet, 2008. **40**(5): p. 663-9.
257. Lorkovic, Z.J., et al., *Involvement of a GHKL ATPase in RNA-directed DNA methylation in Arabidopsis thaliana.* Curr Biol, 2012. **22**(10): p. 933-8.
258. Takahashi, K., et al., *Dynamic regulation of p53 subnuclear localization and senescence by MORC3.* Mol Biol Cell, 2007. **18**(5): p. 1701-9.
259. Mimura, Y., et al., *Two-step colocalization of MORC3 with PML nuclear bodies.* J Cell Sci, 2010. **123**(Pt 12): p. 2014-24.
260. Rosendorff, A., et al., *NXP-2 association with SUMO-2 depends on lysines required for transcriptional repression.* Proc Natl Acad Sci U S A, 2006. **103**(14): p. 5308-13.
261. Li, D.Q., et al., *MORC2 signaling integrates phosphorylation-dependent, ATPase-coupled chromatin remodeling during the DNA damage response.* Cell Rep, 2012. **2**(6): p. 1657-69.
262. Nottke, A.C., et al., *SPR-5 is a histone H3K4 demethylase with a role in meiotic double-strand break repair.* Proc Natl Acad Sci U S A, 2011. **108**(31): p. 12805-10.
263. Kang, H.G., et al., *CRT1 is a nuclear-translocated MORC endonuclease that participates in multiple levels of plant immunity.* Nat Commun, 2012. **3**: p. 1297.
264. Holoch, D. and D. Moazed, *RNA-mediated epigenetic regulation of gene expression.* Nat Rev Genet, 2015. **16**(2): p. 71-84.
265. Wierzbicki, A.T., et al., *RNA polymerase V transcription guides ARGONAUTE4 to chromatin.* Nat Genet, 2009. **41**(5): p. 630-4.
266. Wierzbicki, A.T., J.R. Haag, and C.S. Pikaard, *Noncoding transcription by RNA polymerase Pol IVb/Pol V mediates transcriptional silencing of overlapping and adjacent genes.* Cell, 2008. **135**(4): p. 635-48.
267. Fransz, P., et al., *Interphase chromosomes in Arabidopsis are organized as well defined chromocenters from which euchromatin loops emanate.* Proc Natl Acad Sci U S A, 2002. **99**(22): p. 14584-9.
268. Brabbs, T.R., et al., *The stochastic silencing phenotype of Arabidopsis morc6 mutants reveals a role in efficient RNA-directed DNA methylation.* Plant J, 2013. **75**(5): p. 836-46.
269. Lorkovic, Z.J., *MORC proteins and epigenetic regulation.*, in *Plant Signal Behav*. 2012. p. 1561-1565.
270. Liu, Z.W., et al., *The SET domain proteins SUVH2 and SUVH9 are required for Pol V occupancy at RNA-directed DNA methylation loci.* PLoS Genet, 2014. **10**(1): p. e1003948.
271. Subramaniam, K. and G. Seydoux, *Dedifferentiation of primary spermatocytes into germ cell tumors in C. elegans lacking the pumilio-like protein PUF-8.* Curr Biol, 2003. **13**(2): p. 134-9.
272. Ariz, M., R. Mainpal, and K. Subramaniam, *C. elegans RNA-binding proteins PUF-8 and MEX-3 function redundantly to promote germline stem cell mitosis.* Dev Biol, 2009. **326**(2): p. 295-304.

273. Vaid, S., et al., *PUF-8 negatively regulates RAS/MAPK signalling to promote differentiation of C. elegans germ cells.* Development, 2013. **140**(8): p. 1645-54.
274. Bagga, S., et al., *Regulation by let-7 and lin-4 miRNAs results in target mRNA degradation.* Cell, 2005. **122**(4): p. 553-63.
275. Pillai, R.S., et al., *Inhibition of translational initiation by Let-7 MicroRNA in human cells.* Science, 2005. **309**(5740): p. 1573-6.
276. Mathonnet, G., et al., *MicroRNA inhibition of translation initiation in vitro by targeting the cap-binding complex eIF4F.* Science, 2007. **317**(5845): p. 1764-7.
277. Zekri, L., D. Kuzuoglu-Ozturk, and E. Izaurralde, *GW182 proteins cause PABP dissociation from silenced miRNA targets in the absence of deadenylation.* EMBO J, 2013. **32**(7): p. 1052-65.
278. Meijer, H.A., et al., *Translational repression and eIF4A2 activity are critical for microRNA-mediated gene regulation.* Science, 2013. **340**(6128): p. 82-5.
279. Nishino, J., et al., *Hmga2 promotes neural stem cell self-renewal in young but not old mice by reducing p16Ink4a and p19Arf Expression.* Cell, 2008. **135**(2): p. 227-39.
280. Worringer, K.A., et al., *The let-7/LIN-41 pathway regulates reprogramming to human induced pluripotent stem cells by controlling expression of prodifferentiation genes.* Cell Stem Cell, 2014. **14**(1): p. 40-52.
281. Rougvie, A.E. and E.G. Moss, *Developmental transitions in C. elegans larval stages.* Curr Top Dev Biol, 2013. **105**: p. 153-80.
282. Slack, F.J., et al., *The lin-41 RBCC gene acts in the C. elegans heterochronic pathway between the let-7 regulatory RNA and the LIN-29 transcription factor.* Mol Cell, 2000. **5**(4): p. 659-69.
283. Abrahante, J.E., et al., *The Caenorhabditis elegans hunchback-like gene lin-57/hbl-1 controls developmental time and is regulated by microRNAs.*, in *Dev Cell*. 2003. p. 625-637.
284. Ecsedi, M., M. Rausch, and H. Grosshans, *The let-7 microRNA directs vulval development through a single target.* Dev Cell, 2015. **32**(3): p. 335-44.
285. Quenault, T., T. Lithgow, and A. Traven, *PUF proteins: repression, activation and mRNA localization.* Trends Cell Biol, 2011. **21**(2): p. 104-12.
286. Bailey, T.L., et al., *MEME SUITE: tools for motif discovery and searching*, in *Nucleic Acids Res*. 2009. p. W202-W208.
287. Gerber, A.P., et al., *Genome-wide identification of mRNAs associated with the translational regulator PUMILIO in Drosophila melanogaster.*, in *Proc Natl Acad Sci U S A*. 2006. p. 4487-4492.
288. Hillier, L.W., et al., *Massively parallel sequencing of the polyadenylated transcriptome of C. elegans*, in *Genome Res*. 2009. p. 657-666.
289. Filipovska, A. and O. Rackham, *Designer RNA-binding proteins: New tools for manipulating the transcriptome.* RNA Biol, 2011. **8**(6): p. 978-83.
290. Lorenz, R., et al., *ViennaRNA Package 2.0.*, in *Algorithms Mol Biol*. 2011. p. 26.
291. Freeberg, M.A., et al., *Pervasive and dynamic protein binding sites of the mRNA transcriptome in Saccharomyces cerevisiae.*, in *Genome Biol*. 2013. p. R13.
292. Wan, Y., et al., *Landscape and variation of RNA secondary structure across the human transcriptome.* Nature, 2014. **505**(7485): p. 706-9.

293. Long, D., et al., *Potent effect of target structure on microRNA function.*, in *Nat Struct Mol Biol*. 2007. p. 287-294.
294. Bracht, J., et al., *Trans-splicing and polyadenylation of let-7 microRNA primary transcripts*, in *RNA*. 2004. p. 1586-1594.
295. Vella, M.C., K. Reinert, and F.J. Slack, *Architecture of a validated microRNA::target interaction.* Chem Biol, 2004. **11**(12): p. 1619-23.
296. Vella, M.C., et al., *The C. elegans microRNA let-7 binds to imperfect let-7 complementary sites from the lin-41 3'UTR.* Genes Dev, 2004. **18**(2): p. 132-7.
297. Livak, K.J. and T.D. Schmittgen, *Analysis of relative gene expression data using real-time quantitative PCR and the 2(-Delta Delta C(T)) Method.* Methods, 2001. **25**(4): p. 402-8.
298. Li, H. and R. Durbin, *Fast and accurate short read alignment with Burrows-Wheeler transform*, in *Bioinformatics*. 2009. p. 1754-1760.
299. Huang, D.W., B.T. Sherman, and R.A. Lempicki, *Systematic and integrative analysis of large gene lists using DAVID bioinformatics resources.*, in *Nat Protoc*. 2009. p. 44-57.
300. Huang, D.W., B.T. Sherman, and R.A. Lempicki, *Bioinformatics enrichment tools: paths toward the comprehensive functional analysis of large gene lists.*, in *Nucleic Acids Res*. 2009. p. 1-13.
301. Pak, J. and A. Fire, *Distinct populations of primary and secondary effectors during RNAi in C. elegans*, in *Science*. 2007. p. 241-244.
302. Luteijn, M.J., et al., *Extremely stable Piwi-induced gene silencing in Caenorhabditis elegans*, in *EMBO J*. 2012. p. 3422-3430.
303. Koh, K. and J.H. Rothman, *ELT-5 and ELT-6 are required continuously to regulate epidermal seam cell differentiation and cell fusion in C. elegans.* Development, 2001. **128**(15): p. 2867-80.
304. Kennedy, S., D. Wang, and G. Ruvkun, *A conserved siRNA-degrading RNase negatively regulates RNA interference in C. elegans.* Nature, 2004. **427**(6975): p. 645-9.
305. Zhou, X., et al., *Nuclear RNAi contributes to the silencing of off-target genes and repetitive sequences in Caenorhabditis elegans.* Genetics, 2014. **197**(1): p. 121-32.
306. Huang, L.S., P. Tzou, and P.W. Sternberg, *The lin-15 locus encodes two negative regulators of Caenorhabditis elegans vulval development.* Mol Biol Cell, 1994. **5**(4): p. 395-411.
307. Zhuang, J.J., S.A. Banse, and C.P. Hunter, *The nuclear argonaute NRDE-3 contributes to transitive RNAi in Caenorhabditis elegans.* Genetics, 2013. **194**(1): p. 117-31.
308. Garrigues, J.M., et al., *Defining heterochromatin in C. elegans through genome-wide analysis of the heterochromatin protein 1 homolog HPL-2.* Genome Res, 2015. **25**(1): p. 76-88.
309. Kim, D.H., et al., *Argonaute-1 directs siRNA-mediated transcriptional gene silencing in human cells.* Nat Struct Mol Biol, 2006. **13**(9): p. 793-7.
310. White, E., et al., *Human nuclear Dicer restricts the deleterious accumulation of endogenous double-stranded RNA.* Nat Struct Mol Biol, 2014. **21**(6): p. 552-9.

311. Seth, M., et al., *The C. elegans CSR-1 argonaute pathway counteracts epigenetic silencing to promote germline gene expression.* Dev Cell, 2013. **27**(6): p. 656-63.
312. Conine, C.C., et al., *Argonautes promote male fertility and provide a paternal memory of germline gene expression in C. elegans.* Cell, 2013. **155**(7): p. 1532-44.
313. Saetrom, P., et al., *Distance constraints between microRNA target sites dictate efficacy and cooperativity.* Nucleic Acids Res, 2007. **35**(7): p. 2333-42.
314. McCann, C., et al., *The Ataxin-2 protein is required for microRNA function and synapse-specific long-term olfactory habituation.* Proc Natl Acad Sci U S A, 2011. **108**(36): p. E655-62.
315. Lall, S., et al., *Squid hnRNP protein promotes apical cytoplasmic transport and localization of Drosophila pair-rule transcripts.* Cell, 1999. **98**(2): p. 171-80.
316. Norvell, A., et al., *Specific isoforms of squid, a Drosophila hnRNP, perform distinct roles in Gurken localization during oogenesis.* Genes Dev, 1999. **13**(7): p. 864-76.
317. Norvell, A., et al., *Squid is required for efficient posterior localization of oskar mRNA during Drosophila oogenesis.* Dev Genes Evol, 2005. **215**(7): p. 340-9.
318. Weidmann, C.A. and A.C. Goldstrohm, *Drosophila Pumilio protein contains multiple autonomous repression domains that regulate mRNAs independently of Nanos and brain tumor.* Mol Cell Biol, 2012. **32**(2): p. 527-40.
319. Weidmann, C.A., et al., *The RNA binding domain of Pumilio antagonizes poly-adenosine binding protein and accelerates deadenylation.* RNA, 2014. **20**(8): p. 1298-319.
320. Ruby, J.G., C.H. Jan, and D.P. Bartel, *Intronic microRNA precursors that bypass Drosha processing.* Nature, 2007. **448**(7149): p. 83-6.
321. Gu, S.G., et al., *Amplification of siRNA in Caenorhabditis elegans generates a transgenerational sequence-targeted histone H3 lysine 9 methylation footprint*, in *Nature Genetics*. 2012. p. 157-164.
322. Smelick, C. and S. Ahmed, *Achieving immortality in the C. elegans germline.* Ageing Res Rev, 2005. **4**(1): p. 67-82.
323. Yochem, J. and R.K. Herman, *Investigating C. elegans development through mosaic analysis.* Development, 2003. **130**(20): p. 4761-8.